



HAL
open science

Extracellular matrix remodeling and angiogenesis : impact of the lysyl oxidase like-2 protein

Marion Marchand

► **To cite this version:**

Marion Marchand. Extracellular matrix remodeling and angiogenesis : impact of the lysyl oxidase like-2 protein. Cellular Biology. Sorbonne Université, 2020. English. NNT : 2020SORUS138 . tel-03466541

HAL Id: tel-03466541

<https://theses.hal.science/tel-03466541>

Submitted on 6 Dec 2021

HAL is a multi-disciplinary open access archive for the deposit and dissemination of scientific research documents, whether they are published or not. The documents may come from teaching and research institutions in France or abroad, or from public or private research centers.

L'archive ouverte pluridisciplinaire **HAL**, est destinée au dépôt et à la diffusion de documents scientifiques de niveau recherche, publiés ou non, émanant des établissements d'enseignement et de recherche français ou étrangers, des laboratoires publics ou privés.



COLLÈGE
DE FRANCE
—1530—

THESE DE DOCTORAT DE SORBONNE UNIVERSITE

Spécialité

Physiologie, Physiopathologie et Thérapeutique

Préparée au sein du Centre Interdisciplinaire de Recherches en Biologie du Collège de France

Présentée par

Marion Marchand

Pour obtenir le grade de

DOCTEUR de SORBONNE UNIVERSITE

Remodelage du microenvironnement et angiogenèse

Impact de la lysyl oxydase like-2

Soutenue le 4 décembre 2020

Devant le jury composé de :

Madame la Professeure Muriel Umbhauer

Madame la Docteure Ellen Van Obberghen-Schilling

Monsieur le Professeur Benoît Ladoux

Monsieur le Docteur Pierre-Henri Puech

Monsieur le Professeur Hans Van Oosterwyck

Monsieur le Docteur Stéphane Germain

Monsieur le Docteur Laurent Muller

Présidente du Jury

Rapportrice

Rapporteur

Examineur

Examineur

Directeur de thèse

Encadrant, membre invité

Table of contents

Abbreviations	5
Introduction	6
1. Vascular capillary morphogenesis: cellular and molecular mechanisms	6
1.1. Cellular mechanisms of sprouting angiogenesis	8
1.1.1. Angiogenic stimuli.....	8
1.1.2. Tip/stalk cell specification	9
1.1.3. Lumen formation, shaping the tube.....	11
1.2. Endothelial cell-cell junctions	13
1.3. Maturation and stabilization of blood vessels	15
2. Vascular microenvironment remodeling: synthesis and degradation during angiogenesis	19
2.1. Interstitial ECM degradation	19
2.2. Basement membrane generation	20
2.3. Main components of the endothelial basement membrane	22
2.3.1. Laminins	22
2.3.2. Collagen IV	23
2.3.4. Fibronectin	26
3. LOXL2, actor of vascular ECM remodeling	30
3.1. Lysyl oxidase family of proteins	30
3.2. LOXL2 substrates	32
3.3. Pathological role of LOXL2 and associated mechanisms	33
3.3.1. Implication of LOXL2 in fibrosis via ECM remodeling	33
3.3.2. Implication of LOXL2 in cancer progression	34
3.3.3. Role of LOXL2 in cardiovascular pathologies / vascular development.....	40
4. Cell-microenvironment interactions or how ECM regulates cell responses	43
4.1. Focal adhesions, the main hub for cell-matrix interactions	45
4.1.1. Main components of focal adhesions	45
4.1.2. Focal adhesion dynamics.....	51
4.2. Cell mechanics: signaling through focal adhesions for force generation	56
4.2.1. Mechanosignaling process.....	56
4.2.2. Actomyosin network organization, mechanics and regulators	57
4.2.3. Implication of actomyosin contractility in angiogenesis and vascular stability	59
4.2.4. Technical approaches to study cell traction forces and rigidity sensing	60
4.3. ECM regulates focal adhesion organization and subsequent cell responses	62

4.3.1. Influence of ECM geometry.....	62
4.3.2. Influence of ECM stiffness	63
4.3.3. Combination of factors	63
4.4. Cross-talks between cell-ECM adhesions and cell-cell contacts.....	65
Aims of the study.....	68
Results.....	71
1. Umana-Diaz et al, Matrix Biol 2020.....	71
2. Marchand et al, in preparation.....	93
Discussion and perspectives.....	139
1. Basement membrane deposition	139
A. LOXL2 interacts with ECM proteins prior to their deposition.....	140
B. Spatio-temporal distribution of basement membrane components.....	141
C. LOXL2 drives ECM spatio-temporal assembly in a context-dependent manner ...	142
2. Mechanotransduction	144
3. Angiogenesis.....	145
4. Link between interstitial ECM and basement membrane generation	146
5. Conclusion.....	147
Appendix 1	149
Marchand et al, Semin. Cell. Dev. Biol. 2019	149
Appendix 2	160
Atlas*, Bidault* et al, in prep.....	160
References	193

Abbreviations

AFM: atomic force microscopy	LN: laminin
AJ: adherens junction	LOX: lysyl oxidase
β -APN: b-aminopropionitrile	LTQ: lysyl tyrosylquinone
BM: basement membrane	MAPKs: mitogen-activated protein kinases
CAF: cancer-associated fibroblast	MLCK: myosin light chain kinase
CCM: cerebral cavernous malformations	MMPs: matrix metalloproteinases
CVP: caudal vein plexus	MRLC: myosin regulatory light chain
Dll4: Delta-like 4	mRNA: messenger RNA
DNA: Deoxyribonucleic acid	MT-MMP: membrane-type matrix metalloproteinase
E-cadherin: epithelial cadherin	PDGF: platelet-derived growth factor
EC: endothelial cell	PDGFR: platelet-derived growth factor receptor
ECM: extracellular matrix	PECAM: platelet endothelial cell adhesion molecule
EDA: extra-domain A	PHSRN: Pro-His-Ser-Arg-Asn
EDB: extra-domain B	PIGF: placenta growth factor
EMT: epithelial-to-mesenchymal transition	PLA: proximity ligation assay
ER: endoplasmic reticulum	pMLC: phosphor-myosin light chain
ERK: extracellular signal regulated kinase	RCC: renal cell carcinoma
FA: focal adhesion	RGD: arginylglycylaspartic acid
FAK: focal adhesion kinase	ROCK: Rho-kinase
FGF: fibroblast growth factor	SAXS: small angle X-ray scattering
FN: fibronectin	SHED: Stem cells from human exfoliated deciduous teeth
FRET: forster (fluorescence) resonance energy transfer	SHG: second harmonic generation
FUD: Functional Upstream Domain	SPARC: secreted protein, acidic, cysteine-rich
GEF: guanine nucleotide-exchange factors	Src: proto-oncogene tyrosine-protein kinase
GFP: green fluorescent protein	SRCR: scavenger receptor cysteine rich
HANAC: hereditary angiopathy, nephropathy, aneurysms and muscle cramps	TFM: traction force microscopy
HIF: hypoxia-inducible transcription factor	TGF: transforming growth factor
Hpf: hours post-fertilization	VASP: vasodilator-stimulated phosphoprotein
Hsp47: heat shock protein 47	VE-cadherin: vascular endothelial cadherin
HSPG: heparan sulfate proteoglycan	VEGF: vascular endothelial growth factor
HUVEC: human umbilical vein endothelial cell	VEGFR: vascular endothelial growth factor receptor
ISV: intersegmental vessels	VHL: von Hippel-Lindau
JAIL: junction-associated intermittent lamellipodia	
JAM: junctional adhesion molecule	
LD: leucine-rich	

Introduction

1. Vascular capillary morphogenesis: cellular and molecular mechanisms

Development of blood vessels plays a key role in both physiological and pathological processes. Blood vessels are critical to supply growing tissues with nutrients and oxygen. In vertebrates, they organize in a tree-like hierarchical structure, that actually exists as two distinct arterial and venous trees, connected to one another at their tips through capillary beds. Arteries transport blood away from the heart and branch into smaller vessels called arterioles, which distribute blood to capillary beds. Capillaries lead back the blood to small vessels called venules that grow into larger veins and reach back the heart. All types of vessels display structural specificities that are required for their function (**see figure 1** for the structure of the vessels). Capillaries, the smallest blood vessels, are the unique sites of exchange of many substances with all tissues and fulfill this way a critical function in the vasculature. They consist of a monolayer of endothelial cells polarized in a luminal/abluminal manner and oriented along blood flow, and devoid of smooth muscle cells which are replaced by pericytes. Pericytes are contractile mural cells that enwrap endothelial cells, communicating with them through both direct physical contacts and paracrine signaling. In these small vessels, the structural and mechanical properties of the vascular wall are thus only relying on the basement membrane, a specialized extracellular matrix (ECM) that separates the endothelium from the surrounding stromal tissue. It forms a continuous sheet-like structure 50 to 150 nm thick that surrounds the basal surface of the endothelial monolayer and ensheathes perivascular cells, which also participate in its synthesis and organization (**figure 1**).

During early embryonic development, the vascular tree is initiated through vasculogenesis, the process of blood vessel formation from mesodermally-derived precursors called angioblasts (processed reviewed in Eichmann et al., 2005). These cells first form masses known as blood islands together with hematopoietic precursor cells. Empty spaces then form in the blood islands and develop into vessel lumens. Vascular tubes eventually connect to one another, and the primary plexus differentiates into either arterial or venous fate in response to a combination of hemodynamic stimuli and genetic factors. Vasculogenesis is followed by angiogenesis, which refers to the formation of new blood vessels from pre-existing ones and accounts for a considerable fraction of vessel growth during development, and then throughout life in physiological as well as pathological situations (Potente et al., 2011). Two angiogenesis

mechanisms have been described until now: splitting of pre-existing vessels through intussusceptive angiogenesis, which mainly concerns arteries and veins, and sprouting angiogenesis, which is involved in capillary growth.

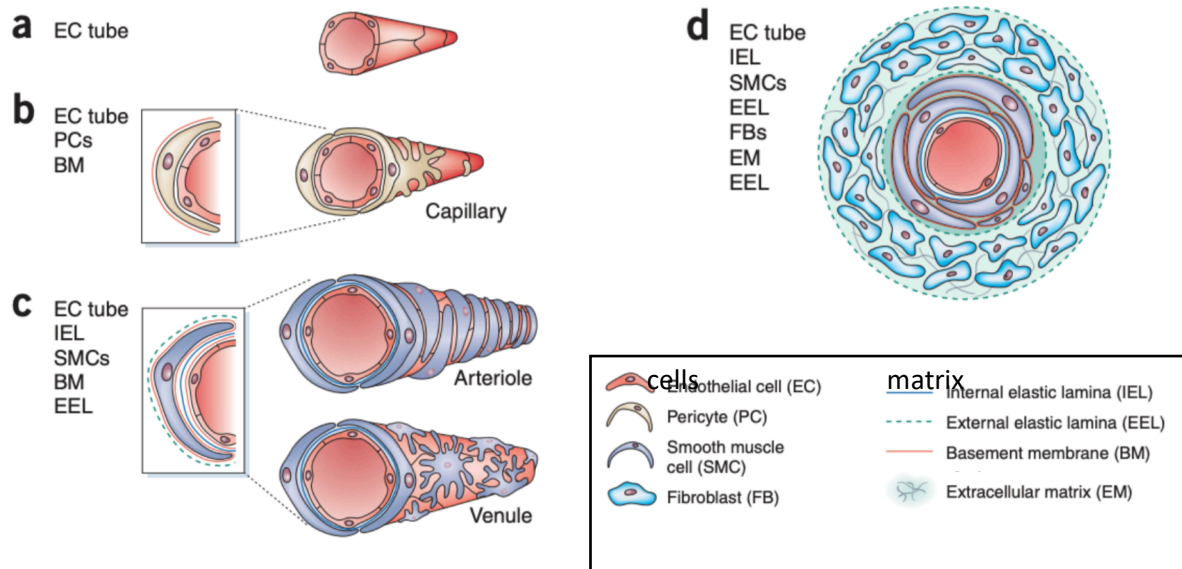


Figure 1. Structure of different types of vessels: capillaries (b), arterioles and venules (c), arteries and veins (d) and associated ECM, adapted from Jain, 2003. EC= endothelial cells, PCs = pericytes, BM= basement membrane, IEL= internal elastic lamina, SMCs=smooth muscle cells, EEL= external elastic lamina, FB= fibroblasts.

Sprouting angiogenesis occurs in conditions that require an increase in blood and oxygen supply, and arises in various pathological circumstances including ischemia, cancer, or retinopathies. Distinct steps of this process include endothelial cell sprouting, elongation and branching, lumen formation, anastomosis, and vessel maturation (**also see figure 2**). One of the key steps in vessel maturation is the generation of a basement membrane by endothelial cells, the structure that supports new vessels and that I will describe in the next chapter of this manuscript. In this chapter, I will detail the cellular and molecular mechanisms involved in sprouting angiogenesis.

1.1. Cellular mechanisms of sprouting angiogenesis

1.1.1. Angiogenic stimuli

Angiogenesis is mainly activated by growth factors expressed in hypoxic tissues, such as vascular endothelial growth factors (VEGF) or fibroblast growth factors (FGF). Hypoxia, a condition in which a tissue is deprived of adequate oxygen supply, occurs in physiological situations, such as embryonic and post-natal development, but also in pathological conditions such as ischemia or cancer. Hypoxia stimulates angiogenesis through multiple pathways including nitric oxide and hypoxia-inducible transcription factors (HIFs). HIF is a constitutively expressed nuclear protein, composed of an α and a β subunits. Half-life of the α subunit is regulated in an oxygen-dependent manner. The actual oxygen sensor is the enzyme prolyl hydroxylase that is involved in post-translational modifications of the α subunit. Upon hydroxylation in normoxia HIF1 α is rapidly degraded via VHL-mediated ubiquitin proteasome pathway. However, under hypoxia, hydroxylation, VHL binding and degradation of HIF1 α are prevented, and the protein accumulates in the nucleus and dimerizes with the β -subunit. HIF α/β heterodimers thus bind to Hypoxic Response Elements on DNA and activate the transcription of a large spectrum of target genes including genes involved in angiogenesis and vascular remodeling, and ECM composition and organization (Germain et al., 2010) (**and see figure 2**).

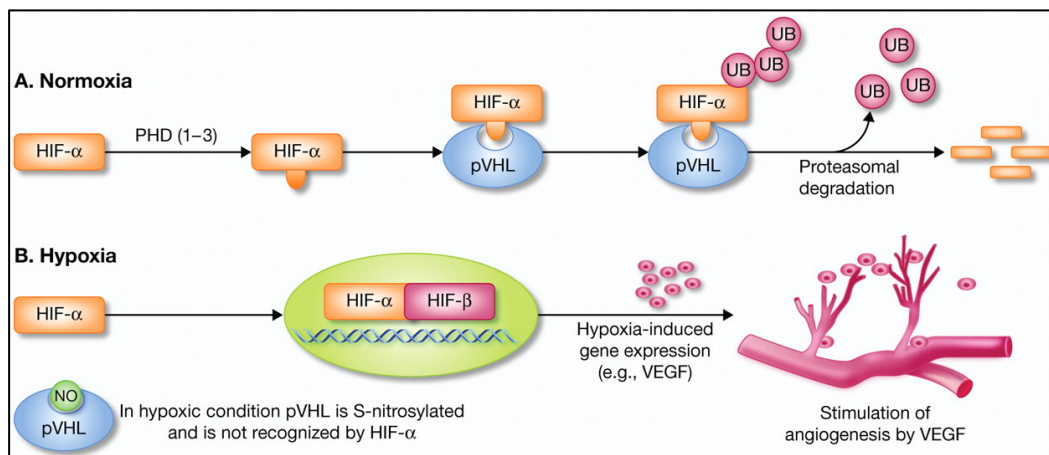


Figure 2. HIF regulation by oxygen levels. A: in normoxia, HIF α is hydroxylated and binds pVHL, causing its degradation through ubiquitination. B: in response to hypoxia, pVHL is S-nitrosylated, preventing its interaction with HIF α . HIF α thus accumulates and associates with the β -subunit. HIF can then be translocated into the nucleus and activate gene expression of pro-angiogenic factors. From Rahimi, 2012.

VEGFs are among the target genes the most activated by hypoxia, and are crucial regulators of angiogenesis (reviewed in Olsson et al., 2006). The VEGF family is composed of secreted dimeric glycoproteins, including placenta growth factor (PlGF), VEGF-A, VEGF-B, VEGF-C, VEGF-D and VEGF-E. Alternative splicing of several members of the VEGF family gives rise to isoforms with different biological activities. Taking VEGF-A as an example, alternative splicing results in five principal forms, the predominant one being VEGF₁₆₅, from which a significant fraction binds to the ECM and cell surface by its heparin-binding sites. This isoform is responsible for inducing physiologically patterned vasculature (Park et al., 1993). Longer forms interact more strongly with the ECM whereas shorter forms that lost their C-terminal heparin-binding domains are more diffusible. Mammalian VEGFs bind to three tyrosine kinase receptors: VEGFR1 (or Flt1) binds VEGF-A, VEGF-B and PlGF; VEGFR2 (or Flk1 or KDR) binds VEGF-A, VEGF-C, VEGF-D and VEGF-E; VEGFR3 binds VEGF-C and VEGF-D. VEGFR1 and VEGFR2 are the most expressed by endothelial cells and play a crucial role in vascular homeostasis. VEGFR1 is somewhat considered to act as a VEGF-A 'trap' as it has high ligand affinity and poor kinase activity, whereas VEGFR2 activation drives most of the VEGF-dependent signaling pathways involved in angiogenesis. Their activation is initiated by binding of VEGF to the N-terminal part of their extracellular domain, by diffusion or by presentation through co-receptors such as heparan sulfate proteoglycans (HSPGs) and integrins. This binding is responsible for homo or hetero-dimerization and activation of the receptors, leading to changes in the intracellular domain conformation and auto-phosphorylation of tyrosine residues in the receptor dimer that trigger activation of downstream signaling pathways involved in vascular homeostasis (Olsson et al., 2006).

1.1.2. Tip/stalk cell specification

In the absence of pro-angiogenic stimuli, endothelial cells are quiescent and VEGF-A signaling is maintained at a low level, allowing endothelial cell survival and homeostasis in an autocrine manner, as demonstrated by the endothelial loss of expression of VEGF resulting in an increase in autophagy leading to cell death (Domigan et al., 2015). However, in the presence of pro-angiogenic stimuli, such as high levels of VEGF, endothelial cells will degrade the basement membrane to allow migration and sprouting of new vessels. In this case, endothelial cells are specified into tip and stalk cells. The tip cell leads the sprouting vessel, whereas the stalk cells proliferate for sprout extension, and form the lumen of the vessel (Geudens and Gerhardt, 2011).

Studies of vascular network formation in mouse retina (Gerhardt, 2003), as well in zebrafish embryo (Blum et al., 2008) have shown that tip cells extend dynamic filopodia and lamellipodia at the leading front, to sense and respond to guidance cues found in the microenvironment. Tip cells guide sprouts and show functional similarities with neuron growth cones that guide axons (Adams and Eichmann, 2010). Stalk cells have the ability to form tubes and extend the vascular network. They produce fewer filopodia, are more proliferative and form the vascular lumen (**figure 3**). They also establish contacts with neighboring cells to ensure integrity of the newly formed vessel. Besides, they downregulate the expression of matrix metalloproteinases (MMPs), that degrade the ECM, and adopt apico-basal polarity.

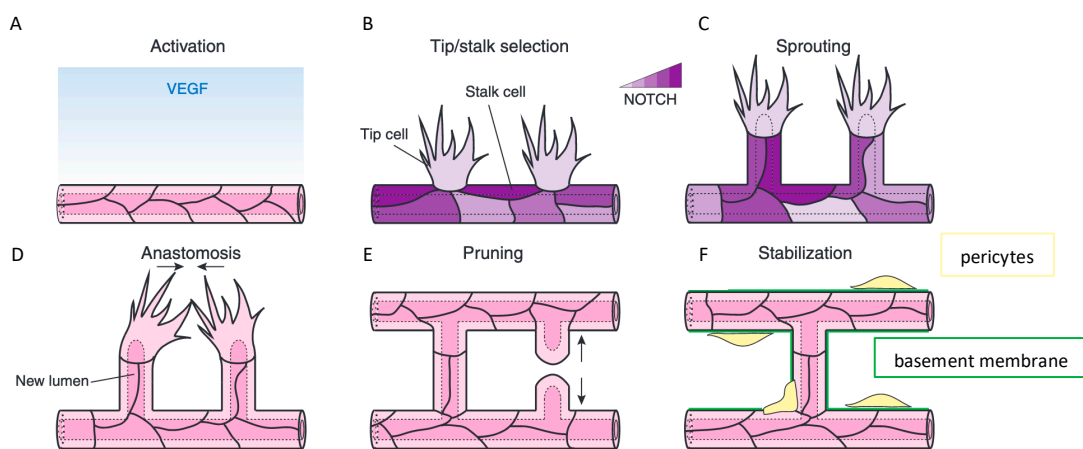


Figure 3. Vascular morphogenesis, schematic representation. Upon activation with VEGF (A), endothelial cells acquire transient tip and stalk cell phenotypes (B) through Notch signaling to form a sprout. They elongate through collective migration and proliferation (C). They fuse by anastomosis to form new vascular loops (D). Elimination of unnecessary branches is led by a process called pruning (E). Eventually, endothelial cells become quiescent and the new vasculature is stabilized by recruitment of pericytes and deposition of ECM (F). Adapted from Szymborska and Gerhardt, 2018

Specification of endothelial cells into tip and stalk cells is controlled by the Notch signaling pathway (**see figure 3 and figure 4**) (Phng and Gerhardt, 2009). Notch activity is high in stalk cells but low in tip cells, which express high levels of the Notch ligand Delta-like 4 (DII4). In response to VEGFA-VEGFR2 signaling, DII4 expression is increased in the tip cells, concomitant with an increase in the expression of Notch receptor in the adjacent stalk cells. The resulting stimulation of Notch in stalk cells leads to the downregulation of VEGFR2 and increased VEGFR1 expression (Suchting et al., 2007). Stalk cells thus become less sensitive to VEGF-A due to the high affinity of VEGFR1 for VEGF ligands and its poor signaling activity.

Inversely, tip cells with low Notch activity have high VEGFR2 and low VEGFR1 expression, resulting in higher levels of Dll4 and maintaining the tip cell specification (**figure 4**). Although endothelial cells express several Notch receptors, Notch1 is critical for suppressing tip cell behavior in stalk cells, as indicated by the hypersprouting phenotype and excessive number of tip cells following Notch1 endothelial-specific deletion (Hellström et al., 2007). Besides, the importance of a balanced tip/stalk specification by Notch is illustrated by the paradoxical effects of gene inactivation of Notch1 or Dll4 in endothelial cells: although more vessels are formed, they are not fully perfused and dysfunctional (Phng and Gerhardt, 2009; Suchting et al., 2007).

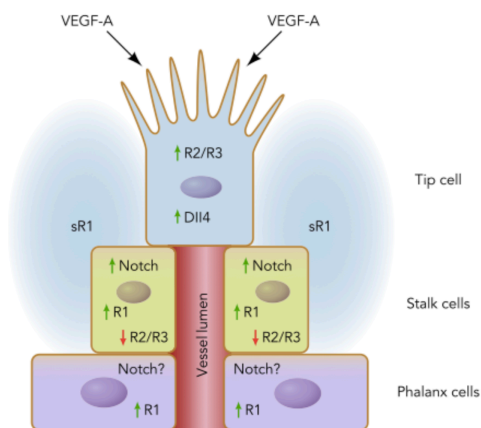


Figure 4. Guidance cues of vessel sprouting. Notch/Dll4 signaling in tip/stalk cells; Dll4 is highly expressed in tip cells, and its receptor Notch is expressed by stalk cells, leading to downregulation of R2 and upregulation of R1. From Lee and Bautch, 2011

1.1.3. Lumen formation, shaping the tube

The capacity to establish an uninterrupted lumen is crucial for blood vessel formation, and endothelial cells engage in this process very early during embryogenesis, following several mechanisms (Ellertsdóttir et al., 2010; Iruela-Arispe and Davis, 2009; Zeeb et al., 2010). Two distinct processes have been discussed: 1) cell hollowing, in which intracellular vacuoles merge and then interconnect with neighboring cells to generate continuous tubes; 2) cord hollowing, involving packed cells undergoing shape changes together with establishment of an apico-basal polarity to create a multicellular tube with a central extracellular lumen (**see figure 5**). The latter model in which endothelial cells define the apico-basal polarity is the most probable one. Indeed, analysis of proteins involved in the establishment of polarity and cell-cell junctions including fibronectin, β -catenin (Jin et al., 2005), podocalyxin, or Par3 (Strilić et al., 2009) has shown that polarization and formation of endothelial cell-cell junctions occur just before creation of the lumen. The mechanisms underlying the establishment of the apico-basal

polarity are not fully understood, however, conserved polarity proteins such as Par6 (Etienne-Manneville and Hall, 2003), podocalyxin, or Par3 (Strilić et al., 2009), with known functions in epithelial polarity are also involved in endothelial cells. In this latter study, authors showed that the first steps of lumen formation in the paired aorta mouse embryos begin upon formation of cell-cell adherens junctions between angioblasts, inducing establishment of an apical interface. Accumulation of negatively charged anti-adhesive glycoproteins at the luminal surface then confers a signal that opens up the lumen (Strilić et al., 2009). Simultaneously to these extracellular events, the actomyosin cytoskeleton is being remodeled and F-actin becomes enriched at junctions between cells shortly before lumenization. If junctional actin cables are not recruited, as it is the case when formin is inhibited, lumens fail to open (Phng et al., 2015).

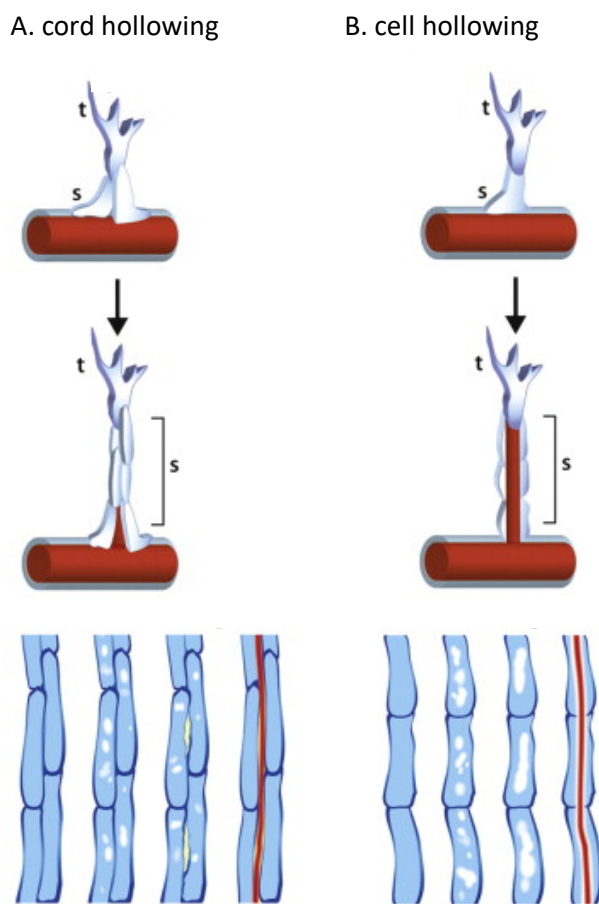


Figure 5. Mechanisms of lumen formation during sprouting angiogenesis by cord hollowing and cell hollowing. t: tip cell; s: stalk cell. A: Cord hollowing process. Endothelial cells grow in a paired configuration maintaining an apical surface in between. Cellular rearrangements will then lead to a continuous apical surface and open up the luminal space. B: Cell hollowing process. Endothelial cells form vacuoles that fuse to give rise to the lumen. Adapted from Ellertsdóttir et al., 2010.

In summary, these studies show that the lumen is formed between apical surfaces of endothelial cells by a cord hollowing process. Signaling from the ECM might also provide initial spatial cues for the organization of cell polarity. As an example, loss of $\beta 1$ integrin in the endothelium increases expression of proteins present in cell-cell junctions such as VE-

cadherin and PECAM-1 and disturbs their polarized localization, leading to disorganization of cell-cell contacts, and blocking lumen formation (Zovein et al., 2010). These results suggest that forces established between endothelial cells but also between endothelial cells and the surrounding ECM must be tightly tuned in order to form a lumen. It is important to note that these processes have been studied in the absence of blood flow and indeed occur before establishment of circulation. In addition to the mechanisms proposed above, a recent work conducted in the zebrafish embryo showed that hemodynamic force exerted by blood flow itself, also plays a role in remodeling of the vascular network and in lumenization of new vascular connections by inducing spherical deformations of the endothelial apical membrane (Gebala et al., 2016). These results demonstrate that blood flow is an additional feature regulating lumen formation during angiogenesis.

1.2. Endothelial cell-cell junctions

The endothelial barrier is regulated by coordination of adherens junctions, basement membrane and pericyte coverage. Endothelial cell-cell junctions comprise both tight junctions (composed of occludins, claudins, JAM adhesion molecules) and adherens junctions, whose main component is VE-cadherin. PECAM (platelet endothelial cell adhesion molecule) also contribute to cell-cell adhesion processes (**figure 6**). Besides, endothelial cells also express N-cadherin, that plays a role in adhesion between endothelial cells and mural cells.

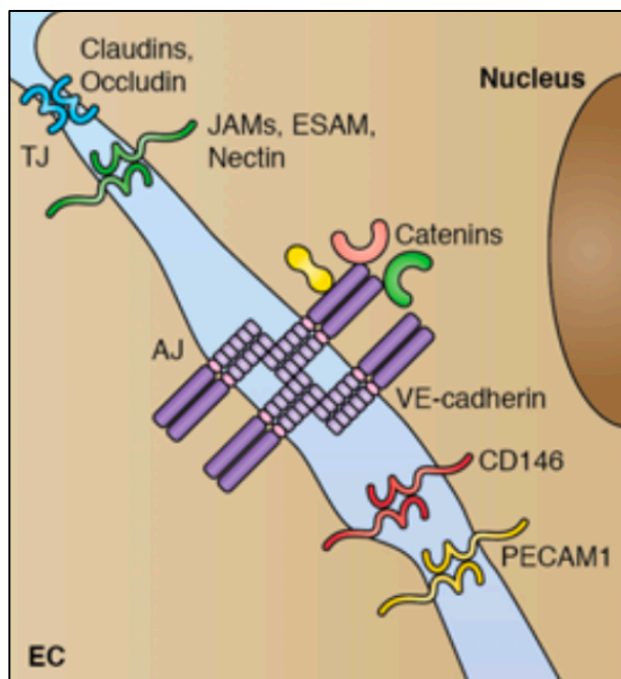


Figure 6. Overview of different endothelial cell junctions. TJ= tight junctions, AJ= adherens junctions, EC= endothelial cells. Adapted from Dejana and Orsenigo, 2013.

VE-cadherin is a glycoprotein that spans across the plasma membrane and is exclusively expressed at the endothelial cell surface. Mice invalidated for VE-cadherin die during development (E9.5) from vascular hemorrhages due to endothelial cell apoptosis (Carmeliet et al., 1999). The intracellular domain of VE-cadherin interacts with several adaptors or effectors such as vinculin, p120-catenin, or β -catenin (**figure 6**). These adaptors are able to bind to proteins that mediate actin cytoskeleton organization and linkage such as α -actinin. The intracellular domain of VE-cadherin contains several tyrosine that can be phosphorylated and are involved in endothelial barrier integrity by regulating interactions between VE-cadherin and its adaptors. At the basal state, VE-cadherin forms a complex at the endothelial cell surface together with VEGFR2 and integrin $\alpha v\beta 3$ that has been demonstrated to regulate vascular stability (Carmeliet et al., 1999; Gomez Perdiguero et al., 2016).

The team of Johan De Rooij has characterized two different organizations for VE-cadherin in endothelial cell-cell junctions: 1) stable adherens junctions, that present a linear organization of VE-cadherin and 2) unstable adherens junctions, that present a Z-shape non-continuous organization of VE-cadherin (Oldenburg and de Rooij, 2014) (and **see figure 7**). Several factors such as thrombin, VEGF or TNF- α trigger the transition between these two morphologies, involving the activation of small GTPases that play a key role in actomyosin organization. For example, VEGF-induced RhoA activation and subsequent ROCK activation leads to increased actomyosin contractility and stress fiber formation. Tensions generated by these stress fibers induce a non-continuous and unstable VE-cadherin organization. Inversely, when the endothelium is in a stable state, actin organizes cortically in the cells, thanks to activation of small GTPases Cdc42 or Rac1. Actomyosin network is therefore associated with VE-cadherin that adopt a linear morphology along cell junctions (Huveneers et al., 2012) (**and see figure 7**).

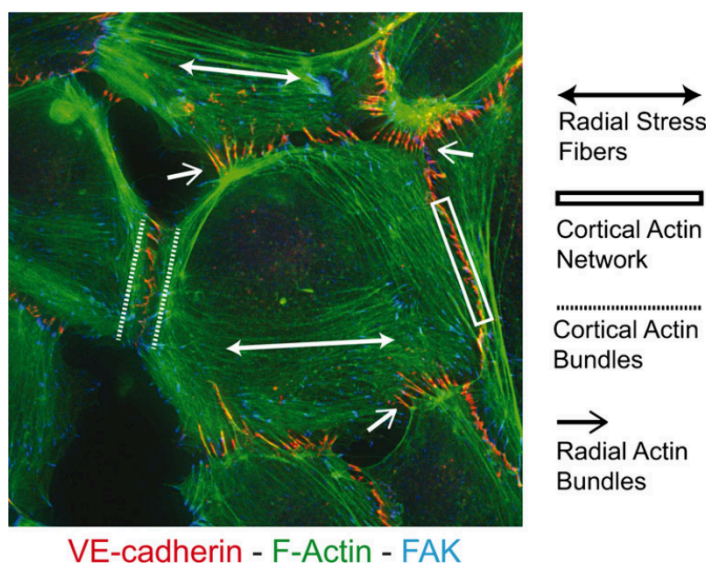


Figure 7. Overview of actin structures involved in endothelial cell-cell adhesion. From Oldenburg and de Rooij, 2014. Adherens junctions are labeled by VE-cadherin antibody in HUVECs. FA are labeled by FAK staining. The actin cytoskeleton is labeled by F-actin staining. Radial stress fibers are located centrally in the cell and connect to focal adhesions on either side. Cortical actin network is hardly visible, very thin.

The actomyosin-mediated contractility and actin remodeling in endothelium has significant impact on shape changes and control of intercellular junctions. Recent studies demonstrated the constitutive appearance of junction-associated intermittent lamellipodia (JAIL) that drives VE-cadherin dynamics and controls endothelial permeability (Cao and Schnittler, 2019). This reticular organization corresponds to overlapping regions of adjacent cells and are characterized by co-localization with PECAM-1. They maintain endothelial stability in regions characterized by low actin tension in the cells. JAILs have also been observed *in vivo* in capillaries (Fernandez-Martin et al, 2012) and are involved in angiogenesis (Cao et al., 2017). Establishment of this type of junction initiates formation of new adhesion plaques of intercellular VE-cadherin and strengthens vascular integrity.

1.3. Maturation and stabilization of blood vessels

For capillaries to be functional, they must mature at multiple levels. At the network level, maturation involves remodeling into a hierarchically branched network and adaptation of vascular patterning to tissue needs. This also involves maturation at the cellular level by recruitment of mural cells and at the subcellular and molecular level by deposition of basement membrane in the vascular wall.

Pericytes are specialized cells found along capillaries that lack vascular smooth muscle cells. They are non-contractile cells displaying long cytoplasmic extensions that surrounds capillaries. Pericyte coverage is very variable from one organ to another, with central nervous system and retina having the most covered capillaries reaching 85% of the endothelium surface. This observation fits with the importance of pericytes as regulators of permeability at the blood-brain barrier. The role of pericytes in capillary stabilization includes regulation of endothelial cell proliferation and migration, as well as participation in basement membrane assembly (Stratman and Davis, 2012). In fact, defects in endothelial cell-pericyte interactions lead to embryonic death due to failures in vascular remodeling and stabilization (Armulik et al., 2011). Recruitment of pericytes at the capillary surface is regulated by platelet-derived growth factor (PDGF) signaling (Lindahl et al., 1997). The ligand PDGF-B is expressed by endothelial tip cells whereas pericytes express its receptor PDGFR- β . PDGF-B is secreted and binds to heparan sulfate proteoglycans in the endothelial ECM, thus generating a gradient that allows pericyte recruitment (Gerhardt and Betsholtz, 2003). Once recruited, pericytes participate in basement membrane generation (Stratman et al., 2010), as suggested by electron microscopy images showing basement membrane between pericytes and endothelial cells but also ensheathing pericytes themselves (Joutel et al., 2016) (**and see figure 8**).

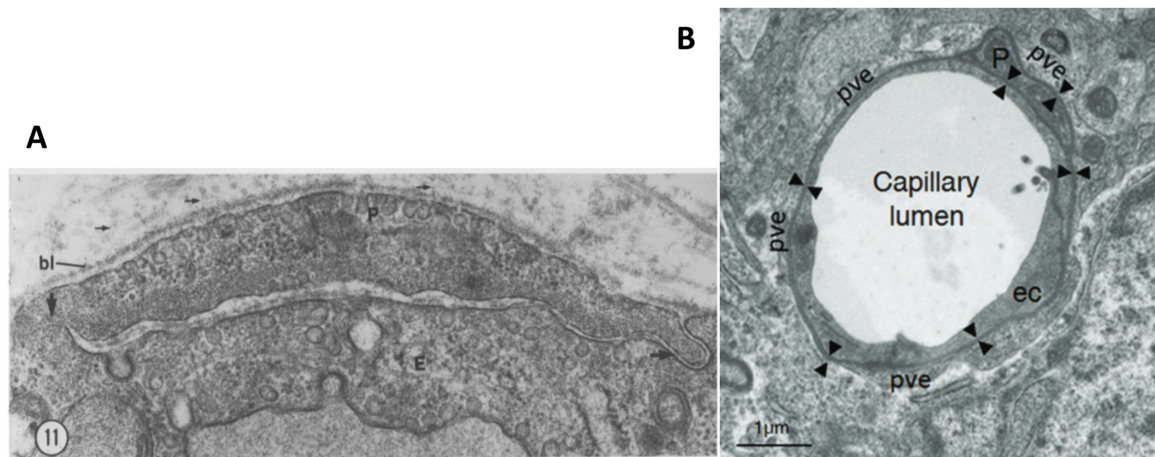


Figure 8. Pericytes and vascular basement membrane. A: Pericyte and endothelial cell of a venule, showing fibrillar connections (small horizontal arrows) between pericyte's basal lamina (bl) and larger collagen bundles (Sims, 1986) B: a capillary in the striatum showing continuous basement membrane (BM) (black arrowheads) covering the basal side of the endothelial cells (EC) and enwrapping the pericyte (P). The BM is surrounded by several perivascular astrocyte endfeet (pve). (Joutel et al., 2016)

It has been difficult to elucidate how capillary tubes form *in vivo*, and there is an increasing requirement for relevant *in vitro* models allowing a molecular analysis of these events. Development of *in vitro* models of capillary morphogenesis in 3D extracellular matrices including type I collagen or fibrin has allowed to shed light on numerous processes involved in capillary elongation, lumen formation and basement membrane deposition by endothelial cells. They have also been developed in order to pre-vascularize tissue constructs in the context of regenerative medicine. One model consists in seeding endothelial cells as single cells into 3D hydrogels. They eventually auto-assemble into 3D tubular networks within 72h when cultured under proper conditions. This model can be used to study tip/stalk cell differentiation and establishment of cell-cell junctions as well as recruitment of perivascular cells (**figure 9**).

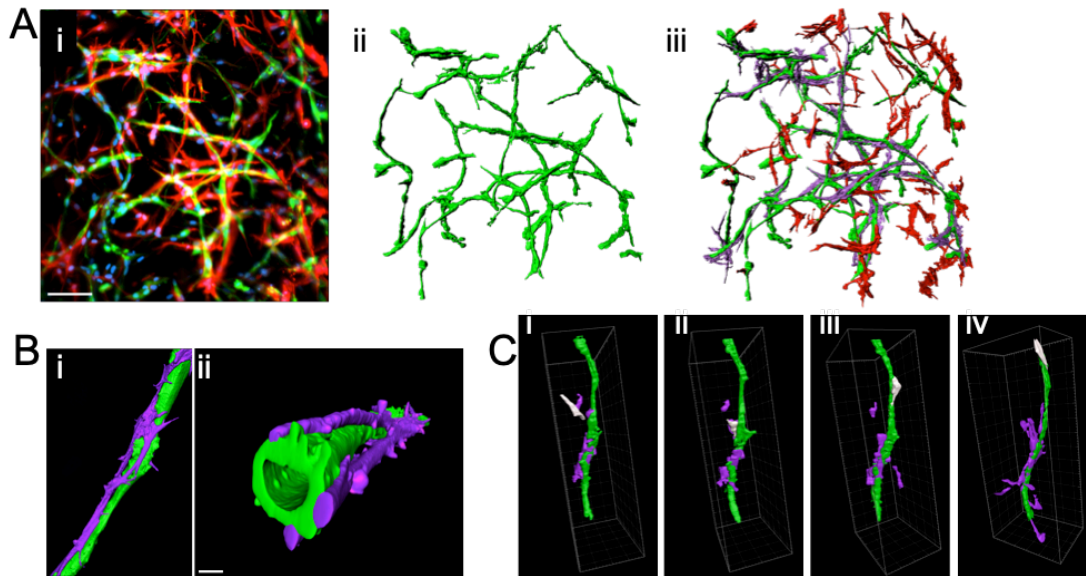


Figure 9. *In vitro* 3D angiogenesis model and perivascular recruitment. **A:** i) Endothelial cells expressing GFP (green) were co-seeded with SHED stem cells expressing LifeAct-Ruby (red) in a collagen hydrogel and cultured for 4 days for capillary formation and perivascular recruitment of stem cells at the capillary surface ii) and iii) SHED were color-coded in red when isolated, and in purple when recruited at the surface of the endothelial network. **B:** 3D reconstruction demonstrated lumen formation and **C:** time-lapse imaging every 20 minutes and cells were color-coded: endothelial cells (green), perivascular SHED (purple) and SHED being recruited and migrating along the capillary (white). Adapted from Atlas*, Gorin* et al, in preparation.

This assay is more closely related to the process of vasculogenesis as opposed to angiogenesis, which can easily be mimicked using the Cytodex bead assay (Nakatsu et al., 2007), a model in which endothelial cells are seeded at the surface of a bead and embedded in a fibrin gel in order to mimic a stable endothelium from which lumenized tubes can sprout (**see figure 9**). In both models, endothelial cells deposit collagen IV in a polarized manner (**figure 8**). These models are relevant to properly study the balance between tip cell migration, establishment of stable adherens junctions and cell-matrix adhesions, as opposed to models in which endothelial cells are only migrating and form unstable capillaries in part due to growth factors overstimulation.

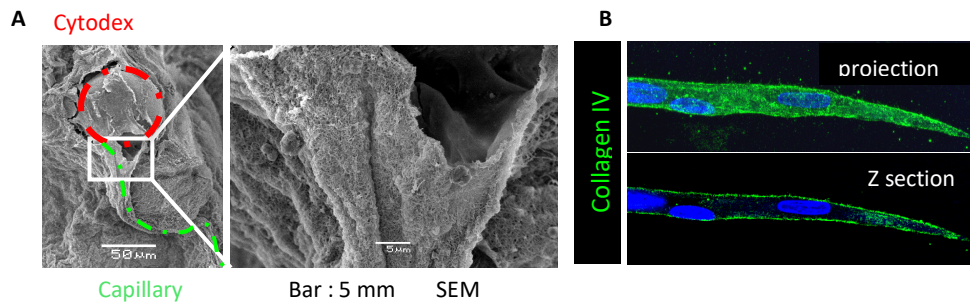


Figure 10. Main features of capillaries in an in vitro 3D model: lumen formation and basement membrane generation. A: scanning electron microscopy of a capillary embedded in fibrin. **B:** immunofluorescence and confocal imaging of collagen IV. Courtesy from Laurent Muller

Basement membrane generated by endothelial cells indeed provides them with a structural and dynamic support. It constitutes the interface between cells and interstitial ECM and is mainly composed of type IV collagen, laminins 411 and 511, fibronectin and heparan sulfate proteoglycans such as perlecan. Defects in assembly of basement membrane often results in angiogenesis defaults (Bignon et al., 2011; Zhou et al., 2008), and the functional role of these proteins and their assembly will be discussed in the next chapter.

2. Vascular microenvironment remodeling: synthesis and degradation during angiogenesis

The vascular microenvironment comprises distinct structures according to the type of blood vessel and their physiological situation, i.e. whether they are angiogenic or quiescent. It includes the vascular basement membrane, present in all blood vessels, and optionally for large blood vessels a conjunctive tissue called the elastic lamina. Finally, the interstitial ECM is surrounding these structures in all vessels (**see figure 1** in the first chapter). During angiogenesis, the vascular microenvironment undergoes an extensive remodeling characterized by synthesis of the basement membrane to support the new vessel, and degradation of the pre-existing interstitial ECM to allow cell migration and capillary morphogenesis. Both processes will be described in the present chapter, and emphasis will be placed on basement membrane formation, that has been the major focus of my work.

2.1. Interstitial ECM degradation

The extracellular microenvironment is a three-dimensional network of macromolecules that provides an architectural support and anchorage for the cells. It includes the interstitial ECM, present in all intercellular spaces and consisting of a complex meshwork of highly cross-linked proteins. Interstitial ECM composition is tissue-specific and alterations of this structure have been associated with various pathologies such as fibrosis or cancer. In 2012, Hynes and colleagues defined the genes within mouse and human genomes that encode all ECM proteins, but also proteins that interact with or modify the ECM. The resultant database was the first comprehensive *in silico* predication of the *in vivo* 'matrisome' (Naba et al., 2012). In the wall of capillaries, this interstitial ECM is mainly composed of elastin and fibrillar collagens, collagen I being by far its major component. Both display distinct functions in the vascular system, respectively elasticity and mechanical stability, as demonstrated by the phenotype of mice invalidated for the $\alpha 1$ chain of collagen I that die between E12 and E14 due to rupture of blood vessels (Löhler et al., 1984). The interstitial ECM is a dynamic structure experiencing deep remodeling during angiogenesis consisting in the degradation of its components to allow cell migration and vessel formation, as sprouting angiogenesis is an invasive process. This highly regulated remodeling, in return affects the mechanical and biochemical properties of the vascular microenvironment and regulates endothelial behavior. The ECM is indeed a reservoir of diverse molecules that can promote or inhibit angiogenesis by modulation of endothelial cell growth, proliferation, and migration. In the first step of angiogenesis, endothelial cells switch

from a quiescent to an angiogenic phenotype, inducing enzymatic degradation of the ECM. Matrix metalloproteinases (MMPs) are proteolytic enzymes that appear to be especially involved in this process. MMPs act not only by facilitating endothelial cell migration by disrupting physical barriers, but they also contribute to release growth factors or cytokines sequestered within the ECM. In a model of corneal neovascularization, it was demonstrated that MMPs can enzymatically release sequestered VEGF and induce angiogenesis (Ebrahem et al., 2010). Podosomes and invadopodia are specialized structures with ability to degrade the ECM and formation of podosomes was shown as an important step in vascular sprouting (Seano et al., 2014).

2.2. Basement membrane generation

Basement membranes are common extracellular matrices that surround the basal side of epithelial and endothelial cells. They act as support of the plasma membrane, protect tissues from mechanical stress and provide a dynamic interface between cells and the surrounding microenvironment (Yurchenco, 2011). They can also act as a physical barrier between two compartments as it is the case in the skin, where it separates the epidermis from the dermis. Another described function is the joining of two tissues through fusion of adjacent basement membranes such as the glomerular basement membrane, an original structure found between the epithelial podocytes and endothelial cells in the kidney glomerulus and that has a filtering role separating blood and urine. In this case, the adjacent basement membranes are very specified and each side differs in their structural and biochemical properties. Basement membranes are indeed highly diverse in terms of structure and molecular composition. They are packed in a dense layer but their thickness is very variable ranging from a few micrometers in the lens capsule of the eye to fifty nanometers for the endothelial basement membrane.

In capillaries, the vascular wall is limited to the basement membrane, since they lack smooth muscle cells and the associated interstitial ECM: the basement membrane alone thus provides the structural and mechanical features supporting the endothelium. It exists as a dense sheet-like structure 50 to 100 nm thick, that enwraps endothelial cells and pericytes, acting as a barrier of capillary blood vessels. The structure and physical properties of the ECM can be different according to the vascular beds, as demonstrated by scanning electron microscopy analysis of the ECM ultrastructure (**figure 11**) showing differences in basement membrane organization in the vena cava and aorta.

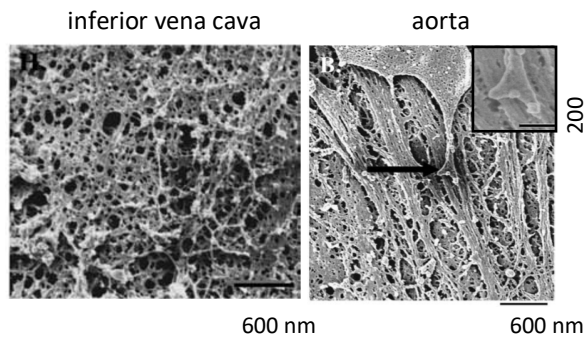


Figure 11. Ultrastructure of different vascular basement membranes. Scanning electron micrographs of endothelial cells and basement membrane in the inferior vena cava and aorta. From Liliensiek et al., 2009

The main components of capillary basement membrane are collagen IV, laminins 411 and 511, fibronectin and heparan sulfate proteoglycans (HSPG) such as perlecan or agrin. In addition to their own specific properties, their scaffolding in the basement membrane is a key process in vascular development and homeostasis. Structurally, basement membranes are composed of two overlaid networks of laminin and collagen IV, arranged parallel to the cell surface and connected together by HSPG such as perlecan and nidogen (**see figure 12**).

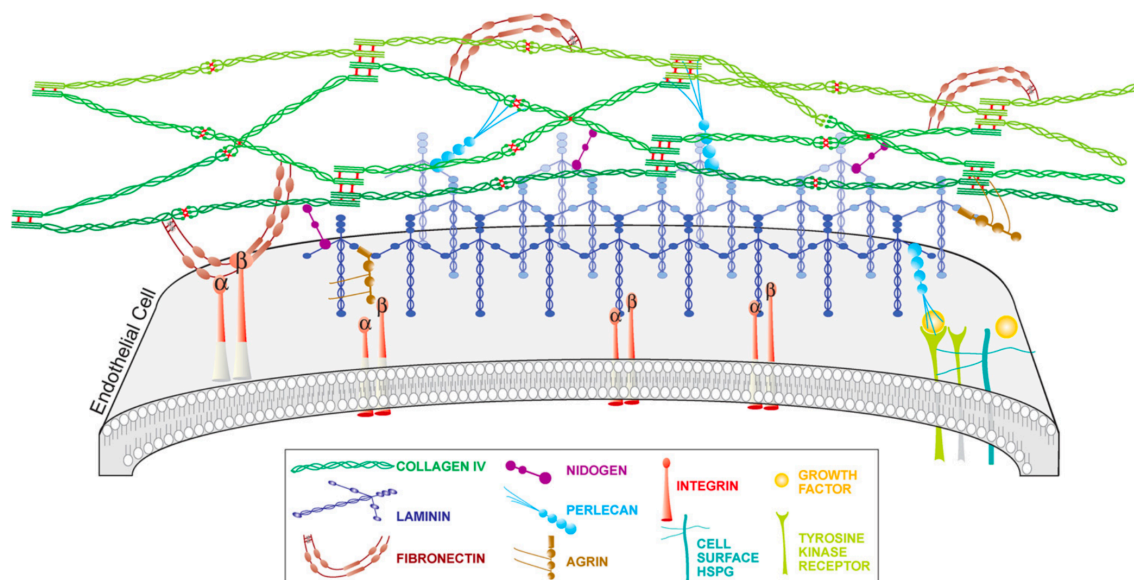


Figure 12. Polarized basement membrane in the capillary wall. From Marchand et al., 2019

A first model for basement membrane assembly proposes that laminin networks first organize into macromolecular sheets through interactions with cell surface receptors. They then support deposition of nidogen and perlecan which both participate to cross-linking the collagen IV network in order to generate the core of the basement membrane (Hohenester and Yurchenco, 2013). This “laminin-centered” vision has been questioned by the group of Billy Hudson, rather proposing that collagen IV would provide a molecular scaffold for interactions with other basement membrane components such as laminins (Brown et al., 2017). These two distinct models could be explained by the differential abundance between collagen IV and laminins

according to the tissue origin of the basement membrane. Indeed, proteomic approaches have focused on analyzing differential ratio between several components in various basement membranes and allowed to shed light on specificities regarding their localization (Uechi et al., 2014). More generally, the exact kinetics of assembly of basement membranes, including capillary basement membrane, and the succession of molecular events leading to their complex scaffolding is not well described, although tight regulation is required for angiogenesis and vascular stability. In this section, I will first describe the main proteins composing the endothelial basement membrane. Then I will detail how these supramolecular complexes assemble and organize.

2.3. Main components of the endothelial basement membrane

2.3.1. Laminins

Laminins are a family of 16 heterotrimeric ($\alpha\beta\gamma$) glycoproteins resulting from combinations of subunits encoded by 5, 4 and 3 genes, respectively (**figure 13**). Laminins 411 and 511, containing $\alpha4$ and $\alpha5$ chains combined to laminin $\beta1$ and $\gamma1$, are the predominant isoforms found in the endothelial basement membrane. Laminin 511 is strongly expressed in the basement membrane of large blood vessels, and its expression appears late in development at around 3 or 4 weeks postnatally (Sorokin et al., 1997), whereas laminin 411 is expressed at all stages in development and in all blood vessels (Thyboll et al., 2002). Mouse genetic studies have demonstrated that both isoforms are required for vessel stability (Song et al., 2017; Thyboll et al., 2002).

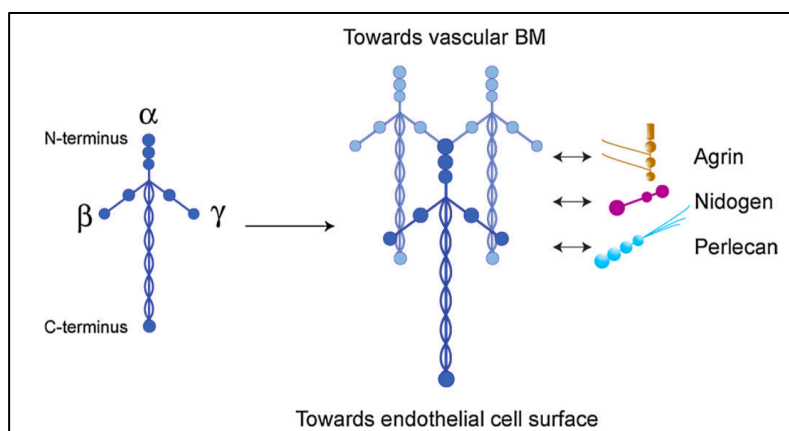


Figure 13. Organization of laminins. The C-terminal long arms are oriented towards the cell surface whereas the N-terminal short arms are oriented towards the vascular BM. The main interacting proteins are agrin, nidogen and perlecan. From Marchand et al., 2019.

Laminin $\alpha 4$ is essential for blood vessel development, indeed $\alpha 4$ knock-out mice present vascular leakage inducing hemorrhages during the embryonic and neonatal periods (Thyboll et al., 2002). Large vessels are not concerned and only capillaries are affected. $\alpha 4$ -null mice display abnormalities in the structure of basement membrane, including reduction in collagen IV deposition, suggesting that laminin $\alpha 4$ is required for the organization of collagen IV in the basement membrane. The vascular alterations of the $\alpha 4$ knock-out mice are not detected after the first weeks of life, suggesting compensation by other laminin α chains. Besides its role in basement membrane stability, $\alpha 4$ chain of laminin is involved in tip/stalk cell specification during angiogenesis. An increase in filopodia and tip cell number was indeed observed in the retina of $\alpha 4$ knock-out mice, concomitant with downregulation of Dll4 (Stenzel et al., 2011a). These results suggest that laminin could induce Dll4 expression in tip cells through integrin $\beta 1$ signaling, and thus regulate endothelial cell behavior during angiogenesis. The role of laminin $\alpha 5$ in vascular homeostasis has not been fully reported. A recent publication indicates that endothelial laminin $\alpha 5$ is essential for proper formation of focal adhesions and cortical stiffness of endothelial cells (Di Russo et al., 2017). Besides, laminin $\alpha 5$ is crucial to shear stress response by stabilizing VE-cadherin at adherens junctions, thus increasing the strength of cell-cell adhesion. In these $\alpha 5$ knock-out mice, authors also describe no effect on collagen IV and fibronectin deposition in endothelial basement membrane, suggesting that laminin $\alpha 5$ was not required for their deposition. Another study has reported the role of laminin $\alpha 5$ in regulating endothelial cell-cell junctions (Song et al., 2017). In this report, analysis of skin capillaries in mice that lack laminin 511 showed VE-cadherin disorganization, demonstrating that laminin $\alpha 5$ stabilizes endothelial junctions. The role of both laminin 411 and 511 isoforms has also been described *in vitro* using the Cytodex bead assay, an angiogenesis model already presented in the first part of the manuscript and useful to study basement membrane deposition by endothelial cells (**figure 10**). In this model, authors show that endothelial cells deposit laminin $\alpha 4$ and $\alpha 5$ and that invalidation of each subunit using siRNA decreased vascular morphogenesis (Xu et al., 2020). Interestingly, laminin $\alpha 5$ deletion had a stronger effect on capillary formation, as compared to laminin $\alpha 4$ deletion, and they did not compensate for one another, suggesting that both isoforms play distinct roles in this process.

2.3.2. Collagen IV

Type IV collagen is the most abundant component of the endothelial basement membrane. Collagen IV comprises six distinct α chains from $\alpha 1$ to $\alpha 6$ that assemble with a great specificity to form only three heterotrimers $\alpha 1\alpha 1\alpha 2$, $\alpha 3\alpha 4\alpha 4$ and $\alpha 5\alpha 5\alpha 6$. $\alpha 1\alpha 1\alpha 2$ is the predominant one in all tissues including the vascular basement membrane. In the glomerular basement

membrane of the kidney, collagen IV $\alpha1\alpha1\alpha2$ protomers produced by the endothelial cells form a network closely juxtaposed to the endothelium, whereas $\alpha3\alpha4\alpha5$ protomers secreted only by epithelial podocytes are tightly attached to the $\alpha1\alpha1\alpha2$ network (Suleiman et al., 2013).

The α chains are approximately 400 nm long and are composed of three domains: a short N-terminal 7S domain, a long middle triple helical collagenous domain, and a C-terminal globular non-collagenous NC1 domain. Assembly of collagen IV heterotrimers is initiated intracellularly by interactions between the NC1 globular domain of three α chains leading to formation of a heterotrimeric protomer. After secretion of the triple-helical protomers, both the 7S and NC1 domains are responsible for the assembly of the networks. Two collagen IV protomers associate through their C-terminal NC1 domains and 7S domains of four protomers associate at their N-terminal domains. In parallel, lateral associations between these assembled molecules form an elaborate supramolecular scaffold and allow formation of the complex mesh network of collagen IV. This mesh organization is a peculiar feature that distinguishes collagen IV from fibrillar collagens such as collagen I, and results from the presence of more than 20 interruptions in the Gly-X-Y motifs present in the central collagenous domain of type IV collagen. Besides, unlike collagen I, the NC1 and 7S domains are not cleaved from the molecule but rather initiate assembly and contribute to its cross-linking. These two major features provide structural flexibility to the molecule and allow mesh-like organization in the basement membrane.

Biosynthesis and secretion of collagen IV requires post-translational modifications including hydroxylation of lysine and proline residues, and is highly dependent on specific molecular chaperone proteins such as Hsp47 or Tango1 (Marutani et al., 2004; Wilson et al., 2011). They ensure proper collagen IV protomer assembly in the endoplasmic reticulum and transit to the cis-Golgi while preventing aberrant aggregation. A similar mechanism has been previously proposed with other ECM proteins such as SPARC, that associate with collagen IV prior to secretion and could thus act as a late chaperone for proper collagen IV secretion (Chioran et al., 2017; Duncan et al., 2020).

Collagen IV assembly is stabilized by specific cross-linking enzymes including peroxidase and lysyl oxidases (LOXs). Peroxidase has been described to cross-link collagen IV through formation of sulfilimine bonds between a methionine sulfur and a lysin nitrogen of the NC1 domains, thus stabilizing the hexameric structure of collagen IV C-terminus (Bhave et al., 2012) (**figure 14**). Cross-linking by peroxidase is responsible for mechanical resistance in the collagen IV molecule as demonstrated by the phenotype of the peroxidase knock-out mice that display reduced stiffness of the renal tubular basement membrane (Bhave et al., 2017).

This is however not sufficient to result in a vascular phenotype in these mice. *In vitro* peroxidase knock-down in endothelial cells resulted in the inhibition of ECM assembly of not only collagen IV but also laminin and fibronectin, suggesting that collagen IV network serves as scaffolds for the assembly of fibronectin and laminin (Lee et al., 2020). Peroxidase was also required for FAK and ERK phosphorylation in endothelial cells, thus demonstrating that proper ECM scaffolding is important for ECM-mediated signaling.

LOXs are secreted copper-containing amine oxidases that catalyze the oxidative deamination of lysine residues in collagens to generate semi-aldehyde known as allysines. These highly reactive groups then undergo spontaneous associations resulting in collagen cross-linking. LOX enzymes thus do not directly cross-link collagens but catalyze the last step required for this process. Even though lysyl oxidase-mediated cross-links have been identified in collagen IV for quite a while (Bailey et al., 1984), we have shown that LOXL2-depletion in endothelial cells results in defects in collagen IV deposition and cross-linking in the ECM (Bignon et al., 2011). More recently, cross-linking of the 7S domain of collagen IV by LOXL2 was demonstrated (Añazco et al., 2016).

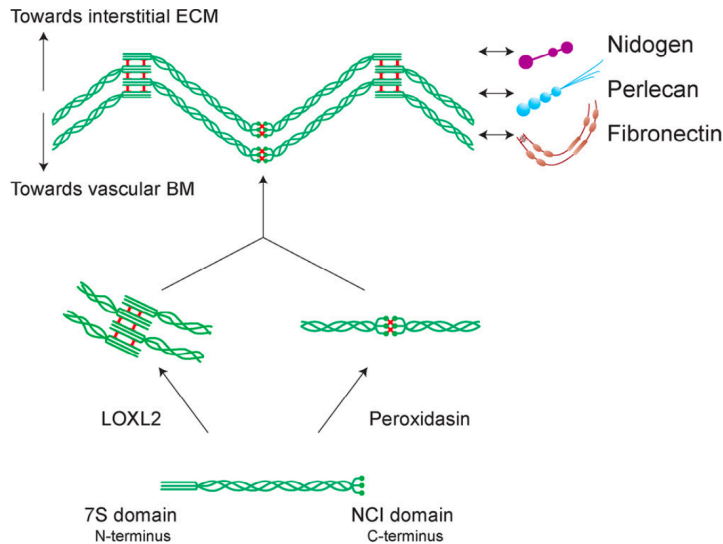


Figure 14. Organization of collagen IV the vascular basement membrane. The NC1 domains crosslinked by the peroxidase enzyme are oriented towards the laminin network. The 7S domains crosslinked after deamination of lysine residues by LOXL2 are oriented towards the interstitial ECM. 7S and NC1 crosslinks are indicated in red. From Marchand et al., 2019.

Interestingly, collagen IV networks display a highly oriented macromolecular organization in the basement membrane. Recent studies have indeed reported a polarized distribution of collagen IV trimers as the N- and C-terminal domains are localized at opposite sides of the basement membrane: the 7S domain is detected at the stromal side whereas the NC1 domain

colocalizes with laminin towards the cell surface, at the stiffer side of the basement membrane (Halfter et al., 2013). This suggests that collagen IV could be organized in such a way that the protein extends throughout the entire width of the basement membrane thus questioning the former horizontal model of organization of collagen IV molecules and also fundamentally questioning the functional role for this organization. These data have been obtained by studying the glomerular basement membrane, a structure that is quite thick (approximately 400nm). Such organization has however never been described in the endothelial one, although collagen IV polarization could be an extracellular cue differentially regulating endothelial cell behavior.

Collagen IV assembly is required for vascular development and homeostasis. Double deletion of Col4a1 and Col4a2 results in embryonic death at E10.5. Embryos display dilated and fragile blood vessels and show many hemorrhages, especially in the brain where capillaries are reduced and perturbed, even though development of large vessels is not affected by the deletion (Pöschl et al., 2004). In accordance with these results, our team showed that downregulating collagen IV in endothelial cells affected capillary formation in a 3D angiogenesis model (Bignon et al., 2011). Collagen IV is however not critically needed for the formation of basement membranes, since deposition of laminin and nidogen was not affected by the absence of collagen IV, supporting the hypothesis that these other components could compensate for collagen IV absence in some basement membranes (Pöschl et al., 2004). Collagen IV is nevertheless crucial for blood vessel integrity at later stages, when mechanical demand is triggered by establishment of blood perfusion. The association of mutations in collagen IV with defects in capillary formation and vessel integrity in human pathologies confirmed these experimental results (Gould et al., 2006; Plaisier et al., 2007). Mutations in collagen IV $\alpha 1$ and $\alpha 2$ were found to cause porencephaly and HANAC syndrome, diseases characterized by intracranial hemorrhages and associated with small-vessel disease. Perturbations of the matrisome of cerebral blood vessels is a possible cause in these pathologies (Joutel et al., 2016).

2.3.4. Fibronectin

Fibronectin is a ubiquitous high molecular weight glycoprotein composed of two subunits linked together through disulfide bonds. Although it is not a specific component of basement membranes, and was even described as absent from certain basement membranes (Halfter et al., 2013), fibronectin is highly expressed in endothelial cells, and used a marker for blood vessels (Bignon et al., 2011; Gerhardt, 2003). Fibronectin is indeed expressed around early

Fibronectin is assembled into a fibrillar matrix in all tissues through a multistep process called fibrillogenesis that is initiated by binding to its major receptor, integrin $\alpha 5\beta 1$. Fibronectin binding induces receptor clustering, providing local high concentrations of fibronectin at the cell surface and thus promoting fibrillogenesis. However, other ECM proteins have been involved in promoting fibronectin fibrillogenesis, such as proteoglycans (Chung and Erickson, 1997) transglutaminase-2 (Akimov and Belkin, 2001) or tenascin-C (Radwanska et al., 2017). Consistent with these results, it has been demonstrated that some fibronectin matrix can be assembled in the absence of RGD- $\alpha 5\beta 1$ integrin interaction (Ichihara-Tanaka et al., 1992; Sechler et al., 1996). More recently, it was described that fibronectin fibrillogenesis is a cell-autonomous process in endothelial cells, that requires endogenous production of fibronectin, demonstrated by the fact that adding soluble fibronectin to fibronectin-depleted cells did not restore fibrillogenesis (Cseh et al., 2010). Cells seeded on a fibronectin coating were nevertheless able to assemble exogenously added soluble fibronectin, suggesting that the nature of the substrate can play a permissive role in fibronectin assembly. Although the fibronectin deposited by cells plated on a coated substrate did not seem different from *de novo* fibronectin at the cell scale, there is no further data about the impact of coating on fibronectin fibrillogenesis at the molecular scale. Recently, the team of Yamada has described promoting effects of basement membrane proteins coating on fibronectin organization by cells (Lu et al., 2020). Indeed, fibronectin deposition was greatly enhanced when cells were plated on collagen IV compared to laminin coating, suggesting preferential interactions between fibronectin and collagen IV. Importantly, and as already described (Cseh et al., 2010), direct interactions between coated proteins and cells were necessary to induce fibronectin deposition, as addition of soluble proteins did not recapitulate the effects on fibronectin organization. Furthermore, basement membrane coating (mimicked using Matrigel) promoted fibronectin deposition by enhancing capacity of cells to assemble fibronectin and not by enhancing fibronectin expression or secretion by cells. All these studies demonstrate that fibronectin assembly is an autocrine process that can be influenced by the substrate through direct interactions between these macromolecular complexes. Interestingly, the same mechanism has been reported with collagen IV remodeling. A recent study has demonstrated that synthetic polymers coated with basement membrane proteins such as fibronectin or laminin could modulate ECM defects due to mutations in collagen IV in fibroblasts (Ngandu Mpoyi et al., 2020). Coated substrates also rescued the reduced stiffness and organization of the deposited matrix by mutant cells. However, no ultrastructural analysis of the basement membrane deposition upon coating was provided in this study.

Interestingly, recent studies demonstrated that disruption of fibronectin fibrillogenesis in cultured cells using the Functional Upstream Domain (FUD) peptide that inhibits fibronectin assembly, disrupted the incorporation of collagen IV and laminin into the ECM (Filla et al., 2017; Miller et al., 2014). In the more recent paper, when authors add FUD after several days of culture, i.e. once the ECM was more established, collagen IV and laminin did not require pre-existing fibronectin fibrils and could be assembled into large macromolecular complexes. This suggested that fibronectin fibrils initially act as organizing centers that allows nascent ECM formation, whereas mature ECM assembly rather seems to be fibronectin-independent. Interestingly, the team of Viola Vogel designed a fibronectin-FRET probe that acts as a strain sensor in the ECM, thus providing unique information on fibronectin mechanical state (Kubow et al., 2015; Smith et al., 2007). Authors showed that tension across fibronectin molecule is able to regulate its interaction with collagen I fibers in the ECM. Indeed, relaxed fibronectin preferentially co-localizes with collagen I. Once assembled, collagen fibers inhibit the ability of fibroblasts to further stretch the matrix, and mechanically become the tension-bearing components in the ECM. These data provide evidence of a reciprocal mechano-regulation among ECM structural proteins that directs hierarchical assembly of the ECM.

Many studies provide evidence for a major role of fibronectin in vascular development. Invalidation of FN1 gene in mice leads to embryonic lethality at E8.5 with severe cardiovascular defects including defects in the embryonic vasculature and aberrant organization of vessels in the yolk sac (George et al., 1993). Endothelial-specific deletion of fibronectin postnatally results in abnormal patterning of the retinal vasculature and mice develop vascular defects despite the presence of exogenous fibronectin secreted by other cell types in the retina (Turner et al., 2017). *In vitro* studies also demonstrated that fibronectin assembly regulates endothelial cell capillary morphogenesis in 3D models (Zhou et al., 2008) or capillary-like tube formation on Matrigel (Cseh et al., 2010). Fibronectin fibrillogenesis also promotes junctional stability for endothelial cells (Cseh et al., 2010). It is likely that fibronectin fibrillogenesis acts through direct effects on endothelial cells by promoting cell adhesion and focal adhesion maturation, and also through indirect effects by providing structural support for deposition of other matrix proteins such as collagens and thus regulate endothelial cell behavior. This hypothesis is supported by the fact that during mouse retina vascularization, filopodia of tip cells extend along the fibronectin network deposited by astrocytes before angiogenesis, suggesting that this primary network supports angiogenesis (Bignon et al., 2011). Vascular guidance by fibronectin secreted by astrocytes was indeed showed to promote the directional migration of tip cells and adhesion of filopodia (Stenzel et al., 2011b).

3. LOXL2, actor of vascular ECM remodeling

3.1. Lysyl oxidase family of proteins

Lysyl oxidases are secreted copper-dependent enzymes that oxidize primary amine groups of lysines and hydroxylysines in collagens and elastin into reactive aldehydes. The highly reactive allysines produced undergo spontaneous association with other lysyl-oxidase derived aldehydes, or with non-modified lysine residues, resulting in cross-linking of the proteins. Deamination by LOX enzymes is an essential step in collagen and elastin assembly and is thus required for the structural integrity of the ECM in various tissues (Moon et al., 2014). The family comprises five members in mammals including LOX and four lysyl oxidase-like proteins (LOXL1 to LOXL4). They are composed of a conserved C-terminal catalytic domain that contains a lysine tyrosylquinone cofactor (LTQ) and a copper binding site, and a variable N-terminal region (**figure 16**). The family is subdivided into two groups regarding the degree of conservation of the catalytic domain and the structure of the N-terminal domains (Moon et al., 2014).

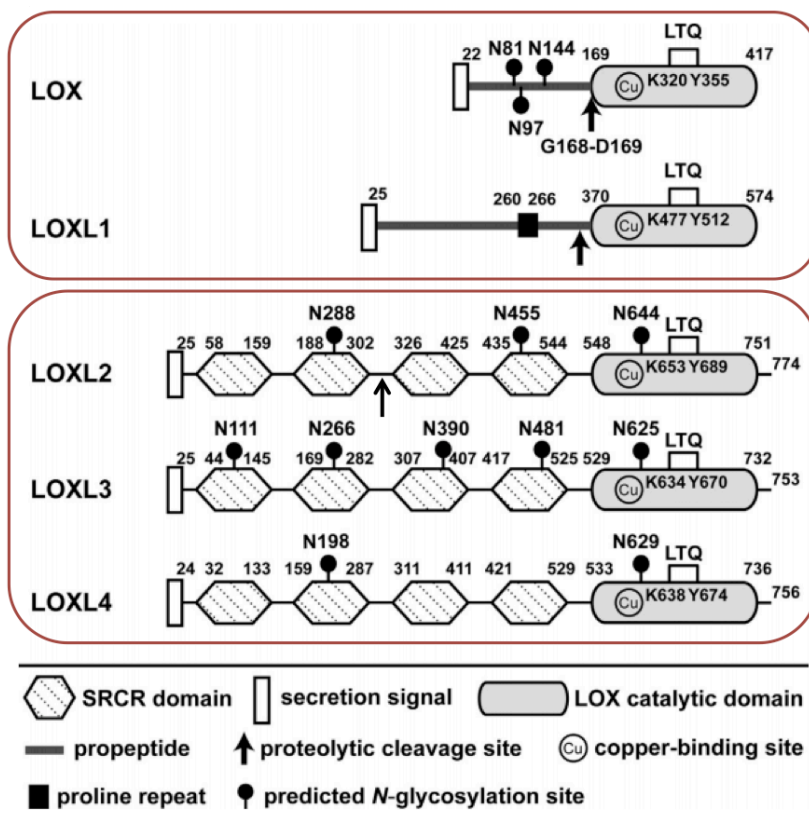


Figure 16. Structure of the lysyl oxidase family members. From Moon et al., 2014.

LOX and LOXL1 share 88% similarity in the catalytic domain, suggesting common substrates, and have N-terminal domains that are proteolytically cleaved by Bone Morphogenetic Protein-1 (BMP1), a procollagen C-proteinase, in order to generate the enzymatically active proteins (**figure 16**). Whereas LOXL2-4 catalytic domains also share 86 to 88% similarity, they only have 64 to 68% similarity with LOX and LOXL1 catalytic domains. LOXL2-4 share an extension of 20-23 amino acids beyond their catalytic domain, and a common specific structure of their N-terminal part consisting in 4 scavenger receptor cysteine rich (SRCR) domains (**figure 16**) whose function is not clear yet. Unlike LOX and LOXL1, LOXL2 N-terminal domain is not entirely cleaved off from the catalytic domain but rather split in two between SRCR2 and SRCR3. Whereas this processing by extracellular serine proteases is not required for activation of its oxidase activity (Okada et al., 2018), it is necessary for LOXL2 to oxidize and cross-link type IV collagen (López-Jiménez et al., 2017). Crystal structure of a truncated inactive recombinant LOXL2 was reported and demonstrated that SRCR4 is the only SRCR domain interacting with the catalytic domain (Zhang et al., 2018). Our SAXS and electron microscopy analyses confirmed this observation and revealed that SRCR domains are organized in a string of pearl way, supporting the processing and release of SRCR1 and SRCR2 domains and suggesting own independent activity of these domains (Schmelzer et al., 2019) (**and see appendix 1**).

Concerning their tissue distribution, expression of LOX and LOXL1 overlap in many tissues including heart, lung, kidney and skin. In contrast, high LOXL2 mRNA levels were found in reproductive tissues such as prostate, uterus and placenta. Immunohistochemistry analyses on various organs showed a general distribution of LOX and LOXL1 in regions presenting fibrillar collagens, whereas LOXL2 was detected in regions presenting type IV collagen and elastin (Csiszar, 2001), suggesting the specificity of LOX family members for distinct substrates. Such complementary distribution was described and well-illustrated in the skin where LOX is expressed in the dermis, while LOXL2 was detected in the basement membrane of the dermal-epidermal junction and of blood vessels (Fujimoto and Tajima, 2009).

In accordance with this pattern of expression, mice invalidated for LOX die at birth due to ruptured aneurysms in the aorta, suggesting a critical weakness in the tensile strength of this collagen-rich tissue. Analysis of collagen I and elastic fibers architecture in knock-out mice demonstrated a loose, diffuse and fragmented organization (Hornstra et al., 2003; Maki, 2002), whereas no change in endothelial basement membrane arrangement was observed (Mäki et al., 2005). Besides, invalidation of LOXL1 in mice leads to impaired deposition of elastin in various tissues, and accumulation of tropoelastin generating vascular abnormalities, with no effect in collagen I cross-linking. These data show that LOX has an essential role in both collagen I and elastin cross-linking, whereas LOXL1 specifically cross-links elastin. As for LOXL2, gene deletion in mice results either in partial embryonic lethality or defects in development of the cardiovascular system, (Martin et al., 2015) or in complete embryonic lethality (Steppan et al., 2019). These studies however did not investigate the potential substrates involved. Unlike LOX and LOXL1, isolation and purification of LOXL2 was made possible and enabled to conduct *in vitro* studies in order to identify substrates for this enzyme.

3.2. LOXL2 substrates

As already mentioned, LOXL2 expression was associated with basement membranes (Csiszar, 2001; Fujimoto and Tajima, 2009) suggesting that collagen IV could be a preferential substrate of this enzyme. Consistent with these observations, our team demonstrated that LOXL2 colocalizes with type IV collagen in the retina of newborn rats, and regulates collagen IV organization in the ECM of endothelial cells. Interestingly, inhibition of lysyl oxidase activity using β -APN increased the amount of collagen IV solubilized from the ECM, suggesting involvement of LOXL2 catalytic activity in this process (Bignon et al., 2011). Direct evidence for collagen IV cross-linking by LOXL2 was indeed demonstrated in the glomerular basement membrane (Añazco et al., 2016). Besides its role in collagen IV cross-linking, LOXL2 is also involved in cross-linking interstitial ECM proteins such as elastin and collagen I. Using mass spectrometry analysis and cross-linked peptide identification, our team has recently demonstrated for the first time the direct involvement of LOXL2 in elastin cross-linking (Schmelzer et al., 2019) (**and see appendix 1**). In addition, *in vitro* use of a LOXL2-specific inhibitor, PXS-5153A, dose-dependently reduced oxidation and cross-linking of collagen I, directly demonstrating that collagen I is a substrate for LOXL2 (Schilter et al., 2019). Recent unpublished data from our group also aimed to better characterize LOXL2-generated cross-links in collagen I (Bidault et al, en preparation) (**see appendix 2**). We indeed demonstrated that human recombinant LOXL2 modulated the structural and mechanical properties of

collagen fibers in hydrogels and we were able to identify specific cross-linked peptides in collagen I telopeptides using mass spectrometry.

In addition to extracellular matrix proteins, recent works have documented deamination by LOXL2 of a cell surface receptor, namely PDGF-R β (Mahjour et al., 2019) and of the nuclear protein histone H3 (Herranz et al., 2016). It is proposed that the ligand PDGF-AB is secreted together with LOXL2 by tumor cells and activates PDGFR β in fibroblasts to promote their proliferation via activation of the ERK1/2 signaling pathway (Mahjour et al., 2019). The intracellular activity of LOXL2 and its consequences on histone deamination and gene transcription will be discussed below.

Altogether, these results demonstrate that LOXL2 cross-links type IV collagen of the basement membrane, as well as ECM interstitial components including collagen I and elastin. This diversity of substrates thus questions the distribution of LOXL2 in the microenvironment, which could be at the interface between basement membrane and interstitial ECM in various tissues.

3.3. Pathological role of LOXL2 and associated mechanisms

Dysregulation of LOXL2 levels has been linked to several pathological conditions, including fibrosis and cancer, as well as cardiovascular pathologies. While perturbations in the function of LOXL2 in ECM remodeling was responsible for generating a pathological microenvironment in fibrosis and cancer (Barry-Hamilton et al., 2010), other unexpected functions of this enzyme were identified in the course of investigation of tumor growth and dissemination. Possible mechanisms and biological activities that have also been proposed include intracellular effects of LOXL2 targeting activation of the FAK/Src signaling pathway, induction of EMT and regulation of gene transcription, and will be further discussed in this section.

3.3.1. Implication of LOXL2 in fibrosis via ECM remodeling

Fibrosis is a dysfunctional response to tissue injury associated with abnormal ECM deposition and progressive loss of tissue function. This pathological state involves multiple cell types, including fibroblasts and myofibroblasts but also other regulators such as growth factors or cytokines in the 3D environment. The involvement of LOXL2 has been demonstrated in multiple fibrotic tissues, including cardiac interstitial fibrosis (Yang et al., 2016), pulmonary fibrosis (Barry-Hamilton et al, 2010; Aumiller et al, 2017; Jones et al., 2018), renal (Cosgrove et al., 2018), and liver fibrosis (Barry-Hamilton et al., 2010; Ikenaga et al., 2017; Klepfish et al.,

2020; Schilter et al., 2019; Vadasz et al., 2005). In these studies, genetic deletion (Yang et al., 2016) or pharmacological inhibition of LOXL2 (Barry-Hamilton et al., 2010; Jones et al., 2018; Schilter et al., 2019; Cosgrove et al., 2018) reduced fibrosis and improved overall tissue function. More precisely, inhibition of LOXL2 was sufficient to decrease the collagen amount and cross-links (Barry-Hamilton et al., 2010; Ikenaga et al., 2017; Schilter et al., 2019). A recent study demonstrated that dysregulation of collagen cross-linking resulted in abnormal fibers at the nanometer scale and was more responsible for ECM stiffening than an increase in collagen concentration (Jones et al., 2018). These authors also demonstrated that LOXL2 inhibition reduced hydroxyallysine-derived collagen cross-links and normalized collagen fibrillogenesis, thus reducing tissue stiffness and improving lung function (Jones et al., 2018). In addition to direct ECM remodeling, LOXL2 inhibition also results in decreased differentiation of cells into more fibrogenic phenotypes (Aumiller et al., 2017; Ikenaga et al., 2017; Yang et al., 2016) or in increased amounts of cells involved in ECM degradation like monocyte-derived macrophages (Klepfish et al., 2020). Overall, these studies support the initial hypothesis that LOXL2 secreted by stromal cells mediates fibroblast activation through ECM remodeling and local stiffness increase, and thus amplifies fibrosis establishment (Barry-Hamilton et al., 2010).

3.3.2. Implication of LOXL2 in cancer progression

A large number of studies have documented increased expression of LOXL2 in many different human cancers including breast, laryngeal, lung, gastric or liver cancers (Ye et al., 2020). Furthermore, inhibition of LOXL2 expression was always shown to decrease tumor growth, invasiveness properties of cancer cells and metastasis dissemination. However, multiple mechanisms for LOXL2 regulation of cancer progression are currently being investigated and give a rather complex overview. Independently of the cancer type and localization, extracellular and intracellular roles for LOXL2 have been described to explain its oncogenic functions (Moon et al., 2014). These distinct propositions will be further discussed in this section.

A/ Cancer and ECM remodeling by LOXL2

LOXL2-mediated ECM remodeling

One of the major hypotheses concerns an extracellular role for LOXL2 in establishment and maintenance of a pathological microenvironment (Barry-Hamilton et al., 2010). The latter study was the first description of a previously unknown role for LOXL2 in ECM remodeling during cancer progression. In different *in vivo* cancer models, targeting LOXL2 with an inhibitory monoclonal antibody reduced primary tumor and metastasis by decreasing cross-linked

collagenous matrix and production of growth factors, thereby targeting the suitable microenvironment for tumor growth and metastasis (Barry-Hamilton et al., 2010). Other studies have since then confirmed a strong correlation between LOXL2 expression, increased collagen deposition and change in the ECM architecture in various cancers (Peng et al., 2017; Saito et al., 2019; Zhou et al., 2017). Besides collagen, other extracellular actors such as fibronectin and MMP, including MT1-MMP and MMP9, play a role in LOXL2-mediated tumor progression (Barker et al., 2011; Moon et al., 2013; Wu et al., 2018a). These effects in ECM remodeling by LOXL2 impact the cytoskeletal reorganization of cancers cells, as demonstrated by enhanced phosphorylation of myosin light chain kinase in hepatocellular carcinomas (Wong et al., 2014). Furthermore, in the context of lung cancer, LOXL2 secreted by tumor cells induced fibronectin deposition by lung fibroblasts, thus promoting the formation of the pre-metastatic niche and enabling tumor progression (Wu et al., 2018a).

Until recently, only correlation between LOXL2 expression and ECM deposition was demonstrated in cancer microenvironment. It was therefore unclear whether the effects of LOXL2 were due to a change in ECM organization or in its composition. A recent study described for the first time the effects of LOXL2 on ECM ultrastructural properties at the fiber level in the context of triple-negative breast cancer (Grossman et al., 2016). Inhibition of LOXL2 had no impact on ECM composition, but decreased the number of cross-links and deeply changed the orientation and thickness of the collagen fibers. The resulting anisotropic fibril organization was responsible for alteration in cancer cell invasion properties. In a 3D spheroid assay, inhibition of LOXL2 locally impacted collagen alignment and subsequent cancer cell migration (Grossman et al., 2016). This study thus clearly demonstrates a tight regulation of ECM structural properties by LOXL2 in tumor and suggests that changes in local stiffness sensed by cancer cells influence their invasive behavior.

LOXL2 as a paracrine factor regulating cancer microenvironment

Identifying the source of extracellular LOXL2 in the microenvironment is a major challenge to address its effects on ECM remodeling. The tumor microenvironment is composed of many actors, and both tumoral and stromal cells such as cancer-associated fibroblasts (CAFs) have been shown to express high levels of LOXL2 in different cancers (Ye et al., 2020). In a recent study, pharmacological inhibition of LOXL2 in CAFs disorganized the ECM and decreased migration of co-cultured prostate tumor cells (Nguyen et al., 2019). These data indicate that CAF-secreted LOXL2 could be an important mediator of intercellular communication within the tumor microenvironment. At the opposite, LOXL2 secreted by tumor cells reciprocally activates stromal fibroblasts in the context of breast (Barker et al., 2013) and oral squamous cell carcinoma (Mahjour et al., 2019). In the latter study, LOXL2 was secreted together with PDGF-

AB by tumor cells, and was able to trans-activate PDGFR β in stromal fibroblasts to promote their activation. Similarly, LOXL2 produced by breast cancer cells increased fibroblast-mediated collagen contraction and invasion through the ECM via activation of integrin/FAK signaling pathway in stromal fibroblasts (Barker et al., 2013). Overall, these data suggest an important role for LOXL2 as a paracrine signal capable of acting *in trans* through ECM remodeling, thereby promoting maintenance of a permissive local niche.

LOXL2-mediated FAK/Src signaling

It is likely that LOXL2-mediated ECM remodeling promotes activation of various signaling pathways regulating tumor cells proliferation and migration, such as the FAK/Src signaling pathway in CAFs (Barker et al., 2013), but also in RCC cell lines (Hong and Yu, 2019), which can be regulated through both extra- and intracellular signals. Extracellular inhibition of LOXL2 in gastric tumors from patients downregulated the Src/FAK signaling pathway, decreasing tumor growth and metastases (Peng et al., 2009). Another autocrine role for LOXL2 has been described in the context of lung tumors, where secreted LOXL2 induced FAK activation through collagen reorganization. In addition, LOXL2 overexpression alone had no effect on migration and invasion unless extrinsic collagen was introduced, also supporting the fact that LOXL2 acts extracellularly in this context (Peng et al., 2017) (**and see figure 17**). Additional data rather suggest that intracellular LOXL2 directly modulates FAK and other signaling pathways in tumor cells, as previously described concerning LOX-mediated activation of FAK in breast cancer (Erler and Giaccia, 2006). Similarly, treatment with catalase reduced intracellular levels of H₂O₂ and thus inhibited LOXL2-mediated phosphorylation of ErbB2 in cancer cells (Chang et al., 2013). Other mediators of intracellular LOXL2 involved in cytoskeleton remodeling include MARCKSL1, which regulate the FAK signaling pathway in breast cancer cells (Kim et al., 2014), and ezrin, whose phosphorylation is regulated by LOXL2 (Zhan et al., 2019).

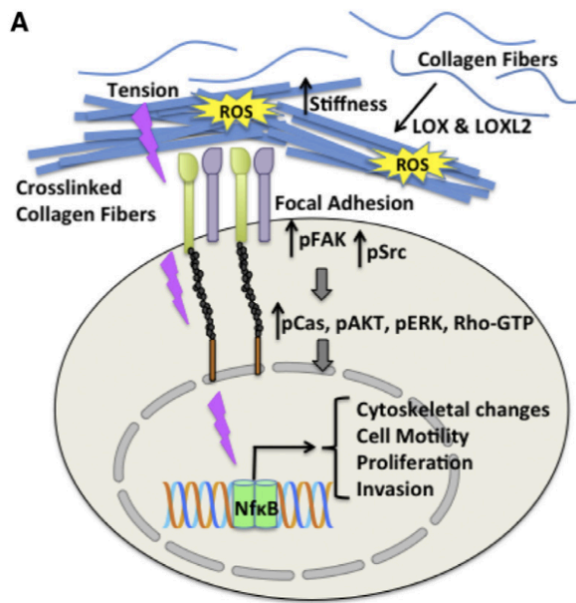


Figure 17. Proposed mechanism for FAK activation by secreted LOXL2. LOXL2 induces ECM stiffening to activate oncogenic signaling pathways including FAK/Src. From [Moon et al., 2014](#).

B/ Cancer and intracellular role of LOXL2

Recent findings suggest an intracellular role for LOXL2 in cancer progression and metastasis through multiple mechanisms including deamination of histone H3, induction of epithelial-to-mesenchymal transition (EMT), ER-stress activation and regulation of cell polarity.

LOXL2 acts intracellularly to regulate EMT

EMT is an important process in tumor progression as it allows epithelial cells to lose their cell-cell adhesions and to acquire invasive properties (**see figure 18**). A previous report demonstrated that LOXL2 intracellularly interacts and cooperates with Snail1, a key EMT transcription factor, to downregulate E-cadherin expression and induce an invasive behavior in cancer cells (Peinado et al., 2005). This study was the first to shed light on potential intracellular effects of LOXL2 in cancer progression. Using expression of LOXL2 catalytically inactive mutants in cancer cells, it was demonstrated that LOXL2 enzymatic activity was not required for the induction of EMT mediated by Snail1 (Cuevas et al., 2014), suggesting that the SRCR domains of the protein can mediate this process.

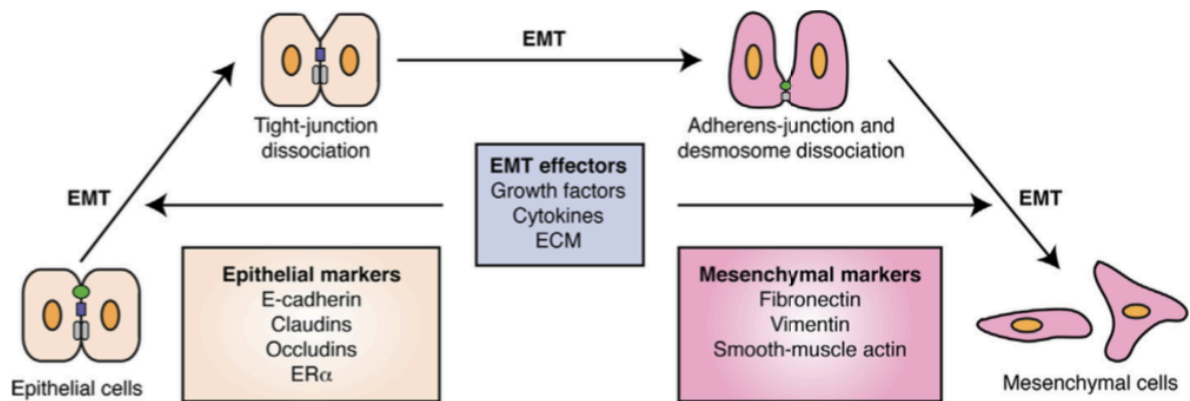


Figure 18. Epithelial-to-mesenchymal transition process. EMT is a process in which epithelial cells are transformed into mesenchymal cells. Cells downregulate adherens junctions and cell polarity proteins and upregulate proteins involved in migration and invasion. From Moon et al., 2014.

Existence of a balance between intra- and extracellular roles of LOXL2 in EMT

This latter study was already raising the possibility of a balance between intra- and extracellular LOXL2 levels in the regulation of EMT. Authors reported that intracellular LOXL2 alone was sufficient to activate FAK in cancer cells, and that induction of EMT thus resulted from indirect intracellular mechanisms (Cuevas et al., 2014). Similarly, another approach consisted in expressing recombinant mutant LOXL2 that could or could not be secreted (Moon et al., 2013). This study reported that intracellular nuclear-associated LOXL2 stabilized Snail1 and induced EMT, whereas cells expressing only the secreted form of LOXL2 kept their epithelial phenotype and showed lower invasive properties, suggesting that only intracellular LOXL2 could mediate this process. These experiments have however been conducted *in vitro* using 2D Matrigel invasion assays, and suggested that EMT regulation by secreted LOXL2 may require a more complex microenvironment involving 3D interactions between LOXL2 and ECM structural proteins to support invasion by cancer cells. Another report clearly demonstrated that intra- and extracellular mechanisms are independent and complementary to induce an invasive phenotype in cancer cells (Peng et al., 2009). While intracellular LOXL2 induced downregulation of E-cadherin via Snail1 activation, secreted LOXL2 was required for FAK/Src activation, therefore potentiating adhesion and invasion of gastric cancer cells (**and see figure 17**).

LOXL2 intracellularly regulates EMT through multiple pathways

A more precise mechanism has recently been proposed to clarify the intracellular role of LOXL2 in EMT. LOXL2 activity is actually involved in oxidation of lysine 4 of histone H3, and thus contributes to cancer progression by affecting transcription of key genes involved in tumorigenesis (Herranz et al., 2016) (**and see figure 19**). Loss of LOXL2 in cancer cells was proved to reduce histone oxidation, therefore modifying chromatin architecture and limiting the EMT process (Millanes-Romero et al., 2013). Furthermore, this genome reorganization by LOXL2 was able to increase chemosensitivity of cancer cells, thus opening new insights into potential therapeutic tools to overcome resistance to cancer treatments (Cebrià-Costa et al., 2020).

In addition to its effects on chromatin regulation, the same laboratory that firstly identified intracellular LOXL2 as a regulator of EMT (Peinado et al., 2005) recently reported a new and original mechanism where overexpression of LOXL2 promotes its accumulation in the endoplasmic reticulum (ER), leading to activation of the IRE1-XBP1 pathway involved in ER-stress response (Cuevas et al., 2017). This activation could trigger the expression of several EMT transcription factors and be responsible for the induction of EMT phenotype in cancer cells. The newly proposed ER-stress regulation suggested that misfolding of LOXL2 and subsequent retention in the ER could be an important feature in establishment of EMT and that previously described intracellular accumulation of LOXL2 could be mediated by such process. This hypothesis thus seems promising and should be considered when studying effects of intracellular LOXL2.

Intracellular LOXL2 involvement was also shown in control of cell polarity, a strongly dysregulated mechanism in EMT. It was proposed that LOXL2 downregulates the expression of tight junctions and cell polarity proteins claudin1 and Lgl2 and induces subsequent disorganization of junctions in breast cancer cells. Invalidation of LOXL2 in these cells resulted in upregulation of these proteins associated with reversion of EMT (Moreno-Bueno et al., 2011).

Interestingly, the role of LOXL2 has also been studied in endothelial-to-mesenchymal transition (EndMT), an important process in vascular development in which endothelial cells differentiate into a mesenchymal phenotype (de Jong et al., 2019; Neumann et al., 2018). Unlike epithelial cells, the expression of LOXL2 alone was not sufficient to induce EndMT in endothelial cells. Both studies however demonstrated that LOXL2 modulates EndMT induced by transforming growth factor- β stimulation (de Jong et al., 2019). These data further suggested that intracellular activity of LOXL2 is differently regulated according to the cell type, and may play a distinct role in endothelial cells as compared to cancer cells.

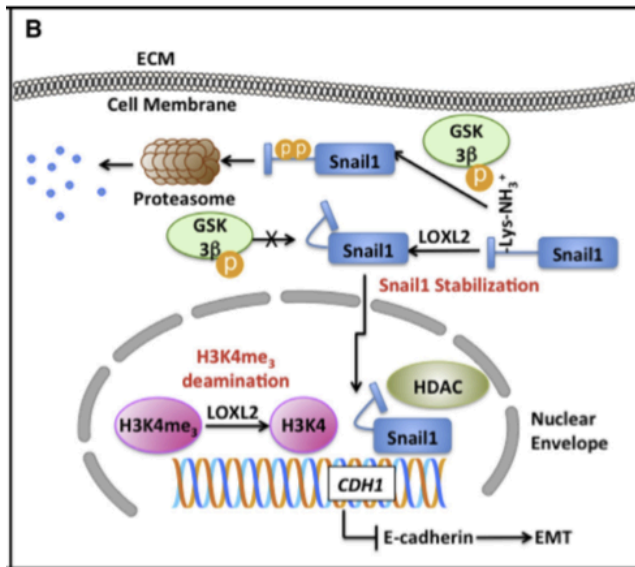


Figure 19. Proposed model for intracellular LOXL2 role in EMT. Intracellular LOXL2 regulates Snail1 or histone H3 to repress E-cadherin expression, leading to EMT. From Moon et al., 2014.

3.3.3. Role of LOXL2 in cardiovascular pathologies / vascular development

It is likely that LOXL2 is involved in development and stability of the cardiovascular system, although no clear consensus about the phenotype of the knock-out mice has been described (Martin et al., 2015; Stepan et al., 2019). LOXL2 is however clearly linked to extracellular matrix cardiovascular disease including aneurysms, suggesting a cross-talk between ECM remodeling by LOXL2 and vascular stability. LOXL2 was indeed screened for genetic susceptibility to intracranial aneurysms in two distinct studies (Akagawa et al., 2007; Wu et al., 2018b). Surprisingly, a paper focusing on retinal small aneurysms showed an increased expression of LOXL2 together with basement membrane components, suggesting that this overproduction could be a compensatory mechanism managed by pericytes or other cell types (López-Luppo et al., 2017).

An additional role for LOXL2 in the regulation of the vascular system is linked to modulation of TGF β -induced EndMT (de Jong et al., 2019). A recent study has identified GATA6-AS as a novel actor in regulation of EndMT by LOXL2 (Neumann et al., 2018). GATA6-AS is a long

non-coding RNA that interacts intracellularly with LOXL2 and negatively regulates nuclear LOXL2 function, modulating endothelial cell gene expression (**figure 20**). As EndMT can be linked to angiogenesis, authors also examined how the interplay between GATA6-AS and LOXL2 could regulate vascular sprouting. Interestingly, GATA6-AS silencing did not alter extracellular levels of LOXL2, and intracellular activity of LOXL2 was not required for sprouting angiogenesis, suggesting that the endothelial sprouting phenotype is rather driven by extracellular LOXL2. Moreover, another study reported that the SRCR domains of LOXL2 interacted with GATA6 independently of the catalytic domain (Peng et al., 2019), suggesting that these effects were not linked with LOXL2 activity.

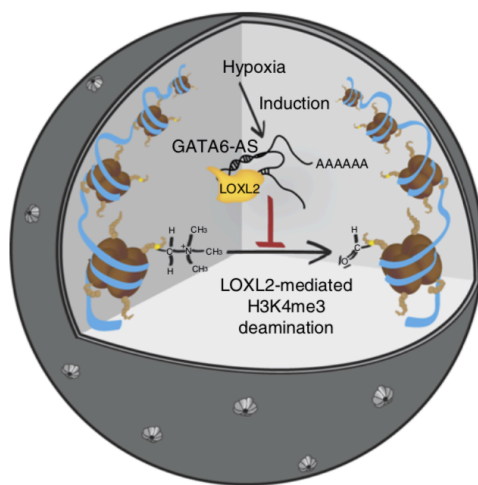


Figure 20. Schematic representation of GATA-AS-regulated LOXL2 function. In the nucleus, LOXL2 catalyzes the oxidative deamination of lysine 4 on histone 3 (Herranz et al., 2016), a process which is negatively regulated by GATA6-AS. (From Neumann et al., 2018).

Furthermore, LOXL2 is involved in vascular development and angiogenesis. Our group demonstrated for the first time that LOXL2 functionally regulates angiogenesis during development (Bignon et al., 2011). Invalidation of LOXL2 in zebrafish embryos impaired development of intersegmental vessels and demonstrated LOXL2 involvement in capillary morphogenesis. *In vitro* studies by loss and gain of function confirmed that LOXL2 was required for angiogenic sprouting in 3D models, and demonstrated that this enzyme is necessary for collagen IV assembly in the endothelial ECM. Inhibition of LOXL2 catalytic activity had no impact on both processes, suggesting a non-catalytic role for LOXL2 in angiogenesis correlated with collagen IV scaffolding (Bignon et al., 2011). However, no specific molecular mechanism had been described to explain its effects on endothelial cells. These results were supported by the proposed distribution of LOXL2 at basement membranes (Csiszar, 2001; Fujimoto and Tajima, 2009) and by the more recent demonstration of collagen IV as a substrate for LOXL2 (Añazco et al., 2016). Besides, LOXL2 has been described to be particularly enriched in endothelial tip cells, the cells that lead the vascular growth (del Toro et al., 2010), also supporting its major role in angiogenesis. Finally, LOXL2 is involved in pathological angiogenesis (Grossman et al., 2016; Zaffryar-Eilot et al., 2013). In lung

carcinoma, the strongest LOXL2 expression was found within the tumor vasculature (Zaffryar-Eilot et al., 2013). Targeting LOXL2 resulted in an anti-angiogenic effect that was not sufficient to inhibit tumor development, suggesting that LOXL2 has more impact on endothelial cells as compared to tumor cells.

4. Cell-microenvironment interactions or how ECM regulates cell responses

Living cells sense and respond to a broad range of external stimuli, both physical and chemical. They integrate these extracellular cues and transduce them into intracellular signals that drive changes in cell processes, including morphology, migration, survival and eventually fate, which are required for tissue and organ development (reviewed in Farge, 2011; Mammoto and Ingber, 2010; Wozniak and Chen, 2009). This overall process is called mechanotransduction and is divided into multiple steps including: i) mechanosensing, or sensitivity to a mechanical stimulus by a cell, ii) mechanosignaling i.e. an intracellular signaling event occurring in response to the mechanical stimulus, iii) mechanotransmission and tension generation, i.e. the act of transmitting a force from outside to the inside or the other way round (Jansen et al., 2017) (and see figure 21). Integrin-based adhesion structures are the main molecular link between cells and the ECM and act as bidirectional hubs transmitting signals between cells and their environment. These proteins sense mechanical signals coming from the ECM by modulating their activation state and rate of turnover. Integrin binding to the ECM results in the recruitment of intracellular adaptors such as talin and paxillin, as well as other signaling proteins such as FAK that are able to modify their level of tyrosine phosphorylation to trigger activation of distinct downstream signaling pathways. These complexes are also platforms that associate with the acto-myosin cytoskeleton and drive its remodeling, stimulating contractility and regulating cell shape (see figure 21).

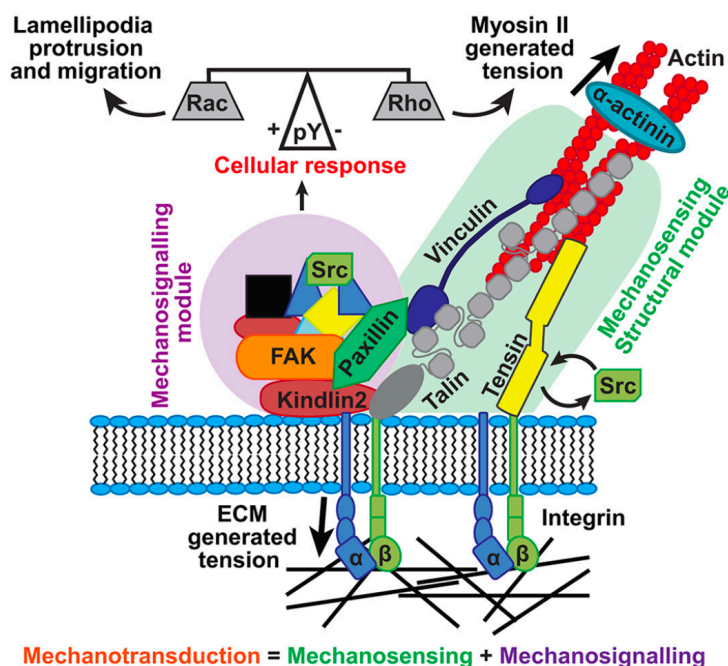


Figure 21. Model of mechanotransduction. This panel distinguishes the mechanosensing structural module from the mechanosignaling one. It also describes the mechanotransmission process through generation of tension forces. From Stutchbury et al., 2017.

In the case of endothelial cells, the role of integrin-mediated adhesions in angiogenesis and vascular stability has been extensively studied. It is now becoming very clear that vascular morphogenesis is influenced by changes in the biomechanical state of endothelial cells that are driven by interactions between cell-cell and cell-ECM adhesions. Indeed, cooperation between these two modes of adhesion is essential to regulate vascular morphogenesis and homeostasis, yet little is known about the precise mechanisms and actors involved in these cross-talks.

In this chapter, I will first describe how cell adhesion machinery is organized and matures in endothelial cells, and how it constitutes a focus point for cell-ECM interactions. I will then move on to mechanosensing through integrin-mediated anchorage to the ECM, and present the main signaling pathways involved in endothelial cell mechanotransduction. Finally, I will examine how ECM regulates endothelial mechanosensing and subsequent cell responses, and discuss about the importance of cell-ECM and cell-cell cross-talks to regulate endothelial contractility.

4.1. Focal adhesions, the main hub for cell-matrix interactions

Focal adhesions are dynamic actin-integrin links, whose assembly and maturation are driven by feedback from interactions with the ECM. Many recent studies have revealed an amazing degree of molecular complexity, illustrated by the great number of core components in these adhesions, and rich selection of regulatory proteins that are able to modulate the structure and dynamics of these hubs. While the integrin adhesome indeed consists of about 160 distinct constituents (Zaidel-Bar et al., 2007), I will here focus on the main components of these structures that have been described as involved in establishment and maturation of focal adhesions in response to the ECM.

4.1.1. Main components of focal adhesions

Integrins

Integrins span across the plasma membrane and link the ECM to the cell cytoskeleton. They have arisen as fundamental adhesion receptors that mediate cell and tissue function in a very broad range of situations, both in health and disease (Kechagia et al., 2019; Winograd-Katz et al., 2014). Several recent reviews have described in detail the biochemical (De Franceschi et al., 2015; Humphries et al., 2019) and mechanical (Chen et al., 2017a; Sun et al., 2016a) regulation of integrins. Recent publications are now shedding light not only on how integrins are affected by these signaling pathways but also on how this tight regulation allows integrins to act as sensors of the environment.

Structure and ligands

Integrins are heterodimeric transmembrane receptors composed of non-covalently interacting α and β subunits. There are at least 24 different integrin receptors in mammals, resulting from combinations of 18 α and 8 β subunits, each recognizing a specific set of ECM ligands. Though some subunits appear in only single heterodimer, 12 integrins contain the β 1-subunit and five the α v-subunit (Humphries, 2006). α and β subunits are both type I transmembrane proteins composed of a large extracellular domain, a single-pass transmembrane helix and a short cytoplasmic domain. Synthesized α and β subunits heterodimerize in the endoplasmic reticulum and are necessarily expressed as heterodimers at the cell membrane (Tiwari et al., 2011). Binding sites for ECM ligands either involve residues from both subunits, for example in the case of α 5 β 1 and α v β 3 integrins, which recognize the RGD motif in proteins such as fibronectin, or reside in a specific domain of the α -subunit as it is the case for the collagen-binding integrins α 1 β 1, α 2 β 1, α 10 β 1 and α 11 β 1 (Kechagia et al., 2019). A hallmark of integrins

is their ability to bind several ECM ligands, that can vice-versa engage different integrin heterodimers. However, a growing hypothesis is that integrins with overlapping ligand specificities have markedly distinct biomechanical features (Kechagia et al., 2019). Endothelial cells express 9 different integrins heterodimers (Hynes, 2007) (**see table 1**).

INTEGRIN HETERODIMER	LIGAND
$\alpha 1\beta 1$	collagen
$\alpha 2\beta 1$	
$\alpha 3\beta 1$	laminin
$\alpha 6\beta 1$	
$\alpha 6\beta 4$	
$\alpha 4\beta 1$	fibronectin
$\alpha 5\beta 1$	
$\alpha V\beta 3$	RGD containing proteins
$\alpha V\beta 5$	

Table 1. Integrins expressed by endothelial cells and their ligands. RGD containing proteins are vitronectin, fibronectin, fibrinogen and osteopontin. Adapted from Hynes, 2007.

Role of integrins in vascular development

The role of integrins in endothelial cell function and angiogenesis has been studied by mutation of either subunits or their ligands, or using selective antagonists to these receptors. The effects of genetic ablation or integrin antagonists on development and angiogenesis are reviewed by Silva and collaborators (Silva et al., 2008). Briefly, complete deletion of $\beta 1$ integrin leads to mice embryonic lethality at E5.5 due to a peri-implantation defect (Fässler and Meyer, 1995). Deletion of $\beta 1$ integrin only in endothelial cells increases the lifespan of mice embryos until E9.5-E10.5, but they eventually die due to severe vascular branching defects, showing the importance of endothelial $\beta 1$ integrin expression in development of the vascular system (Tanjore et al., 2008). Blocking antibodies against $\alpha 2\beta 1$ and $\alpha 1\beta 1$ integrins, both collagen receptors, induce a decrease in VEGF-mediated angiogenesis *in vivo*, and a decrease in tumor angiogenesis (Senger et al., 1997). Using the model of zebrafish embryo, injection of morpholino targeting $\alpha 2$ subunit induced abnormal and stunted intersegmental vessels and absence of dorsal longitudinal anastomotic vessel, providing evidence for a central role of $\alpha 2\beta 1$ integrin in developmental angiogenesis (San Antonio et al., 2009). Concerning fibronectin receptors, mice invalidated for the $\alpha 5$ integrin gene present dilatation and aberrant distribution of vessels of the yolk sac, which is lethal between E10 and E11 (Yang et al., 1993). Furthermore, treatments of endothelial cells with $\alpha 5\beta 1$ antagonists decrease physiological and

pathological angiogenesis (Kim et al., 2000). Antibodies targeting $\alpha v\beta 3$ integrins inhibit cell adhesion to vitronectin, and repress neovascularization in a variety of *in vivo* models including tumor angiogenesis and retinal angiogenesis (Eliceiri and Cheresch, 1998, 1999; Friedlander et al., 1996). However, more recent studies question these data, and suggest that $\alpha v\beta 3$ integrins may have an inhibitory role in angiogenesis (Hodivala-Dilke, 2008; Reynolds et al., 2002). Additionally, other studies have demonstrated that $\alpha 6$ integrin plays a role in tumor angiogenesis (Bouvard et al., 2014). These conflicting data about the role of integrins in vascular development could be explained by potential compensatory mechanisms implemented by subunits of other integrins depending on the biological system and context.

Mechanosensing through integrin-mediated anchorage to the ECM

The ability of cells to sense biochemical and mechanical features of their microenvironment through integrin-based adhesion hubs is called mechanosensing. Cell mechanosensing is a multistep process initiated by binding of integrins to their ECM ligands. Integrin molecular bonds display a behavior termed 'catch-bond' or more precisely 'catch-slip bond'. In a catch-slip bond, force applied on integrins first strengthens the bond (catch regime) but once a given threshold is reached, force starts weakening the bond (slip regime). Catch bonds seem to be a usual feature of integrin-ligand interactions and occur in different bonds with RGD-containing ligands such as bonds between fibronectin and $\alpha 5\beta 1$ (Kong et al., 2009) or $\alpha v\beta 3$ (Chen et al., 2017b; Elosegui-Artola et al., 2016). It is relevant to note that while the properties under force of integrin-RGD bonds have been extensively studied, there are unfortunately no report depicting force-dependent lifetimes of bonds between integrins and non-RGD ECM ligands such as collagens or laminins. Integrin binding to ECM ligands and their subsequent clustering provide bidirectional signaling by mechanisms known as 'outside-in signaling' and 'inside-out signaling' which are associated to receptor conformational changes. Integrin clustering at the cell surface indeed triggers accumulation of several adaptors and hubs of signaling proteins (Horton et al., 2015), regulating signaling pathways, such as activation of FAK, Src, Akt, and Erk pathways, and also downstream regulation of small GTPases of the Rho family. These signaling molecules are essential for regulation of cytoskeletal dynamics, as they provide platforms for organization of acto-myosin, including actin polymerization and myosin activation, and subsequent tension generation.

Talin, paxillin, vinculin

Focal adhesions are composed of a complex network of adaptor proteins organized into functional modules and each are responsible for regulating distinct aspects of mechanotransduction. The main signal transduction adaptor proteins include talin, paxillin and vinculin. Whereas talin and vinculin are part of the structural module proteins in focal adhesions, paxillin is involved in the signaling module (Stutchbury et al., 2017) (**and see figure 21**).

Talin has a unique role in formation and maintenance of focal adhesions. It forms the core of integrin adhesion complexes by directly linking integrins to actin, increasing the affinity of integrin for ligands and engaging several proteins. Talin serves as a platform to recruit other focal adhesion structural proteins such as vinculin via multiple binding sites present along the molecule (**see figure 22**).

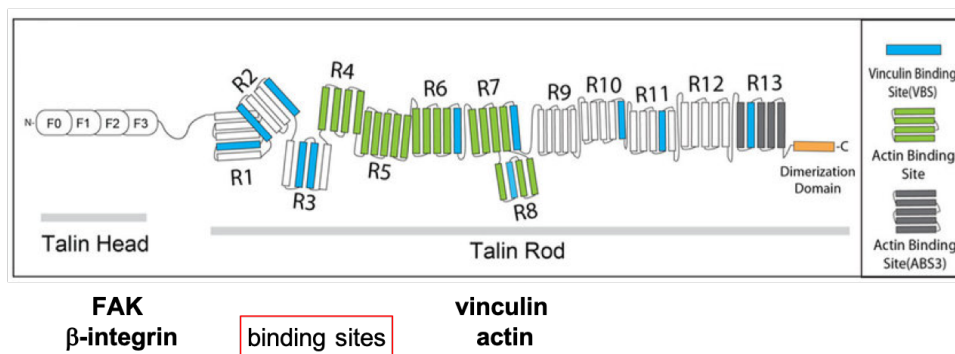


Figure 22. Talin structure. The protein is composed of a head which interacts with FAK and integrins, whereas the talin rod has binding sites for vinculin and actin. Adapted from Hu et al., 2016

Talin is indeed required for integrin activation, focal adhesion formation and cell spreading, as demonstrated in cells lacking talin 1 and talin 2 isoforms that fail to form focal adhesion, and present an abolished integrin-cytoskeleton linkage (Zhang et al., 2008). Whereas integrin needs talin for all of its functions, the opposite is not true; for example, talin regulates cadherin gene expression independently of integrins in drosophila (Bécam et al., 2005). Endothelial-specific inactivation of the talin1 gene in mouse embryo leads to embryonic lethality at E8.5-E9.5 from vascular defects, as observed in the head and yolk sac vessels. In endothelial cells, talin2 was not able to compensate for talin1 depletion, suggesting distinct roles for the two isoforms in these cells (Monkley et al., 2011). Tamoxifen-induced endothelial cell-specific deletion of talin1 in adult mice results in weakened stability of intestinal microvascular blood vessels, vascular leakage and death. Confocal analysis of intestinal villi revealed morphological alterations of the vasculature and the basement membrane. Interestingly,

intestinal capillary junctions were discontinuous, and endothelial cells detached from neighboring cells in absence of talin1. This effect was emphasized in the retina, where endothelial talin1 depletion induced disorganized capillary cell-cell junctions and decreased recruitment of VE-cadherin at these sites. Loss of talin1 in endothelial cells *in vitro* resulted in increased cell contractility, altered VE-cadherin organization, and induced vascular permeability (Pulous et al., 2019). These data suggest that talin is required for endothelial barrier function.

Paxillin is a multi-domain scaffold protein that works as a platform for the recruitment of various regulatory and structural proteins that together govern dynamic changes in cell adhesion (**figure 23**). The C-terminal half of paxillin contains four LIM (Lin11, Isl-1, Mec-3) domains, which are double-zinc-finger motifs mediating protein-protein interactions and that function as an anchor to the plasma membrane. The N-terminus part of paxillin contains repetitive leucine-rich domains and a proline-rich sequence that binds SH3-containing proteins such as tyrosine kinases and controls this way most of the signaling activity of paxillin. Integrin binding to the ECM promotes paxillin phosphorylation at Y118 by Src and FAK, as well as Y31 by FAK, which allows paxillin interaction with downstream effectors such as p130cas, and transduction of external signals mediated by mitogen-activated protein kinases (MAPKs). Tyrosine phosphorylation of paxillin has been shown to regulate both assembly and turnover of adhesion sites (Zaidel-Bar et al., 2007).

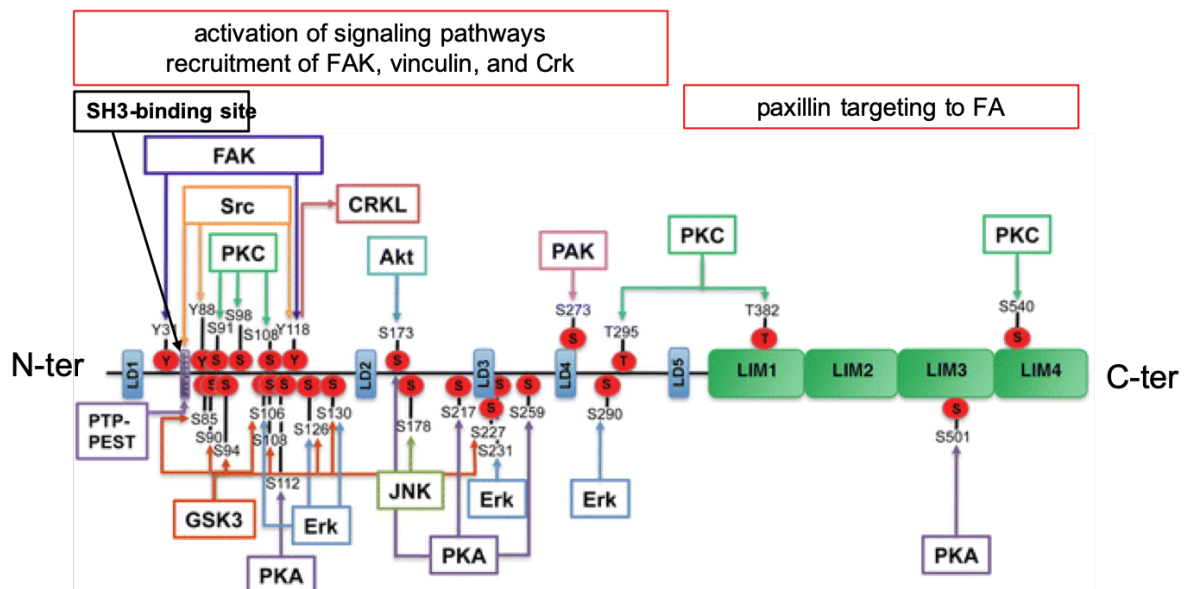


Figure 23. Paxillin structural and functional organization. The N-terminus contains a proline-rich region that anchors SH3-containing proteins and five leucine-rich LD domains, which include docking sequences for the recruitment of signaling and structural molecules such as FAK, vinculin, and Crk. The C-terminus contains four cysteine-histidine-enriched LIM domains, involved in the anchoring of paxillin to

the plasma membrane and its targeting to focal adhesions. Subsequent recruitment of signaling and adapter proteins are highly dependent on phosphorylation and are indicated on the figure. Adapted from [López-Colomé et al., 2017](#).

Paxillin is essential for normal mouse development, and has been found to critically regulate the development of mesodermally-derived structures such as heart and somites. The knockout mouse closely looks like the knock-out mouse for fibronectin (Hagel et al., 2002). In endothelial cells, paxillin rapidly becomes phosphorylated in response to VEGF (Abedi and Zachary, 1997). Paxillin knock-down in endothelial cells increases migration and invasiveness of endothelial cells, in a model of Matrigel implant but also during neonatal retinal angiogenesis (German et al., 2014). Consistent with this study, recent data show that paxillin-dependent Cdc42 activation is essential for cell polarity and angiogenic sprouting (Boscher et al., 2019).

Vinculin is so far the most characterized adhesion adaptor-protein. It is structurally composed of 5 domains distributed in 3 groups, vinculin head, linker domain and vinculin tail domains. The head has binding sites for talin and β -catenin while the linker binds vasodilator-stimulated phosphoprotein (VASP) and the tail contains binding domains for paxillin, and actin filaments (**see figure 24**). Vinculin exists in two conformations: an open active form and a closed auto-inhibited state in which the tail domain interacts with the head. Different studies suggest that activation of vinculin towards the open conformation could be regulated by interaction with talin, phosphorylation of vinculin, or increase of tension on adhesion sites (reviewed in Bays and DeMali, 2017).

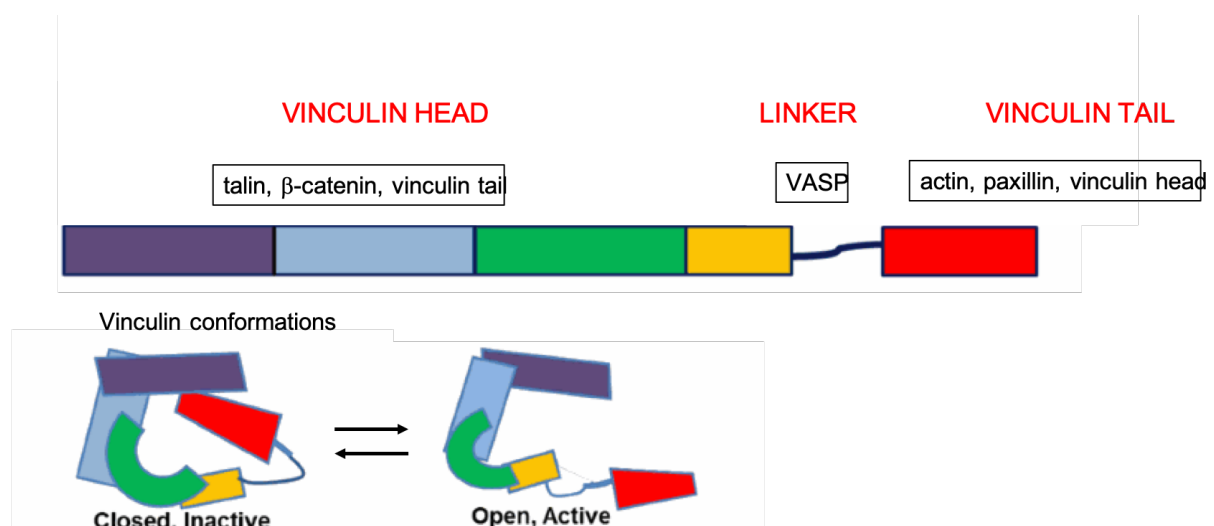


Figure 24. Vinculin structure and binding partners. Also represented a schematic of vinculin in closed, inactive and open, active conformations. Adapted from [Bays and DeMali, 2017](#).

In fact, vinculin is critical for generation of traction force in cells, which will be further developed in the next chapter. Phosphorylation of vinculin at Y100 and Y1065 by Src kinase is required during focal adhesion development and maturation and may affect vinculin binding to other proteins by modifying its conformational changes. Interestingly, vinculin implication has been demonstrated in the formation of podosomes, which are mechanosensitive structures able to protrude into the ECM and to degrade it (van den Dries et al., 2019). Recruitment of vinculin seems to play a critical role in podosomes force generation and protrusive force transmission to the substrate. This suggested that vinculin could play a role in vascular patterning, since the formation of podosomes has been described as an important step in sprouting angiogenesis (Seano et al., 2014; Warren and Iruela-Arispe, 2014). Paxillin has also similarly been shown to be crucial for formation of invadosomes, other actin-based structures able to digest the ECM (Petropoulos et al., 2016). Another aspect that supports a role for vinculin in angiogenesis, is that vinculin is involved in mechanical coupling at cell-cell junctions (Seddiki et al., 2018) (and see chapter on vascular morphogenesis, and endothelial cell-cell junctions). Accordingly, abolition of vinculin expression in endothelial cells resulted in defects in vascular morphogenesis in the mouse retina (Carvalho et al., 2019). In zebrafish embryo, vinculin mutant fish die at 21 days post fertilization, also displaying defects in juvenile cardiovascular development. Vinculin does not seem to affect initial vasculogenesis, but impacts the formation of a well-organized vascular network, especially in the coronary vasculature. Coronary vessels are indeed over-present, disorganized, and mispatterned in these fish. It is suggested that this effect is mediated by ERK hyperactivity causing overproliferation of endocardial cells, leading to abnormal alignment of endothelial cells and impaired angiogenesis. These results indicate that vinculin is essential for proper vascular morphogenesis (Cheng et al., 2016).

4.1.2. Focal adhesion dynamics

Cell-ECM adhesions are categorized into several types corresponding to their level of maturation, according to their size, stability, location, and molecular composition: nascent adhesions also called focal complexes, focal adhesions, and fibrillar adhesions (**figure 25**, and reviewed in Parsons et al., 2010). They mature through the recruitment of a repertoire of adhesion plaque proteins, including actinin (to facilitate actin association) and adaptor proteins such as paxillin, which, as already described, promotes interactions between multiple signaling complexes.

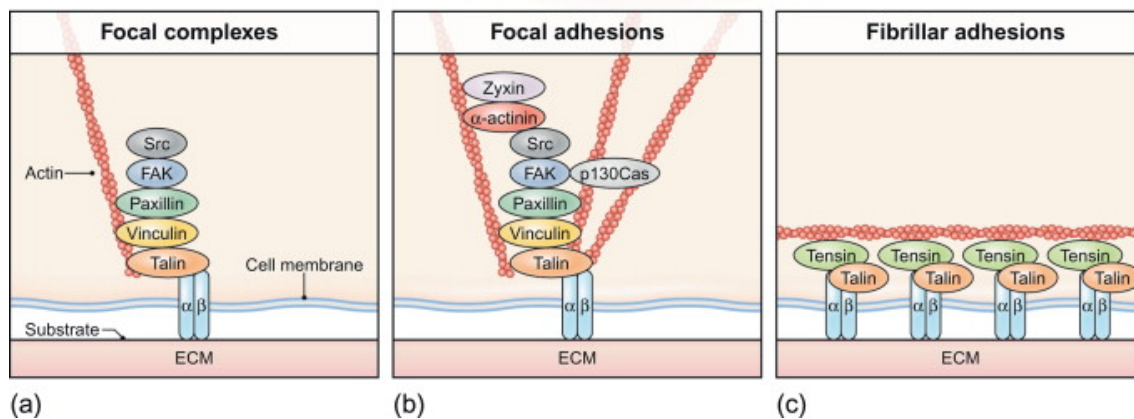


Figure 25. Adhesion dynamics at a glance; from Joo and Yamada, *Stem Cell Biology and Tissue Engineering in Dental Sciences*, 2015. Adhesions are classified in focal complexes (a), focal adhesions (b) and fibrillar adhesions (c).

Formation of nascent adhesions

Upon cell adhesion, the first structures assemble by nucleating three to six integrins at the leading edge of cell protrusions, as well as at the cell periphery, and form nascent adhesions (Bachir et al., 2014) (and **see figure 26**). The mechanism by which they first assemble remains quite unclear and the exact molecular nature of these complexes is not well described. It has been shown that they comprise at least two molecules of talin that link α/β integrin dimers to actin filaments (Kukkurainen et al., 2014). At this step, inside-out signals regulate displacement of intracellular integrin inhibitors and allow talin binding to integrin β -tails. Integrin activation is also promoted by an outside-in mechanism through ECM binding and ECM force application (**see figure 27**) that slows the diffusion of integrin dimers within the cell membrane. Integrin activation by this process is thought to increase affinity for ECM ligand binding (Takagi et al., 2002).

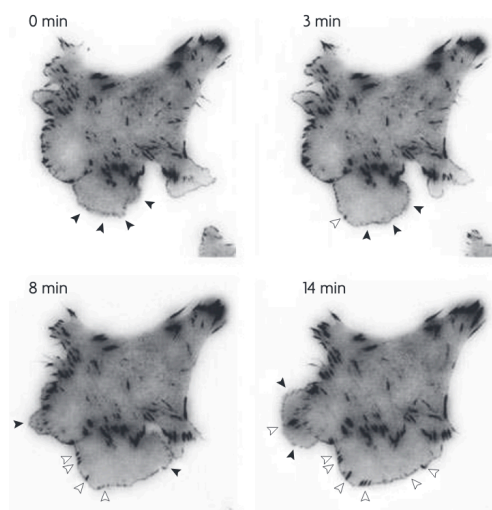


Figure 26. TIRF micrographs of a Chinese hamster ovary (CHO) cell expressing paxillin-mEGFP on glass coated with fibronectin. Closed arrowheads show nascent adhesions assembling and turning over in protrusions. Open arrowheads indicate maturing adhesions that begin to elongate centripetally. From (Choi et al., 2008).

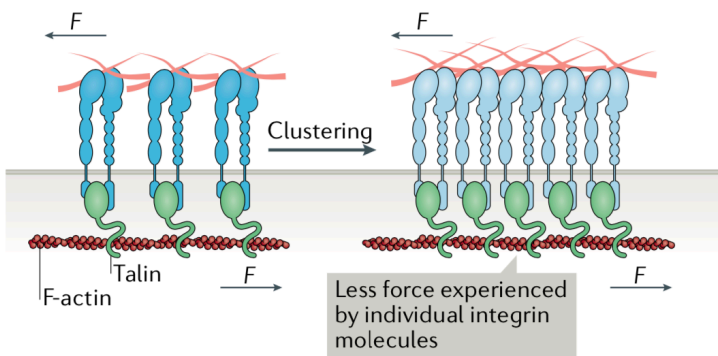


Figure 27. How forces from the ECM regulate integrin properties. Adapted from (Kechagia et al., 2019). Integrin-ECM binding follows a catch bond behavior. When force (F) applied to the ECM-bound integrin is below the optimal bond force (F_b) the strength of the bond increases with force. When F exceeds F_b , the bond lifetime decays with force.

Further ECM force application leads to integrin clustering (**see figure 28**) and the initiation of integrin downstream signaling through the coupling of integrins *via* talin and vinculin to the actin cytoskeleton. Reciprocally, actin can pull on integrins, contributing to force generation directly from the cell. To summarize, there are two principal factors that contribute to mechanical stress experienced by cells during focal adhesion formation: 1) the biochemical and physical cues of the ECM-generated force, and 2) the contractile activity of the cells pulling on this environment. ECM and cell contractility both contribute to the cellular mechanical stresses that lead mechanotransduction.

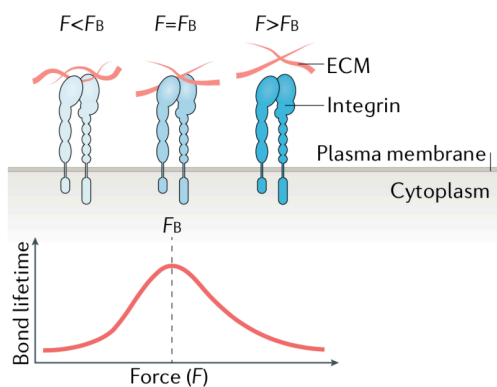


Figure 28. Force regulates integrin clustering. Adapted from Kechagia et al., 2019. If a force (F) is applied to an adhesion site, further integrin clustering decreases the force applied to individual integrin dimers, minimizing elastic energy since it decreases the applied strain.

Next step in focal complexes assembly involves opening of binding sites within the talin rod domain for recruitment of additional proteins that reinforce integrin-cytoskeleton bonds. This process has been studied using various methods including magnetic tweezers and AFM (del Rio et al., 2009), and high-resolution microscopy (Margadant et al., 2011) to explore the unfolding pathways of talin. Both studies revealed that the length of talin increases over time due to mechanical stress, and that physical extension of talin rod exposes cryptic hydrophobic binding sites for other proteins including vinculin.

Maturation of focal complexes into focal adhesions

At this stage, the width of integrin-based adhesions is usually below 1 μm , corresponding to the scale of the diameter of a single ECM fiber (Gasiorowski et al., 2013; Kim and Wirtz, 2013). Subsequent step is maturation of focal complexes into focal adhesions, which are elongated structures 3 to 10 μm long associated with stress fibers. Binding of vinculin to talin triggers the clustering of activated integrins (Humphries et al., 2007). Interactions between talin and the vinculin tail promote their association with actin, therefore reinforcing actin-integrin link (Galbraith et al., 2002). Besides, simulations of molecular dynamics of focal adhesion formation show that vinculin recruitment might be locally enhanced by applied tensile forces (Hytönen and Vogel, 2008). Using a FRET-based tension sensor, Grashoff and collaborators have shown that vinculin molecules are under a force of 2.5 pN in stable adhesions, and are in a stretched configuration in assembling focal adhesions, and in a non-stretched configuration in disassembling focal adhesions (Grashoff et al., 2010). This suggests an important role for vinculin in focal adhesion maturation and force transmission to the actin cytoskeleton. In fact, successful binding of vinculin to talin is essential to stabilize talin-F-actin interaction and thus to transfer the mechanical signal inward (Humphries et al., 2007).

Formation of fibrillar adhesions

The last step is maturation of focal adhesions into fibrillar adhesions where talin is replaced by tensin (McCleverty et al., 2007) (see figure 29). Fibrillar adhesions are rich in $\alpha 5 \beta 1$ integrins and their main function is to promote fibronectin fibrillogenesis, and reorganization of the ECM (Pankov et al., 2000; Zamir et al., 2000). Tyrosine phosphorylation of the cytoplasmic tail of integrin has been suggested to induce integrin-tensin interaction and abrogate talin binding in fibrillar adhesions (McCleverty et al., 2007). However, the precise mechanistic details of talin-tensin switch remain unclear. Tensin silencing reduces force generation, indicating an important role for tensins in mechanotransduction to the ECM (Georgiadou et al., 2017). Besides, it has been demonstrated that substrate stiffness promotes growth of fibrillar adhesions in a tensin-dependent manner (Barber-Pérez et al., 2020).

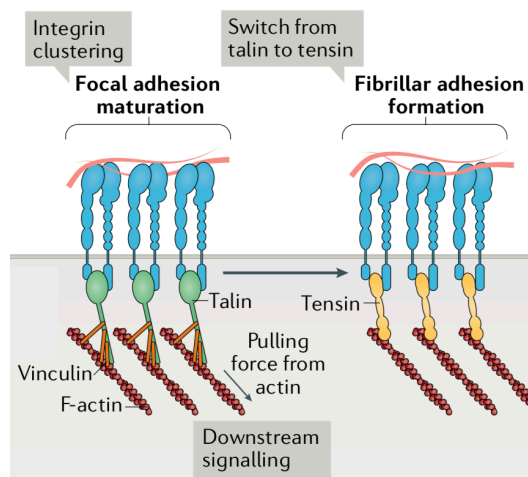


Figure 29. From focal to fibrillar adhesions. Talin-tensin switch and downstream signaling. Adapted from Kechagia et al., 2019.

Other studies have identified the Kank (N motif and ankyrin repeat domains) family of proteins as talin-binding components of focal adhesions (Bouchet et al., 2016; Sun et al., 2016b). Similar to tensins, Kanks promote integrin activation, formation of fibrillar adhesions and fibronectin fibrillogenesis. However, they reduce traction force, in contrast with tensins (Sun et al., 2016b). It is still unknown whether Kanks and tensins co-operate or compete during the process of adhesion maturation and what their respective contributions to fibrillar adhesions and ECM assembly are (Georgiadou and Ivaska, 2017). Zyxin is also a hallmark of mature focal adhesions (Zaidel-Bar et al., 2003) and was shown to be needed for force-dependent actin polymerization (Hirata et al., 2008). Zyxin is a mechanosensory component whose association with both focal adhesions and stress fibers depends on application of mechanical forces to these structures. Its effects on actin polymerization and stress fibers remodeling might involve a collaboration with VASP (Hoffman et al., 2006). Using live-cell super resolution microscopy, recent findings identify zyxin as a physiological regulator of endothelial ECM exocytosis components through reorganizing local actin network in the final stage of exocytosis (Han et al., 2017).

4.2. Cell mechanics: signaling through focal adhesions for force generation

4.2.1. Mechanosignaling process

Many of the integrin-associated proteins are tyrosine-phosphorylated after engagement to activate specific signaling pathways. Activated molecules play crucial roles in regulating multiple events, including cell adhesion and migration. For example, and amongst others, Focal Adhesion Kinase (FAK) is rapidly recruited after integrin activation and auto-phosphorylated, serving as a binding site for Src family members. FAK is a ubiquitous tyrosine kinase protein inducing intracellular signal transduction pathways downstream of integrins. FAK is recruited at sites of integrin clustering *via* interactions between its C-terminal domain and integrin-associated proteins such as talin or paxillin. Stimulation of FAK autophosphorylation at Y397 generated by integrin binding creates a high-affinity binding site for Src. This leads to the formation of a FAK-Src signaling complex that phosphorylates distinct focal adhesion proteins including FAK, paxillin and p130cas, which is involved in the regulation of Rho family GTPases (DeMali et al., 2003). As an example, phosphorylated p130Cas recruits the adaptor protein Crk into the developing focal adhesion site, and this complex activates Rac1 (Brugnera et al., 2002). FAK has also been shown to transmit integrin-stimulated signals to c-Jun N-terminal kinase (JNK), one of the major effectors of the MAPK signaling pathway. Several studies have highlighted the potential role of FAK in vascular morphogenesis and homeostasis. Endothelial deletion of FAK in mice leads to embryonic death at E11.5 with primary vascular defects, including bleeding, dilated capillaries in the yolk sac and impaired sprouting angiogenesis in the neuroepithelium. Interestingly, there was no effect on cell migration in FAK-null endothelial cells, but defective lamellipodia and cell spreading were observed, whether the cells were seeded on laminin or on fibronectin coatings. These results further suggested that the vascular defects observed in mice could be explained by ECM-dependent mechanisms (Braren et al., 2006). Furthermore, it has been proven that VEGF stimulation in endothelial cells increases FAK recruitment to cell-cell junctions, suggesting a role for FAK in endothelial cell barrier function (Chen et al., 2012). FAK is also involved in tumor angiogenesis (Jean et al., 2014; Mitra and Schlaepfer, 2006; Tavora et al., 2010) and was actually found to form a complex containing integrin $\alpha\beta 5$ in a Src-dependent manner, which was required for VEGF-stimulated angiogenesis in a mouse model (Eliceiri et al., 2002). Many other downstream signaling pathways are regulated by integrin activation. In all cases, reorganization of actin cytoskeleton is a direct outcome in focal adhesion assembly and modulation of cell contractility is part of the mechanotransduction process. In the next section,

I will expose the mechanisms of force transmission within the actin cytoskeleton and at focal adhesion sites.

4.2.2. Actomyosin network organization, mechanics and regulators

Each step of assembly of focal adhesions depends on the application of mechanical force by the actin system. Many studies indeed show that focal adhesions themselves cannot fully explain all the mechanosensing process, and that the actin cytoskeleton plays an important role at a larger scale (Gupta et al., 2015, 2016; Trichet et al., 2012). One striking example is provided by the study of the cell response to substrate stiffness. A set-up suspending cells between 2 microplates was developed in order to measure the forces involved during substrate stiffness sensing (Mitrossilis et al., 2009). In these experiments, authors tuned the apparent stiffness sensed by cells by controlling one of the microplates in real-time, and measuring the force exerted by cells at the same time. They found that the rapid time-scale (second-scale) at which cells respond to changes in substrate stiffness could not be due to minutes-long biochemical signaling at focal adhesions, whereas including the actin cytoskeleton in the equation could explain such fast response. A similar set-up has been described using an AFM stiffness-clamp model to investigate cell contractility in response to stiffness (Webster et al., 2011). Other recent studies showed that the number of actin stress fibers increases with stiffness of the substrate, and that they tend to align parallel to each other, thus polarizing the cell (Trichet et al., 2012). This change of organization could be due to regulation of molecular actors involved in actin cytoskeleton dynamics that are sensitive to tension. This notion is also demonstrated by experiments consisting in plating cells on micropatterned substrates, which spatially restricts the localization of adhesions (Lehnert et al., 2004; Theyry et al., 2006). Cells that are placed on flat, triangular adhesive islands form focal adhesions and stress fibers along the edges of the triangles (Théry et al., 2006) whereas plating cells on islands that consist of straight and semicircular strips induces the development of a fan-like morphology of the actin cytoskeleton, with an actin-rich lamellipodium associated with the curved strip, and a tail located at the end of the straight strip (Theyry et al., 2006). This kind of experiment demonstrates that the actomyosin system plays an important role in mechanosensing, and that integrin adhesions are able to control organization of the actin cytoskeleton. In this chapter, I will focus on actomyosin network organization and mechanics, and actomyosin regulators to explain how cell contractility is modulated in response to the ECM. I will then

describe how cell contractility and cytoskeleton rearrangements are involved in angiogenesis and vascular development.

Actomyosin contractility results from the mechanical action of myosin II motors, which use energy from ATP hydrolysis to exert forces on actin. Actin filaments (F-actin) have structural polarity resulting from the head-to-tail assembly of the actin monomers, leading to two distinct filament ends named *minus* and *plus* ends. Myosin II motors have two globular head domains linked by a long tail domain. Head domains bind to actin while the tail domains serve to assemble myosin II molecules into bipolar filaments. This bipolar architecture allows myosin filaments to slide anti-parallel actin filaments and this sliding activity can give rise to either a contractile or an extensible force (Koenderink and Paluch, 2018). Non-muscle myosin II is a hexamer composed of two heavy chains, two essential myosin light chains (MLC) and two regulatory myosin light chains. MLC can be phosphorylated by Myosin Light Chain Kinase (MLCK) which regulates vascular smooth muscle cells contraction (Loirand and Pacaud, 2014). MLCK1 is expressed by endothelial cells and regulates MLC phosphorylation to control traction force generation and subsequent regulation of endothelial cell shape (Faurobert et al., 2013). Besides, phosphorylation of MLC is involved in endothelial barrier function as pMLC is detected at cell-cell junctions and associated either with reinforcement of barrier function (Moreno et al., 2014) or with contractility-induced barrier disruption (Stockton et al., 2010).

Arp2/3 is the most common regulator of actin filament nucleation. Arp2/3 colocalizes with VE-cadherin at endothelial cell-cell junctions where it is involved in small actin-driven protrusions called JAILs (Abu Taha and Schnittler, 2014) (**and see figure 30**). This type of junction is critical to control endothelial barrier function and remodeling. Indeed, actin bundles consist of two oppositely oriented branched networks that push the plasma membrane of neighboring cells against each other and thus maintain strong interactions between VE-cadherins. Inhibition of the Arp2/3 complex in endothelial cells thus leads to breakdown of linear adherens junctions (Efimova and Svitkina, 2018 and **see figure 30**). Similar to Arp2/3, formins are a family of ubiquitous Rho-GTPase effector proteins that are also involved in the actin polymerization. In the zebrafish embryo, knocking-down formin-like 3 expression leads to unstable endothelial junctions, that results in defects in blood vessels lumen formation (Phng et al., 2015). These data highlight the importance of actin nucleation in endothelial cells, and the consequences of actin cytoskeleton rearrangements on vascular morphogenesis will be further detailed in the next chapter.

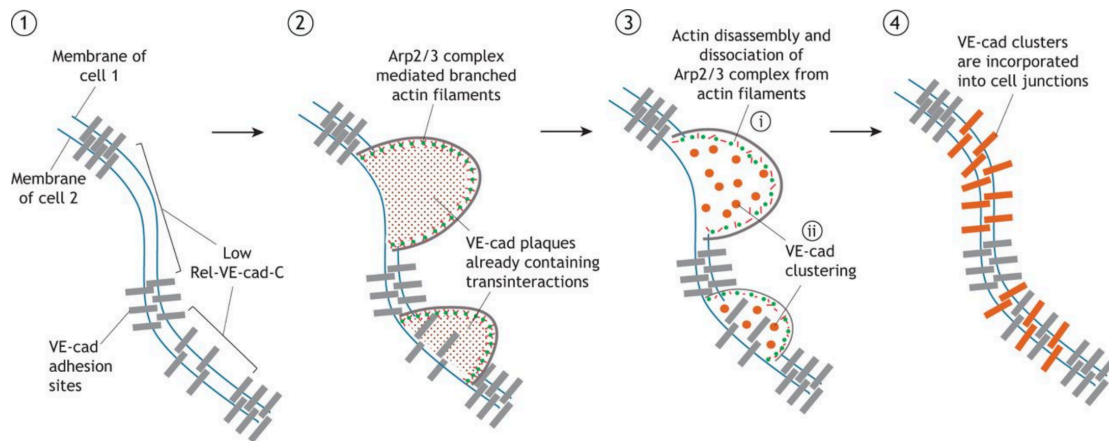


Figure 30. Sequential steps in JAIL-mediated VE-cadherin dynamics, and role of the Arp2/3 complex. 1) a region with a low VE-cadherin density forms 2) branched actin filaments develop at these sites in an Arp2/3-dependent manner, during this process VE-cadherin on each side of the membrane can associate in trans and form a VE-cadherin plaque; 3) JAIL extension is done by the disassembly of branched actin networks, dissociation of the Arp2/3 complex from actin filaments and by recruiting VE-cadherin molecules present in the plaque clusters; 4) the formed VE-cadherin clusters move to the junctions and become new junctional sites. From Cao and Schnittler, 2019.

4.2.3. Implication of actomyosin contractility in angiogenesis and vascular stability

As already mentioned, sprouting angiogenesis depends on coordinated migration and proliferation of endothelial cells, both processes relying on cell rearrangements mediated by actin structures. Besides, the role of actomyosin contractility is important for stabilization, remodeling and mechanosensing properties of adherens cell-cell junctions (Ladoux et al., 2015). Endothelial actomyosin contractility is thus supposed to be involved in regulation of vascular stability.

Important regulators of every aspect of actin cytoskeleton function are the small Rho family GTPases, mainly Rho and Rac (Burrige and Wennerberg, 2004). Among many Rho GTPases, Cdc42 has been demonstrated to regulate actin cytoskeletal dynamics, and to be involved in vascular development, as demonstrated by endothelial-specific knock-out mice for Cdc42 that lacked branched vascular structures in the trunk and heart (Jin et al., 2013). In another 3D *in vitro* set-up of sprouting angiogenesis, inhibition of Cdc42 impaired vascular morphogenesis, and increased the number of migrating single cells, suggesting that Cdc42 is

crucial to maintain cell-cell contacts in multicellular angiogenic sprouts (Nguyen et al., 2017). Consistent with this study, recent data described that inhibition of Cdc42 in endothelial cells led to reduction of cell-cell junction stability, and reduced the association of actin stress fibers and VE-cadherin at junctional sites. Cdc42 inhibition thus induced defects in endothelial cell polarity during sprouting angiogenesis in the mouse retina (Carvalho et al., 2019). These data suggest that Cdc42 maintains collective cell migration and stabilizes endothelial cell junctions by promoting endothelial cell contractility, both processes being required during vascular morphogenesis. A similar phenomenon has been described in the zebrafish embryo, where coupling between endothelial cell junctions and cortical actin cytoskeleton is needed and provides structural support to polymerize F-actin cables and generate force during endothelial cell sprouting and elongation in the context of vascular morphogenesis (Sauteur et al., 2014).

More originally, actomyosin contractility of the surrounding cells of the microenvironment is also capable to modulate blood vessel formation *in trans*. In a recent study in pancreatic islets, the biomechanical properties of islet cells, such as their actomyosin-mediated cortex tension and force of adhesion to endothelial cells are driving endothelial network formation. Indeed, increasing actomyosin-mediated cell contractility by downregulating integrin-linked kinase (ILK) expression in pancreatic cells inhibited their adhesion to endothelial cells and reduced vascularization. These results indicate that the actomyosin mechanical state of the surrounding environment can determine whether the blood vasculature envelops and invades the growing tissue (Kragl et al., 2016).

4.2.4. Technical approaches to study cell traction forces and rigidity sensing

Technical approaches to study cell traction forces and rigidity sensing have been recently reviewed (Gupta et al., 2016; Polacheck and Chen, 2016). Generally, force measurements rely on measuring the displacement of the substrate in response to force generated by cells. In the context of cell-ECM interactions, the standard approach that has been conventionally established over the last decades is traction force microscopy (TFM). In order to carry out these experiments, cells are seeded on deformable substrates such as polyacrylamide hydrogels, that will undergo linear elastic deformations upon cell tractions. Fluorescent beads are embedded into these hydrogels and are used as fiducial markers. Microscopy tracking allows to produce a displacement map for the substrate, and established integrated workflows and force reconstruction gives access to cellular traction forces with μm resolution. Recent

data have demonstrated that it is also possible to reliably measure traction forces exerted by cells embedded in 3D hydrogels, either by quantifying bead displacement, or cell-induced ECM deformations (Jorge-Peñas et al., 2017). This technique has been well characterized to measure live ECM displacement around endothelial cells at high resolution in the context of vascular sprouting (Steuwe et al., 2020). Development of FRET-based molecular tension sensors has also enabled intracellular tension measurements at molecular scale in a range of few pN/molecule. These sensors use Förster (fluorescence) resonance energy transfer (FRET) between a donor and an acceptor fluorophore, and the energy transfer depends on the distance between the two fluorophores. Increasing distance means less energy transfer, means stretching of the protein, and tension applied on it. As already mentioned, a vinculin-FRET sensor has been described (Grashoff et al., 2010) and similar force probes have been developed to sense tension in VE-cadherin and PECAM1 (Conway et al., 2013) or E-cadherin (Borghi et al., 2012). Interestingly, the team of Viola Vogel described a fibronectin-FRET probe that gives information on fibronectin mechanical state (Kubow et al., 2015; Smith et al., 2007).

Atomic force microscopy (AFM) is another technique that can be used in many ways to evaluate the mechanical and/or structural state of substrates or cells. AFM is a surface probe technique that uses a soft cantilever to image surfaces or cells, or to apply forces while interacting with them. It can be used to measure tension in the cell cortex by deforming the surface of single cells and simultaneously recording force-indentation curves (Krieg et al., 2008). AFM can also be used to physically separate adherent single cells and measure adhesion force between them (Puech et al., 2006), or to stretch single molecules (El-Kirat-Chatel and Beaussart, 2018). Interestingly, AFM allows to determine the force required to deform ECM, and to measure in this way the strain stiffening of the substrate (van Helvert and Friedl, 2016). To detect strain stiffening at the leading edge of cells migrating on collagen I fibrillar hydrogels, authors used AFM nanoindentation and observed elevation of Young's modulus along the leading edge of cells. This technique can now be used simultaneously to optical fluorescence imaging in order to follow a structure, its dynamics and localization (Cazaux et al., 2016).

4.3. ECM regulates focal adhesion organization and subsequent cell responses

Several parameters contribute to the strength of adhesion between a cell and its environment such as organization of adhesion receptors at the cell surface, and their affinity for the ligand (Albiges-Rizo et al., 2009). As an example, distance between individual integrins is important to modulate and reinforce cell adhesion (Selhuber-Unkel et al., 2008). However, one of the key features able to modulate reinforcement of adhesion structures reside in ECM organization. Spatial distribution of ECM ligands, nanotopography of the ECM and mechanical properties such as stiffness are factors involved in control of integrin organization and maturation of adhesion complexes. In the next sections, I will provide information about the influence of ECM geometry and mechanical properties on endothelial cell responses.

4.3.1. Influence of ECM geometry

Physical parameters such as spatial organization of the extracellular environment is important in regulating cell-ECM interactions. The work of Christopher Chen has determined how ECM geometry governs endothelial cell survival in the context of capillary morphogenesis. Using micropatterned substrates to control cell shape, it was further demonstrated that the area of cell spreading could drive changes in endothelial cell proliferation and apoptosis (Chen et al., 1997). More recently, his team used micropatterning technique to organize endothelial cells into capillaries that can be implanted *in vivo*, and demonstrated that the diameter of the channel in which cells are first seeded is important to trigger proper vascularization after implantation (Chaturvedi et al., 2015). In another model of lumen formation, based on hepatocytes canaliculi, geometry of the ECM was also shown to be crucial to induce proper lumen morphogenesis (Li et al., 2016). ECM geometry can also be modulated by ligand spacing and density and can subsequently influence endothelial responses. Indeed, high ECM densities are able to resist to cell-generated traction forces and to promote endothelial cell spreading and growth, whereas low ECM densities inhibits endothelial cell spreading, thus proposing that context-dependent enrichment of ECM components has a role in endothelial cell responses (Ingber and Folkman, 1989). Another descriptor of ECM geometry is its orientation, that has also been shown to modulate cell morphology and intracellular signaling. Using a microcontact printing approach to orthogonally vary ECM alignment, density and size, a recent paper described that increasing ECM alignment led cells to adopt an elongated uniaxial morphology, polarized the cell, and modulated cell migration (Wang et al., 2018a).

4.3.2. Influence of ECM stiffness

Many studies have characterized the response of cells to substrate stiffness and agreed that cells are unable to spread on softer substrates, whereas they completely spread on stiffer substrates. In agreement, focal adhesions are larger, actin cytoskeleton is more polarized and cells exert higher traction forces on stiffer substrates (Balaban et al., 2001; Discher, 2005; Lo et al., 2000; Prager-Khoutorsky et al., 2011; Trichet et al., 2012), demonstrating their involvement in sensing the substrate stiffness. Following the same idea, while cells are not able to polarize on soft substrates, they do on stiffer ones through a mechanism that is dependent on myosin II activity and α -actinin in fibroblasts (Doss et al., 2020). During development of drosophila egg chamber, it was demonstrated that the ECM basement membrane is secreted in such a way that a stiffness gradient is sensed by epithelial cell and regulates organ and cell shape (Chlasta et al., 2017; Crest et al., 2017). In endothelial cells, ECM stiffening has been shown to induce β 1 integrin activity, as well as traction force generation, without major changes in the endothelial transcriptome, suggesting that the biomechanical response of endothelial cells is not mediated by changes in gene expression (Bastounis et al., 2019). The impact of ECM stiffening on endothelial response has been further evaluated using 3D collagen hydrogels of controlled stiffness: by increasing the collagen concentration, and thereby ECM stiffness, endothelial cells were able to better organize *in vitro*, demonstrating a level of regulation of endothelial behavior imposed by the substrate (Raghavan et al., 2010).

4.3.3. Combination of factors

As ECM stiffness and geometry are linked to one another, influence of combination of these two parameters on cell responses have also been studied. Using micropatterned substrates of controlled stiffness, it was recently shown that increasing ECM ligand spacing promotes growth of focal adhesion complexes in endothelial cells on intermediate-rigidity substrates, but induces their collapse on higher stiffnesses, suggesting that there is an optimal stiffness that decreases as ligand spacing increases (Oria et al., 2017). These data suggest that ECM geometry together with the mechanical properties of the substrate are able to modulate cell adhesion. However, it has been suggested that ECM stiffness ultimately controls the cellular response, over the amount of ECM ligands presented. Indeed, when cells are cultured on ECM substrates of varying rigidities, focal adhesion fail to assemble when cells are cultured on ECM substrates below a critical stiffness threshold, even when ECM ligands are presented at saturated levels (Cavalcanti-Adam et al., 2007). This was also the case in zebrafish epicardial

explants, where stiffness exerted by the ECM is responsible for impaired cytokinesis, and increasing ECM ligand density was not able to restore failed divisions (Uroz et al., 2019).

Altogether, these data demonstrate that both ECM geometry and stiffness are important features regulating endothelial adhesion and subsequent cell responses required for angiogenesis. As already mentioned, a proper balance between cell-ECM and cell-cell junctions is also required during this process, as numerous cross-talks exist between these two modes of adhesion. In the next section, I will develop how these cross-talks are balanced and regulated in endothelial cells.

4.4. Cross-talks between cell-ECM adhesions and cell-cell contacts

Junctional properties of endothelial cells were already described the first section of the manuscript. During embryonic development and angiogenesis, cells often show collective migration, characterized by cooperation between assembly and disassembly of cell-ECM adhesions and cell-cell adhesions. However, little is known about the mechanisms and molecules involved in the cross-talks between these two modes of adhesion. Cell-ECM and cell-cell adhesions share similarities in structure and organization (Han and de Rooij, 2016; Lecuit et al., 2011) (**see figure 31**). Both form clusters whose properties are relying on actomyosin contractility. In the case of cell-cell junctions, VE-cadherins associate with the actin cytoskeleton through specific adaptors such as α -catenin and β -catenin, as well as shared ones including vinculin and FAK. Both structures are composed of a signaling layer, a force transduction layer and actin-regulatory layer (Han and de Rooij, 2016) (**and see figure 31**).

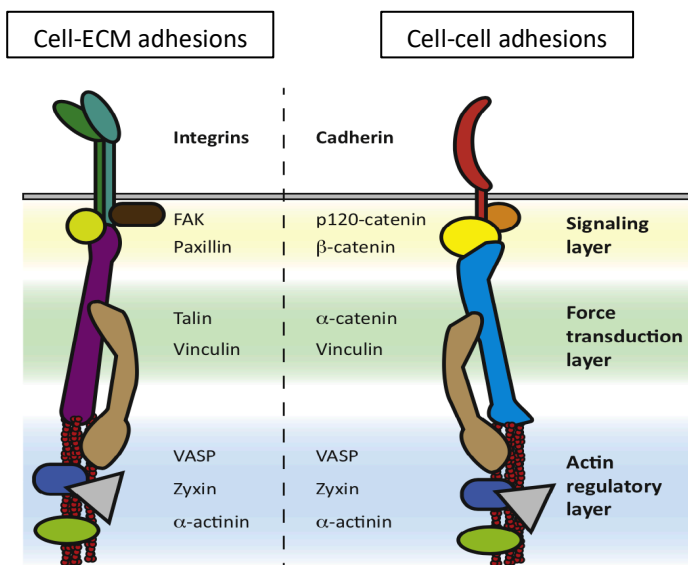


Figure 31. Structure and organization of integrin and cadherin adhesion complexes. Adapted from Han and de Rooij, 2016.

Vinculin is a key mediator of integrin signaling that also regulates cell-cell junctions. Vinculin is indeed present in both complexes (**figure 31**) and is necessary for force transmission (Geiger et al., 1980). Vinculin depletion affects both integrin adhesion (Rodríguez Fernández et al., 1993) and actomyosin contractility (Mierke et al., 2008). It acts as a cytoskeleton anchoring protein in both cases and is involved in reinforcement and stabilization of cell-cell junctions (Bays et al., 2014) (**figure 32**). Previous data have shown that vinculin enrichment at cell-cell contacts was dependent on tension, either by experiments inhibiting intracellular contractility (le Duc et al., 2010; Sumida et al., 2011) or by experiments in which external forces were applied to cells (Dufour et al., 2013). A proposed mechanism regulating vinculin

recruitment and mechanotransduction at cell-cell junctions involves the conformation changes of α -catenin that are dependent on force generated by myosin-II (le Duc et al., 2010). Phosphorylation of vinculin at Y822 has been shown to regulate vinculin function and activation at sites of cell-cell junctions but not cell-ECM adhesions (Bays et al., 2014). Vinculin function in endothelial cell-cell junctions has also been more specifically described (Huveneers et al., 2012). In this study, authors expressed a vinculin binding-deficient mutant of β -catenin in endothelial cells, and showed that adherens junctions formed normally. This demonstrated that vinculin recruitment was not required for formation of adherens junctions in endothelial cells. However, when submitted to thrombin treatment for induction of vascular permeability, adherens junctions devoid of vinculin were more severely disrupted and failed to return to their stable state for a longer time. These results suggested a role for vinculin in the protection against force-dependent remodeling of endothelial junctions. Interestingly, talin was also reported to localize at endothelial cell junctions, and the same types of vascular defects were reported in endothelial-specific talin knockout mice, also supporting a link between integrin activation and maintenance of endothelial barrier (Pulous et al., 2019).

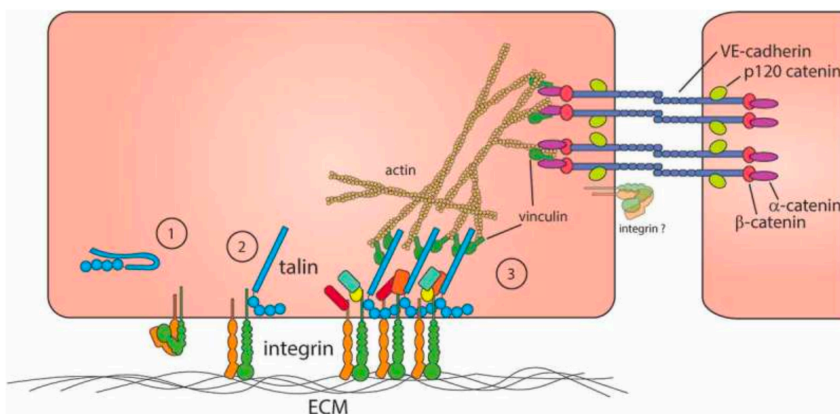


Figure 32. Vinculin is localized at cell-ECM and cell-cell junctions. From Pulous and Petrich, 2019.

Cell-ECM interactions have indeed been demonstrated to influence cell-cell junctions in several contexts, mainly using epithelial cells on micro-patterned substrates (Maruthamuthu et al., 2011; Tseng et al., 2012). The role of ECM in regulating vinculin recruitment at cell-cell junctions has been precisely addressed. By plating cells on fibronectin-patterned polyacrylamide gels of controlled stiffness, recent data suggest that junctional recruitment of vinculin, β -catenin and F-actin is significantly increased with substrate stiffness. These experiments suggested that ECM stiffness imposes intercellular tension that positively controls vinculin recruitment at cell-cell junctions (Seddiki et al., 2018). In monolayers of endothelial cells, localization at intercellular contacts of integrin $\alpha 2\beta 1$ and $\alpha 5\beta 3$ has been described and this distribution was independent of the initial plating substrate (Lampugnani et al., 1991). $\beta 1$

integrin was also localized to cell junctions in another more recent report (Pulous et al., 2019). After cell adhesion, endothelial cells synthesize and organize their own ECM that can eventually redistribute integrin receptors. Interestingly, authors reported deposition of matrix at cell junctions and suggested that this was representing potential ligands for the integrins found at the same locations. Since localization of integrin molecules at cell-cell junctions did not depend on the nature of the plating substrate, it is possible that the ECM produced by endothelial cells during these experiments could mediate integrin redistribution at cell-cell contacts. This hypothesis is supported by the very early deposition of ECM by endothelial cells after spreading. In adipocytes of *Drosophila* fat body, addressed secretion of collagen IV in the basement membrane at epithelial cell-cell contacts was also detected (Ke et al., 2018) and supports the hypothesis of autocrine ECM deposition that could mediate cell-cell junctions in this cell type. More recently, links between integrin $\beta 1$ and VE-cadherins have been investigated in endothelial-specific gene inactivation of integrin $\beta 1$. Deleted mice display major defects in cell-cell junction establishment during vascular development, leading to vascular leakage and hemorrhages (Yamamoto et al., 2015). These results clearly indicate that alterations in integrin activity as a result of defective cell-ECM interactions affect the stability of endothelial cell-cell contacts.

Aims of the study

The work of my PhD thesis was conducted at the Center for Interdisciplinary Research in Biology in College de France, within the team “Matrix proteins in hypoxia and angiogenesis” led by Stephane Germain. How hypoxic endothelial cells integrate chemical signals with mechanical cues from their local microenvironment in order to build and maintain functional capillary networks remains an open question and is driving our team’s research. We are indeed interested in understanding how angiogenesis and vascular integrity are regulated with a focus on the vascular microenvironment and remodeling of the extracellular matrix during this process. The team has thus been using a multidisciplinary approach based on animal models of vascular pathology including myocardial infarct, stroke, retinopathies to understand the role of matrix proteins in blood vessel formation and vascular integrity (Bouleti et al., 2013; Galaup et al., 2012). The team has also developed *in vitro* 3D capillary formation models in the context of tissue engineering (Gorin et al., 2016) and to decipher the mechanisms involved in regulation of capillary morphogenesis (Beckouche et al., 2015; Bignon et al., 2011).

We are studying the role of hypoxia-target proteins of the microenvironment in vascular development and stability, and more specifically of ECM modifying enzymes that regulate matrix proteins assembly and growth factor availability. Studies of the laboratory thus aim at better understanding the complex interplay between endothelial cells and ECM that will eventually affect angiogenesis, which is indeed characterized by remodeling of the vascular microenvironment through interstitial ECM degradation and formation of the basement membrane. The team had previously identified the lysyl oxidase like-2 protein (LOXL2) as a secreted hypoxia-target in developmental angiogenesis and in the context of ischemic diseases. Further studies had then suggested a role for this enzyme in ECM remodeling during angiogenesis. However, the precise molecular mechanisms involved in building and remodeling the vascular microenvironment remained to be elucidated, although basement membrane components are essential for proper vascular morphogenesis (Bignon et al., 2011; Gould, 2005; Turner et al., 2017; Zhou et al., 2008).

In this context, my research project aims at understanding: -1/ how endothelial cells build their own microenvironment during angiogenesis and especially how the endothelial basement membrane is secreted and assembled; and -2/ how cell response to the matrix resulting from this scaffolding could modulate vascular morphogenesis.

1. How is basement membrane deposited and organized by endothelial cells?

A little is known about the molecular mechanisms leading basement membrane deposition and organization by endothelial cells in the context of angiogenesis. I first aimed to identify the succession of molecular events leading to autocrine secretion and scaffolding of the macromolecular complexes composing the endothelial basement membrane, and was interested in understanding the role of LOXL2 in this process. I thus explored the dynamics of association between several basement membrane components, and characterized their spatio-temporal distribution leading to matrix organization. For this purpose, I developed a correlative atomic force/fluorescence microscopy approach in order to better characterize basement membrane topography and structural properties together with identity of some components involved at high resolution. The aim of this work was thus to propose a model of assembly of the endothelial basement membrane and to get a better insight into how LOXL2 could participate to this scaffolding.

2. What are the effects of basement membrane scaffolding on cell responses and angiogenesis?

I then focused on understanding the impact of this autocrine basement membrane and investigated a possible link between basement membrane deposition by endothelial cells and their angiogenic response. I was therefore interested in evaluating how endothelial cells could sense and integrate information from the basement membrane and used LOXL2-depleted cells as a tool to characterize the impact of a defective basement membrane scaffolding on endothelial cell adhesion, contractility, and spreading. Besides, as cooperation between cell-ECM and cell-cell adhesions are essential in the angiogenic process (Han and de Rooij, 2016), I was interested in understanding how these two types of adhesion could be regulated in our set-up.

Overall, this work will provide new insights into the mechanisms connecting the impact of LOXL2 on ECM scaffolding to the angiogenic response of endothelial cells.

Results

1. Umana-Diaz et al, Matrix Biol 2020

The following paper aimed to characterize the role of LOXL2 domains in matrix deposition and angiogenesis, using directed mutagenesis. This paper demonstrated that both processes do not require LOXL2 catalytic activity. My contribution to this paper consists in the *in vitro* analysis of basement membrane deposition by LOXL2-depleted cells, together with investigating ECM partners for LOXL2. I also used time-lapse TIRF microscopy to investigate LOXL2 direct incorporation in the basement membrane.



Scavenger Receptor Cysteine-Rich domains of Lysyl Oxidase-Like2 regulate endothelial ECM and angiogenesis through non-catalytic scaffolding mechanisms

Claudia Umana-Diaz^{a,b,3}, Cathy Pichol-Thievend^{a,b,1,4}, Marion F. Marchand^{a,b,1}, Yoann Atlas^{a,b}, Romain Salza^c, Marilynne Malbouyres^d, Alain Barret^a, Jérémie Teillon^{a,5}, Corinne Ardidie-Robouant^a, Florence Ruggiero^d, Catherine Monnot^a, Philippe Girard^{e,f}, Christophe Guilluy^g, Sylvie Ricard-Blum^c, Stéphane Germain^{a,2} and Laurent Muller^{a,2}

a - Center for Interdisciplinary Research in Biology (CIRB), Collège de France, CNRS, INSERM, PSL Research University, Paris, France

b - Sorbonne Université, Collège Doctoral, Paris, France

c - University Claude Bernard Lyon 1, CNRS, INSA Lyon, CPE, Institute of Molecular and Supramolecular Chemistry and Biochemistry, UMR, 5246, Villeurbanne, France

d - Institut de Génomique Fonctionnelle (IGFL), ENS-Lyon, UMR CNRS, 5242, Université de Lyon, Lyon, France

e - Institut Jacques Monod, UMR7592 CNRS, Université Paris Diderot, Sorbonne Paris Cité, Paris, France

f - Biomedical and Fundamental Science Faculty, Université Paris Descartes, Sorbonne Paris Cité, Paris, France

g - Institute for Advanced Biosciences, INSERM U1209, CNRS UMR 5309, Université Grenoble Alpes, La Tronche, France

Correspondence to Laurent Muller: Center for Interdisciplinary Research in Biology, Collège de France, Paris, 11 Place Marcelin Berthelot, F-75005, France. laurent.muller@college-de-france.fr
<https://doi.org/10.1016/j.matbio.2019.11.003>

Abstract

Lysyl oxidases are major actors of microenvironment and extracellular matrix (ECM) remodeling. These cross-linking enzymes are thus involved in many aspects of physiopathology, including tumor progression, fibrosis and cardiovascular diseases. We have already shown that Lysyl Oxidase-Like 2 (LOXL2) regulates collagen IV deposition by endothelial cells and angiogenesis. We here provide evidence that LOXL2 also affects deposition of other ECM components, including fibronectin, thus altering structural and mechanical properties of the matrix generated by endothelial cells. LOXL2 interacts intracellularly and directly with collagen IV and fibronectin before incorporation into ECM fibrillar structures upon exocytosis, as demonstrated by TIRF time-lapse microscopy. Furthermore, surface plasmon resonance experiments using recombinant scavenger receptor cysteine-rich (SRCR) domains truncated for the catalytic domain demonstrated their direct binding to collagen IV. We thus used directed mutagenesis to investigate the role of LOXL2 catalytic domain. Neither enzyme activity nor catalytic domain were necessary for collagen IV deposition and angiogenesis, whereas the SRCR domains were effective for these processes. Finally, surface coating with recombinant SRCR domains restored deposition of collagen IV by LOXL2-depleted cells. We thus propose that LOXL2 SRCR domains orchestrate scaffolding of the vascular basement membrane and angiogenesis through interactions with collagen IV and fibronectin, independently of the enzymatic cross-linking activity.

© 2019 Elsevier B.V. All rights reserved.

Introduction

Lysyl oxidases (LOX and LOX-Like 1 to 4) are responsible for the covalent cross-linking of ECM proteins and participate to the remodeling of the

microenvironment associated with tissue development and pathologies including cardiovascular diseases, fibrosis and cancer [1,2]. These copper-dependent enzymes catalyze the deamination of hydroxylysines and lysines in collagens and elastin.

0022-2836/© 2019 Elsevier B.V. All rights reserved.

Matrix Biology. (xxxx) xx, xxx

Please cite this article as: C. Umana-Diaz, C. Pichol-Thievend, M. F. Marchand, et al., Scavenger Receptor Cysteine-Rich domains of Lysyl Oxidase-Like2 regulate endothelial ECM and angiogenesis thro..., Matrix Biology, <https://doi.org/10.1016/j.matbio.2019.11.003>

They all share the copper-binding residues and the catalytic tyrosine and lysine that form the lysyl tyrosylquinone cofactor (LTQ) (Fig. S4A). This family of enzymes is subdivided in two groups that differ in the degree of conservation of both the catalytic and the N-terminal domains [3]. LOX and LOXL1 share 88% similarity in the catalytic domain. They have unique N-terminal domains that act as propeptides whose cleavage is required for activation of the amine oxidase activity. Whereas the catalytic domains of LOXL2-4 also share 86–88% similarity, they only have 64–68% similarity with the catalytic domains of LOX and LOXL1. In addition, LOXL2-4 share a common specific structure of their N-terminus consisting in 4 repeats of scavenger receptor cysteine rich (SRCR) domains whose function remains quite elusive. SRCR domains are ancient and highly conserved domains of 100–115 residues characterized by 3 or 4 intradomain disulfide bonds that are present in secreted and cell surface proteins associated with pattern recognition of extracellular proteins [4]. LOXL2 has mainly been associated with pathological microenvironments in fibrosis and cancer because of its increased expression and of the impact of its inhibition on disease progression in animal models [5–7]. Whereas oxidation of collagen I and tropoelastin by LOXL2 had been described for long, it is only recently that their LOXL2-mediated cross-linking has been demonstrated [8,9]. Similarly, LOXL2-mediated cross-linking of collagen IV, which had already been proposed [10,11], was only recently demonstrated [12]. Interactions of LOXL2 that do not involve catalytic activity have also been recently identified, including with other ECM components like ADAMTS10 and ADAMTSL2, and fibulins [13,14], further suggesting that LOXL2 could be involved in elastogenesis [15]. In addition to ECM remodeling, a non-collagenous substrate of LOXL2 has been proposed to affect tumor progression through the regulation of the paracrine PDGF-AB signaling pathway [16]. Finally, intracellular functions of LOXL2 have also been proposed, mainly in the context of tumor progression and epithelial-mesenchymal transition through the regulation of Snail [17,18]. Even though LOXL2 was a promising therapeutic target in fibrosis and cancer, recent clinical trials using a LOXL2 specific antibody inhibiting enzyme activity did not prove up to the expectations [2,19,20].

LOXL2 was also described as a regulator of the cardiovascular system both during development and in extracellular matrix cardiovascular disease like aneurysm [21–23]. Gene deletion of LOXL2 in mouse results either in defects in the development of the cardiovascular system associated to partial [24] or complete lethality [25], whereas aged heterozygous LOXL2^{+/-} mice are protected from vascular stiffening [25]. LOXL2 was identified as one of the most up-regulated genes in endothelial tip cells during retina

vascularization [26] and its expression follows growth of intersomitic vessels (ISV) during zebrafish embryo development [10]. The involvement of LOXL2 in the regulation of angiogenesis has been demonstrated in physiological [10] and pathological contexts [27–29]. Sprouting angiogenesis, the formation of new blood vessels budding from pre-existing ones, involves proliferation and migration of endothelial cells, as well as capillary morphogenesis [30]. These processes are associated with extensive remodeling of the microenvironment, including degradation of the pre-existing extracellular matrix (ECM) and *de novo* generation of the vascular basement membrane [31]. Basement membrane provides the only structural support to capillaries, as these vessels lack a smooth muscle wall, and participates to neovessel stabilization and pericyte recruitment. It thus regulates dynamic processes including cell adhesion, migration and survival, as well as signaling. We have reported that LOXL2 is co-localized with collagen IV in the basement membrane of newly formed capillaries in the retina of newborn rat [10], and LOXL2 is indeed considered as part of the machinery involved in formation of the collagen IV core of the basement membrane [32]. The involvement of collagen IV in the regulation of sprouting angiogenesis was demonstrated by defects in brain microvasculature detected in collagen IV-deficient mouse embryos, even though deposition of other basement membrane components and formation of large vessels were not affected [33].

Basement membrane is a complex network of entangled self-assembled macromolecular complexes that require organization into supra-structures for achieving its multifunctional biologic roles [34,35]. Interaction of ECM-associated proteins with the core of basement membrane remains poorly understood, even though their role is essential for capillary formation, as demonstrated for fibronectin [36,37]. We have previously shown that LOXL2 depletion in endothelial cells resulted in defects in collagen IV deposition *in vitro* that were correlated with inhibition of capillary formation in 3D angiogenesis models and during zebrafish embryo development. The effect of LOXL2 depletion was however not mimicked by inhibition of lysyl oxidase enzyme activity, neither *in vitro* nor in zebrafish embryos [10], suggesting that non-catalytic activity of LOXL2 was involved in ECM organization and/or angiogenesis. In the present paper, we have thus investigated the role of LOXL2 domains in the organization of the vascular ECM and how they impact the formation of ISV during zebrafish development, and of capillaries *in vitro*. Altogether, our data demonstrated that the SRCR domains of LOXL2 alone are effective for both ECM scaffolding and 3D capillary morphogenesis, whereas its catalytic activity is not necessary for these processes.

Results

LOXL2 regulates deposition of ECM components through direct interactions

We have already shown that LOXL2 is colocalized with collagen IV and fibronectin in fibrillar structures of the ECM deposited *in vitro* by endothelial cells, but not with the matricellular protein Cyr61 [10]. Depleting LOXL2 in these cells resulted in

defects in collagen IV deposition in the ECM without altering mRNA synthesis and secretion of the protein [10]. We here investigated the impact of LOXL2 depletion on deposition of other basement membrane components. Endothelial cells were seeded at confluency and maintained for 2 and 3 days prior to immunofluorescence or extraction of ECM proteins for immunoblotting, respectively (Fig. 1). Perlecan and fibronectin deposition was strongly affected, whereas laminin deposition was inhibited by only 25%, as assessed by western blotting. These

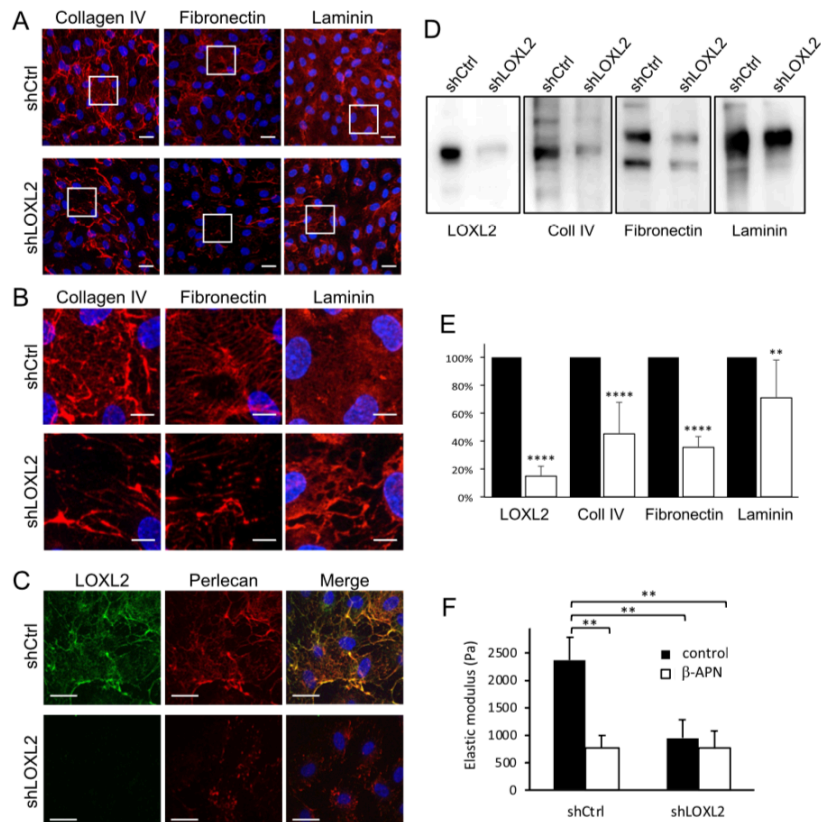


Fig. 1. LOXL2 regulates the deposition of ECM proteins. A–C: Control (shCtrl) and LOXL2-depleted (shLOXL2) endothelial cells were seeded on coverslips. Immunostaining of perlecan, collagen IV, fibronectin, and laminin was performed 48 h after seeding. Nuclei were stained with DAPI. Boxed areas are illustrated in **B**. Bars: 25 μm (**A** and **C**) and 10 μm (**B**). **D** and **E**: ECM proteins from endothelial cells cultured for 72 h were solubilized and separated by SDS-PAGE. LOXL2, collagen IV, fibronectin and laminin were immunodetected (**D**). Amounts of each protein in the ECM of control (black box) and LOXL2-depleted (white box) cells was normalized to the mean of controls (**E**). Graph presents the mean of 4 independent experiments. Values are presented ± SD. ** $P < 0.005$ and **** $P < 0.0001$. (**F**) The stiffness of cell-derived matrix was measured using atomic force microscopy. Graph presents the mean of 3 independent experiments. Values are presented ± SD. ** $P < 0.005$.

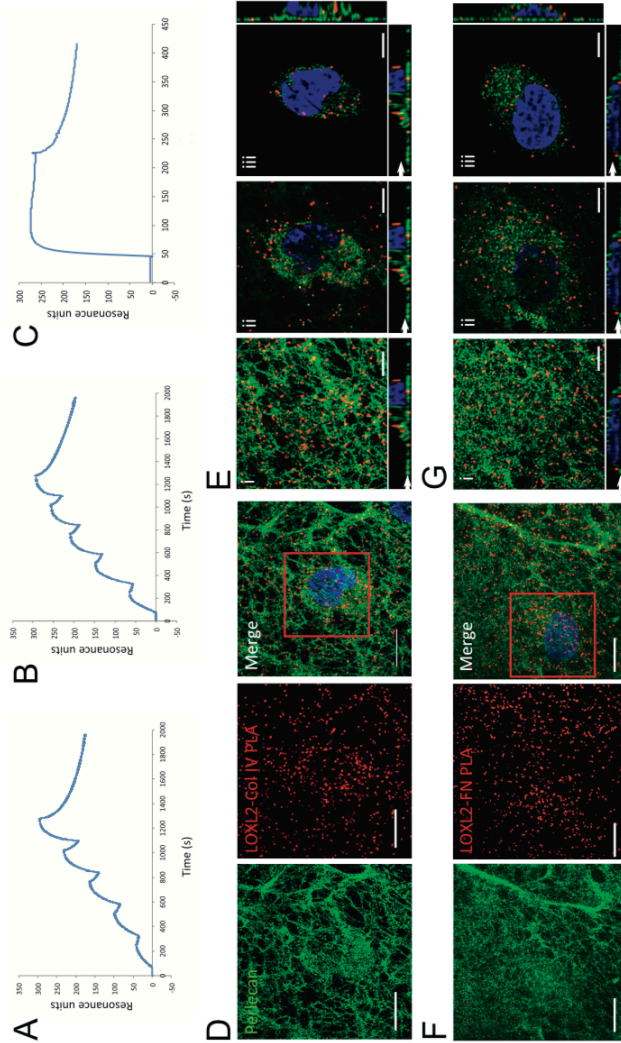


Fig. 2. LOXL2 directly interacts with collagen IV and fibronectin intracellularly prior to incorporation in the ECM upon exocytosis. A–C: LOXL2 directly binds to collagen IV and fibronectin. Several concentrations of full-length LOXL2 (8, 16, 32, 64 and 128 nM - A) or SRCR12 (62.5, 125, 250, 500 nM and 1 μ M - B) were injected at 30 μ L/min for 180s over immobilized collagen IV. 500 nM LOXL2 was injected at 30 μ L/min over immobilized fibronectin (C). D–G: Subcellular distribution of the interactions of LOXL2 with collagen IV and fibronectin. PLA was performed for analysis of the distribution of LOXL2 interactions with collagen IV (D and E) or fibronectin (F and G) on confluent endothelial cells that had deposited ECM. PLA signal (red) corresponding to LOXL2 interactions was analyzed by confocal microscopy. D and E display z projections of the whole stacks. Boxed areas are presented in E and G, which display 3 z-planes (i-iii) and the orthogonal views. White arrows indicate the z positions of the 3 single planes above. Perfectcan immunostaining (green) was used to localize the ECM layer (i) and nuclei staining with DAPI to localize the intracellular layer (iii). Bar: 10 μ m (D and F), and 5 μ m (E and G). The 3D reconstructions are presented in the online movies 1 (for collagen IV) and 2 (for fibronectin). H and I: Incorporation of LOXL2-GFP in the ECM was followed by time-lapse TIRF microscopy. H: A mixed population of confluent endothelial cells expressing or not LOXL2-GFP was imaged 24 h after seeding. Two cells expressing LOXL2-GFP sequentially migrate in the field of view. Arrows indicate the edge of each cell (the first in green, and the second in red). Arrowheads indicate stable fibrillar structures that have incorporated LOXL2-GFP, with a similar color-code as for the cells. Time is indicated in minutes. Bar: 20 μ m. See online movie 3. (I) An isolated migrating cell was imaged 24 h after seeding. GFP fluorescence is illustrated at the starting point (0' - green) and after 15 min (red). The merged image illustrates ECM remodeling associated to cell migration: LOXL2 is incorporated into nascent fibrillar structures at the migration front. White arrow indicates the direction of migration (top row). Bar: 10 μ m. A zoomed area (white box) illustrates incorporation of LOXL2-GFP in nascent fibrillar structures (arrows; bottom row). Time is indicated in minutes. Bar: 5 μ m. See online movie 4.

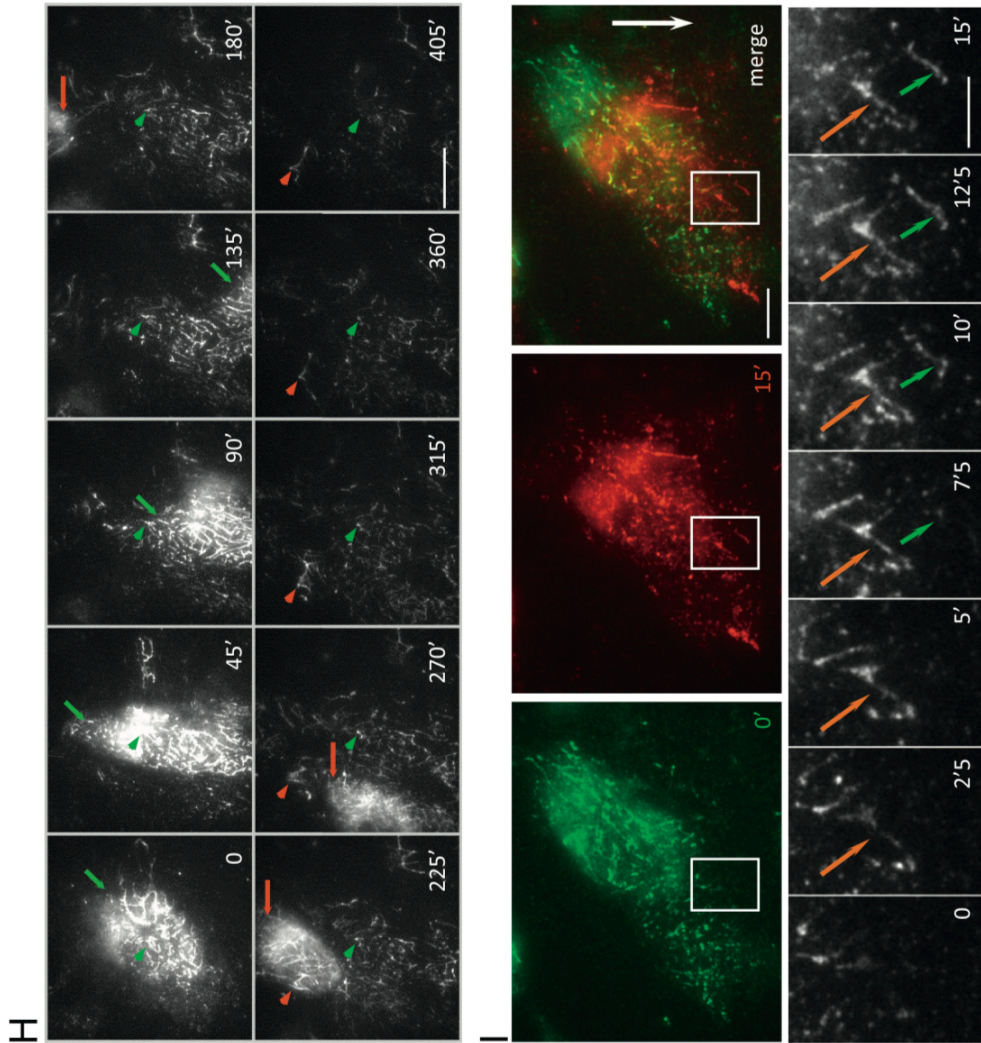


Fig. 2. (continued).

Please cite this article as: C. Umana-Diaz, C. Pichol-Thievend, M. F. Marchand, et al., Scavenger Receptor Cysteine-Rich domains of Lysyl Oxidase-Like2 regulate endothelial ECM and angiogenesis thro..., Matrix Biology, <https://doi.org/10.1016/j.matbio.2019.11.003>

defaults of deposition of matrix proteins were not associated with down-regulation of their expression (Fig. S1). Furthermore, the fibronectin that was not deposited in the ECM was detected in the secretion medium as already described for collagen IV (Fig. S2) [10], suggesting that LOXL2-depletion affected their assembly in the ECM rather than their secretion. The stiffness of the ECM generated by endothelial cells was measured using atomic force microscopy. The defects in organization and composition of the ECM observed upon LOXL2 depletion were correlated with decreased stiffness to a comparable level as in the presence of β -APN, a pharmacological pan-inhibitor of lysyl oxidase activity (Fig. 1F).

Preliminary experiments analyzing the kinetics of co-localization of LOXL2 suggested that it was associated earlier and to a higher level with fibronectin than with collagen IV (Fig. S3). To gain insight into the mechanisms involved in the regulation of their deposition by LOXL2, we investigated direct interactions between these proteins using surface plasmon resonance (Fig. 2A–C). We characterized two binding sites of LOXL2 to collagen IV, including one of very high affinity, with equilibrium dissociation constants: $K_{D1} = 8.9 \pm 2.9$ nM and $K_{D2} = 0.016 \pm 0.009$ nM. The LOXL2-collagen IV interactions displayed the following association rates of $7.54E+05$ Ms^{-1} and $4.93E+04$ Ms^{-1} , and dissociation rates of $6.1E-03$ s^{-1} and $7.47E-07$ s^{-1} . We also investigated the interactions of a recombinant protein corresponding to the N-terminal SRCR domains 1 and 2 (SRCR12) (Fig. S4). We could detect direct binding of SRCR12 to collagen IV (Fig. 2B). SPR experiments also demonstrated the direct binding of LOXL2 to fibronectin (Fig. 2C). We could however not calculate kinetic parameters and affinity for these interactions since the signal decreased before the end of the association phase. We then investigated the subcellular distribution of the interactions of LOXL2 with these proteins using proximity ligation assay (PLA). The experimental conditions were first set up by quantifying PLA dots in isolated LOXL2-depleted endothelial cells for identification of specific interactions with collagen IV or fibronectin (Fig. S5). Using confocal microscopy, these interactions were then analyzed in confluent monolayers that had generated a polarized ECM. Most of the PLA signal was detected in the ECM focal planes, which were identified using perlecan as a marker. We also identified intracellular PLA dots corresponding to LOXL2-collagen IV and LOXL2-fibronectin interactions in the perinuclear region (Fig. 2D–G; movies 1 and 2).

Supplementary video related to this article can be found at <https://doi.org/10.1016/j.matbio.2019.11.003>.

The incorporation of LOXL2 in the ECM was further investigated by time-lapse TIRF microscopy.

A mosaic population of cells expressing a LOXL2-GFP construct or not was cultured at confluency (Fig. 2H, Movie 3). LOXL2-GFP was directly incorporated in filamentous structures of the ECM underneath the endothelial cell expressing the chimera. Cells loaded the matrix locally as they migrated (Fig. 2H, arrows) without diffusion of LOXL2-GFP to the ECM located under the neighboring cells. After cells had passed through the field of view, an important pool of fluorescent LOXL2 was rapidly released from the matrix (within 10 min), whereas a smaller fraction of fluorescent LOXL2 remained bound to the ECM for several hours (Fig. 2H, arrowheads). These two pools of LOXL2-GFP could correspond to the two rates of dissociation of LOXL2 from collagen IV that were measured in SPR experiments. In order to investigate more precisely LOXL2 incorporation into the ECM, we acquired closer time-lapse images of migrating endothelial cells (Fig. 2I, Movie 4). LOXL2-GFP was deposited into nascent ECM fibrillar structures at the migration front. Incorporation in these fibrillar structures appeared as blinking spots of high intensity typical of exocytosis [38]. Altogether, these data suggest that LOXL2 has a scaffolding activity responsible for building up a network of macromolecules, including collagen IV and fibronectin, in the basement membrane.

Supplementary video related to this article can be found at <https://doi.org/10.1016/j.matbio.2019.11.003>.

LOXL2 catalytic activity is not required for collagen IV deposition and capillary formation

Considering the direct interaction of the SRCR domains with collagen IV, we then investigated whether LOXL2 function in ECM deposition requires its amine oxidase activity. We have already shown that pharmacological inhibition of lysyl oxidase activity by β -APN: i) does not affect collagen IV deposition in the ECM *in vitro*; -ii) only partially inhibits capillary formation in 3D assays; -iii) does not affect ISV formation in zebrafish embryo [10]. Considering the wide spectrum of inhibition of β -APN and the conflicting results concerning its efficacy in cell culture [3], we further investigated the involvement of LOXL2 catalytic activity using site directed mutagenesis. A point mutation of the tyrosine residue in the LTQ was generated (LOXL2-Y689A; Fig. S6) to inactivate the catalytic activity, as previously described for LOX [39]. The LOXL2-Y689A mutant was secreted by transfected CHO cells but inactive, as monitored by measuring the total β -APN-sensitive lysyl oxidase activity in the secretion medium (Fig. 3A and B). We have already shown that transducing LOXL2-depleted cells with wild-type LOXL2 restored both ECM deposition and capillary formation [10]. We here performed similar

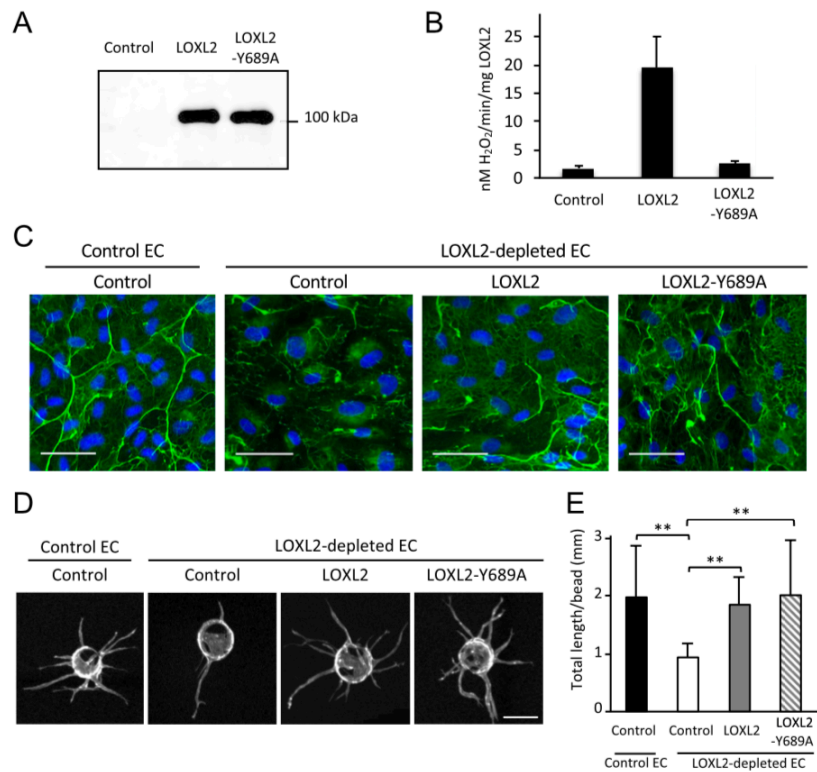


Fig. 3. LOXL2 catalytic activity is not necessary for collagen IV deposition and capillary formation. **A** and **B**: CHO cells were transfected with a control plasmid or with plasmids encoding either wild type LOXL2 or the Y689A mutant. Overnight secretion media were collected. Amounts of secreted LOXL2 were assessed by Western blot (**A**) and lysyl oxidase activity was measured (**B**). **C** to **E**: Control and LOXL2-depleted endothelial cells (EC) were transfected with lentivirus encoding either GFP (control) or LOXL2 or the LOXL2-Y689A mutant. **C**: Immunostaining of collagen IV was performed 5 days after seeding. Bar: 50 μ m. **D** and **E**: Capillary formation was assessed after 6 days of culture using the cytodex bead assay. Bar: 200 μ m. Capillary length was measured in 3 independent experiments of duplicate wells (**E**). Graph presents the mean value of total sprout length/bead \pm SD. ** $P < 0.005$.

experiments using mutant LOXL2. The expression of wild type and mutant LOXL2 in endothelial cells was assessed by Western blot, using antibodies directed against either LOXL2 catalytic domain or the myc epitope tag in order to distinguish between endogenous and transduced LOXL2 (Fig. S6B). Similar levels of wild-type and Y689A mutant LOXL2 were detected. Cells expressing the different LOXL2 constructs were seeded at confluency in order to promote collagen IV deposition. Whereas deposition of collagen IV by LOXL2-depleted cells was inhibited, re-expressing LOXL2 reversed this effect (Fig. 3C). Collagen IV deposition by endothelial cells expressing the LOXL2-Y689A was also

restored and displayed a similar distribution as when deposited by cells expressing wild-type LOXL2 (Fig. 3C). In vitro capillary formation in 3D fibrin hydrogels was also inhibited using LOXL2-depleted cells, and restored to control levels by wild type LOXL2 or LOXL2-Y689A (Fig. 3D and E).

A parallel approach based on re-expression of human LOXL2 was performed in LOXL2 knocked-down zebrafish embryos. ISV formation was altered upon LOXL2 depletion, resulting in misguiding of vessels and absence of dorsal longitudinal anastomotic vessel, as well as loss of connection with the aorta (Fig. 4 Aii, and movie 5), and lack of perfusion of ISV (Fig. 4B). Co-injection of the mRNA encoding

wild-type human LOXL2 together with the translation morpholino that down-regulates endogenous LOXL2 rescued this phenotype, as previously described [10]. The involvement of LOXL2 catalytic activity in the regulation of angiogenesis was then investigated using an mRNA encoding the human LOXL2-Y689A mutant. ISV formation and perfusion were rescued to the same extent as with wild-type human mRNA (Fig. 4), suggesting that LOXL2 catalytic activity was not required.

Supplementary video related to this article can be found at <https://doi.org/10.1016/j.matbio.2019.11.003>.

The SRCR domains of LOXL2 are effective for collagen IV deposition and capillary formation

We then investigated the function of the different domains of LOXL2. In addition to the copper-binding site and LTQ, the catalytic domain contains a cytokine receptor-like domain (CRL) (Fig. S6A) whose function remains unknown. Moreover, processing of LOXL2 between SRCR domains 2 and 3 has been described [40,41], suggesting that these domains could be involved in different functions. We thus assessed the proteolytic processing of LOXL2 by endothelial cells using antibodies targeting the N- or C-terminus. These experiments revealed the presence of full length LOXL2 (105 kDa) together with processed forms not detected when cells were LOXL2-depleted (Fig. 5A): an N-terminal fragment of 37 kDa, and a complementary C-terminal fragment of 68 kDa. Both proteolytic fragments were detected in the ECM and the secretion medium, but absent from the cell extracts. Indeed, bands of smaller molecular weight were detected in cell lysates only with the C-terminal antibody, and those were not altered by shRNA targeting LOXL2. These data are consistent with the processing of LOXL2 by extracellular proprotein convertases releasing a molecular form consisting in SRCR domains 1 and 2 (SRCR12) [40,41]. The ratio of these proteolytic fragments to full length LOXL2 was higher in the ECM than in the secretion medium, but our experiments do not allow to distinguish between processing in the ECM or in the secretion medium.

LOXL2-depleted endothelial cells were transduced with lentiviruses encoding either wild type or SRCR12 or SRCR14 forms of LOXL2. Expressing any of these three forms restored collagen IV deposition in the ECM (Fig. 5B), even though SRCR12 and SRCR14 did not reach as high levels of expression as full length LOXL2 (Fig. S6). The three constructs also restored capillary formation to the same extent as control cells (Fig. 5C), demonstrating that the two N-terminal SRCR domains are sufficient for collagen IV deposition and capillary formation *in vitro*.

In order to perform a similar investigation in zebrafish embryos, two complementary approaches were used: i) injection of a splicing morpholino; and –ii) co-injection of a translation morpholino with an mRNA. A splicing morpholino targeting the sequence joining intron 8 and exon 9, thus splicing exon 9, was designed to result in the insertion of a stop codon in the open reading frame, and thus in translation of a protein truncated for the whole catalytic domain. Splicing of LOXL2 mRNA was confirmed by RT-PCR (Fig. 6A). The only antibody directed against LOXL2 that recognizes the zebrafish protein, in our hands, targets the catalytic domain. Investigating deletion of the catalytic domain by Western blot using this antibody resulted in loss of the band present in control embryos and absent in embryos injected with a translation morpholino (Fig. 6B). Vessel formation and perfusion were restored in 77.8% of zebrafish embryos expressing truncated LOXL2 (Fig. 6C and D). We also co-injected the translation morpholino with an mRNA encoding human LOXL2 deleted for its catalytic domain (SRCR14). Semi-quantitative RT-PCR revealed that similar amounts of the injected mRNA were still present at 10 and 22 h post-fertilization (hpf) (Fig. 6E), demonstrating the presence of Loxl2a mRNA at the developmental stage of ISV growth. We could however not detect the truncated human LOXL2 using an antibody directed against the myc epitope. Nevertheless, formation and perfusion were completely rescued in 63%, and partially rescued in 19% of LOXL2-SRCR14 injected embryos (Fig. 6F and G; movie 5). These data demonstrate that the catalytic domain is not required for deposition of collagen IV in the ECM and formation of capillaries.

LOXL2 regulates ECM deposition in a context-dependent manner

We further characterized the ECM scaffolding function of LOXL2 using recombinant full length and truncated forms of LOXL2 as surface coating. Secretion and proper glycosylation profile of the recombinant proteins were verified by SDS-PAGE, suggesting the correct folding of these proteins (Fig. S4). Control and LOXL2-depleted endothelial cells were seeded in tissue culture dishes coated or not with the recombinant proteins and collagen IV deposition was analyzed by immunofluorescence 3 days after seeding (Fig. 7A). All three forms of LOXL2 restored collagen IV deposition. The pattern of collagen IV was however lacking the thick filamentous material that was generated by endothelial cells in the absence of coating. These data showed that LOXL2 and its two N-terminal SRCR domains could provide binding sites for collagen IV, as suggested by the direct interaction between these

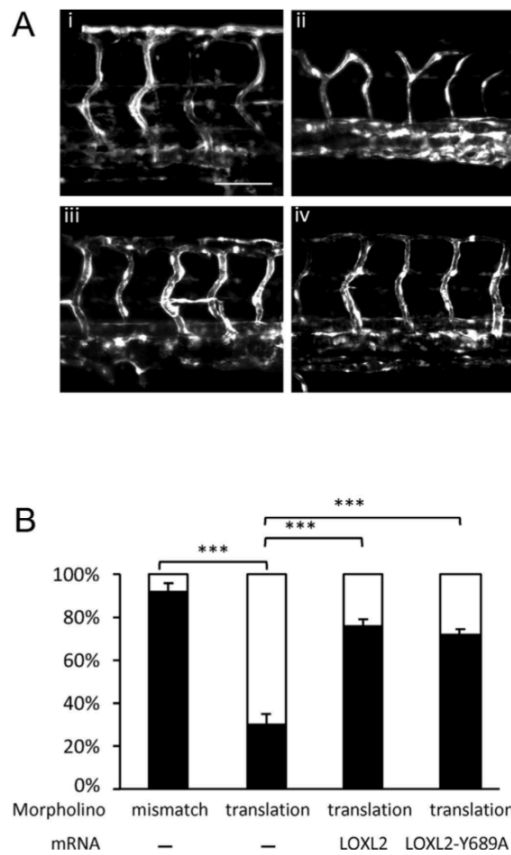


Fig. 4. LOXL2 catalytic activity is not necessary for ISV formation. **A** and **B**: Zebrafish embryos were co-injected with a mismatch morpholino (i) or a morpholino targeting LOXL2 translation (ii-iv), and co-injected with an mRNA encoding either human wild type LOXL2 (iii) or the Y689A catalytic site mutant of human LOXL2 (iv). **A**: Capillary formation was analyzed in $tg(fli1:EGFP)y^1$ zebrafish embryos by lightsheet microscopy. Bar: 100 μ m **B**: ISV displaying blood circulation were counted at 72 hpf. Graph presents the quantification of embryos displaying less (black box) and more (white box) than 5 non-circulating ISV of 5 independent experiments \pm SD. $***P < 0.0001$.

proteins. A similar pattern of collagen IV deposition lacking large fibrillar structures was also observed when endothelial cells were seeded on collagen I or fibronectin (Fig. 7B). Under such culture conditions, LOXL2 followed the same pattern of deposition as collagen IV: the large fibrillar structures detected when cells were seeded in the absence of coating were lost when cells were seeded on fibronectin or collagen I (Fig. 7B). Quite remarkably, LOXL2 depletion only altered collagen IV deposition in the absence of coating (Fig. 7C-left column) but did not affect the fine and homogenous distribution of

collagen IV in the ECM when endothelial cells were seeded on collagen I or fibronectin (Fig. 7C- middle and right column). These data suggest that LOXL2 is part of large macromolecular complexes of ECM proteins whose deposition is mutually relying on the presence of one of the components in the ECM.

Discussion

Morphogenetic processes are tightly regulated by remodeling of the microenvironment, including

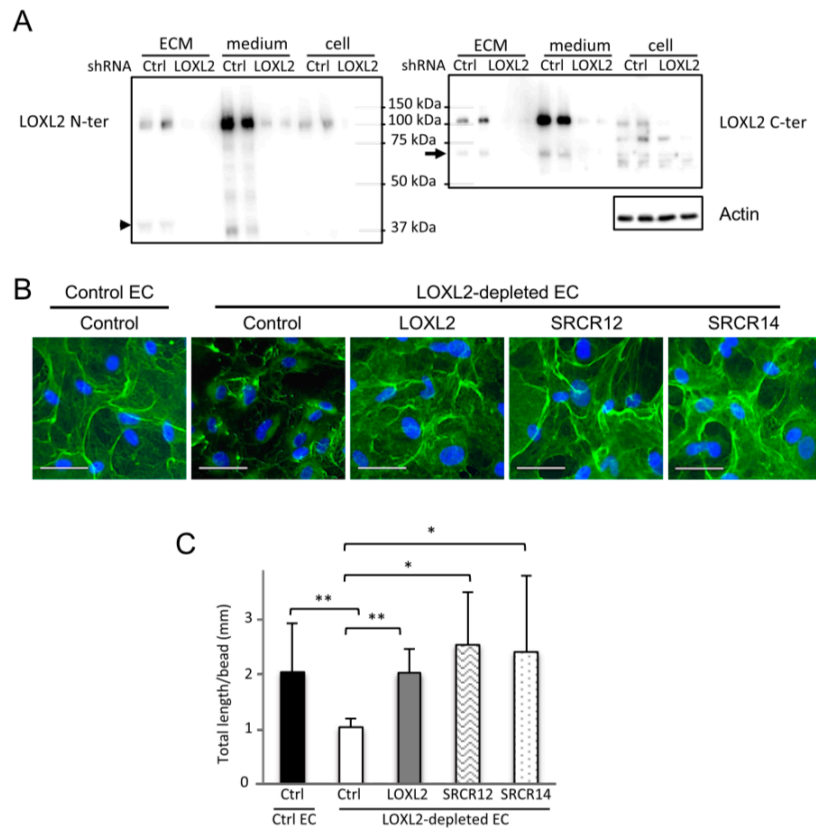


Fig. 5. LOXL2 SRCR domains are effective for collagen IV deposition and capillary formation. **A:** Overnight medium of control and LOXL2-depleted cells was collected, and cell and ECM lysates were prepared. Proteins from duplicate culture wells were separated by SDS-PAGE and LOXL2 was identified by Western blot using antibodies directed against either the N-terminus (left panel) or the C-terminal catalytic domain (top right panel). Arrowhead indicates the N-terminal 42 kDa fragment, and arrow indicates the 65 kDa C-terminal fragment. Similar amounts of proteins were loaded on both gels. Actin was detected in cell lysates as a loading control (bottom right panel). **B:** Control and LOXL2-depleted endothelial cells (EC) were transduced with lentivirus encoding either GFP (control) or LOXL2 or LOXL2 deleted for the catalytic domain and SRCR domains 3 and 4 (SRCR12) or for the catalytic domain only (SRCR14). Immunostaining of collagen IV was performed 5 days after seeding. Bar: 25 μ m **C:** Capillary formation was assessed after 6 days of culture using the cytodex bead assay. Sprout length was measured in 3 independent experiments performed in duplicate wells. Graph presents the mean value of total sprout length/bead \pm SD. * $P < 0.05$ and ** $P < 0.005$.

composition and physical properties of basement membrane [35,42]. Sprouting angiogenesis indeed requires *de novo* building of the vascular basement membrane at the surface of growing capillaries, as demonstrated for several components, including collagen IV [33] and fibronectin [37]. We have previously demonstrated the impact of LOXL2 depletion on collagen IV deposition and angiogenesis [10]. We here describe impairment of the

deposition of fibronectin and perlecan, suggesting that LOXL2 acts as a key regulator of the organization of the vascular basement membrane. Our data also demonstrate that the catalytic activity of LOXL2 is not involved in these processes. Using a structure-function approach, we actually found that LOXL2 SRCR domains alone play a central role in ECM generation and capillary formation. Our data thus suggest that LOXL2 could act as a scaffolding

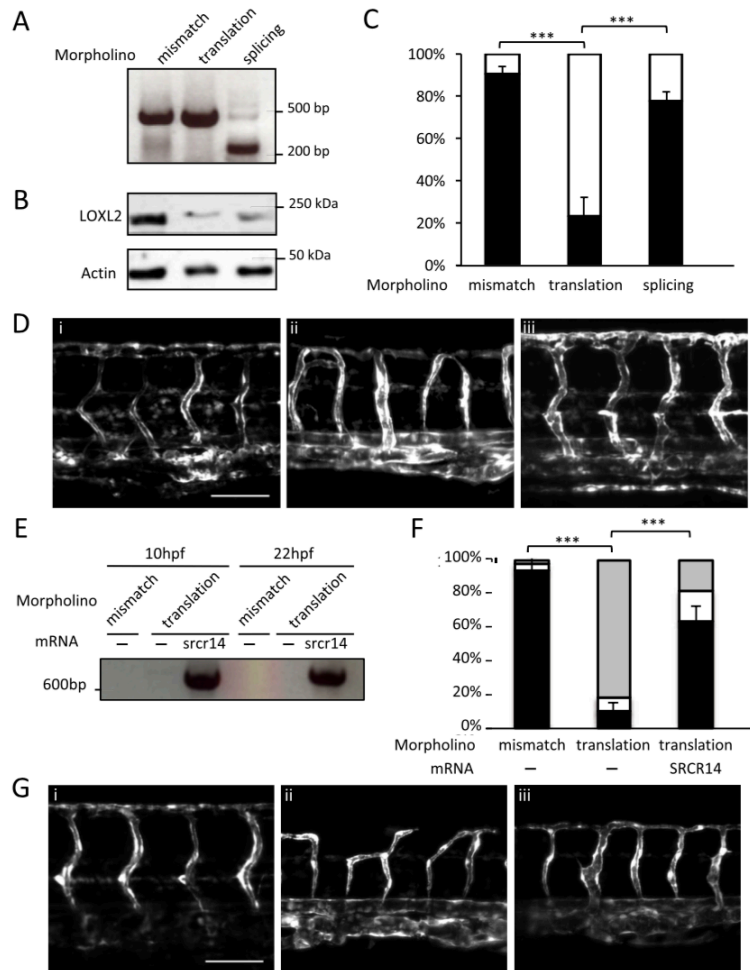


Fig. 6. LOXL2 SRCR domains regulate ISV formation in zebrafish embryo. A-D. Zebrafish embryos were injected with a mismatch (i) or a translation morpholino targeting LOXL2 (ii), or a splicing morpholino targeting exon 9 (iii). Splicing of *loxl2* was verified by RT-PCR (A) and deletion of the catalytic domain was confirmed by Western blot using an antibody directed against the catalytic domain (B). ISV displaying blood circulation were counted at 72 hpf (C). Graph presents the quantification of embryos displaying less (black box) and more (white box) than 5 non-circulating ISV of 4 independent experiments \pm SD. $***P < 0.0001$. Capillary formation was investigated in *tg(fli1:EGFP)¹* zebrafish embryos by lightsheet microscopy. Bar: 100 μ m (D). E-G. Zebrafish embryos were injected with mismatch (i) or translation morpholino targeting LOXL2 (ii), and co-injected with an mRNA encoding human LOXL2 deleted for the catalytic domain (SRCR14) (iii). Amount of human mRNA was assessed by RT-PCR (E). ISV displaying blood circulation were counted at 72 hpf (F). Embryos were distributed in three groups displaying less than 5 (black box), 5 to 10 (white box) or more than 10 (grey box) non-circulating ISV. Graph presents the mean value of 5 independent experiments \pm SD. $***P < 0.0001$. G: Capillary formation was investigated in *tg(fli1:EGFP)¹* zebrafish embryos by lightsheet microscopy. Bar: 100 μ m.

protein participating to the macromolecular organization of the ECM, thus providing the appropriate microenvironment to blood vessels.

Organization of the vascular basement membrane is mediated by the autocrine deposition of ECM components by endothelial cells. Whereas some proteins like laminins and collagen IV undergo self-assembly, the key components and mechanisms that regulate the organization of these macromolecules into supra-structures remain largely unknown. LOXL2 could be a regulator of this process as its depletion alters deposition of several components and mechanical properties of the ECM generated by endothelial cells. Such scaffolding activity would then be completed by LOXL2-mediated crosslinking of collagen IV [32]. A similar function was described for LOX in elastogenesis, as it binds both fibulin-4 and tropoelastin, which is then a substrate for LOX [43]. We detected direct and intracellular interactions of LOXL2 with collagen IV and fibronectin. Progression of collagen IV from the endoplasmic reticulum to secretory vesicles requires post-translational modifications including hydroxylation of lysines and prolines [42], and is regulated by the intracellular specific chaperones HSP47 and Tango1 [44,45]. An appealing hypothesis would be that LOXL2 interacts with the trimeric protomer of collagen IV in the late secretory pathway, and acts as a specific chaperone prior to deposition in the ECM network. Since processing of the SRCR domains is required for cross-linking of collagen IV [40], the N-terminal SRCR domains 1 and 2 could protect collagen IV from premature cross-linking in the secretory pathway, thus promoting the correct formation of the 7S domain in the ECM. Such chaperone activity associated with post-Golgi intracellular trafficking and conserved through evolution has been proposed for other secreted enzymes and for SPARC interaction with collagen IV [46,47]. Antibodies specific for the NC1 and 7S domains of collagen $\alpha 3(\text{IV})$ demonstrated the polarized deposition of collagen IV in the basement membrane, with the 7S pointing to the interstitial matrix [48]. Interaction of LOXL2 with the 7S domain [12] could thus participate to such molecular polarization in the basement membrane. We also detected intracellular and direct interactions of LOXL2 with fibronectin. Binding of fibronectin to LOX catalytic domain had already been described [49]. This interaction was critical for LOX activation even though fibronectin was not a substrate for LOX. Together with the early and high co-localization of LOXL2 and fibronectin in the ECM, these data suggest that a complex between these two proteins could participate in organization of the endothelial ECM.

Whereas the core machinery involved in the trafficking of basement membrane components starts to be established, the mechanisms involved in sorting and targeting these cargo proteins remain

unknown [42]. TIRF microscopy demonstrated that LOXL2 was directly incorporated upon exocytosis into the basal ECM underneath the secreting cell, corresponding to the polarized deposition of ECM. Hot spots of exocytosis appeared to be distributed along filamentous structures, demonstrating intracellular targeting of LOXL2 to the sites of its deposition. Furthermore, LOXL2 was incorporated within the fibrillar structures of the ECM, rather than at their tip, suggesting that it added up proteins in these structures rather than participated to their elongation. In addition, persistence of part of the LOXL2-GFP signal in the ECM for hours after secretion could correspond to the cross-linking of this enzyme to collagen IV [40].

Knocking-down *Loxl2a* expression in zebrafish embryo altered ISV formation, whereas β -APN had no effect. β -APN also hardly inhibited *in vitro* capillary formation by HUVEC [10]. Mutation of the LTQ did not affect capillary formation *in vivo* and *in vitro* either. Similar mutations also had no effect on other LOXL2-mediated functions [11], including regulation of epithelial [50] or endothelial [29] to mesenchymal transition or expression of cell polarity factors [51] or keratinocyte differentiation [52]. In this latter study, an antibody targeting SRCR domain 4 however inhibited LOXL2 impact on differentiation, suggesting that protein interactions of the SRCR domains could be mediating LOXL2 effect. In our study, complete deletion of the catalytic domain further demonstrated the lack of involvement of the enzyme activity, and ruled out the possibility that LOXL2 acts through the CRL domain. Interestingly, intracellular activity of LOXL2 SRCR domains was also demonstrated through their interaction with GATA6 [53].

Propeptides of enzymes are known to regulate their catalytic activity, either by intramolecular promotion of the folding of the catalytic site and/or by inhibition of the enzyme activity [54,55]. Similar function holds true for LOX and LOXL1 propeptides [56,57], but not for LOXL2, as processing of its propeptide is not associated with activation of the amine oxidase activity [40,41]. Other roles have been proposed for processed propeptides of lysyl oxidases, and are still under investigation [43]. Unlike LOX and LOXL1, LOXL2 propeptide is actually not cleaved off from the catalytic domain, but processed in two halves, which releases only the 2 N-terminal SRCR domains (SRCR12). Our recent SAXS and electron microscopy analyses of LOXL2 structure revealed that only SRCR4 is interacting with the catalytic domain, and that the SRCR domains are organized in a string of pearl manner that supports processing and release of SRCR12 domains [9]. This fragment was not detected in endothelial cell lysates, but was naturally occurring after secretion, in agreement with its generation by extracellular serine proteases [40,41]. After

secretion SRCR12 was in both the medium and the ECM, where the ratio of SRCR12 to full length LOXL2 was the highest. We also demonstrated the direct interaction of SRCR12 with collagen IV using SPR. Whereas we did not succeed in expressing the two N-terminal SRCR domains alone in zebrafish embryo, using either splicing morpholino or injection of mRNA, SRCR12 was successfully expressed in endothelial cells and mimicked LOXL2 impact on matrix deposition and capillary formation. Finally, collagen IV deposition by LOXL2-depleted cells was restored when culture support was coated with SRCR12. A general feature of SRCR domains is binding to cell surface and ECM molecules through wide spectrum pattern recognition [3], and dimerization of class A SRCR domains is particularly adapted to recognition of large ligands [58], which corresponds to the proposed interaction between LOXL2 SRCR domains and the 7S domain of collagen IV. These data thus support a novel function for LOXL2 SRCR domains as scaffolding domains in the ECM.

Many mechanisms have been proposed explaining the impact of LOXL2 on cell behavior [3], including through expression of Snail [17,50] or activation of FAK/Src [29,59], both through catalytic or non-catalytic mechanisms. In endothelial cells, intracellular LOXL2 also regulates gene expression through direct interaction of intracellular LOXL2 with GATA6-AS [60]. These authors demonstrated that these effects are distinct from the regulation of angiogenesis, which only involves extracellular LOXL2. Another recent study proposes that LOXL2 and its enzyme-dead mutant regulate similarly the endothelial to mesenchymal transition [29]. The non-catalytic regulation of basement membrane deposition by LOXL2 that we describe fits quite well with these hypotheses. Scaffolding of collagen IV and fibronectin by the ECM-localized LOXL2 could thus play a major role in angiogenesis considering the importance of cell-mediated remodeling of the basement membrane for acquisition of function [42]. Inactivation of genes encoding collagen $\alpha 1$ (IV) and collagen $\alpha 2$ (IV) in mouse resulted in inhibition of sprouting angiogenesis in the developing brain [33]. Fibronectin is also required for angiogenesis, and more particularly cellular fibronectin released by endothelial cells in a polarized and autocrine manner [61,62]. In addition, direct interactions of fibronectin with collagen IV have been known for long and more recent studies have proposed that fibronectin fibrillogenesis is required for collagen IV deposition [63,64]. A complex involving collagen IV, fibronectin and LOXL2 at the interface between endothelial cells and interstitial ECM could thus be required for regulation of angiogenesis. Altogether, our data extend the catalytic function of LOXL2 in biosynthesis of the collagen IV core [32] to a wider role as a non-catalytic scaffolding organizer in the basement membrane at its interface with ECM.

The non-catalytic mechanisms that we identified could participate to the development of pathologies of the vascular basement membrane, including intracranial and retinal aneurysms [21–23]. Such mechanisms should therefore be considered in the context of inhibitor development, especially after failure of recent clinical trials targeting LOXL2 catalytic activity [2,19,20]. Indeed, collagen IV mutations impact the endothelium function in pathologies including small vessel diseases, which are associated with tortuous blood vessels, hemorrhages and aneurysms [65]. Even though collagen IV is present in the basement membrane in these pathologies, transmission electron microscopy reveals interruptions and dilations of the vascular basement membranes. Affecting LOXL2 function in the organization of the vascular basement membrane could thus have long-term effects on endothelial integrity and function.

Experimental procedures

Antibodies and reagents

LOXL2 antibodies were purchased from Cell Signaling Technology (rabbit mAb #69301) (Boston, MA, USA.) and Abnova (mouse mAb #H00004017-M01) (Heidelberg, Germany); type IV collagen antibodies from Novotec (rabbit polyclonal #20411) (Lyon, France); anti-myc clone 9E10 mouse mAb # 11-667-203-001), fluorescent secondary antibodies, DAPI, Amplex Red were purchased from Life Technologies (Carlsbad CA, USA); fibrinogen (#341578) and thrombin (#605190) from Calbiochem/merck (Darmstadt, Germany), VEGF (#293-VE-050) from R&D, horseradish peroxidase, 1,5-diaminopentane and β -APN from Sigma-Aldrich (Saint-Louis, MO, USA).

Cell culture

Human umbilical vein endothelial cells (HUVEC) were prepared and grown as previously described [66] in endothelial cell growth medium (ECGM2). Experiments were performed using HUVEC between passages 2 and 5. Normal human dermal fibroblasts were purchased from Promocell (Heidelberg, Germany) and grown in Fibroblast Growth Medium 2 (Promocell).

Immunofluorescence

Confluent (40,000 cells/cm²) cells were seeded on glass coverslips or in 6 channels ibiTreat microslides ibidi® (Martinsried, Germany) and cultured for 2–5 days before fixation with 4% paraformaldehyde and permeabilization with Triton-X-100 (0.5%). In some experiments, coverslips were coated with 230 μ M of recombinant protein (full length LOXL2-myc-His, LOXL2-SRCR14-myc-His, LOXL2-SRCR12-myc-His) for 1 h at 37 °C. Primary and secondary antibodies were incubated in the presence of 1% normal goat serum. Coverslips were mounted in

Mowiol and for 6 channels ibidi micro-slides, liquid mounting medium was added into each channel. Images were acquired with a spinning disk confocal microscope equipped with an HQ2 coolsnap camera using a 63× objective (Nikon-Roper).

Protein extraction and immunoblotting

For cell lysate, confluent HUVECs were directly extracted with Laemmli buffer containing DTT (50 mM) before separation by SDS-PAGE. For HUVEC ECM proteins, cells were detached on ice with 0.5% DOC, washed with PBS prior to similar protein extraction. For secreted protein, overnight serum-free ECGM2 was collected and centrifuged. Proteins were precipitated with 1% TCA followed with acetone and ether washes, before treatment with Laemmli buffer.

For zebrafish analysis, 10 dechorionated embryos were lysed in 25 mM Tris pH 7.5, 100 mM NaCl, 5 mM EDTA, 0.5% DOC, 0.5% NP40® containing protease inhibitor cocktail (Sigma-Aldrich). Lysates were centrifuged 15 min at 15000 rpm and pellets were solubilized in Laemmli buffer containing DTT.

Proteins were then separated by SDS-PAGE and transferred to PVDF membranes before incubation with the appropriate antibodies in 25 mM Tris-HCl, pH 7.4, 0.1% Tween 20, and 5% milk. Immunological detection was performed with streptavidin-horseradish peroxidase (HRP) conjugated secondary antibodies, using ECL (Life Technologies) as a substrate.

Atomic force microscopy

Matrix stiffness was determined by probe force spectroscopy using an atomic force microscope (NanoWizard 3, JPK Instruments, Berlin, Germany) placed on a vibration isolation table. A silicon nitride cantilever with conical tip (0.06 N/m) was used. Exact spring constant was determined upon calibration in PBS by the thermal noise method prior to each experiment. We used the Young's modulus of the endothelial ECM as a measurement of matrix elasticity. AFM force-distance curves were transformed to force-indentation curves and fitted using the JPK data processing software. Automated curve fitting was applied using the first 500 nm of indentation as a fitting range, and using the contact-point independent linear Hertz-Sneddon model modified for a cone [67].

SPR binding assays

SPR binding assays were carried out in a Biacore T100 system (GE Healthcare, Protein Science Facility, UMS 3444, Lyon, France) using human placenta collagen IV and human plasma fibronectin (C7521 and F2006, Sigma). They were covalently immobilized on a dextran-covered CM5 sensor chip using the amine coupling kit (GE Healthcare) according to the manufacturer's instructions at a flow rate of 5 μ L/min with 10 mM Hepes, 150 mM NaCl, P20 0.05% pH 7.4 as running buffer. The carboxyl groups of CM5 sensor chips were activated by injecting N-hydroxysuccinimide/1-ethyl-3-(3-dimethylaminopropyl) carbodiimide for 420 s. Ligands were injected for 420 s at

100 μ g/mL over the activated sensor chip. The residual activated groups were blocked by injecting 1 M ethanolamine pH 8.5 for 420 s. Two injections of running buffer of 60 s each were then performed. The immobilization levels were 4039 RUs for collagen IV and 3000 RUs for fibronectin.

Several concentrations of full-length LOXL2 (8, 16, 32, 64 and 128 nM) and SRCR12 domains (62.5, 125, 250, 500 nM and 1 μ M) were injected at 30 μ L/min for 180s over immobilized ligands and over a control flow cell submitted to the coupling steps without ligand to evaluate non specific binding, which was subtracted from raw data. The association (k_a) and dissociation rate (k_d) constants and the equilibrium dissociation constant (KD) were calculated using the Biaevaluation software (version 2.0.3).

Proximity ligation assay (PLA)

Proximity ligation assay was performed using the Duolink® In Situ Red Starter Kit mouse/rabbit (Sigma-Aldrich) following the manufacturer's instructions. Briefly, HUVEC were grown on 6-channel micro-slides (ibidi, Martinsried, Germany). Cells were washed once with PBS, fixed with 4% paraformaldehyde in PBS and permeabilized with TritonX-100 (0.5%). LOXL2 was detected with a primary rabbit anti-human antibody (Cell signaling technologies), while collagen IV and fibronectin were detected using mouse anti-human antibodies (Millipore). The kit provided the corresponding probes of anti-rabbit PLUS and anti-mouse MINUS. Nuclei were then stained with DAPI containing mounting medium. Stacks of 26–30 images with a 300 nm step were acquired with a Nikon Ti-Roper iLas confocal spinning disk microscope, equipped with an HQ2 cool snap camera with a 100× objective.

TIRF microscopy

LOXL2-GFP cells were seeded in a glass bottom micro-dish (ibidi, Martinsried, Germany) in ECGM2. Cells were maintained in an environmental control system at 37 °C, 5% CO₂ (Life Imaging System, Basel, Switzerland) and imaged after 24 or 48 h. One solid-state laser line (488 nm) was coupled to a TIRF condenser and time-lapse images were collected with a Nikon Ti-Roper iLas TIRF microscope, equipped with an Evolve EMCCD camera (Roper Scientific, Evry, France).

Expression vector, lentivirus, and shRNA tools

cDNA encoding human wild-type and mutant LOXL2 constructs were cloned in pLenti6/V5-DEST using the Gateway LR clonase™ II (Life Technologies, Grand Island, NY, USA).

HUVEC from each umbilical cord were infected with non-targeting (control) or LOXL2 shRNA. Plasmids encoding shRNA were purchased from Sigma-Aldrich. Lentiviral production was performed using Mission lentiviral packaging mix (Sigma-Aldrich) according to the manufacturer's instructions. For rescue experiments, these cells were super-transduced with virus encoding Green Fluorescent Protein (GFP), LOXL2-GFP, wild-type LOXL2, catalytic

site mutant LOXL2-Y689A, LOXL2-SRCR14 (without catalytic domain) and LOXL2-SRCR12 (without catalytic domain and SRCR 3 and 4). These constructs were silently mutated at the shRNA recognition site. Transductions were repeated using HUVEC from different umbilical cords. Transduced cells were selected for 7 days with puromycin (2 µg/mL) for shRNA-mediated down-regulation and with blasticidin (2 µg/mL) for re-expression.

Lysyl oxidase activity assay

Lysyl oxidase activity was determined using cadaverine as a substrate in a fluorescent assay based on oxidation of Amplex Red to resorufin [68]. Overnight secretion medium from cells expressing wild-type LOXL2 or the catalytic mutant LOXL2-Y689A were incubated in 1.2 M urea, 0.05 M sodium borate, pH 8.2, 1 unit/mL horseradish peroxidase, 10 mM Amplex red, 10 mM of cadaverin at 37 °C for 1 h. Lysyl oxidase activity was calculated as the difference between total amine oxidase and the activity measured in the presence of 500 µM β-APN.

3D capillary formation assay

Three-dimensional fibrin gel assays were carried out as previously described [69]. Briefly, HUVEC were seeded on cytodex beads (GE Healthcare) 24 h before embedding in a 2.5 mg/mL fibrin gel. In some experiments, 230 µM recombinant LOXL2 proteins (LOXL2, LOXL2-SRCR14, LOXL2-SRCR12) were added to the hydrogels. Normal human dermal fibroblasts were plated on top of the gel. Capillaries were allowed to grow for 5–6 days in the presence of complete medium containing 10 ng/mL VEGF. Hydrogels were then fixed with 4% paraformaldehyde, stained with phalloidin-Alexa Fluor 488 and imaged with a Nikon Ti-Roper iLas confocal spinning disk microscope equipped with an HQ2 cool snap camera using a 10× objective (Nikon-Roper). Total tube length per bead was measured using ImageJ.

Downregulation of *Loxl2a* and ISV analysis in zebrafish embryo

Wild-type, Tg(*flil1*:EGFP)¹ and Tg(*kdrl*:EGFP) zebrafish embryos were maintained according to common practices at 28 °C in embryo medium. Four ng of the translation morpholino targeting *loxl2a* or a control morpholino or a splicing morpholino targeting exons 5 and 6 of *loxl2a*, were microinjected into one- to two-cell stage embryos as previously described. Morpholinos were purchased from Gene Tools, LLC (Philomath, OR, USA). The following primers were used to detect splicing: forward 5'-AGCTGTAGACTAGGCAAAGCT-3'; reverse: 5'-CCATTTGAAGGACGTGTGGAA-3'.

For mRNA injection, 100 ng of each mRNA coding for LOXL2, LOXL2-Y689A or SRCR14-LOXL2, were co-microinjected into one- to two-cell stage embryos with 4 ng of the translation morpholino. The following primers were used to detect *srcr14-loxl2* mRNA: forward 5'-GACCGTCTGCGACGACAAG-3'; reverse 5'-GGTGATGATGACCGGTATGC-3'. Morphology of capillaries was investi-

gated at 72 hpf using a home-built digital scanned laser light sheet microscope (DSLIM) based on Keller and collaborators report [70] using a single illumination. Embryos were mounted in 1% low-melting agarose in a glass capillary (2 mm diameter) and extruded in an immersion chamber with a transferpiston (Brand, Wertheim, Germany). Samples were excited at 488 nm (Coherent, USA) with a 10×/0.3 objective lens (Leica, Germany). The focal plane of a 20×/0.5 U-V-I water-immersion objective lens (Leica, Germany) was imaged onto an sCMOS Orca Flash4 2.0 camera (Hamamatsu, Japan) through emission filter (Semrock, Rochester, NY, USA). Sample was moved using three motorized linear stage (M-111.1DG) and one rotative stage (M-660.55) (Physik Instrumente, Karlsruhe, Germany) controlled with custom-made software written in Labview (National Instruments, Austin, TX, USA). Stacks of 200-300 slices were processed with Fiji and orientated using the Interactive Stack Rotation plugin [71]. Images are presented as the maximum intensity projection of one half of the embryo.

Recombinant protein purification

The cDNA encoding either full length human LOXL2 or forms consisting of the four or two N-terminal SRCR domains were inserted in pcDNA3.1-myc-His at HindIII and XbaI restriction sites. PCR fragments were generated using the following primers: 5'-AAGCTTATGGAGAGGCCTCTG-3' and 5'-TCTAGACTGCGGGGACAGCTG-3' for LOXL2, 5'-TCTAGAGTTCTGAGCAGGC-3' for SRCR14 and 5'-TCTAGAGAATCTTGAGGGTCC-3' for SRCR12. Co-expression in dihydrofolate reductase-deficient CHO cells with the *dhfr* gene was performed using lipofectamine 2000 according to the manufacturer recommendations (Thermo Fischer Scientific, Waltham, MA). High expression clones were generated by serial subcloning in the presence of increasing concentrations of methotrexate (Sigma-Aldrich, St Louis, MO). Production and purification of recombinant proteins was performed on HisTrap columns (GE Healthcare, Pittsburgh, PA) as previously described [9].

Statistics

Statistical analysis of data was performed with Student t-test, unless otherwise stated and considered significant when P value < 0.05 (GraphPad Prism 4, GraphPad Software). Error bars represent the standard deviation.

Acknowledgements

We thank Yves Dupraz for fabrication of parts of the lightsheet microscope, Matthieu Boukaissi and Christine Rampon from the zebrafish facility, and Carole Gauron for help with zebrafish injections, and Sabrina Martin for RT-qPCR experiments.

Appendix A. Supplementary data

Supplementary data to this article can be found online at <https://doi.org/10.1016/j.matbio.2019.11.003>.

⁵ JT is now at Bordeaux Imaging Center, Photonic Unit, Bordeaux, France, France.

Funding

Building the lightsheet microscope was supported by grants from Fondation pour la Recherche Médicale (DBS20131128438) and ANR PulpCell to LM. AFM was acquired through an ERPT grant from Fondation Leducq to SG.

SPR assays were supported by grants from Fondation pour la Recherche Médicale (DBI20141231336 to SRB).

CUD was supported by Ministère de l'enseignement et de la Recherche. CPT was supported by Association pour la Recherche sur le Cancer (ARC); MFM by Fondation pour la Recherche Médicale (FRM); YA by la Ligue Nationale contre le Cancer.

Author contributions

Conceptualization: CUD, CPT, LM - Investigation: CUD, CPT, MFM, YA, RS, MM, AB, CAR - Methodology: YA, JT, PG, MFM - Visualization: CUD, YA, MFM, SRB - Funding acquisition: SG, LM - Writing: Original draft: LM - Review and editing: SRB, PG, MFM, CM, SG.

Competing financial interests

Authors declare no competing financial interests.

Received 8 August 2019;

Received in revised form 8 November 2019;

Accepted 12 November 2019

Available online xxxx

Keywords:

Lysyl oxidase;
Angiogenesis;
ECM organization;
Vascular basement membrane;
Microenvironment remodeling

¹ Contributed equally as second author to this work.

² Contributed equally as last author to this work.

³ CUD is now at INSERM U944, CNRS UMR7212, Institut Universitaire d'Hématologie, Sorbonne Paris Cité, Université Paris Diderot, Hôpital St. Louis, Paris, France.

⁴ CPT is now at Institut Curie, PSL Research University, INSERM U1021, CNRS UMR3347, Orsay, France.

References

- [1] J.M. Mäki, Lysyl oxidases in mammalian development and certain pathological conditions, *Histol. Histopathol.* 24 (2009) 651–660.
- [2] P.C. Trackman, Lysyl oxidase isoforms and potential therapeutic opportunities for fibrosis and cancer, *Expert Opin. Ther. Targets* 20 (2016) 935–945.
- [3] H.J. Moon, J. Finney, T. Ronnebaum, M. Mure, Human lysyl oxidase-like 2, *Bioorg. Chem.* 57 (2014) 231–241.
- [4] V.G. Martinez, S.K. Moestrup, U. Holmskov, J. Mollenhauer, F. Lozano, The conserved scavenger receptor cysteine-rich superfamily in therapy and diagnosis, *Pharmacol. Rev.* 63 (2011) 967–1000.
- [5] V. Barry-Hamilton, R. Spangler, D. Marshall, S. McCauley, H.M. Rodriguez, M. Oyasu, A. Mikels, M. Vaysberg, H. Ghermazien, C. Wai, C.A. Garcia, A.C. Velayo, B. Jorgensen, D. Biermann, D. Tsai, J. Green, S. Zaffryar-Eliot, A. Holzer, S. Ogg, D. Thai, G. Neufeld, P. Van Vlasselaer, V. Smith, Allosteric inhibition of lysyl oxidase-like-2 impedes the development of a pathologic microenvironment, *Nat. Med.* 16 (2010) 1009–1017.
- [6] J. Yang, K. Savvatis, J.S. Kang, P. Fan, H. Zhong, K. Schwartz, V. Barry, A. Mikels-Vigdal, S. Karpinski, D. Korniyev, J. Adamkewicz, X. Feng, Q. Zhou, C. Shang, P. Kumar, D. Phan, M. Kasner, B. López, J. Diez, K.C. Wright, R.L. Kovacs, P.S. Chen, T. Quertermous, V. Smith, L. Yao, C. Tschöpe, C.P. Chang, Targeting LOXL2 for cardiac interstitial fibrosis and heart failure treatment, *Nat. Commun.* 7 (2016) 13710.
- [7] Y. Wei, T.J. Kim, D.H. Peng, D. Duan, D.L. Gibbons, M. Yamauchi, J.R. Jackson, C.J. Le Saux, C. Calhoun, J. Peters, R. Derynck, B.J. Backes, H.A. Chapman, Fibroblast-specific inhibition of TGF- β 1 signaling attenuates lung and tumor fibrosis, *J. Clin. Investig.* 127 (2017) 3675–3688.
- [8] H. Schilter, A.D. Findlay, L. Perryman, T.T. Yow, J. Moses, A. Zahoor, C.I. Turner, M. Deodhar, J.S. Foot, W. Zhou, A. Greco, A. Joshi, B. Rayner, S. Townsend, A. Buson, W. Jarolimek, The lysyl oxidase like 2/3 enzymatic inhibitor, PXS-5153A, reduces crosslinks and ameliorates fibrosis, *J. Cell Mol. Med.* 23 (2019) 1759–1770.
- [9] C.E.H. Schmelzer, A. Heinz, H. Troilo, M.P. Lockhart-Cairns, T.A. Jowitt, M.F. Marchand, L. Bidault, M. Bignon, T. Hedtke, A. Barret, J.C. McConnell, M.J. Sherratt, S. Germain, D.J.S. Hulmes, C. Baldock, L. Muller, Lysyl oxidase-like 2 (LOXL2)-mediated cross-linking of tropoelastin, *FASEB J.* 33 (2019) 5468–5481.
- [10] M. Bignon, C. Pichol-Thievend, J. Hardouin, M. Malbouyres, N. Bréchet, L. Nasciutti, A. Barret, J. Teillon, E. Guillon, E. Etienne, M. Caron, R. Joubert-Caron, C. Monnot, F. Ruggiero, L. Muller, S. Germain, Lysyl oxidase-like protein-2 regulates sprouting angiogenesis and type IV collagen assembly in the endothelial basement membrane, *Blood* 118 (2011) 3979–3989.

Please cite this article as: C. Umana-Diaz, C. Pichol-Thievend, M. F. Marchand, et al., Scavenger Receptor Cysteine-Rich domains of Lysyl Oxidase-Like2 regulate endothelial ECM and angiogenesis thro..., *Matrix Biology*, <https://doi.org/10.1016/j.matbio.2019.11.003>

- [11] P.C. Trackman, Enzymatic and non-enzymatic functions of the lysyl oxidase family in bone, *Matrix Biol.* 52–54 (2016) 7–18.
- [12] C. Anazco, A.J. López-Jiménez, M. Rafi, L. Vega-Montoto, M.Z. Zhang, B.G. Hudson, R.M. Vanacore, Lysyl oxidase-like-2 cross-links collagen IV of glomerular basement membrane, *J. Biol. Chem.* 291 (2016) 25999–26012.
- [13] R. Aviram, S. Zaffryar-Eilot, D. Hubmacher, H. Grunwald, J.M. Mäki, J. Myllyharju, S.S. Apte, P. Hasson, Interactions between lysyl oxidases and ADAMTS proteins suggest a novel crosstalk between two extracellular matrix families, *Matrix Biol.* 75–76 (2019) 114–125.
- [14] T. Sasaki, F.G. Hanisch, R. Deutzmann, L.Y. Sakai, T. Sakuma, T. Miyamoto, T. Yamamoto, E. Hannappel, M.L. Chu, H. Lanig, K. von der Mark, Functional consequence of fibulin-4 missense mutations associated with vascular and skeletal abnormalities and cutis laxa, *Matrix Biol.* 56 (2016) 132–149.
- [15] A.R.F. Godwin, M. Singh, M.P. Lockhart-Cairns, Y.F. Alanazi, S.A. Cain, C. Baldock, The role of fibrillin and microfibril binding proteins in elastin and elastic fibre assembly, *Matrix Biol.* (2019). [Epub ahead of print].
- [16] F. Mahjour, V. Dambal, N. Shrestha, V. Singh, V. Noonan, A. Kantarci, P.C. Trackman, Mechanism for oral tumor cell lysyl oxidase like-2 in cancer development: synergy with PDGF-AB, *Oncogenesis* 8 (2019) 34.
- [17] H. Peinado, M. Del Carmen Iglesias-de la Cruz, D. Olmeda, K. Csiszar, K.S. Fong, S. Vega, M.A. Nieto, A. Cano, F. Portillo, A molecular role for lysyl oxidase-like 2 enzyme in snail regulation and tumor progression, *EMBO J.* 24 (2005) 3446–3458.
- [18] A. Millanes-Romero, N. Herranz, V. Perra, A. Iturbide, J. Loubat-Casanovas, J. Gil, T. Jenuwein, A. Garcia de Herreros, S. Peiró, Regulation of heterochromatin transcription by Snail1/LOXL2 during epithelial-to-mesenchymal transition, *Mol. Cell* 52 (2013) 746–757.
- [19] D. Schuppan, M. Ashfaq-Khan, A.T. Yang, Y.O. Kim, Liver fibrosis: direct antifibrotic agents and targeted therapies, *Matrix Biol.* 68–69 (2018) 435–451.
- [20] A.J. Muir, C. Levy, H.L.A. Janssen, A.J. Montano-Loza, M.L. Shiffman, S. Caldwell, V. Luketic, D. Ding, C. Jia, B.J. McColgan, J.G. McHutchison, G. Mani Subramanian, R.P. Myers, M. Manns, R. Chapman, N.H. Afdhal, Z. Goodman, B. Eksteen, C.L. Bowlus, GS-US-321-0102 investigators, simtuzumab for primary sclerosing cholangitis: phase 2 study results with insights on the natural history of the disease, *Hepatology* 69 (2019) 684–698.
- [21] H. Akagawa, A. Narita, H. Yamada, A. Tajima, B. Krischek, H. Kasuya, T. Hori, M. Kubota, N. Saeki, A. Hata, T. Mizutani, I. Inoue, Systematic screening of lysyl oxidase-like (LOXL) family genes demonstrates that LOXL2 is a susceptibility gene to intracranial aneurysms, *Hum. Genet.* 121 (2007) 377–387.
- [22] M. López-Luppo, V. Nacher, D. Ramos, J. Catita, M. Navarro, A. Carretero, A. Rodriguez-Baeza, L. Mendes-Jorge, J. Ruberte, Blood vessel basement membrane alterations in human retinal microaneurysms during aging, *Investig. Ophthalmol. Vis. Sci.* 58 (2017) 1116–1131.
- [23] Y. Wu, Z. Li, Y. Shi, L. Chen, H. Tan, Z. Wang, C. Yin, L. Liu, J. Hu, Exome sequencing identifies LOXL2 mutation as a cause of familial intracranial aneurysm, *World Neurosurg* 109 (2018) e812–e818.
- [24] A. Martín, F. Salvador, G. Moreno-Bueno, A. Floristán, C. Ruiz-Herguido, E.P. Cuevas, S. Morales, V. Santos, K. Csiszar, P. Dubus, J.J. Haigh, A. Bigas, F. Portillo, A. Cano, Lysyl oxidase-like 2 represses Notch1 expression in the skin to promote squamous cell carcinoma progression, *EMBO J.* 34 (2015) 1090–1109.
- [25] J. Steppan, H. Wang, Y. Bergman, M.J. Rauer, S. Tan, S. Jandu, K. Nandakumar, S. Barreto-Ortiz, R.N. Cole, T.N. Boronina, W. Zhu, M.K. Halushka, S.S. An, D.E. Berkowitz, L. Santhanam, Lysyl oxidase-like 2 depletion is protective in age-associated vascular stiffening, *Am. J. Physiol. Heart Circ. Physiol.* 317 (2019) H49–H59.
- [26] R. del Toro, C. Prahst, T. Mathivet, G. Siegfried, J.S. Kaminker, B. Larrivee, C. Breant, A. Duarte, N. Takakura, A. Fukamizu, J. Penninger, A. Eichmann, Identification and functional analysis of endothelial tip cell-enriched genes, *Blood* 116 (2010) 4025–4033.
- [27] T. Van Bergen, R. Spangler, D. Marshall, K. Hollanders, S. Van de Veire, E. Vandewalle, L. Moons, J. Herman, V. Smith, I. Stalmans, The role of LOX and LOXL2 in the pathogenesis of an experimental model of choroidal neovascularization, *Investig. Ophthalmol. Vis. Sci.* 56 (2015) 5280–5289.
- [28] S. Zaffryar-Eilot, D. Marshall, T. Voloshin, A. Bar-Zion, R. Spangler, O. Kessler, H. Ghermazien, V. Brekman, E. Suss-Toby, D. Adam, Y. Shaked, V. Smith, G. Neufeld, Lysyl oxidase-like-2 promotes tumour angiogenesis and is a potential therapeutic target in angiogenic tumours, *Carcinogenesis* 34 (2013) 2370–2379.
- [29] O.G. de Jong, L.M. van der Waals, F.R.W. Kools, M.C. Verhaar, B.W.M. van Balkom, Lysyl oxidase-like 2 is a regulator of angiogenesis through modulation of endothelial-to-mesenchymal transition, *J. Cell. Physiol.* 234 (2019) 10260–10269.
- [30] M. Potente, H. Gerhardt, P. Carmeliet, Basic and therapeutic aspects of angiogenesis, *Cell* 146 (2011) 873–887.
- [31] M. Marchand, C. Monnot, L. Muller, S. Germain, Extracellular matrix scaffolding in angiogenesis and capillary homeostasis, *Semin. Cell Dev. Biol.* 69 (2019) 147–156.
- [32] K.L. Brown, C.F. Cummings, R.M. Vanacore, B.G. Hudson, Building collagen IV smart scaffolds on the outside of cells, *Protein Sci.* 26 (2017) 2151–2161.
- [33] E. Pöschl, U. Schlötzer-Schrehardt, B. Brachvogel, K. Saito, Y. Ninomiya, U. Mayer, Collagen IV is essential for basement membrane stability but dispensable for initiation of its assembly during early development, *Development* 131 (2004) 1619–1628.
- [34] W. Halfter, P. Oertle, C.A. Monnier, L. Camenzind, M. Reyes-Lua, H. Hu, J. Candiello, A. Labilloy, M. Balasubramani, P.B. Henrich, M. Plodinec, New concepts in basement membrane biology, *FEBS J.* 282 (2015) 4466–4479.
- [35] A. Pozzi, P.D. Yurchenco, R.V. Iozzo, The nature and biology of basement membranes, *Matrix Biol.* 57–58 (2017) 1–11.
- [36] E.L. George, E.N. Georges-Labouesse, R.S. Patel-King, H. Rayburn, R.O. Hynes, Defects in mesoderm, neural tube and vascular development in mouse embryos lacking fibronectin, *Development* 119 (1993) 1079–1091.
- [37] X. Zhou, R.G. Rowe, N. Hiraoka, J.P. George, D. Wirtz, D.F. Mosher, I. Virtanen, M.A. Chermousov, S.J. Weiss, Fibronectin fibrillogenesis regulates three-dimensional neovessel formation, *Genes Dev.* 22 (2008) 1231–1243.
- [38] D. Toomre, J.A. Steyer, P. Keller, W. Almers, K. Simons, Fusion of constitutive membrane traffic with the cell surface observed by evanescent wave microscopy, *J. Cell Biol.* 149 (2000) 33–40.

- [39] S.X. Wang, M. Mure, K.F. Medzihradsky, A.L. Burlingame, D.E. Brown, D.M. Dooley, A.J. Smith, H.M. Kagan, J.P. Klinman, A crosslinked cofactor in lysyl oxidase: redox function for amino acid side chains, *Science* 273 (1996) 1078–1084.
- [40] A.J. Lopez-Jimenez, T. Basak, R.M. Vanacore, Proteolytic processing of lysyl oxidase like-2 in the extracellular matrix is required for crosslinking of basement membrane collagen IV, *J. Biol. Chem.* 292 (2017) 16970–16982.
- [41] K. Okada, H.J. Moon, J. Finney, A. Meier, M. Mure, Extracellular processing of lysyl oxidase-like 2 and its effect on amine oxidase activity, *Biochemistry* 57 (2018) 6973–6983.
- [42] A.J. Isabella, S. Horne-Badovinac, Building from the ground up: basement membranes in *Drosophila* development, *Curr. Top. Membr.* 76 (2015) 305–336.
- [43] P.C. Trackman, Functional importance of lysyl oxidase family propeptide regions, *J Cell Commun Signal* 12 (2018) 45–53.
- [44] T. Marutani, A. Yamamoto, N. Nagai, H. Kubota, K. Nagata, Accumulation of type IV collagen in dilated ER leads to apoptosis in Hsp47-knockout mouse embryos via induction of CHOP, *J. Cell Sci.* 117 (2004) 5913–5922.
- [45] D.G. Wilson, K. Phamluong, L. Li, M. Sun, T.C. Cao, P.S. Liu, Z. Modrusan, W.N. Sandoval, L. Rangell, R.A. Carano, A.S. Peterson, M.J. Solloway, Global defects in collagen secretion in a Mia3/TANGO1 knockout mouse, *J. Cell Biol.* 193 (2011) 935–951.
- [46] I. Lindberg, B. Tu, L. Muller, I.M. Dickerson, Cloning and functional analysis of *C. elegans* 7B2, *DNA Cell Biol.* 17 (1998) 727–734.
- [47] A. Chioran, S. Duncan, A. Catalano, T.J. Brown, M.J. Ringuette, Collagen IV trafficking: the inside-out and beyond story, *Dev. Biol.* 431 (2017) 124–133.
- [48] W. Halfter, C. Monnier, D. Müller, P. Oertle, G. Uechi, M. Balasubramani, F. Safi, R. Lim, M. Loparic, P.B. Henrich, The bi-functional organization of human basement membranes, *PLoS One* 8 (2013), e67660.
- [49] B. Fogelgren, N. Polgár, K.M. Szauder, Z. Ujfaludi, R. Laczkó, K.S. Fong, K. Csiszar, Cellular fibronectin binds to lysyl oxidase with high affinity and is critical for its proteolytic activation, *J. Biol. Chem.* 280 (2005) 24690–24697.
- [50] E.P. Cuevas, G. Moreno-Bueno, G. Canesin, V. Santos, F. Portillo, A. Cano, LOXL2 catalytically inactive mutants mediate epithelial-to-mesenchymal transition, *Biol. Open* 3 (2014) 129–137.
- [51] G. Moreno-Bueno, F. Salvador, A. Martín, A. Floristán, E.P. Cuevas, V. Santos, A. Montes, S. Morales, M.A. Castilla, A. Rojo-Sebastián, A. Martínez, D. Hardisson, K. Csiszar, F. Portillo, H. Peinado, J. Palacios, A. Cano, Lysyl oxidase-like 2 (LOXL2), a new regulator of cell polarity required for metastatic dissemination of basal-like breast carcinomas, *EMBO Mol. Med.* 3 (2011) 528–544.
- [52] J. Lugassy, S. Zaffryar-Eilat, S. Soueid, A. Mordoviz, V. Smith, O. Kessler, G. Neufeld, The enzymatic activity of lysyl oxidase-like-2 (LOXL2) is not required for LOXL2-induced inhibition of keratinocyte differentiation, *J. Biol. Chem.* 287 (2012) 3541–3549.
- [53] T. Peng, X. Deng, F. Tian, Z. Li, P. Jiang, X. Zhao, G. Chen, Y. Chen, P. Zheng, D. Li, S. Wang, The interaction of LOXL2 with GATA6 induces VEGFA expression and angiogenesis in cholangiocarcinoma, *Int. J. Oncol.* 55 (2019) 657–670.
- [54] R. Rozenfeld, L. Muller, S. El Messari, C. Llorens-Cortes, The C-terminal domain of aminopeptidase A is an intramolecular chaperone required for the correct folding, cell surface expression, and activity of this monozinc aminopeptidase, *J. Biol. Chem.* 279 (2004) 43285–43295.
- [55] L. Muller, A. Cameron, Y. Fortenberry, E.V. Apletalina, I. Lindberg, Processing and sorting of the prohormone convertase 2 propeptide, *J. Biol. Chem.* 275 (2000) 39213–39222.
- [56] M.V. Panchenko, W.G. Stetler-Stevenson, O.V. Trubetskoy, S.N. Gacheru, H.M. Kagan, Metalloproteinase activity secreted by fibrogenic cells in the processing of prolysin oxidase. Potential role of procollagen C-proteinase, *J. Biol. Chem.* 271 (1996) 7113–7119.
- [57] A. Borel, D. Eichenberger, J. Farjanel, E. Kessler, C. Gleyzal, D.J. Hulmes, P. Sommer, B. Font, Lysyl oxidase-like protein from bovine aorta. Isolation and maturation to an active form by bone morphogenetic protein-1, *J. Biol. Chem.* 276 (2001) 48944–48949.
- [58] J.R. Ojala, T. Pikkarainen, A. Tuuttila, T. Sandalova, K. Tryggvason, Crystal structure of the cysteine-rich domain of scavenger receptor MARCO reveals the presence of a basic and an acidic cluster that both contribute to ligand recognition, *J. Biol. Chem.* 282 (2007) 16654–16666.
- [59] H.E. Barker, D. Bird, G. Lang, J.T. Erler, Tumor-secreted LOXL2 activates fibroblasts through FAK signaling, *Mol. Cancer Res.* 11 (2013) 1425–1436.
- [60] P. Neumann, N. Jaé, A. Knau, S.F. Glaser, Y. Fouani, O. Rossbach, M. Krüger, D. John, A. Bindereif, P. Grote, R.A. Boon, S. Dimmeler, The lncRNA GATA6-AS epigenetically regulates endothelial gene expression via interaction with LOXL2, *Nat. Commun.* 9 (2018) 237.
- [61] B. Cseh, S. Fernandez-Sauze, D. Grall, S. Schaub, E. Doma, E. Van Obberghen-Schilling, Autocrine fibronectin directs matrix assembly and crosstalk between cell-matrix and cell-cell adhesion in vascular endothelial cells, *J. Cell Sci.* 123 (2010) 3989–3999.
- [62] G. Mana, F. Clapero, E. Panieri, V. Panero, R.T. Böttcher, H.Y. Tseng, F. Saltarin, E. Astanina, K.I. Wolanska, M.R. Morgan, M.J. Humphries, M.M. Santoro, G. Serini, D. Valdembrì, PPFIA1 drives active $\alpha 5 \beta 1$ integrin recycling and controls fibronectin fibrillogenesis and vascular morphogenesis, *Nat. Commun.* 7 (2016) 13546.
- [63] C.G. Miller, A. Pozzi, R. Zent, J.E. Schwarzbauer, Effects of high glucose on integrin activity and fibronectin matrix assembly by mesangial cells, *Mol. Biol. Cell* 25 (2014) 2342–2350.
- [64] M.S. Filla, K.D. Dimeo, T. Tong, D.M. Peters, Disruption of fibronectin matrix affects type IV collagen, fibrillin and laminin deposition into extracellular matrix of human trabecular meshwork (HTM) cells, *Exp. Eye Res.* 165 (2017) 7–19.
- [65] M. Jeanne, D.B. Gould, Genotype-phenotype correlations in pathology caused by collagen type IV alpha 1 and 2 mutations, *Matrix Biol.* 57–58 (2017) 29–44.
- [66] A. Cazes, A. Galaup, C. Chomel, M. Bignon, N. Bréchet, S. Le Jan, H. Weber, P. Corvol, L. Muller, S. Germain, C. Monnot, Extracellular matrix-bound angiotensin-like 4 inhibits endothelial cell adhesion, migration, and sprouting and alters actin cytoskeleton, *Circ. Res.* 99 (2006) 1207–1215.
- [67] P. Carl, H. Schillers, Elasticity measurement of living cells with an atomic force microscope: data acquisition and processing, *Pflüg. Arch.* 457 (2008) 551–559.

- [68] A.H. Palamakumbura, P.C. Trackman, A fluorometric assay for detection of lysyl oxidase enzyme activity in biological samples, *Anal. Biochem.* 300 (2002) 245–251.
- [69] N. Beckouche, M. Bignon, V. Lelarge, T. Mathivet, C. Pichol-Thievend, S. Berndt, J. Hardouin, M. Garand, C. Ardidie-Robouant, A. Barret, G. Melino, H. Lortat-Jacob, L. Muller, C. Monnot, S. Germain, The interaction of heparan sulfate proteoglycans with endothelial transglutaminase-2 limits VEGF165-induced angiogenesis, *Sci. Signal.* 8 (2015) ra70.
- [70] P.J. Keller, A.D. Schmidt, J. Wittbrodt, E.H. Stelzer, Reconstruction of zebrafish early embryonic development by scanned light sheet microscopy, *Science* 322 (2008) 1065–1069.
- [71] J. Schindelin, I. Arganda-Carreras, E. Frise, V. Kaynig, M. Longair, T. Pietzsch, S. Preibisch, C. Rueden, S. Saalfeld, B. Schmid, J.Y. Tinevez, D.J. White, V. Hartenstein, K. Eliceiri, P. Tomancak, A. Cardona, Fiji: an open-source platform for biological-image analysis, *Nat. Methods* 9 (2012) 676–682.

Please cite this article as: C. Umana-Diaz, C. Pichol-Thievend, M. F. Marchand, et al., Scavenger Receptor Cysteine-Rich domains of Lysyl Oxidase-Like2 regulate endothelial ECM and angiogenesis thro..., *Matrix Biology*, <https://doi.org/10.1016/j.matbio.2019.11.003>

2. Marchand et al, in preparation

The following paper aims to characterize basement membrane supramolecular assembly by endothelial cells and to address the role of LOXL2 in regulating this scaffolding. We finally investigating the molecular mechanisms connecting LOXL2 function in basement membrane assembly to the angiogenic response of endothelial cells.

Autocrine regulation of endothelial mechanotransduction by LOXL2-mediated assembly of basement membrane

Marion F Marchand^{1,2}, Claudia Umana-Diaz¹, Corinne Ardidie-Robouant¹, Tristan Pilot¹, Sabrina Martin¹, Philippe Mailly¹, Emmanuel Pauthe³, Christophe Guilluy⁴, Catherine Monnot¹, Stéphane Germain^{1,†}, Laurent Muller^{1,†,*}

¹: Center for Interdisciplinary Research in Biology (CIRB), Collège de France, CNRS UMR7241, INSERM U1050, PSL Research University, Paris, France

²: Sorbonne Université, Collège doctoral, Paris, France

³ Equipe de Recherche sur les Relations Matrice Extracellulaire-Cellules (ERRMECe), Institut des Matériaux, Maison International de la Recherche, Université de Cergy-Pontoise, 95000, Neuville sur Oise, France

⁴ : Institute for Advanced Biosciences, INSERM U1209, CNRS UMR 5309, University Grenoble Alpes, La Tronche, France

[†] : contributed equally to this work

^{*} : corresponding author

Present address:

CUD: Centre for Cell Biology, Development and Disease, Department of Biological Sciences, Simon Fraser University, Burnaby, BC V5A 1S6, Canada

Short title: Basement membrane-mediated regulation of mechanotransduction

ABSTRACT

Vascular basement membrane provides the only structural support to blood capillaries at the interface between endothelial cells and tissues. Even though it regulates capillary formation as well as integrity and function, the assembly of capillary basement membrane during angiogenesis is still poorly characterized. In addition to the structural core proteins including laminin, collagen IV and fibronectin, many associated proteins and post-translational modifying enzymes are involved in the generation of basement membrane. We have shown that lysyl oxidase-like 2 regulates both collagen IV assembly and angiogenesis. The precise mechanisms connecting the functional roles of LOXL2 in these processes however remain unknown. We here characterized the early steps of deposition and assembly of basement membrane components by endothelial cells using high resolution correlative atomic force/fluorescence microscopy. We demonstrated that collagen IV, laminin and fibronectin are deposited independently before association of fibronectin microfibrils with self-assembled collagen IV. LOXL2 was involved in linking these two structures and promoted further enrichment and thickening of the basement membrane. We then analyzed the mechanotransduction response of endothelial cells to the defective basement membranes generated upon LOXL2 depletion. Adhesion and contractility machineries were not altered in these cells, but the formation of focal adhesions and their long-term maturation were nonetheless affected, also resulting in defaults in translocation of vinculin and pY118-paxillin to cell-cell junctions. Altogether, we identified a novel autocrine mechanism regulating mechanotransduction through the supramolecular assembly of collagen IV and fibronectin in the basement membrane. Such a pathway could entirely resume the angiogenesis defaults triggered by LOXL2 down-regulation.

251 words

Keywords: angiogenesis, basement membrane, lysyl oxidase, mechanotransduction

ABBREVIATIONS

AFM: atomic force microscopy

BM: basement membrane

CDM: cell-derived matrix

ECIS: Electric Cell-substrate Impedance Sensing

ECM: extracellular matrix

ERK: extracellular signal regulated kinase

FAK: focal adhesion kinase

FN: fibronectin

GFP: green fluorescent protein

HANAC: hereditary angiopathy, nephropathy, aneurysms and muscle cramps

HUVEC: human umbilical vein endothelial cell

LN: laminin

LOX: lysyl oxidase

LOXL2: lysyl oxidase like-2

PHSRN: Pro-His-Ser-Arg-Asn

RGD: arginylglycylaspartic acid

SPARC: secreted protein, acidic, cysteine-rich

SRCR: scavenger receptor cysteine rich

TIRF: total internal reflection fluorescence

VEGF: vascular endothelial growth factor

INTRODUCTION

Basement membranes (BMs) are specialized extracellular matrices developed at the interface of tissues that play major roles for both tissue development and homeostasis. Whereas their function has been restricted to structural support for long, recent studies have highlighted their dynamic roles in the regulation of multiple cellular processes (Jayadev and Sherwood, 2017; Pozzi et al., 2017). Vascular BMs thus provide structural support to blood vessels at the interface between endothelial cells and tissues and are also involved in angiogenesis (Marchand et al., 2019). The diversity of composition and structure of vascular BMs depending on vessel type and vascularized tissue further supports specific roles in the regulation of vascular functions (Liliensiek et al., 2009; Uechi et al., 2014). Many components of vascular BMs are required for the formation of blood capillaries. This has been described for the core components laminins (Estrach et al., 2011; Stenzel et al., 2011) and collagen IV (Bignon et al., 2011; Pöschl et al., 2004), as well as for associated proteins like fibronectin (Turner et al., 2017; Zhou et al., 2008), or for the network linker perlecan (Aviezer et al., 1994; Sharma et al., 1998). Assembly of capillary BM during angiogenesis is however still poorly characterized, mainly for experimental reasons considering the limited access to such structure *in vivo*. Both structural support and regulatory functions of BM have to be effective within hours after initiation of angiogenesis. Indeed, BM assembly is initiated by tip cells (Stenzel et al., 2011), and blood perfusion and perivascular cell recruitment are detected in the first stalk cells in contact with tip cells, as extensively demonstrated in dynamic models including vascularization of the mouse retina and formation of zebrafish intersomitic vessels (Potente et al., 2011).

BM is generated by association of two distinct networks of laminin and collagen IV. Laminin is considered as the foundational building block for assembly through tight association with the cell surface and is then connected to a self-assembled collagen IV network. Recent studies have provided more evidence for the highly organized supramolecular assembly of these proteins within the BM. A major aspect is their polarized distribution that results in specific adhesion and regulatory properties of each side of the BM (Halfter et al., 2013, 2015). The essential role of this supramolecular assembly is illustrated by the impact of point mutations in collagen IV on long term vascular function, which results in many vascular diseases including small vessel disease and HANAC syndrome (Gould et al., 2006; Jeanne and Gould, 2017; Plaisier et al., 2007). We have demonstrated that lysyl oxidase-like 2 is involved in the regulation of BM assembly by endothelial cells (Bignon et al., 2011). More specifically, the involvement of LOXL2 concerned collagen IV assembly, whereas laminin deposition was hardly affected (Umana-Diaz et al., 2020). In addition, LOXL2 is expressed in tip cells in mouse retina (del Toro et al., 2010) and in growing zebrafish intersomitic vessels (Bignon et al., 2011) and regulates both developmental and pathological angiogenesis (Bignon et al., 2011; de Jong et al., 2019; Van Bergen et

al., 2015; Zaffryar-Eilot et al., 2013). Lysyl oxidases (LOX and LOXL-1 to 4) are involved in remodeling the microenvironment both during development and in pathologies including cardiovascular diseases, fibrosis and cancer (Mäki, 2009; Trackman, 2016). These secreted enzymes catalyze the deamination of hydroxylysines and lysines in collagens and elastin. In addition to the conserved catalytic domain, LOXL2 contains 4 repeats of SRCR domains that are organized as a rod-like structure presenting the catalytic domain at its tip (Schmelzer et al., 2019). In agreement with such structure, we have demonstrated that SRCR domains alone were effective in the assembly of collagen IV by endothelial cells, independently of the catalytic domain and activity (Umana-Diaz et al., 2020). LOXL2 also participates to the tensile force of the BM through cross-linking of the 7S domains of collagen IV (Añazco et al., 2016), along with peroxidase that generates sulfilimine crosslinks between NC1 domains (Bhave et al., 2012), and with formation of disulfides. Mechanisms connecting LOXL2 function in BM assembly to angiogenesis however remain to be deciphered considering that multiple functions have been ascribed to LOXL2. These consist in either extracellular activity maintaining a pathological microenvironment (Barry-Hamilton et al., 2010) or intracellular functions involving LOXL2 in epithelial-mesenchymal transition and regulation of gene expression in the context of tumor growth (Millanes-Romero et al., 2013; Peinado et al., 2005). In endothelial cells, LOXL2 also displays intracellular functions regulating gene expression through GATA6-AS interactions (Neumann et al., 2018). LOXL2 alone however does not trigger endothelial-mesenchymal transition, but is only associated with TGF- β -induced endothelial-mesenchymal transition (de Jong et al., 2019; Neumann et al., 2018). Furthermore, these authors also excluded the participation of intracellular function of LOXL2 to the regulation of angiogenesis, providing evidence for the sole extracellular LOXL2 in the regulation of this process (Neumann et al., 2018). Endothelial LOXL2 is also involved in cardiovascular pathologies of the BM including vascular stiffening and aneurysm (Akagawa et al., 2007; López-Luppo et al., 2017; Stepan et al., 2019; Wu et al., 2018). In order to get a better understanding of the mechanisms connecting the involvement of LOXL2 in collagen IV assembly with angiogenesis, we here investigated the assembly of endothelial BM by correlative atomic force/fluorescence microscopy. We demonstrated that LOXL2 finely tunes the association between collagen IV and fibronectin. We then characterized endothelial mechanotransduction in response to the BM they generated and identified paxillin as a mediator of the defaults in adhesion and cell-cell junctions that could mediate the regulation of angiogenesis.

RESULTS

Assembly of endothelial basement membrane

Angiogenesis-associated matrix remodeling was assessed during postnatal vascularization of mouse retina by investigating the distribution of fibronectin and collagen IV in the vascular front (Fig.1). Fibronectin was detected in the avascular microenvironment where it provides tracks to endothelial tip cell filopodia. Higher fibronectin staining was detected at the surface of endothelial tip cells and in the abluminal basement membrane of capillaries. In contrast, collagen IV distribution was restricted to endothelial cell surface, and tip cell processes were protruding out of the collagen IV staining. Such distribution indicated early cell interaction with microenvironment fibronectin followed by its remodeling and incorporation in the basement membrane together with collagen IV. They also suggested the tight regulation of this process during vascular morphogenesis, which could be achieved by LOXL2 since it has been identified as a marker for tip cells in mouse retina (del Toro et al., 2010) and as a regulator of angiogenesis and collagen IV deposition (Bignon et al., 2011). We have indeed already demonstrated that LOXL2 depletion affects collagen IV overall assembly by endothelial cells independently of enzyme activity (Umana-Diaz et al., 2020). We here further characterized ECM deposition using high resolution structural analysis by AFM and fluorescence microscopy. We first established conditions for the preparation of endothelial cell-derived matrix (CDM) and found that six hours was the minimal culture time that ensured the decellularization process did not alter the material deposited (Fig.S1A). Expression of a LOXL2/GFP construct which colocalized with fibronectin in the ECM allowed characterization of the culture conditions required for appropriate basement membrane deposition (Fig.S1B and C). Generation of a homogenous basement membrane-like matrix required cell seeding at confluency and culture over a period of three days. Analysis of topography by AFM 6h post-seeding showed deposition of nascent ECM fibers that were approximately 5 μm long and 30 to 80 nm high (Fig.2A). While these structures displayed only little connection, they extended laterally and connected to form a uniform lattice at 24 hours (Fig.2B) as they also increased in diameter (Fig.2D). Forty-eight hours later, a homogeneous network had been generated, consisting in overlapping fibrillar material that was at least 200 nm high and heightened up to 600 nm (Fig.2C). Extension of the fibrillar network was quantified by calculating the image proportion covered by fibrillar material higher than 50 nm in each condition. Lateral extension of the fibrillar network persisted during the whole process, covering from 2% of the field at 6h to 95% at 72h (Fig.2E). ECM thickening was assessed as the mean height of the fibers in 75 or 5% of the highest structures detected (Fig.2F). Whatever the proportion of fibers analyzed, there was no difference between 6 and 24h, whereas major thickening of the ECM occurred between 24 and 72h (Fig.2F). BM deposition thus

appears as a continuous and progressive process that develops through a biphasic growth involving first lateral elongation, followed by ECM thickening and organization into multiple layers.

We then analyzed the spatio-temporal distribution of ECM components in these structures and thus performed correlative AFM-fluorescence microscopy. CDM generated for 6h and 24h of culture were analyzed for the distribution of fibronectin, collagen IV, laminin and LOXL2 before topography measurements by AFM (Fig.2G-I). We detected a strong colocalization of fibronectin and LOXL2 at both time points (Fig.2G), whereas collagen IV was less co-localized with LOXL2 at 6h and increased over time (Fig.2H), as previously described (Umana-Diaz et al., 2020). We then calculated the correlation rate between the fluorescence signal and AFM-detected structures (Fig.S2). At 6h, ECM nascent fibers mainly contained fibronectin and LOXL2 ($64.20\% \pm 19\%$ and $62.66\% \pm 15\%$ respectively) (Fig.2Gi) and about two and a half times less collagen IV ($26.11\% \pm 9\%$) (Fig.2Hi). Indeed, collagen IV appeared as a granular staining with no specific structure (Fig.2Hi). Collagen IV was however redistributed over time and correlated with the fibrillar structures detected by AFM at 24h ($70.39\% \pm 10\%$) (Fig.2Hii), while no significant change was detected for fibronectin and LOXL2 ($58.18\% \pm 12\%$ and $56.59\% \pm 9\%$) (Fig.2Gii). During the whole process, laminin displayed a diffuse distribution with poor co-localization with fibronectin, and very limited association with the fibrillar structures detected by AFM (Fig.2I) with only $32.05\% \pm 13\%$ correlation at 24h (Fig.2Ii-ii). This analysis suggested that fibronectin and collagen IV were first deposited independently by cells, with high and low rates of association with LOXL2, respectively. These proteins were then redistributed to common supramolecular structures organized as a network over the first 24h, which then matured as supra-structures through overlay of interconnected networks.

LOXL2 drives BM spatio-temporal assembly and cell morphology in a context-dependent manner

We then analyzed the impact of LOXL2-depletion on the early steps of BM deposition by endothelial cells (Fig.3A). Nascent fibrils of fibronectin and granular staining of collagen IV were still generated by cells depleted for LOXL2 at 6h (Fig.3Ai). Fibronectin remodeling was however impacted by LOXL2-depletion at 24h: whereas control cells had remodeled fibronectin into a homogenous meshwork, LOXL2-depleted cells had generated long aligned fibrils of fibronectin (Fig.3Aii). In contrast, collagen IV meshwork formation was not affected by LOXL2-depletion at 24h (Fig.3Aii). As a result, collagen IV co-localization with FN was limited (Fig.3B), and correlative AFM-fluorescence microscopy at 24h allowed detection of granular material alongside the fibrillar structures that was identified as collagen IV by immunostaining (Fig.3C). These data suggested that LOXL2 was responsible for ECM maturation by promoting association of the fibronectin fibrillar material with the collagen IV meshwork

over time. We thus investigated consequences of this maturation impairment by measuring the characteristics of CDM generated after 3 days in culture (Fig.3D-F). LOXL2 depletion highly impacted ECM topography (Fig.3D). The homogeneous multi-layered control ECM was replaced by large sparse aggregates, with a limited network of thin fibrillar structures (Fig.3Dii). LOXL2 depletion indeed induced formation of much thicker structures about twice higher than the fibers generated by control cells (Fig.3E). Correlative AFM-fluorescence microscopy showed that these aggregated structures contained fibronectin and collagen IV (Fig.3F), in agreement with our former fluorescence data (Bignon et al, 2011; Umana-Diaz et al, 2020). These data suggested that LOXL2 stabilizes the structures generated at 24h that otherwise aggregated in the absence of the enzyme. Noticeably, LOXL2 displayed a more punctiform distribution at 72h than at the earlier time points (Fig.3F). A fibrillar distribution of LOXL2/GFP was however detected in the ECM at 72h (Fig.S3), suggesting that maturation of BM over time was accompanied with decrease of access of the antibody to the N-terminus of LOXL2, most probably as a result of steric hindrance. We also performed immunostaining using an antibody directed against the C-terminal half of the protein, but could only detect intracellular LOXL2 and no staining was observed in the ECM (Fig.S4A). In addition, these antibodies did not detect LOXL2/GFP in secretory vesicles (Fig.S4B), further supporting protein interactions of LOXL2 in the late secretory pathway, as we previously described with fibronectin and collagen IV (Umana-Diaz et al, 2020). Overall, this structural analysis demonstrated that LOXL2 was not involved in the secretion/deposition of ECM proteins but was regulating their supramolecular assembly for meshwork extension and thickening. These data suggested that: -1/ fibronectin and collagen IV were independently deposited in the matrix with high and low association with LOXL2, respectively; -2/ fibronectin was deposited as fibrillar structures, while collagen IV assembled in a meshwork pattern after deposition; -3/ these complexes were then remodeled into supramolecular structures in a LOXL2-dependent manner that associated fibronectin to collagen IV following a pattern led by the latter.

The dramatic shift in fibronectin and collagen IV organization between 24h and 72h observed upon knock-down of LOXL2 expression suggested a strong cell-mediated remodeling of the matrix. We thus analyzed the impact of impaired ECM scaffolding on cell morphology and cytoskeleton remodeling. Cell shape was assessed using immunostaining of β -catenin on confluent monolayers and morphometric parameters were calculated (Fig.S5). LOXL2-depleted cells underwent important shape modifications resulting in aligned and more elongated cells as compared to control cells (Fig.4A). Indeed, cell circularity was 30% lower for LOXL2-depleted cells (Fig.4B), and maximum Feret diameter was increased by 1.8-fold in LOXL2-depleted cells (Fig.4C). Whereas F-actin was distributed subcortically in confluent control cells, with a random overall distribution, it was localized in transversal bundles of stress fibers oriented along a preferential axis in LOXL2-depleted cells (Fig.4D-

F). These data suggested that the defects in fibronectin organization detected at 24h impacted cell shape at longer term.

In order to confirm that LOXL2-mediated scaffolding impacted endothelial cell response, we experimentally modulated ECM organization by surface coating fibronectin before seeding cells. We have already shown that such coating modified collagen IV distribution by control cells and rescued its assembly by LOXL2-depleted cells (Umana-Diaz et al., 2020; Fig.5A). The first steps in deposition of fibronectin and collagen IV at 6h were not affected, and only fibronectin remodeling at 24h was slightly impacted (Fig.S6). Furthermore, seeding cells on a gradient of fibronectin demonstrated that a minimal amount of 0.09 $\mu\text{g}/\text{cm}^2$ was sufficient to induce the remodeling of collagen IV thick filamentous structures into a homogeneous network by control cells, while restoration of collagen IV deposition by LOXL2-depleted endothelial cells was only achieved at 1.5 $\mu\text{g}/\text{cm}^2$ fibronectin (Fig.5A). In order to investigate whether these effects were directly mediated by interactions between ECM proteins or induced by enhanced cell adhesion, we compared the impact of fibronectin whole protein to its RGD and PHSRN peptides that mediate cell attachment (Fig.5B) (Akiyama et al., 1995). Surface coating with either RGD or PHSRN did not modify ECM deposition and only full-length fibronectin induced collagen IV remodeling by endothelial cells (Fig.5C), thus supporting that interactions between ECM proteins are driving basement membrane remodeling.

We thus investigated how modulating BM deposition by LOXL2-depleted cells through surface coating with fibronectin impacted cortical actin distribution and cell morphology (Fig.5D-F). No change in either factor was detected in control cells. While LOXL2-depleted cells were elongated and displayed aligned stress fibers at low fibronectin concentration, both cell shape and cytoskeleton organization were shifted to values of control cells when seeded on fibronectin coatings at 1.5 $\mu\text{g}/\text{cm}^2$ (Fig5D-F), the concentration that also rescued matrix deposition by these cells (Fig5A). Altogether, these data demonstrated that ECM scaffolding by LOXL2 was responsible for regulation of cell shape and cytoskeleton remodeling in endothelial cells.

LOXL2 affects endothelial cell mechanotransduction through ECM scaffolding

In order to test whether LOXL2 depletion affected mechanotransduction through ECM organization, we first characterized the intrinsic capacity of cells expressing LOXL2 or not to respond to similar ECM stimuli, without any influence of the ECM they produced. For that purpose, endothelial cells were seeded on fibronectin or collagen I coating one hour before analysis of focal adhesion and cell spreading. Focal adhesions were then visualized with paxillin staining and their morphologic characteristics including surface area, circularity, aspect ratio and mean distance from the edge of cells

were calculated. These experiments revealed equal formation of nascent adhesions at the cell edges and maturation into focal adhesions towards the cell center (Fig.6A-B). Besides, global architecture of the actin cytoskeleton was similar in control and LOXL2-depleted cells in these conditions (Fig.6A). In agreement with these observations, cell spreading was not affected by LOXL2 depletion either (Fig.6C). These results suggested that traction forces developed by endothelial cells during the initial steps of cell adhesion and spreading were not depending on LOXL2 expression. We further investigated mechanotransduction in these cells by measuring cell response to stiffness and thus performed AFM stiffness-clamp experiments. This setup allows to evaluate single endothelial cell mechanosensing by tuning the apparent stiffness of the cell microenvironment in real time (Mitrossilis et al., 2010). Traction force was dynamically recorded while applying a broad range of stiffness values, from 10mN/m to 400mN/m during a continuous single-cell traction force experiment. Control and LOXL2-depleted cells displayed the same increasing traction rate, as the stiffness applied was raised (Fig.6D), indicating that LOXL2 does not impact cell contractility *per se* in response to stiffness. We thus tested whether the defective cytoskeleton organization and cell morphology could result from cell response to the autocrine ECM generated by endothelial cells. Control cells were seeded on cell-derived matrices generated by either control cells or LOXL2-depleted cells and focal adhesions were analyzed 60 minutes after plating. The distribution of paxillin and pY397-FAK in cells seeded on control matrices were similar to that previously described on ECM surface coating (Fig.7A). While matrices prepared from LOXL2-depleted cells were supporting cell adhesion and spreading, they were however not able to promote proper maturation of nascent adhesions into focal adhesions.

To further assess the impact of the defective basement membrane generated in the absence of LOXL2, confluent cells were cultured for three days before analysis of the distribution of adhesion proteins. Phosphorylated FAK was detected in focal adhesions whether cells expressed LOXL2 or not (Fig.7B). The shape and distribution of these adhesion structures was however quite different, with the presence of elongated and aligned adhesions in LOXL2-depleted cells that were reminiscent of the stress fibers described above. Vinculin was detected in similar focal adhesions in these cells, with limited localization to cell-cell junctions, whereas it was mainly co-localized with β -catenin in control cells (Fig.7B). Vinculin expression and recruitment to adhesion on ECM surface coating were however not affected by loss of LOXL2 expression (Fig.S7AB). Considering its role in the control of the turnover of focal adhesions, we also investigated the distribution of pY118-paxillin (Fig.7C). Surprisingly, pY118-paxillin was mainly localized at cell-cell junctions in control cells. Furthermore, it was redistributed from cell-cell junctions to ECM adhesions that displayed similar shape and distribution as those detected with phosphorylated FAK in LOXL2-depleted cells. In addition, we observed a modification of the organization of pY118-paxillin at adherens junctions. While pY118-paxillin was localized on top of the adherens junctions immunostained for β -catenin in control cells, the few pY118-paxillin still

associated with junctions in LOXL2-depleted cells was either co-localized in the same focal plane or located beside β -catenin staining (Fig.7Cii). We thus investigated phosphorylation of paxillin together with activation of ERK and Akt signaling pathways in cells that had been seeded at confluency and maintained for three days for BM assembly (Fig.7D). Paxillin basal phosphorylation was decreased by 40%, while its expression was slightly increased. On the opposite, ERK and Akt expression was not affected by LOXL2-depletion. While basal phosphorylation of Akt was not affected, phosphorylated ERK was increased 1.6-fold. To assess cell response to angiogenic stimulus, cells were treated with VEGF. Whereas VEGF triggered more phosphorylation of ERK in control cells than in LOXL2-depleted cells, this should be balanced by the increased basal level of p-ERK detected in the latter cells. Phosphorylation of paxillin and Akt was increased by VEGF only in LOXL2-depleted cells. The altered distribution of pY118-paxillin and vinculin in adherens junctions, together with modifications of the expression and phosphorylation of paxillin drove us to investigate the permeability properties of LOXL2-depleted cells using impedance measurement. Even though these cells reached a plateau with similar kinetics as control cells, their basal permeability as well as thrombin-induced response were altered (Fig.S8).

Altogether, these data suggested that the defective basement membrane generated by LOXL2-depleted cells was responsible for the default in mechanotransduction response of endothelial cells through altered maturation of cell-ECM adhesions and translocation to adherens junctions. They also suggested that paxillin is a major regulator of these defaults considering the alteration in its distribution and activation both under basal conditions and in response to VEGF.

DISCUSSION

Endothelial basement membrane is crucial for developmental angiogenesis as demonstrated by the phenotype of mice lacking collagen IV (Pöschl et al., 2004), fibronectin (George et al., 1993; Turner et al., 2017) and laminin (Thyboll et al., 2002). In the case of collagen IV, mutations in $\alpha 1$ or $\alpha 2$ chains result in vascular pathologies at longer term, including aneurysms and vascular leakage (Jeanne and Gould, 2017; Plaisier et al., 2007). Little is however known about the structural organization of the basement membrane of capillaries, the vascular unit responsible for angiogenesis. We already demonstrated that LOXL2 has a functional role both in angiogenesis and in organisation of endothelial basement membrane components (Bignon et al., 2011; Umana-Diaz et al., 2020). We thus aimed to identify the molecular events leading to scaffolding of the endothelial basement membrane and to decipher the mechanisms connecting LOXL2-mediated ECM scaffolding to the mechanotransduction response of endothelial cells.

Using correlative atomic force/fluorescence microscopy, we identified nascent ECM fibrillar structures containing fibronectin and LOXL2. Collagen IV immunofluorescence was also colocalized with LOXL2 but as a granular staining that was not correlated with AFM structures. The intracellular interactions between LOXL2 and fibronectin or collagen IV that we had already identified (Umana-Diaz et al., 2020) support their co-secretion in such structures in the matrix. The lack of binding of antibodies to LOXL2 in the secretory vesicles, most probably as a result of steric hindrance, further support interactions with these proteins in the late secretory pathway. Such interactions could protect collagen IV and fibronectin from misfolding or aggregation prior to their deposition in the basement membrane, as already proposed for collagen IV and SPARC (Chioran et al., 2017). These intracellular interactions do not affect deposition of collagen IV and fibronectin to their respective ECM structures, but could target LOXL2 to fibronectin fibrils and to collagen IV granular deposits, as already suggested by our time-lapse TIRF acquisitions (Umana-Diaz et al., 2020). Fibronectin fibrillogenesis is a cell-autonomous process requiring endogenous synthesis (Cseh et al., 2010; Turner et al., 2017) and is essential for basement membrane deposition as an ECM organizing center (Filla et al., 2017; Miller et al., 2014). Our results demonstrate that LOXL2 does not regulate these first steps of matrix deposition.

Kinetics of collagen IV, fibronectin, laminin and LOXL2 organization showed that the independent fibronectin and collagen IV deposits co-assembled over time into a network that resembles neither early deposit of these proteins. LOXL2 was colocalized in this network, in agreement with our previous data (Umana-Diaz et al., 2020). At this step of matrix deposition, LOXL2 depletion impacted fibronectin remodeling, resulting in a dense layer of elongated and aligned fibrils, but collagen IV remodeling into a homogenous network was not impacted. Self-assembly of collagen IV thus appears to be the driving force of basement membrane assembly at this step. Indeed, topography imaging could identify

material stained for collagen IV alongside fibronectin fibrils upon LOXL2 knock-down, supporting uncoupling of fibronectin and collagen IV reorganization. In agreement with these data, Lu and collaborators have recently proposed a new basement-membrane triggered mechanism responsible for fibronectin fibrillogenesis using surface coating with collagen IV (Lu et al., 2020). Our observations of increasing ECM fiber diameter during this remodeling also supports the supramolecular assembly of fibronectin and self-assembled collagen IV in the basement membrane. Even though fibronectin-collagen IV association has been described for long (Aumailley and Timpl, 1986; Miller et al., 2014), there is still no binding site identified for their direct interaction. LOXL2 could cross-link both proteins as we have identified direct interactions of LOXL2 with each of these proteins (Umana-Diaz et al., 2020).

Maturation of basement membrane is further achieved by continuous accumulation of multiple layers of such structures resulting in thicker and denser network. Our former TIRF analysis had already provided evidence for matrix reloading with LOXL2 and deposition of extra-layers on pre-existing fibers during cell migration (Umana-Diaz et al., 2020). Such mechanism for building up basement membrane has been described during egg chamber elongation in drosophila (Haigo and Bilder, 2011; Isabella and Horne-Badovinac, 2016). Furthermore, LOXL2 stabilizes basement membrane organization during this process since its knock-down resulted in large aggregates containing both fibronectin and collagen IV after three days in culture. Such stabilization activity thus prevented the cell-driven aggregation of basement membrane that resulted from adhesion through integrins or other ECM receptors and traction forces associated with cell migration. Tension level in fibronectin regulates its interactions with collagen I and reciprocally fibrillar collagen shields fibronectin from cellular traction (Kubow et al., 2015). In basement membrane, LOXL2 interaction with collagen IV-fibronectin complexes could maintain fibronectin in a low-tension state, thus protecting these supramolecular complexes from cell-driven tractions, and preventing the aggregation observed upon LOXL2 depletion. Indeed, in LOXL2-depleted cells, organization of cytoskeleton stress fibers directly corresponded to fibronectin organization in long aligned fibrils, whereas the meshwork organization of fibronectin resulted in cortical actin distribution in control cells.

Surface coating with matrix proteins including fibronectin and collagen I prevented their aggregation in the absence of LOXL2 by providing anchor points to the matrix deposited by cells. Similar rescue of a defect in collagen IV deposition was recently proposed for collagen IV mutation (Ngandu Mpoyi et al., 2020). Moreover, we here show that cell adhesion peptides of fibronectin did not affect matrix organization whereas full length protein resulted in a homogenous network. Quite remarkably, surface coating with LOXL2 SRCR domains also affected matrix deposition and even rescued LOXL2 knock-down (Umana-Diaz et al., 2020). These results also demonstrated that stabilization of the fibronectin-collagen IV network by LOXL2 was not mediated by its catalytic activity but rather relied

on non-catalytic cross-linking of these ECM proteins by LOXL2 SRCR domains. LOXL2 was indeed recently proposed to act as a major component of basement membrane building blocks (Brown et al., 2017). Our analysis provides details concerning the involvement of LOXL2 in this process. Altogether, we showed that LOXL2 interaction with collagen IV and fibronectin regulates their supramolecular assembly and stabilizes the basement membrane. Laminin has been considered as an organizer of basement membranes for long by providing a scaffold to other basement membrane components including collagen IV self-assembled network (Hohenester and Yurchenco, 2013). In our model, laminin is indeed not associated with early deposition or assembly of the fibronectin-LOXL2-collagen IV network. Furthermore, we had already shown that LOXL2 depletion had very limited effect on laminin deposition by endothelial cells (Umana-Diaz et al., 2020). These data are thus in agreement with the late association of independent supra-structures of laminin and collagen IV through cross-linking by nidogen and perlecan.

LOXL2 depletion impacted cell morphology and cytoskeleton redistribution resulting in elongated cells with bundles of actin stress fibers. This organization was correlated with fibronectin alignment, thus suggesting that LOXL2-mediated matrix organization could directly impact cell mechanotransduction. It has been known for long that local geometric control of ECM (Chen et al., 1997) and ECM ligand micropatterning (Cavalcanti-Adam et al., 2007; Oria et al., 2017) drive cytoskeleton organization and cell fate. There is however limited transfer of such results to analysis of endogenous ECM production. The submicron defaults in basement membrane assembly that we detected in absence of LOXL2 could correspond to the modifications driven by micropatterning of ECM components. Indeed, modifying ECM-deposition by LOXL2-depleted cells using surface coating with fibronectin rescued not only basement membrane deposition but also cytoskeleton organization and cell shape. Similar results were described in the case of collagen IV point mutation which also affected cell morphology (Ngandu Mpoyi et al., 2020).

We thus analyzed characteristics of endothelial cell adhesion to their autocrine basement membrane, and demonstrated that distribution of the focal adhesion proteins pY397-FAK, vinculin and pY118-paxillin was impaired in LOXL2-depleted cells. Vinculin and pY397-FAK were detected in long focal adhesions evenly distributed at the cell-matrix interface, in a pattern reminiscent of fibronectin and cytoskeleton alignment. Such matrix-driven distribution of adhesions was described when cells were seeded on microcontact-printed ECM and also resulted in cell elongation and alignment (Wang et al., 2018). In a context where matrix deposition by cells was abrogated, i.e. cell seeding on ECM surface coating followed by short term analysis, there was no default in focal adhesion formation and maturation. Cell spreading was not impacted either, thus indicating that adhesion machinery was not altered in these cells. A similar protocol applied to matrix derived from LOXL2-depleted cells however allowed detection of defaults in maturation of nascent adhesions into focal adhesions, thus

highlighting the major autocrine role of endothelial basement membrane in mechanotransduction. Stiffness is also affected in matrices generated by LOXL2-depleted cells, resulting in 70% less stiff matrices compared to control cells (2,3 kPa as measured by nanoindentation) (Umana-Diaz et al., 2020). Whereas this could be responsible for the defective response in cell-ECM adhesion (van Geemen et al., 2014), we nevertheless observed an increased number and a global redistribution of focal adhesions, suggesting that matrix topography prevails over stiffness. In line with this, cell contractility in response to a wide range of stiffness was not sensitive to LOXL2 expression.

Vinculin is a force-sensor both at cell-ECM and cell-cell junctions in epithelial (le Duc et al., 2010; Thomas et al., 2013) and endothelial cells (Huveneers et al., 2012). In these cells, vinculin is part of focal adherens junctions and regulates junction stability. In parallel with increased ECM focal adhesions labelled with pY397-FAK and vinculin, colocalization of the latter with β -catenin was decreased in LOXL2-depleted cells. Vinculin redistribution out of the adherens junction could be explained by the decrease in basement membrane stiffness resulting from LOXL2 depletion (Umana-Diaz et al., 2020). Indeed, ECM stiffness has been shown to positively regulate vinculin recruitment to cell-cell junctions (Seddiki et al., 2018). Whereas vinculin translocation from cell-ECM to cell-cell junctions is well documented, only a few studies describe paxillin localization to adherens junctions. It has been shown at cell-cell borders in epithelial zebrafish tissues (Crawford et al., 2003) and in endothelial cells where it interacts with β -catenin (Birukova et al., 2007; van Geemen et al., 2014). We detected pY118-paxillin co-localized with β -catenin at the level of cell-cell junctions in control cells. Most of pY118-paxillin was not maintained in cell-cell junctions in LOXL2-depleted cells. The local distribution of pY118-paxillin still present in adherens junction was shifted from accumulation on top of β -catenin in control cells, to within or beside β -catenin staining in LOXL2-depleted cells. Basal phosphorylation of paxillin was decreased in these cells. Dephosphorylation of paxillin has been linked to stabilization and decreased turnover of focal adhesions (Zaidel-Bar et al., 2007). In agreement, we detected increased cell-ECM adhesions stained for pY397-FAK and vinculin with limited staining of pY118-paxillin. Our data however challenged such a role for phosphorylation of paxillin in adherens junction, as decreased overall phosphorylation of paxillin was accompanied with decreased vinculin in the junctions. Such opposite mechanisms of adhesion stabilization could rely on the nature of the binding partner of paxillin in each compartment, i.e. FAK in focal adhesions and β -catenin in adherens junctions (Dubrovskiy et al., 2012).

Altogether, our study demonstrates that loss of LOXL2 expression in endothelial cells leads to dramatic default in basement membrane assembly, and subsequent altered mechanotransduction response at the level of cell-ECM as well as cell-cell adhesion. This autocrine matrix-mediated signaling

might be responsible for the impaired angiogenesis that we previously described both during zebrafish embryo development and in *in vitro* 3D models (Bignon et al., 2011; Umana-Diaz et al., 2020). Indeed, endothelial-specific knock-out of vinculin in mice leads to defects in vascular morphogenesis through loss of α -catenin-mediated coupling of adherens junctions to actin cytoskeleton (Carvalho et al., 2019). In a similar manner, endothelial-specific knockout of FAK inhibited angiogenesis without perturbation of vasculogenesis (Shen et al., 2005). Considering that surface coating restored ECM components deposition *in vitro*, the defaults in basement membrane assembly resulting from LOXL2 depletion that we described *in vitro* might not result in as complete default in basement membrane generation *in vivo*. They might rather trigger fine rearrangements of basement membrane as observed in the endothelial-specific deletion of fibronectin in mice (Turner et al., 2017) and in patients with point mutations in collagen IV responsible for small vessel disease or HANAC syndrom (Jeanne and Gould, 2017; Plaisier et al., 2007). In agreement with this hypothesis, LOXL2 is considered a candidate gene in the vascular matrix pathologies like intracranial aneurysm (Akagawa et al., 2007; López-Luppo et al., 2017; Wu et al., 2018) and vascular stiffening (Steppan et al., 2019).

MATERIALS AND METHODS

Antibodies

Primary and secondary antibodies are listed in table 1.

Cell culture, expression vectors, lentivirus and shRNA tools

Human umbilical vein endothelial cells (HUVECs) were prepared and grown as already described (Chomel et al, FASEB J 2009) in endothelial cell growth medium (ECGM2, Promocell). Experiments were performed using HUVECs between passages 2 and 5. pLKO.1 plasmids encoding shRNA were purchased from Sigma-Aldrich (Saint-Louis, MO, USA). Lentiviral production was performed in HEK293FT cells using Mission lentiviral Packaging Mix, Sigma-Aldrich (Saint-Louis, MO, USA). Endothelial cells isolated from 1 umbilical cord were split in 2 and infected before the first passage with control or LOXL2 targeting lentivirus. Transductions were repeated using HUVECs from different umbilical cords. Transduced cells were selected for 7 days with puromycin at 2 µg/mL for shRNA-mediated down-regulation. For coating experiments, collagen I purchased from Corning (Corning, NY, USA) or human purified fibronectin purchased from Sigma-Aldrich (Saint-Louis, MO, USA) were respectively diluted in 20 mM acetic acid or 1X PBS before coating petri dishes for one hour at 37°C. RGD or PHSRN coating experiments were realized using DenovoMatrix (Dresden, Germany) coated plates.

Preparation of cell-derived extracellular matrices

HUVECs were seeded at confluency in low petridishes (Ibidi, Martinsried, Germany) and cultured in ECGM2 for the desired amount of time. Before decellularization, cells were washed in cold PBS and detached on ice, using a solution containing 0,3% Triton X-100 and 20 mM ammonium hydroxide in cold PBS. Samples were checked under a light microscope to ensure proper decellularization. The matrices were washed several times with cold PBS before further processing.

Immunofluorescence

HUVECs were seeded at confluency in µ-slides ibiTreat 8 wells (Ibidi, Martinsried, Germany) and cultured from 6h to 72h before fixation with 4% paraformaldehyde and permeabilization with 0,5 % Triton-X-100. Appropriate primary and secondary antibodies were incubated in the presence of 1% normal goat serum and 0,01% Triton-X-100. Images were acquired with either a Zeiss (Oberkochen, Germany) W1 spinning-disk microscope or a Zeiss (Oberkochen, Germany) Axio Observer epifluorescence microscope equipped with an apotome module using 63x or 40x objectives. For image analysis, image J software was used.

Whole-mount retina immunofluorescence

For whole mount retina stainings, eyes were fixed in 4% PFA and retinas were dissected and stained as previously described (del Toro et al., 2010). Briefly, isolectin B4 was incubated overnight in PBS, 1 mM CaCl₂, 1 mM MgCl₂ and 1% Triton-X-100. Retinas were washed and secondary antibodies/streptavidin were incubated in the presence of 0,25 % Triton-X-100. Retinas were mounted and imaged with a Zeiss (Oberkochen, Germany) W1 spinning-disk microscope using 25x or 40x objectives.

Protein extraction and immunoblotting

HUVECs were directly lysed with Laemmli buffer containing 4% SDS and 50 mM DTT, before separation by SDS-PAGE. Proteins were transferred to PVDF membranes before incubation with the appropriate antibodies in 25 mM Tris-HCl, pH 7.4, 0.1% Tween 20, and 5% milk. Immunological detection was performed with streptavidin-horseradish peroxidase (HRP) conjugated secondary antibodies, using ECL (Life Technologies) as a substrate.

Correlative fluorescence/atomic force microscopy

Analysis of ECM topography was determined using a scanning force microscope NanoWizard 4, JPK-BioAFM (Berlin, Germany) mounted on a Zeiss (Oberkochen, Germany) Axio Observer epifluorescence microscope equipped with an apotome module, placed on a vibration isolation table. Topography was determined using a conical shape probe with typical tip radius of curvature < 10 nm mounted on a gold coated cantilever (0.03-0.09 N/m) (Biolever Mini, Olympus). Spring constant was determined upon calibration by the thermal noise method (Hutter J and Bechhoefer J, Rev of Sci Instr 1993). Quantitative imaging (QI) (JPK, Berlin, Germany) was conducted in PBS. Typically, an AFM map of 20 x 20 µm corresponding to 256x256 pixels was acquired at an appropriate scan speed (100 to 200 µm/s) and the lower setpoint possible (typically 0.1 nN) to prevent damage to the sample. AFM image processing and analysis were performed using JPK data processing software and ImageJ. Second order flattening is applied to AFM topography images to remove tilt and bow. Median filter and Gaussian convolution were also applied when necessary. Correlative with fluorescence was achieved based on the optical calibration module (JPK). Quantification of fluorescence content was achieved as described (Fig.S2) by thresholding both AFM and fluorescence images and calculating integrated density of pixelized images.

Stiffness-clamp experiments

Measurements for stiffness clamp were carried out as previously described (Webster KD et al, Plos One 2011; Mitrossilis D et al, PNAS 2009). Briefly, experiments were conducted using a NanoWizard 4, JPK-BioAFM (Berlin, Germany) associated with the module CellHesion 200. Tipless cantilevers Arrow TL1 purchased from NanoWorld) were coated with 40 µg/mL fibronectin for 20 min at room temperature. Cells were seeded in a 35mm µ-dish coated with fibronectin for 2 min. The cantilever was put in contact with individual cells, and measures were started after 150 s.

Transendothelial electrical resistance

Transendothelial electrical resistance was used as an indicator of the barrier function of the endothelial monolayer and was determined using an electrical cellular impedance sensor (ECIS) Applied Biophysics, Troy, NY). Endothelial cells were seeded at confluency on gold microelectrodes coated with fibronectin. Real time transendothelial electrical resistance was continuously measured in a 37°C , 5% CO₂ incubator over several days. Cultures were maintained 20h after reaching a plateau before measurement of thrombin-induced permeability.

Table 1: Antibodies and fluorescent probes

	target	supplier	reference	species	dilution	
					immuno-fluorescence	western blotting
primary antibodies	type IV collagen	Novotec	#20411	Rabbit polyclonal	1:1000	
	type IV collagen a2 chain	Merck-Millipore	mab1910	Mouse monoclonal	1:500	
	fibronectin	Merck-Millipore	mab1936	Mouse monoclonal	1:500	
	fibronectin	Merck-Millipore	mab1926	Mouse monoclonal	1:500	
	laminin	Novotec	#24811	Rabbit polyclonal	1:200	
	LOXL2	Cell Signalling	69301	Rabbit monoclonal	1:500	
	LOXL2	Abcam	96233	Rabbit polyclonal	1:200	
	paxillin	R&D	af4259	Sheep polyclonal	1:100	1:1000
	β -actin	Abcam	#8227	Rabbit polyclonal	1:5000	
	Akt	Cell Signalling	#9272S	Rabbit polyclonal	1:1000	
	pAkt	Cell Signalling	#9271S	Rabbit polyclonal	1:500	
	ERK 1/2	Merck-Millipore	06-182	Rabbit polyclonal	1:1000	
	pERK 1/2	Cell Signalling	9106	Mouse monoclonal	1:500	
	pFAK Y397	Thermofisher Scientific	44-624G	Rabbit monoclonal	1:500	
	vinculin	Sigma-Aldrich	V9131	Mouse monoclonal	1:400	1:1000
pPaxillin Y118	Thermofisher Scientific	44-722G	Rabbit polyclonal	1:100	1:500	
β -catenin-647	Cell Signalling	#4627	Mouse monoclonal	1:500		
secondary antibodies	anti-mouse Alexa Fluor 488	Thermofisher Scientific				
	anti-mouse Alexa Fluor 555	Thermofisher Scientific				
	anti-mouse Alexa Fluor 647	Thermofisher Scientific				
	anti-rabbit Alexa Fluor 488	Thermofisher Scientific				
	anti-rabbit Alexa Fluor 555	Thermofisher Scientific				
	anti-rabbit Alexa Fluor 647	Thermofisher Scientific				
	anti-sheep Alexa Fluor 555	Thermofisher Scientific				
probes	phalloidin-Alexa Fluor 488	Thermofisher Scientific	A12379	1:200		
	isolectin B4 from GS-biotin conjugate	Thermofisher Scientific	I21414	1:50		
	Streptavidin-Cy3	Amersham	GEPA42001	1:100		

REFERENCES

- Akagawa, H., Narita, A., Yamada, H., Tajima, A., Krischek, B., Kasuya, H., Hori, T., Kubota, M., Saeki, N., Hata, A., et al. (2007). Systematic screening of lysyl oxidase-like (LOXL) family genes demonstrates that LOXL2 is a susceptibility gene to intracranial aneurysms. *Hum. Genet.* *121*, 377–387.
- Akiyama, S.K., Olden, K., and Yamada, K.M. (1995). Fibronectin and integrins in invasion and metastasis. *Cancer Metastasis Rev.* *14*, 173–189.
- Añazco, C., López-Jiménez, A.J., Rafi, M., Vega-Montoto, L., Zhang, M.-Z., Hudson, B.G., and Vanacore, R.M. (2016). Lysyl Oxidase-like-2 Cross-links Collagen IV of Glomerular Basement Membrane. *J. Biol. Chem.* *291*, 25999–26012.
- Aumailley, M., and Timpl, R. (1986). Attachment of cells to basement membrane collagen type IV. *J. Cell Biol.* *103*, 1569–1575.
- Aviezer, D., Hecht, D., Safran, M., Eisinger, M., David, G., and Yayon, A. (1994). Perlecan, basal lamina proteoglycan, promotes basic fibroblast growth factor-receptor binding, mitogenesis, and angiogenesis. *Cell* *79*, 1005–1013.
- Barry-Hamilton, V., Spangler, R., Marshall, D., McCauley, S., Rodriguez, H.M., Oyasu, M., Mikels, A., Vaysberg, M., Ghermazien, H., Wai, C., et al. (2010). Allosteric inhibition of lysyl oxidase-like-2 impedes the development of a pathologic microenvironment. *Nat. Med.* *16*, 1009–1017.
- Bhave, G., Cummings, C.F., Vanacore, R.M., Kumagai-Cresse, C., Ero-Tolliver, I.A., Rafi, M., Kang, J.-S., Pedchenko, V., Fessler, L.I., Fessler, J.H., et al. (2012). Peroxidase forms sulfilimine chemical bonds using hypohalous acids in tissue genesis. *Nat. Chem. Biol.* *8*, 784–790.
- Bignon, M., Pichol-Thieuvend, C., Hardouin, J., Malbouyres, M., Brechot, N., Nasciutti, L., Barret, A., Teillon, J., Guillon, E., Etienne, E., et al. (2011). Lysyl oxidase-like protein-2 regulates sprouting angiogenesis and type IV collagen assembly in the endothelial basement membrane. *Blood* *118*, 3979–3989.
- Birukova, A.A., Malyukova, I., Poroyko, V., and Birukov, K.G. (2007). Paxillin-beta-catenin interactions are involved in Rac/Cdc42-mediated endothelial barrier-protective response to oxidized phospholipids. *Am. J. Physiol. Lung Cell. Mol. Physiol.* *293*, L199–211.
- Brown, K.L., Cummings, C.F., Vanacore, R.M., and Hudson, B.G. (2017). Building collagen IV smart scaffolds on the outside of cells. *Protein Sci.* *26*, 2151–2161.
- Carvalho, J.R., Fortunato, I.C., Fonseca, C.G., Pezzarossa, A., Barbacena, P., Dominguez-Cejudo, M.A., Vasconcelos, F.F., Santos, N.C., Carvalho, F.A., and Franco, C.A. (2019). Non-canonical Wnt signaling regulates junctional mechanocoupling during angiogenic collective cell migration. *ELife* *8*, E45853.
- Cavalcanti-Adam, E.A., Volberg, T., Micoulet, A., Kessler, H., Geiger, B., and Spatz, J.P. (2007). Cell Spreading and Focal Adhesion Dynamics Are Regulated by Spacing of Integrin Ligands. *Biophys. J.* *92*, 2964–2974.
- Chen, C.S., Mrksich, M., Huang, S., Whitesides, G.M., and Ingber, D.E. (1997). Geometric control of cell life and death. *Science* *276*, 1425–1428.
- Chioran, A., Duncan, S., Catalano, A., Brown, T.J., and Ringuette, M.J. (2017). Collagen IV trafficking: The inside-out and beyond story. *Dev. Biol.* *431*, 124–133.
- Crawford, B.D., Henry, C.A., Clason, T.A., Becker, A.L., and Hille, M.B. (2003). Activity and distribution of paxillin, focal adhesion kinase, and cadherin indicate cooperative roles during zebrafish morphogenesis. *Mol. Biol. Cell* *14*, 3065–3081.
- Cseh, B., Fernandez-Sauze, S., Grall, D., Schaub, S., Doma, E., and Van Obberghen-Schilling, E. (2010). Autocrine fibronectin directs matrix assembly and crosstalk between cell-matrix and cell-cell adhesion in vascular endothelial cells. *J. Cell Sci.* *123*, 3989–3999.
- Dubrovskiy, O., Tian, X., Poroyko, V., Yakubov, B., Birukova, A.A., and Birukov, K.G. (2012). Identification of paxillin domains interacting with β -catenin. *FEBS Lett.* *586*, 2294–2299.
- le Duc, Q., Shi, Q., Blonk, I., Sonnenberg, A., Wang, N., Leckband, D., and de Rooij, J. (2010). Vinculin potentiates E-cadherin mechanosensing and is recruited to actin-anchored sites within adherens junctions in a myosin II-dependent manner. *J. Cell Biol.* *189*, 1107–1115.
- Estrach, S., Cailleateau, L., Franco, C.A., Gerhardt, H., Stefani, C., Lemichez, E., Gagnoux-Palacios, L., Meneguzzi, G., and Mettouchi, A. (2011). Laminin-binding integrins induce Dll4 expression and Notch signaling in endothelial cells. *Circ. Res.* *109*, 172–182.
- Filla, M.S., Dimeo, K.D., Tong, T., and Peters, D.M. (2017). Disruption of fibronectin matrix affects type IV collagen, fibrillin and laminin deposition into extracellular matrix of human trabecular meshwork (HTM) cells. *Exp. Eye Res.* *165*, 7–19.

van Geemen, D., Smeets, M.W.J., van Stalborch, A.-M.D., Woerdeman, L.A.E., Daemen, M.J.A.P., Hordijk, P.L., and Huvencers, S. (2014). F-actin-anchored focal adhesions distinguish endothelial phenotypes of human arteries and veins. *Arterioscler. Thromb. Vasc. Biol.* 34, 2059–2067.

George, E.L., Georges-Labouesse, E.N., Patel-King, R.S., Rayburn, H., and Hynes, R.O. (1993). Defects in mesoderm, neural tube and vascular development in mouse embryos lacking fibronectin. *Development* 119, 1079–1091.

Gould, D.B., Phalan, F.C., van Mil, S.E., Sundberg, J.P., Vahedi, K., Massin, P., Bousser, M.G., Heutink, P., Miner, J.H., Tournier-Lasserre, E., et al. (2006). Role of COL4A1 in small-vessel disease and hemorrhagic stroke. *N. Engl. J. Med.* 354, 1489–1496.

Haigo, S.L., and Bilder, D. (2011). Global tissue revolutions in a morphogenetic movement controlling elongation. *Science* 331, 1071–1074.

Halfter, W., Monnier, C., Müller, D., Oertle, P., Uechi, G., Balasubramani, M., Safi, F., Lim, R., Loparic, M., and Henrich, P.B. (2013). The bi-functional organization of human basement membranes. *PLoS One* 8, e67660.

Halfter, W., Oertle, P., Monnier, C.A., Camenzind, L., Reyes-Lua, M., Hu, H., Candiello, J., Labilloy, A., Balasubramani, M., Henrich, P.B., et al. (2015). New concepts in basement membrane biology. *FEBS J.* 282, 4466–4479.

Hohenester, E., and Yurchenco, P.D. (2013). Laminins in basement membrane assembly. *Cell Adhes. Migr.* 7, 56–63.

Huvencers, S., Oldenburg, J., Spanjaard, E., van der Krogt, G., Grigoriev, I., Akhmanova, A., Rehmann, H., and de Rooij, J. (2012). Vinculin associates with endothelial VE-cadherin junctions to control force-dependent remodeling. *J. Cell Biol.* 196, 641–652.

Isabella, A.J., and Horne-Badovinac, S. (2016). Rab10-Mediated Secretion Synergizes with Tissue Movement to Build a Polarized Basement Membrane Architecture for Organ Morphogenesis. *Dev. Cell.* 38, 47–60.

Jayadev, R., and Sherwood, D.R. (2017). Basement membranes. *Curr. Biol.* 27, R207–R211.

Jeanne, M., and Gould, D.B. (2017). Genotype-phenotype correlations in pathology caused by collagen type IV alpha 1 and 2 mutations. *Matrix Biol.* 57–58, 29–44.

de Jong, O.G., van der Waals, L.M., Kools, F.R.W., Verhaar, M.C., and van Balkom, B.W.M. (2019). Lysyl oxidase-like 2 is a regulator of angiogenesis through modulation of endothelial-to-mesenchymal transition. *J. Cell. Physiol.* 234, 10260–10269.

Kubow, K.E., Vukmirovic, R., Zhe, L., Klotzsch, E., Smith, M.L., Gourdon, D., Luna, S., and Vogel, V. (2015). Mechanical forces regulate the interactions of fibronectin and collagen I in extracellular matrix. *Nat. Commun.* 6, 8026.

Liliensiek, S.J., Nealey, P., and Murphy, C.J. (2009). Characterization of Endothelial Basement Membrane Nanotopography in Rhesus Macaque as a Guide for Vessel Tissue Engineering. *Tissue Eng. Part A* 15, 2643–2651.

López-Luppo, M., Nacher, V., Ramos, D., Catita, J., Navarro, M., Carretero, A., Rodriguez-Baeza, A., Mendes-Jorge, L., and Ruberte, J. (2017). Blood Vessel Basement Membrane Alterations in Human Retinal Microaneurysms During Aging. *Invest. Ophthalmol. Vis. Sci.* 58, 1116–1131.

Lu, J., Doyle, A.D., Shinsato, Y., Wang, S., Bodendorfer, M.A., Zheng, M., and Yamada, K.M. (2020). Basement Membrane Regulates Fibronectin Organization Using Sliding Focal Adhesions Driven by a Contractile Winch. *Dev. Cell* 52, 631–646.

Mäki, J.M. (2009). Lysyl oxidases in mammalian development and certain pathological conditions. *Histol Histopathol.* 24, 651–60.

Marchand, M., Monnot, C., Muller, L., and Germain, S. (2019). Extracellular matrix scaffolding in angiogenesis and capillary homeostasis. *Semin. Cell Dev. Biol.* 89, 147–156.

Millanes-Romero, A., Herranz, N., Perrera, V., Iturbide, A., Loubat-Casanovas, J., Gil, J., Jenuwein, T., García de Herreros, A., and Peiró, S. (2013). Regulation of heterochromatin transcription by Snail1/LOXL2 during epithelial-to-mesenchymal transition. *Mol. Cell* 52, 746–757.

Miller, C.G., Pozzi, A., Zent, R., and Schwarzbauer, J.E. (2014). Effects of high glucose on integrin activity and fibronectin matrix assembly by mesangial cells. *Mol. Biol. Cell* 25, 2342–2350.

Mitrossilis, D., Fouchard, J., Pereira, D., Postic, F., Richert, A., Saint-Jean, M., and Asnacios, A. (2010). Real-time single-cell response to stiffness. *Proc. Natl. Acad. Sci.* 107, 16518–16523.

Neumann, P., Jaé, N., Knau, A., Glaser, S.F., Fouani, Y., Rossbach, O., Krüger, M., John, D., Bindereif, A., Grote, P., et al. (2018). The lncRNA GATA6-AS epigenetically regulates endothelial gene expression via interaction with LOXL2. *Nat. Commun.* 9, 237.

Ngandu Mpoyi, E., Cantini, M., Sin, Y.Y., Fleming, L., Zhou, D.W., Costell, M., Lu, Y., Kadler, K., García, A.J., Van Agtmael, T., et al. (2020). Material-driven fibronectin assembly rescues matrix defects due to mutations in collagen IV in fibroblasts. *Biomaterials* 252, 120090.

Oria, R., Wiegand, T., Escribano, J., Elosegui-Artola, A., Uriarte, J.J., Moreno-Pulido, C., Platzman, I., Delcanale, P., Albertazzi, L., Navajas, D., et al. (2017). Force loading explains spatial sensing of ligands by cells. *Nature* 552, 219–224.

Peinado, H., Del Carmen Iglesias-de la Cruz, M., Olmeda, D., Csiszar, K., Fong, K.S.K., Vega, S., Nieto, M.A., Cano, A., and Portillo, F. (2005). A molecular role for lysyl oxidase-like 2 enzyme in snail regulation and tumor progression. *EMBO J.* 24, 3446–3458.

Plaisier, E., Gribouval, O., Alamowitch, S., Mougenot, B., Prost, C., Verpont, M.C., Marro, B., Desmettre, T., Cohen, S.Y., Rouillet, E., et al. (2007). COL4A1 mutations and hereditary angiopathy, nephropathy, aneurysms, and muscle cramps. *N. Engl. J. Med.* 357, 2687–2695.

Pöschl, E., Schlötzer-Schrehardt, U., Brachvogel, B., Saito, K., Ninomiya, Y., and Mayer, U. (2004). Collagen IV is essential for basement membrane stability but dispensable for initiation of its assembly during early development. *Development.* 131, 1619–1628.

Potente, M., Gerhardt, H., and Carmeliet, P. (2011). Basic and therapeutic aspects of angiogenesis. *Cell* 146, 873–887.

Pozzi, A., Yurchenco, P.D., and Iozzo, R.V. (2017). The nature and biology of basement membranes. *Matrix Biol.* 57–58, 1–11.

Schmelzer, C.E.H., Heinz, A., Troilo, H., Lockhart-Cairns, M.P., Jowitt, T.A., Marchand, M.F., Bidault, L., Bignon, M., Hedtke, T., Barret, A., et al. (2019). Lysyl oxidase-like 2 (LOXL2)-mediated cross-linking of tropoelastin. *FASEB J.* 33, 5468–5481.

Seddiki, R., Narayana, G.H.N.S., Strale, P.-O., Balcioglu, H.E., Peyret, G., Yao, M., Le, A.P., Teck Lim, C., Yan, J., Ladoux, B., et al. (2018). Force-dependent binding of vinculin to α -catenin regulates cell-cell contact stability and collective cell behavior. *Mol. Biol. Cell* 29, 380–388.

Sharma, B., Handler, M., Eichstetter, I., Whitelock, J.M., Nugent, M.A., and Iozzo, R.V. (1998). Antisense targeting of perlecan blocks tumor growth and angiogenesis in vivo. *J. Clin. Invest.* 102, 1599–1608.

Shen, T.-L., Park, A.Y.-J., Alcaraz, A., Peng, X., Jang, I., Koni, P., Flavell, R.A., Gu, H., and Guan, J.-L. (2005). Conditional knockout of focal adhesion kinase in endothelial cells reveals its role in angiogenesis and vascular development in late embryogenesis. *J. Cell Biol.* 169, 941–952.

Stenzel, D., Franco, C.A., Estrach, S., Mettouchi, A., Sauvaget, D., Rosewell, I., Schertel, A., Armer, H., Domogatskaya, A., Rodin, S., et al. (2011). Endothelial basement membrane limits tip cell formation by inducing Dll4/Notch signalling in vivo. *EMBO Rep.* 12, 1135–1143.

Steppan, J., Wang, H., Bergman, Y., Rauer, M.J., Tan, S., Jandu, S., Nandakumar, K., Barreto-Ortiz, S., Cole, R.N., Boronina, T.N., et al. (2019). Lysyl oxidase-like 2 depletion is protective in age-associated vascular stiffening. *Am. J. Physiol. Heart Circ. Physiol.* 317, H49–H59.

Thomas, W.A., Boscher, C., Chu, Y.-S., Cuvelier, D., Martinez-Rico, C., Seddiki, R., Heysch, J., Ladoux, B., Thiery, J.P., Mege, R.-M., et al. (2013). α -Catenin and vinculin cooperate to promote high E-cadherin-based adhesion strength. *J. Biol. Chem.* 288, 4957–4969.

Thyboll, J., Kortessmaa, J., Cao, R., Soininen, R., Wang, L., Iivanainen, A., Sorokin, L., Risling, M., Cao, Y., and Tryggvason, K. (2002). Deletion of the Laminin 4 Chain Leads to Impaired Microvessel Maturation. *Mol. Cell. Biol.* 22, 1194–1202.

del Toro, R., Prahst, C., Mathivet, T., Siegfried, G., Kaminker, J.S., Larrivee, B., Breant, C., Duarte, A., Takakura, N., Fukamizu, A., et al. (2010). Identification and functional analysis of endothelial tip cell-enriched genes. *Blood* 116, 4025–4033.

Trackman, P.C. (2016). Enzymatic and non-enzymatic functions of the lysyl oxidase family in bone. *Matrix Biol.* 52–54, 7–18.

Turner, C.J., Badu-Nkansah, K., and Hynes, R.O. (2017). Endothelium-derived fibronectin regulates neonatal vascular morphogenesis in an autocrine fashion. *Angiogenesis* 20, 519–531.

Uechi, G., Sun, Z., Schreiber, E.M., Halfter, W., and Balasubramani, M. (2014). Proteomic View of Basement Membranes from Human Retinal Blood Vessels, Inner Limiting Membranes, and Lens Capsules. *J. Proteome Res.* 13, 3693–3705.

Umana-Diaz, C., Pichol-Thievent, C., Marchand, M.F., Atlas, Y., Salza, R., Malbouyres, M., Barret, A., Teillon, J., Ardidie-Robouant, C., Ruggiero, F., et al. (2020). Scavenger Receptor Cysteine-Rich domains of Lysyl Oxidase-Like2 regulate endothelial ECM and angiogenesis through non-catalytic scaffolding mechanisms. *Matrix Biol.* 88, 33–52.

Van Bergen, T., Spangler, R., Marshall, D., Hollanders, K., Van de Veire, S., Vandewalle, E., Moons, L., Herman, J., Smith, V., and Stalmans, I. (2015). The Role of LOX and LOXL2 in the Pathogenesis of an Experimental Model of Choroidal Neovascularization. *Invest. Ophthalmol. Vis. Sci.* 56, 5280–5289.

Wang, W.Y., Pearson, A.T., Kutys, M.L., Choi, C.K., Wozniak, M.A., Baker, B.M., and Chen, C.S. (2018). Extracellular matrix alignment dictates the organization of focal adhesions and directs uniaxial cell migration. *APL Bioeng.* 2, 046107.

Wu, Y., Li, Z., Shi, Y., Chen, L., Tan, H., Wang, Z., Yin, C., Liu, L., and Hu, J. (2018). Exome Sequencing Identifies LOXL2 Mutation as a Cause of Familial Intracranial Aneurysm. *World Neurosurg.* 109, e812–e818.

Zaffryar-Eilot, S., Marshall, D., Voloshin, T., Bar-Zion, A., Spangler, R., Kessler, O., Ghermazien, H., Brekhman, V., Suss-Toby, E., Adam, D., et al. (2013). Lysyl oxidase-like-2 promotes tumour angiogenesis and is a potential therapeutic target in angiogenic tumours. *Carcinogenesis* 34, 2370–2379.

Zaidel-Bar, R., Milo, R., Kam, Z., and Geiger, B. (2007). A paxillin tyrosine phosphorylation switch regulates the assembly and form of cell-matrix adhesions. *J. Cell Sci.* 120, 137–148.

Zhou, X., Rowe, R.G., Hiraoka, N., George, J.P., Wirtz, D., Mosher, D.F., Virtanen, I., Chernousov, M.A., and Weiss, S.J. (2008). Fibronectin fibrillogenesis regulates three-dimensional neovessel formation. *Genes Dev.* 22, 1231–1243.

FIGURE LEGENDS

Figure 1. Angiogenesis-associated extracellular matrix remodeling

Fibronectin and collagen IV were immunostained (green) in postnatal mouse retina (P5). Endothelial cells were detected using Isolectin B4 (red) as a marker. Scale bar: 10 μm .

Figure 2. Endothelial basement membrane topography and assembly

A-F: Endothelial cells were seeded at confluency and maintained for 6h (**A**), 24h (**B**) or 72h (**C**) before preparation of CDM. Topographical analysis was performed by AFM. Height maps representative of at least 3 independent experiments are shown. For each map, a two-dimensional scan line of height (white-dotted line) was measured. Scale bar: 5 μm . Height maps were quantified for ECM fiber diameter (**D**), matrix coverage (**E**) and mean height (**F**). Matrix coverage was assessed as the proportion of pixels higher than 50 nm. Mean height was calculated for either 75 or 5% of the highest pixels. Two (6h-orange) and 3 (24h-purple, 72h green) independent experiments with a minimum of 4 maps/experiment were performed. For fiber diameters, Mann-Whitney test for non-Gaussian distribution was performed (**** $p < 0.0001$), for matrix coverage, Kruskal-Wallis test was performed for non-Gaussian distribution (* $p < 0.0225$, ** $p < 0.0011$, **** $p < 0.0001$), for mean height, two-way ANOVA was performed (**** $p < 0.0001$). **G-I:** Correlative AFM-fluorescence analysis was performed on CDM prepared from confluent cells cultured for 6h (**i**) or 24h (**ii**) and immunostained for LOXL2 and fibronectin (**G**), or LOXL2 and collagen IV (**H**) or fibronectin and laminin (**I**). Scale bar: 5 μm . Quantification of the proportion of AFM-detected structures containing fluorescent signal was performed in $n=2$ distinct experiments and at least 3 maps of 20x20 μm for each condition. Statistical analysis was done using paired t-tests (* $p < 0.03$, *** $p < 0.0002$, **** $p < 0.0001$).

Figure 3. LOXL2-depletion affects spatio-temporal distribution of basement membrane components

A : Control (shControl) or LOXL2-depleted (shLOXL2) endothelial cells were seeded at confluency and maintained for 6h (**i**) or 24h (**ii**) before preparation of CDM and immunostaining of fibronectin or collagen IV (green) and LOXL2 (red). Scale bar: 50 μm (3 top rows) and 5 μm (lower row). **B:** Control (shControl) or LOXL2-depleted (shLOXL2) endothelial cells were seeded at confluency and maintained for 24h before preparation of CDM and immunostaining of fibronectin (green) or collagen IV (red). Scale bar: 10 μm . **C:** Correlative AFM-fluorescence analysis was performed on CDM prepared from control (shControl) or LOXL2-depleted (shLOXL2) endothelial cells seeded at confluency and maintained for 24h before preparation of CDM and immunostaining of collagen IV (green). Field of view is 8 x 12 μm . **D-E:** Control (shControl) or LOXL2-depleted (shLOXL2) endothelial cells were seeded

at confluency and maintained for 72h before preparation of CDM. Topographical analysis was performed by AFM. For each height map, a two-dimensional scan line of height (white dotted line) was measured. Scale bar: 5 μm . **E:** Height of individual fibers was extracted from two-dimensional scan-lines on 2-5 images from 4 distinct experiments. Unpaired Student t-test was performed ($p < 0.0001$). **F:** Correlative AFM-fluorescence analysis was performed on CDM prepared from control (shControl) or LOXL2-depleted (shLOXL2) endothelial cells seeded at confluency and maintained for 72h before preparation of CDM and immunostaining of fibronectin (i) or collagen IV (ii) (green) and LOXL2 (red). Scale bar: 5 μm .

Figure 4. LOXL2-depletion affects cell morphology and cytoskeleton organization.

Control (shControl) or LOXL2-depleted (shLOXL2) endothelial cells were seeded at confluency and maintained for 72h before immunostaining of β -catenin (**A**) or detection of F-actin with phalloidin-AlexaFluor 488 and of nuclei with DAPI (blue) (**D**). Morphometric parameters (cell circularity (**B**) and Ferret diameter (**C**)). Cytoskeleton orientation was measured and is presented as the average of vector proportion within 20° from the main axis (**E**) and as average of orientation per field of view per experiment (**F**). Scale bar: 20 (**A**) and 10 (**D**) μm . Statistical analysis was done using unpaired t-tests (**** $p < 0.0001$).

Figure 5. Fibronectin surface coating modulates ECM assembly, cell morphology and cytoskeleton organization

A: Control (shControl) or LOXL2-depleted (shLOXL2) endothelial cells were seeded at confluency on tissue culture plastic (no coating) or on surface coating of fibronectin at the indicated concentration ranging from 0.09 to 3 $\mu\text{g}/\text{cm}^2$. Cells were maintained for 72h before immunostaining of collagen IV (green). Nuclei were stained with DAPI (blue). Scale bar: 25 μm . **B-C:** Schematic representation of fibronectin indicating the position of the PHSRN and RGD peptides (**B**). Endothelial cells were seeded at confluency and maintained for 72h before staining of fibronectin (top row and magenta) and collagen IV (central row and green). Scale bar: 50 μm . **D-F:** Control (shControl) or LOXL2-depleted (shLOXL2) endothelial cells were seeded at confluency on tissue culture plastic (no coating) or on surface coating of fibronectin at the indicated concentration ranging from 0.09 to 3 $\mu\text{g}/\text{cm}^2$. Cells were maintained for 72h before immunostaining of β -catenin (magenta) or detection of F-actin with phalloidin-AlexaFluor 488 (green) and of nuclei with DAPI (blue) (**D**). Cell circularity (**E**) and cytoskeleton orientation (**F**) were measured for shControl (dark boxes) and shLOXL2 (clear boxes) cells. Scale bar: 30 μm . Statistical analysis was done using two-way ANOVAs (# $p < 0.05$, ## $p < 0.05$, #### $p < 0.0001$).

Figure 6. LOXL2-depletion does not alter the adhesion and contractility capacities of endothelial cells

A-C: Control (shControl) or LOXL2-depleted (shLOXL2) endothelial cells were plated on surface coating of fibronectin (i) or collagen I (ii) for 1h. **A:** Paxillin was immunostained (top row - magenta) and F-actin was detected with phalloidin-AlexaFluor 488 (green). Nuclei were stained with DAPI (blue). Scale bar: 20 μm . Morphometric parameters of focal adhesions (mean area, circularity, aspect ratio, distance from the edge of the cell) (**B**) and surface area of individual cells (**C**) were calculated were calculated for shControl (dark boxes) and shLOXL2 (clear boxes) cells in 4 independent experiments. n=42 to 52 cells. t- tests were performed. **D:** Control (shControl) or LOXL2-depleted (shLOXL2) endothelial cells were captured on an AFM cantilever coated with fibronectin and immobilized on a fibronectin coating for measurement of their mean traction rate in an AFM-stiffness clamp set-up. Statistical analysis was performed using unpaired t-tests.

Figure 7. Matrices generated by LOXL2-depletion alter distribution of adhesion proteins and signaling pathways

A: Control (shControl) or LOXL2-depleted (shLOXL2) endothelial cells were seeded at confluency and cultured 72h before preparation of CDM. Control cells were then plated for 1h before immunostaining of paxillin (magenta and middle row) or pY397-FAK (pFAK - green and bottom row). Scale bar: 50 μm (top row) and 5 μm (middle and bottom rows). **B-C:** Control (shControl) or LOXL2-depleted (shLOXL2) endothelial cells were seeded at confluency and cultured 72h before immunostaining of pY397-FAK (pFAK - cyan-**B**) or vinculin (green-**B**) or pY118-paxillin (pPAX – green-**C**). β -catenin was immunostained (red) and nuclei were detected with DAPI (blue). Orthogonal views are presented for merged images of the pY118-paxillin and β -catenin double-immunostaining (**Cii**). Scale bar: 25 μm (**B** and **Ci**) and 10 μm (**Cii**). **D:** Control (shCt) or LOXL2-depleted (shLOXL2) endothelial cells were seeded at confluency and cultured 72h before cell lysis and western blotting for the indicated proteins (i). The level of expression (ii), basal phosphorylation (iii) and VEGF-induced phosphorylation (iv) were quantified in 4 independent experiments performed in duplicate culture wells (n=8). Statistical analysis was performed using unpaired t-tests (* p < 0.05, ** p < 0.005, *** p < 0.0005, **** p < 0.0001).

SUPPLEMENTARY FIGURES

Figure S1. Characterization of CDM

A: Endothelial cells were seeded at confluency and maintained 6h before either fixation (top row) or preparation of CDM (bottom row). Fibronectin (left column and magenta) and LOXL2 (central column and green) were immunostained. Nuclei were stained with DAPI (blue). Scale bar: 20 μm . **B:** Endothelial cells expressing LOXL2/GFP were seeded at confluency and cultured for 72h before immunostaining of fibronectin (red). Scale bar: 20 μm . **C:** Endothelial cells expressing LOXL2/GFP were seeded below (30 000 cells/cm²) or above (60 000 cells/cm²) confluency. They were fixed after 72h in culture and immunostained for LOXL2 (red). Scale bar: 100 μm .

Figure S2. Quantification method for correlative/AFM images

To quantify the correlation rate between the fluorescence signal and the AFM-detected structures, images were cropped and manually thresholded for all channels using image J software. Integrated density (ID) was calculated for thresholded AFM and after image calculation of pixels containing both thresholded AFM and fluorescence signals. Proportion of fibers containing fluorescent signal was then calculated as the ratio of integrated densities.

Figure S3. Deterioration of LOXL2 immunoreactivity during matrix maturation

Endothelial cells expressing LOXL2/GFP were seeded at confluency and cultured for 24h (top row) or 72h (bottom row) before immunostaining of LOXL2 (red). White box indicates the zoomed area. bar: 25 μm (left column) and 5 μm (middle and right columns).

Figure S4. LOXL2 subcellular immunoreactivity

Endothelial cells expressing LOXL2/GFP were seeded at confluency and cultured for 72h before immunostaining of LOXL2 using either an antibody directed against the C-terminal half of the protein (AbCam #96233-red – **Ai** and **B** top row) or the antibody targeting the N-terminus (CST #96301-red – **Aii** and **B** bottom row). White box in left column corresponds to the zoomed area in right column. Scale bars: 25 μm (**A** left columns) and 10 μm (**A** right columns) and 5 μm (**B**).

Figure S5. Segmentation and image analysis for calculation of morphometric parameters

β -catenin signal was thresholded to generate binary images before applying MorphoLibJ plugin (Image J) in order to segment and obtain morphological parameters on the confluent monolayers including

area, perimeter, circularity, and maximum Feret diameter. Cells located at the border were removed from the analysis.

Figure S6. Matrix deposition on fibronectin coating

Control (shControl) or LOXL2-depleted (shLOXL2) endothelial cells were seeded at confluency on fibronectin surface coating and maintained for 6h (A) or 24h (B) before immunostaining of fibronectin (green - left panels) or collagen IV (green – right panels). Scale bars: 50 μm (i) and 10 μm (ii).

Figure S7. Vinculin expression and early association to focal adhesion is not affected by LOXL2 knock-down

A: Control (shControl) or LOXL2-depleted (shLOXL2) endothelial cells were plated on surface coating of fibronectin or collagen I for 1h. Vinculin was immunostained (top row - magenta) and F-actin was detected with phalloidin-AlexaFluor 488 (green). Nuclei were stained with DAPI (blue). Scale bar: 10 μm . **B:** Control (shControl) or LOXL2-depleted (shLOXL2) endothelial cells were seeded at confluency and cultured 24h before cell lysis and western blotting for the indicated proteins.

Figure S8. Vascular permeability is affected by LOXL2 knock down

Control (shControl) or LOXL2-depleted (shLOXL2) endothelial cells were seeded at confluency on fibronectin surface coating. Cells were stimulated with thrombin at 88h. Impedance was measured over 72h for assessment of permeability. Culture medium changes are indicated at 24h and 68 h.

FIGURE 1

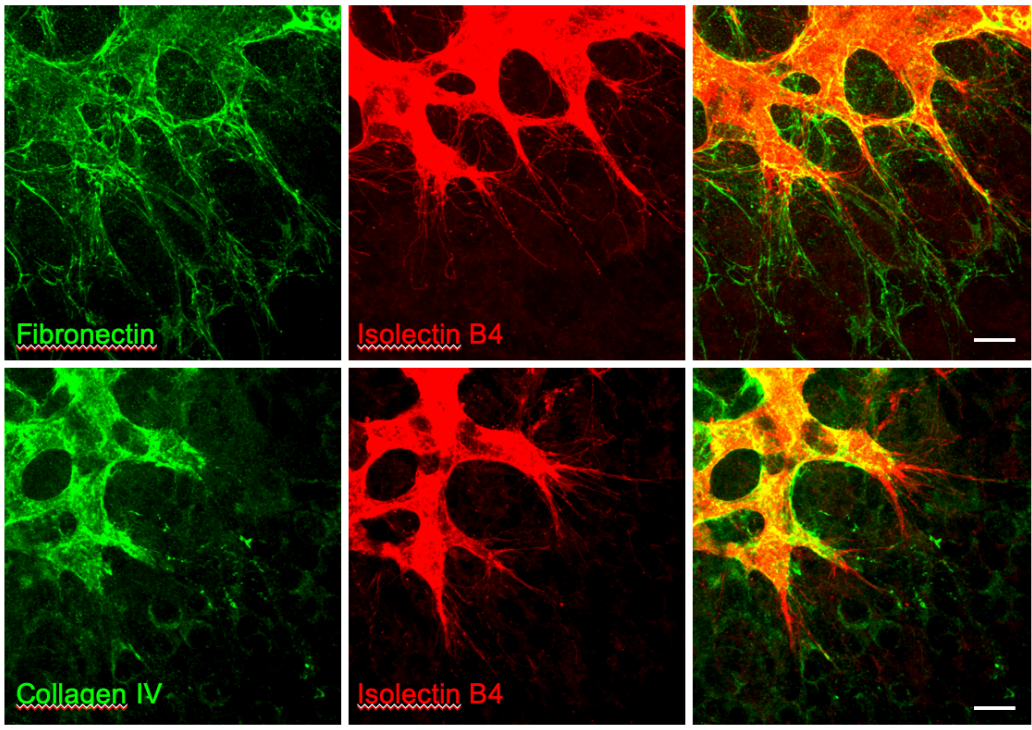


FIGURE 2

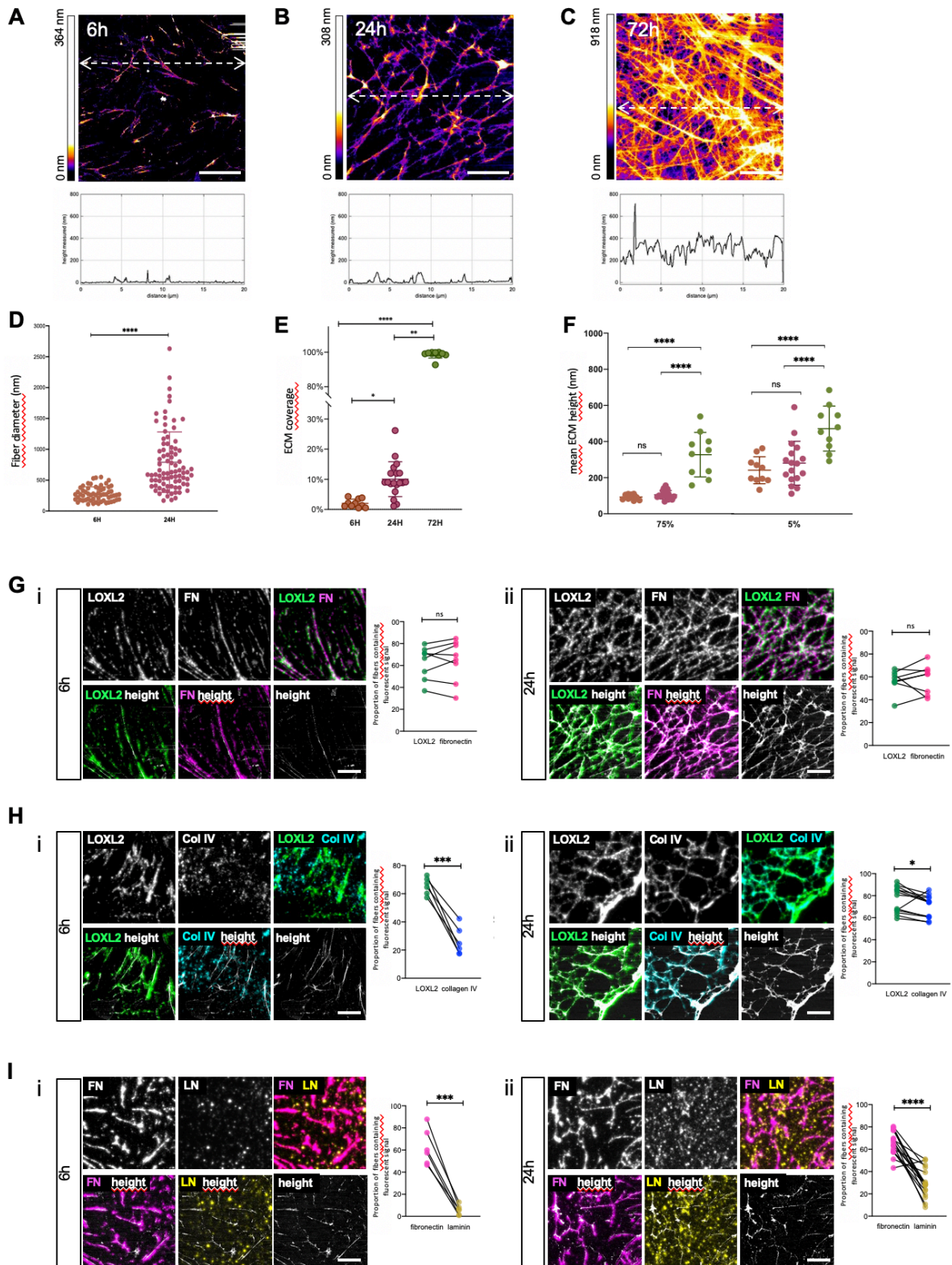


FIGURE 3

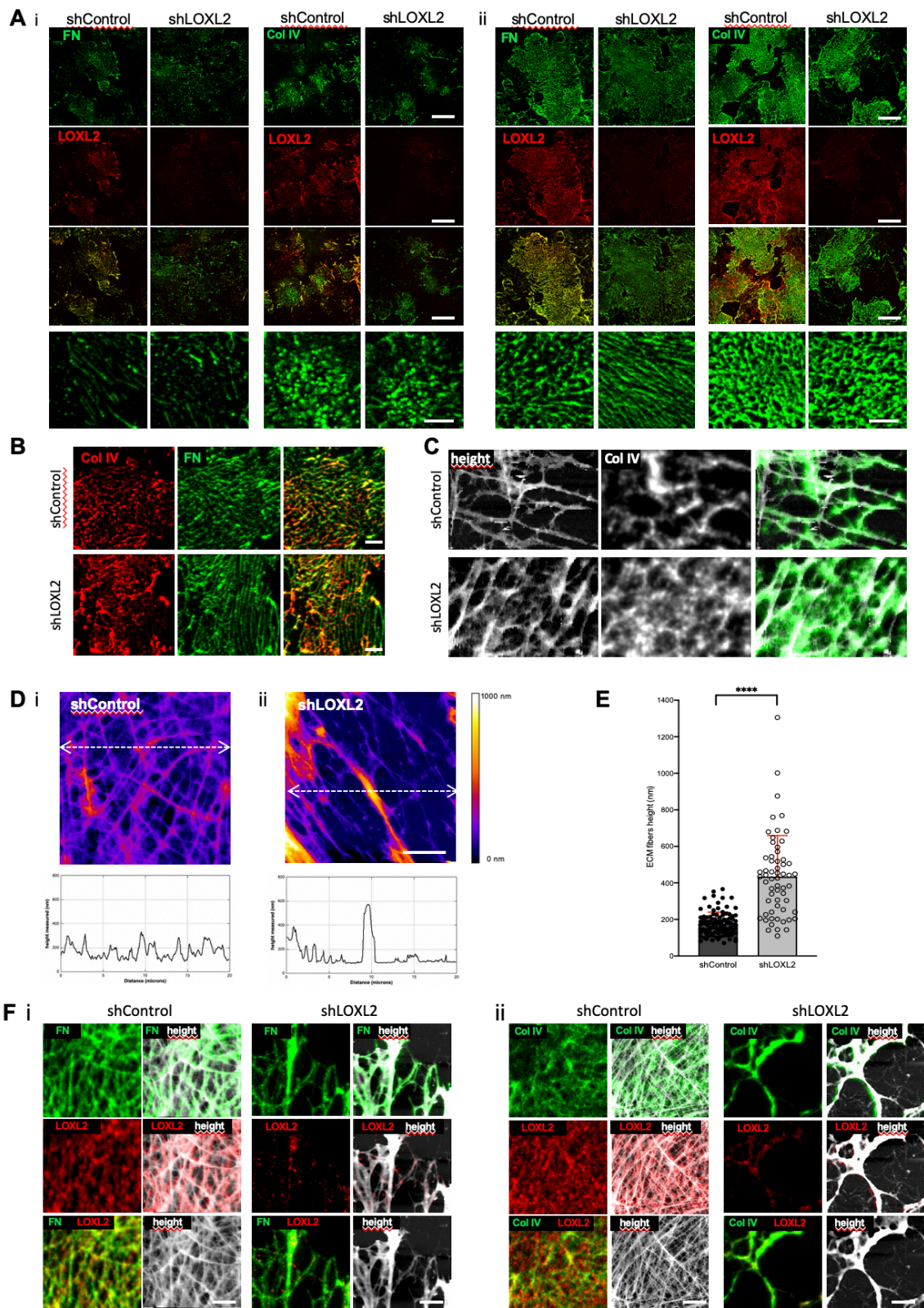


FIGURE 4

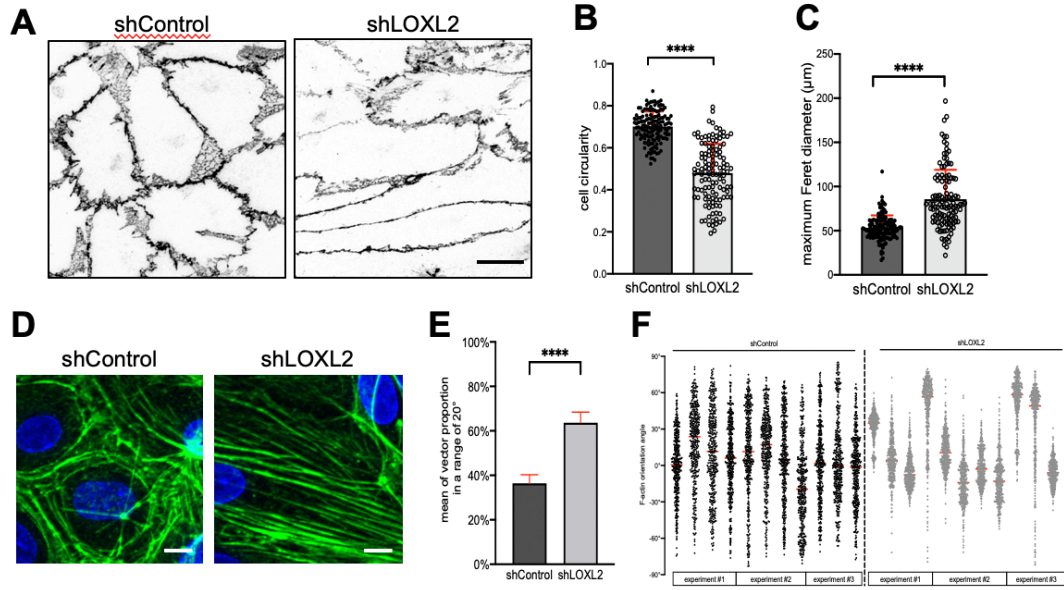


FIGURE 5

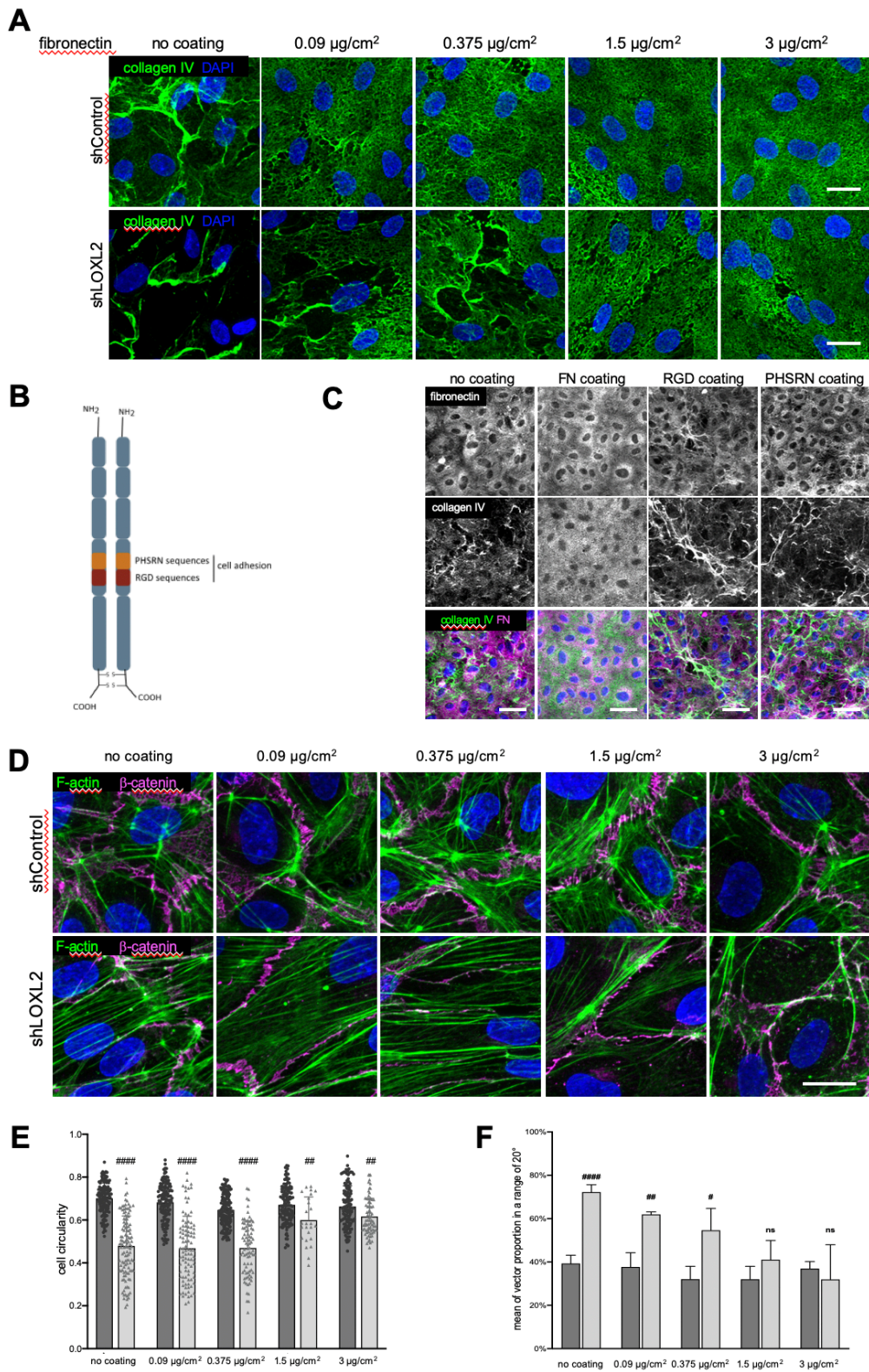


FIGURE 6

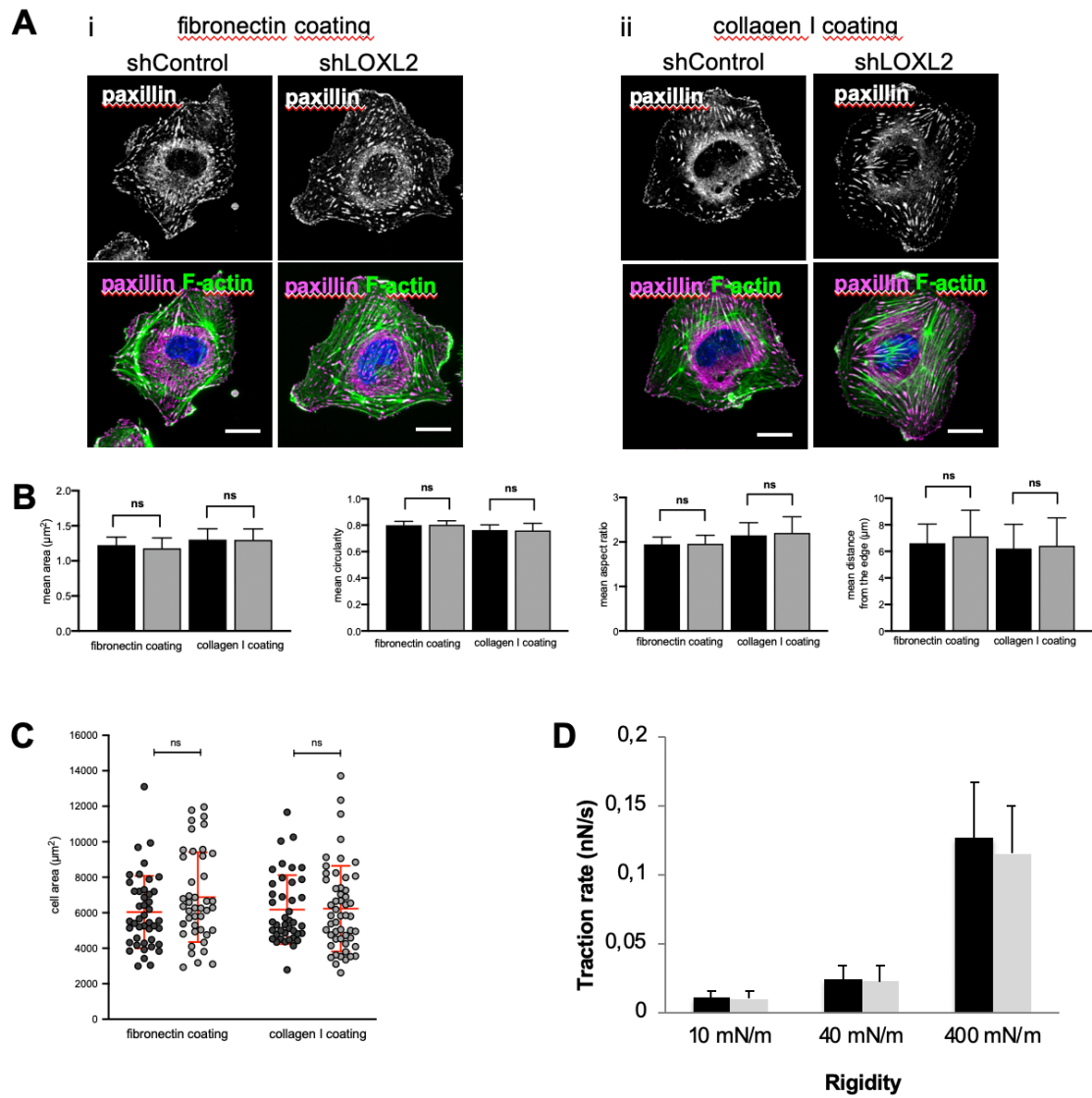
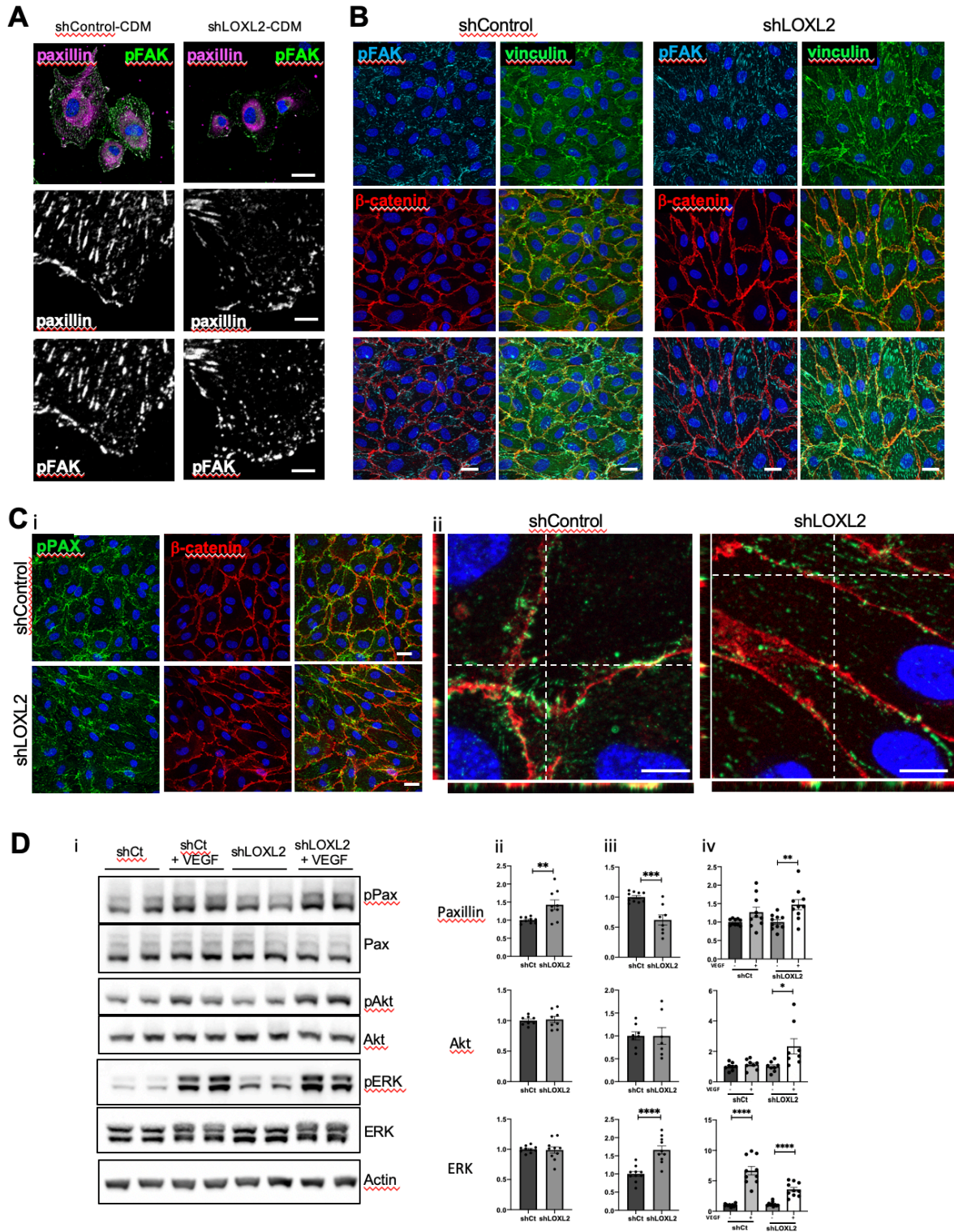
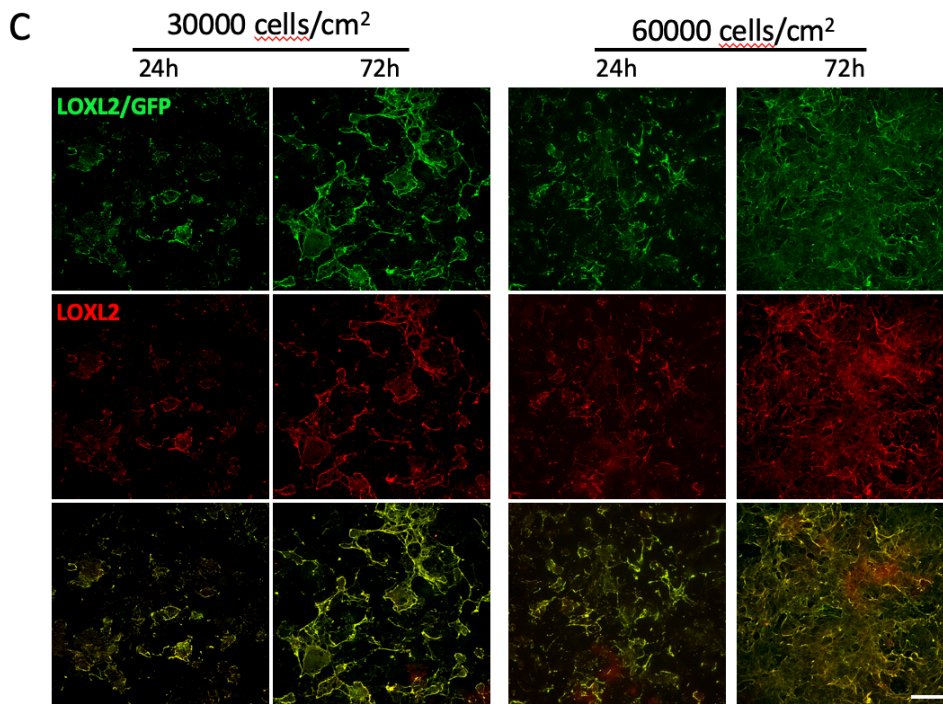
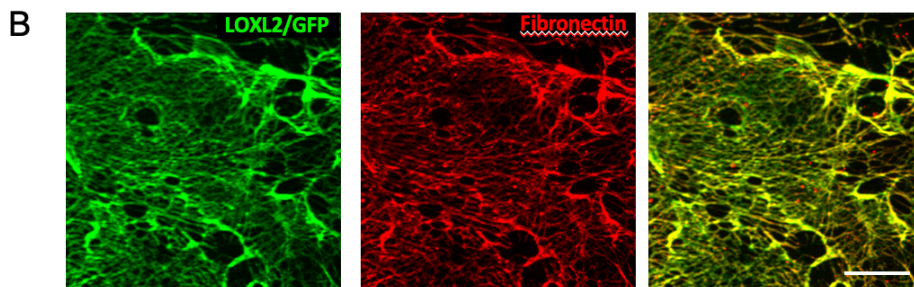
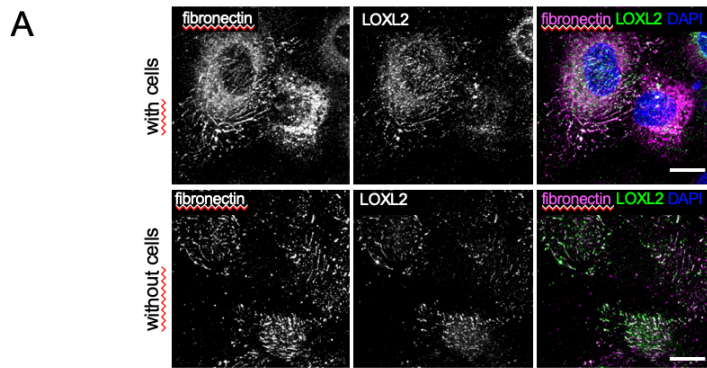


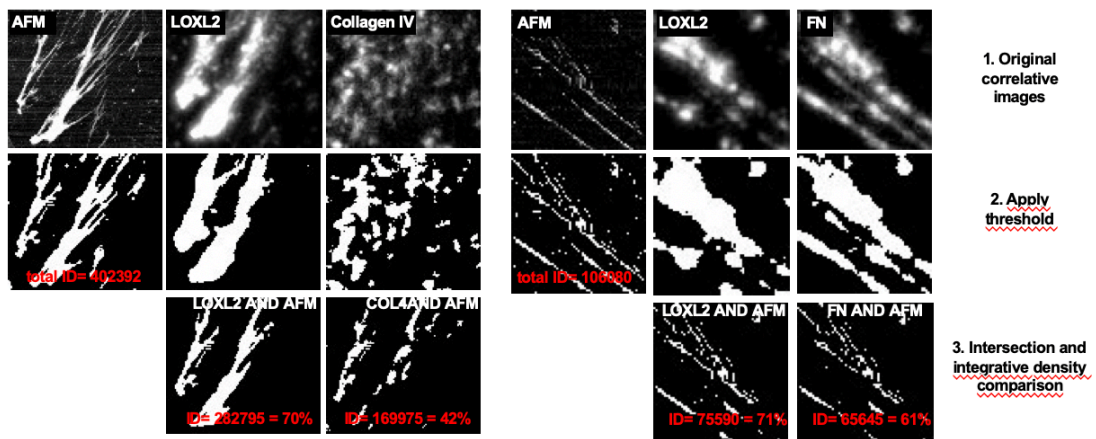
FIGURE 7



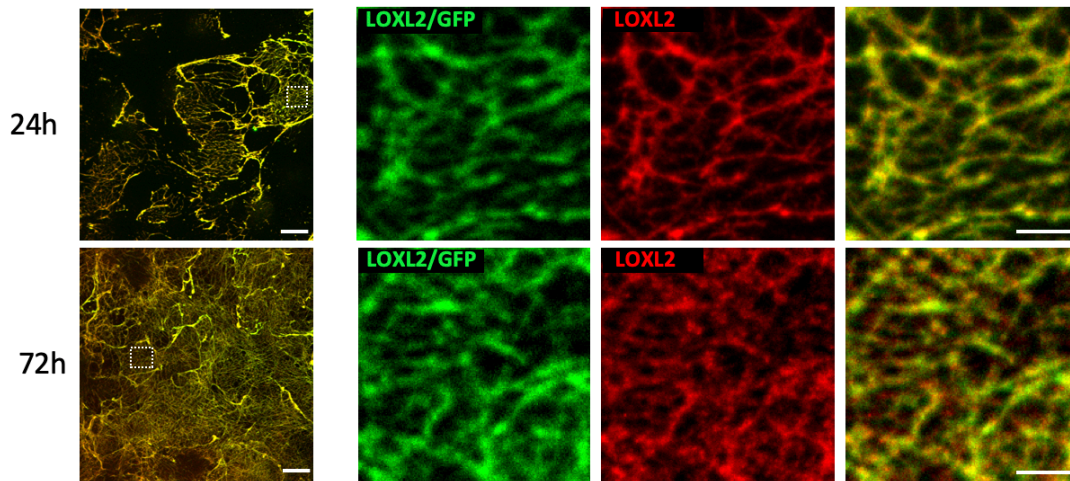
SUPPLEMENTARY FIGURE 1



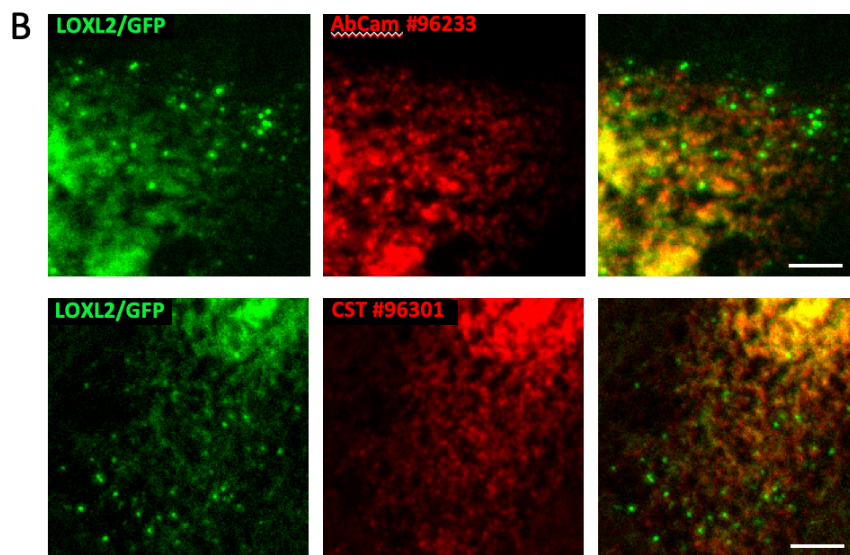
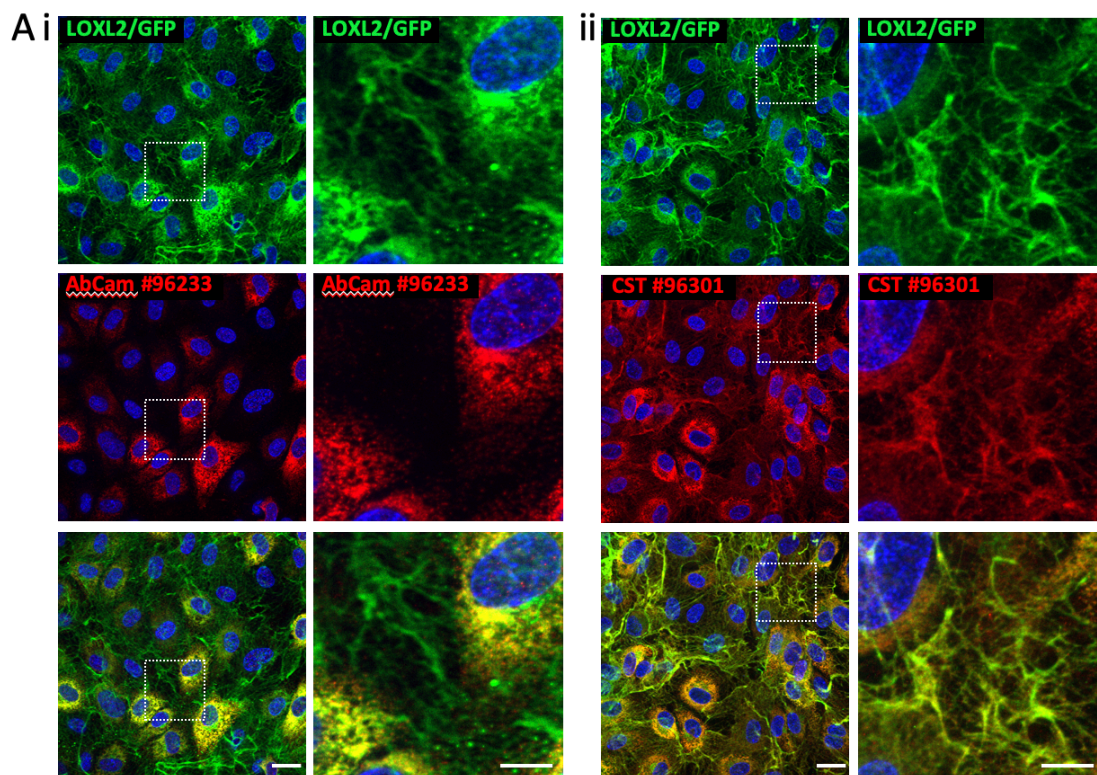
SUPPLEMENTARY FIGURE 2



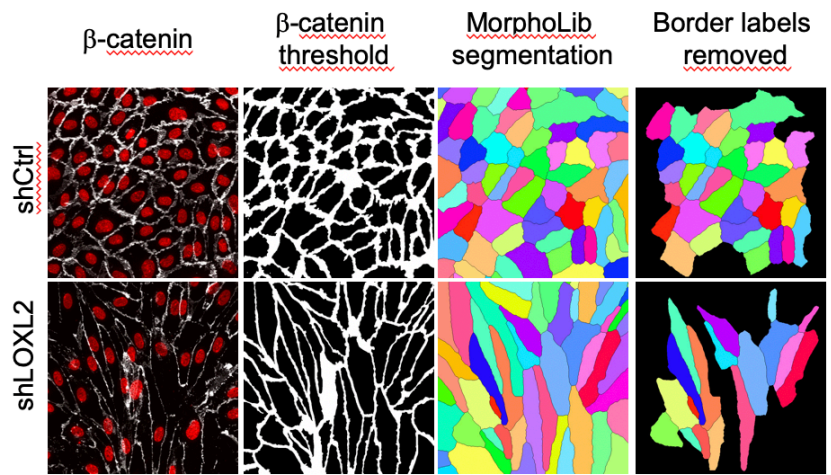
SUPPLEMENTARY FIGURE 3



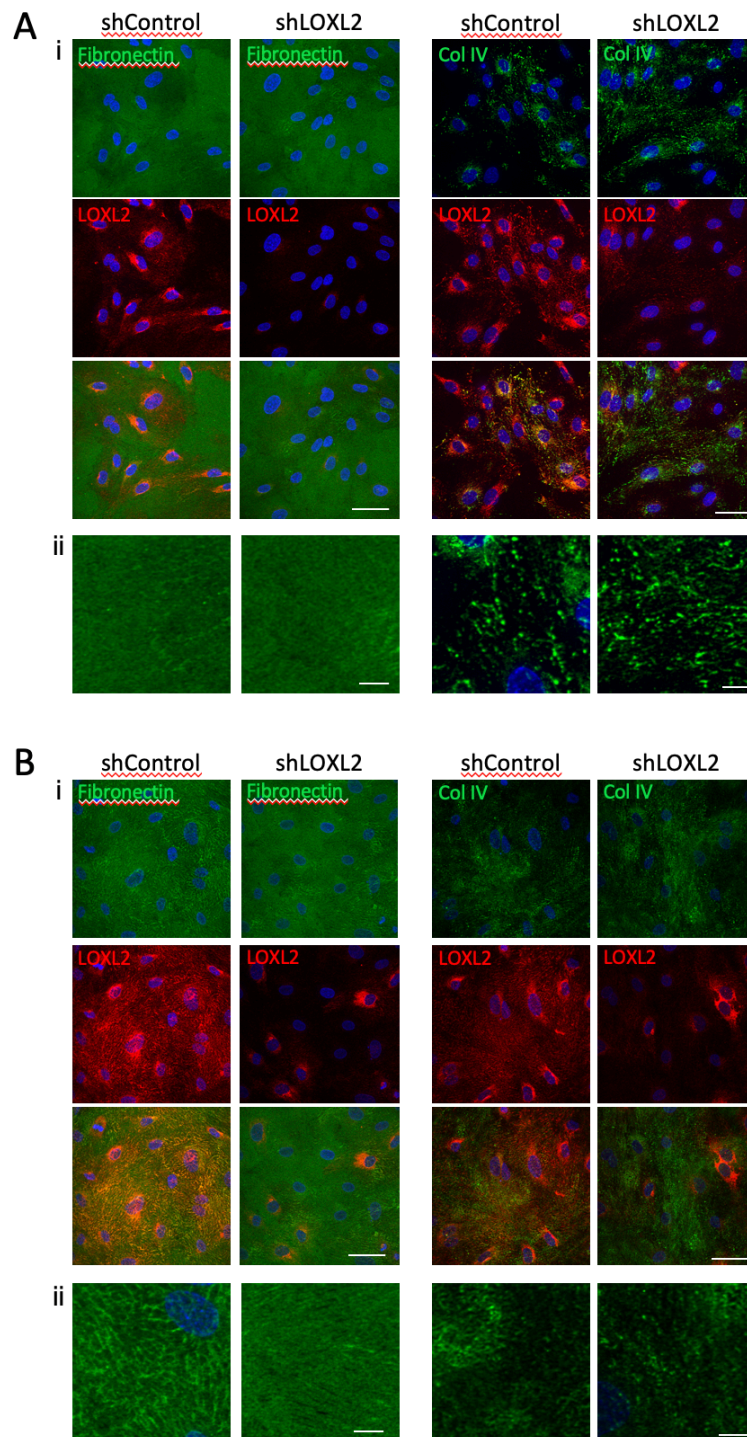
SUPPLEMENTARY FIGURE 4



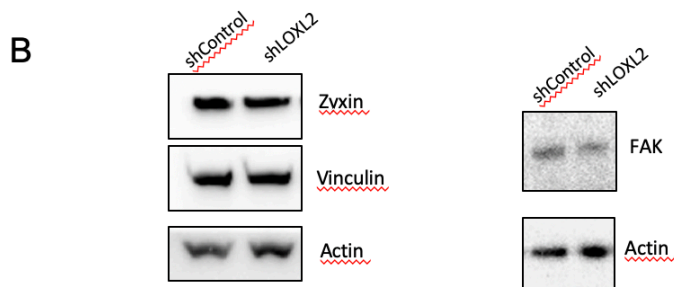
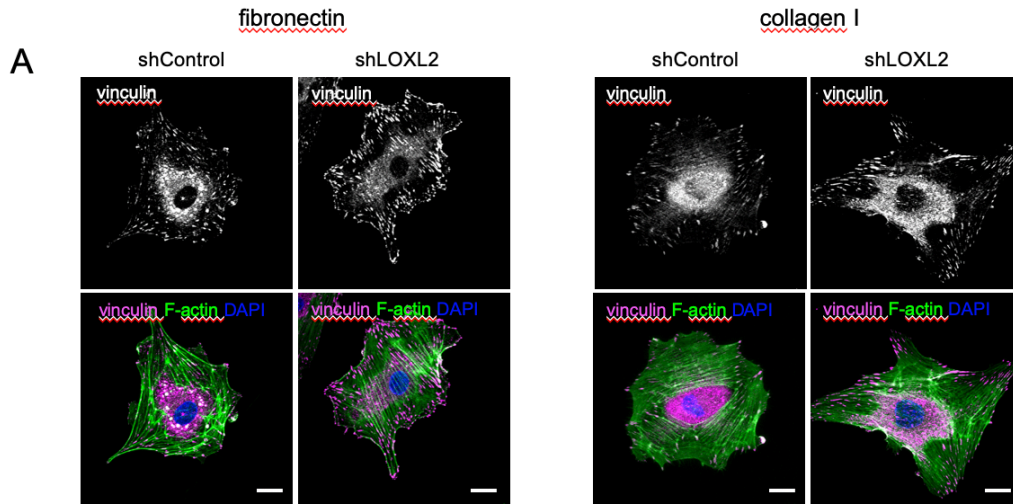
SUPPLEMENTARY FIGURE 5



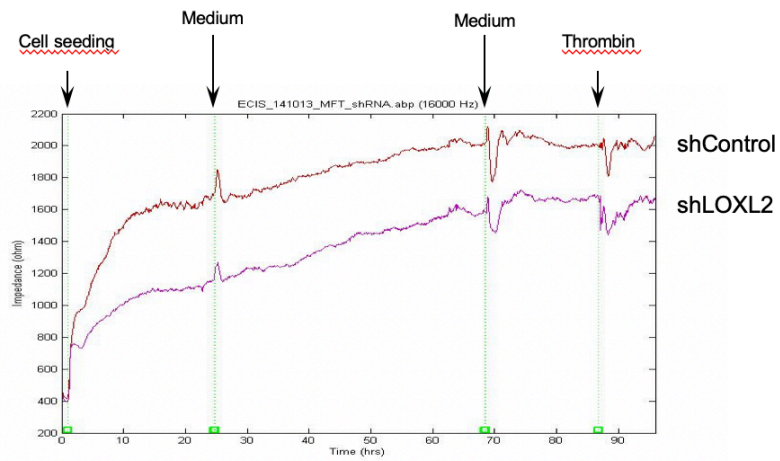
SUPPLEMENTARY FIGURE 6



SUPPLEMENTARY FIGURE 7



SUPPLEMENTARY FIGURE 8



Discussion and perspectives

Sprouting angiogenesis is associated with extensive ECM remodeling, including basement membrane deposition by endothelial cells. Although this structure is a crucial component of the vasculature required for capillary morphogenesis and maintenance of vascular integrity, the structural and molecular mechanisms involved in building and remodeling this extracellular microenvironment are not completely understood. Our team previously identified LOXL2 as a protein expressed in the endothelial basement membrane in hypoxic conditions and demonstrated that LOXL2 regulates capillary formation and collagen IV deposition (Bignon et al., 2011). The present work thus aimed to link the major role of LOXL2 in regulating the organization of the endothelial basement membrane to the downstream mechanotransduction properties of endothelial cells that are required for angiogenesis. I have first characterized generation of the basement membrane and the functional role of LOXL2 in this process, and then analyzed the consequences of LOXL2 depletion on the mechanosensing and response of endothelial cells to their defective microenvironment. I was also involved in a project focused on the role of LOXL2 in cross-linking the interstitial ECM. This complementary function of LOXL2 associated to pathologies including cancer and fibrosis provided information concerning the complexity of targeting LOXL2 in pathological microenvironments.

1. Basement membrane deposition

The first part of the present work aimed to characterize basement membrane deposition by endothelial cells and to investigate the role of LOXL2 in regulating this process. Little is known about the structural organization and molecular composition of the capillary basement membrane, even though each of its core components is essential to vascular development and homeostasis (Marchand et al., 2019). Indeed, mice lacking collagen IV, laminin or fibronectin display defects in capillary formation (George et al., 1993; Pöschl et al., 2004; Thyboll et al., 2002) and 3D *in vitro* angiogenesis models also confirmed these observations (Bignon et al., 2011; Xu et al., 2020; Zhou et al., 2008). However, very few models are available i) to study the structure of capillary basement membrane and ii) to decipher the succession of events leading to the supramolecular assembly of its components. Indeed, accessing capillary basement membrane topography remains a challenge. In order to study the role of LOXL2 in structural mechanisms involved in basement membrane deposition and molecular assembly by endothelial cells, we used *in vitro* cell-derived extracellular matrices, which had already been described before for endothelial cells and mesenchymal cells (Bignon et al., 2011; Tello et al., 2016). We took advantage of polarization of basement membrane deposition below the

cells and modulated its assembly by tuning several factors including culture time, confluency and physical support, but also coating conditions.

We first demonstrated that basement membrane deposition by endothelial cells is an autocrine process, initiated upon cell seeding consisting in deposition of nascent fibrillar structures building up a meshwork. This process is continuous and progressive over periods of days, and develops via two major steps involving lateral elongation before thickening/assembly into multiple layers. The historical model of basement membrane organization consists in association of self-assembled laminin sheet and collagen IV network, connected through binding to heparan sulfate proteoglycans and nidogen (Hohenester and Yurchenco, 2013). In parallel, fibronectin is proposed to be associated to this structure rather than a structural component (LeBleu et al., 2007). We here demonstrated that basement membrane assembly relies on the organization of collagen IV and fibronectin supramolecular complexes and were therefore interested in characterizing the involvement of LOXL2 in this process.

A. LOXL2 interacts with ECM proteins prior to their deposition

A transcriptomic analysis demonstrated high expression of LOXL2 in endothelial tip cells (del Toro et al., 2010), suggesting its early deposition in the basement membrane during sprouting angiogenesis. Indeed, using a LOXL2-GFP construct, time-lapse TIRF microscopy experiments showed direct incorporation upon exocytosis in the first fibrillar structures of the matrix underneath migrating cells (Umana-Diaz et al., 2020), raising the question of the mechanisms involved in targeting LOXL2 to these exocytosis hotspots. A previous report has demonstrated that the exocyst, an octameric protein complex involved in the tethering of secretory vesicles to the plasma membrane prior to SNARE-mediated fusion and secretion is involved in matrix degradation by locally releasing MT1-MMP-containing vesicles (Monteiro et al., 2013). A similar mechanism could be proposed for matrix generation and LOXL2 exocytosis.

LOXL2 could be co-deposited with other basement membrane components, as we detected intracellular interactions with collagen IV and fibronectin using proximity ligation assay and surface plasmon resonance experiments (Umana-Diaz et al., 2020). Interactions with collagen IV fits with the fact that it is a substrate of LOXL2 (Añazco et al., 2016). The result was less expected concerning LOXL2-fibronectin interaction, although binding of fibronectin to LOX catalytic domain (very conserved in the whole LOX family) had already been described (Fogelgren et al., 2005). Another function of LOXL2 intracellular interactions could correspond

to a late-chaperone activity, to ensure proper folding prior to deposition in the ECM. Similar activity has already been proposed for SPARC protecting collagen IV from misfolding during intracellular trafficking in the drosophila embryo (Chioran et al., 2017). This hypothesis is also supported by our immunofluorescence results showing that two antibodies targeting the N- and C-terminus of LOXL2 do not detect LOXL2/GFP in the Golgi apparatus nor in secretory vesicles. Intracellular interactions of LOXL2 with other ECM proteins in the late secretory pathway could prevent antibody recognition. This is also consistent with the structural analysis of LOXL2 that we investigated using small-angle X-ray scattering demonstrating that the 4 SRCR domains and the catalytic domain are organized as a string of pearls, free from any steric hindrance, making these domains available for interactions with other proteins (Schmelzer et al., 2019). A protective role of LOXL2 on collagen IV was further suggested by the requirement for cleavage of the SRCR domains 1 and 2 prior to cross-linking collagen IV 7S domains (López-Jiménez et al., 2017). Altogether, our data suggest that LOXL2 interacts intracellularly with collagen IV and fibronectin and stabilizes these proteins before deposition in ECM structures upon exocytosis.

B. Spatio-temporal distribution of basement membrane components

Whereas initial deposition of collagen IV appeared as a diffuse granular staining, fibronectin was incorporated into short fibrils of approximately 50 nm diameter and 5 μ m long. Consistent with our results, fibronectin fibrillogenesis is a cell-autonomous process that requires endogenous synthesis of fibronectin in endothelial cells (Cseh et al., 2010). LOXL2 was detected in both ECM nascent fibers and granular structures. Using immunofluorescence (Umana-Diaz et al., 2020) and correlative high-resolution topography analysis, we then followed the remodeling of these fibronectin fibrils and collagen IV granular deposits. Collagen IV was associated with fibronectin in ECM fibers only after 24h of culture in a pattern of elongated and connected fibrillar structures that resembles neither early fibronectin fibrils, nor collagen IV granular deposition. Two recent hypotheses were proposed for association of these proteins in the basement membrane: on one hand, fibronectin fibrils could be the organizing centers allowing nascent ECM formation (Filla et al., 2017); on the other hand, collagen IV surface coating was proposed to promote fibronectin fibrillogenesis (Lu et al., 2020). In both situations, our data nevertheless demonstrate that laminin is not a scaffold for collagen IV and fibronectin assembly, but is rather organized independently, in agreement with the historical two-layered model of basement membranes (Hohenester and Yurchenco, 2013).

Generation of endothelial cells depleted for each of these components including laminin could provide more details on the sequential events leading to basement membrane organization.

Further maturation of the collagen IV-fibronectin network consists in accumulation of multiple layers of these fibrillar structures, as detected by AFM and TIRF experiments. Overnight time-lapse TIRF movies showed that endothelial cells kept on loading the matrix locally with LOXL2 as they migrated, suggesting a continuous deposition process and a role for LOXL2 in matrix maturation. These results were consistent with work conducted in the drosophila egg chamber, which constitutes an interesting system to study basement membrane deposition. Live-imaging analysis showed that elongation of the egg chamber is coupled to basement membrane production by migrating follicle cells and extracellular fibrils of collagen IV eventually align along the elongation axis (Isabella and Horne-Badovinac, 2015). Our data therefore suggest that LOXL2 incorporation in the basement membrane is a dynamic process associated with cell migration.

C. LOXL2 drives ECM spatio-temporal assembly in a context-dependent manner

We had already demonstrated that LOXL2 regulates collagen IV deposition (Bignon et al., 2011) and further established that these effects are not dependent on its catalytic activity but require the SRCR12 domains of the protein (Umana-Diaz et al., 2020). We here demonstrated that LOXL2 promotes association of the fibronectin fibrillar material with the collagen IV meshwork over time and stabilizes basement membrane at later stages. Indeed, LOXL2 is not involved in the first steps of matrix deposition, but rather drives supramolecular organization of its components over time. In a first step, LOXL2-depletion results in inhibition of fibronectin remodeling, whereas collagen IV organization can still proceed. At longer term, maturation of the collagen IV network is also impaired and both fibronectin and collagen IV end up in huge aggregates with damaged topographical distribution as detected by AFM. Interactions between collagen IV and fibronectin have been known for long (Aumailley and Timpl, 1986; Miller et al., 2014). However, to our knowledge, no binding site has been identified yet in either protein. An interesting hypothesis is that LOXL2 participates to the supramolecular assembly of fibronectin to self-assembling collagen IV by providing a link between these two complexes. Even though collagen IV cross-linking has an important role in basement membrane stability (Añazco et al., 2016; Lee et al., 2020), we have shown that LOXL2 function in basement membrane scaffolding does not require its catalytic activity (Umana-Diaz et al., 2020). Inhibition of fibronectin remodeling in LOXL2-depleted basement membranes, characterized by alignment

of fibronectin fibrils, could be explained by increased intramolecular tension. Using FRET-based sensors, regulation of fibronectin-collagen I interactions by fibronectin tension has been demonstrated (Kubow et al., 2015). Similarly, LOXL2-mediated collagen IV-fibronectin association could regulate subsequent mechanoregulation between ECM proteins.

We were also interested in understanding how basement membrane scaffolding was influenced by substrate coating conditions. Indeed, basement membrane deposition *in vivo* is known to be modulated by the molecular composition/stiffness of the surrounding micro-environment as demonstrated by structural distinctions between several basement membranes according to the vascular bed (Liliensiek et al., 2009). We demonstrated that surface coating with collagen I or fibronectin induced remodeling of collagen IV by control cells and also rescued collagen IV organization by LOXL2-depleted cells (Umana-Diaz et al., 2020). We further demonstrated that these effects were dose-dependent, as already suggested for fibronectin fibrillogenesis by fibroblasts upon coating with collagen IV, laminin or Matrigel (Lu et al., 2020). Furthermore, using the RGD and PHSRN cell-adhesion peptides, we demonstrated that this process was mediated by interactions between ECM proteins and not induced by improved cell adhesion.

Our results concerning fibronectin alignment at 24h in the LOXL2-depleted cells suggested a strong cell-mediated remodeling of the matrix. We propose that LOXL2 protects the matrix from being subjected to cell tractions mediated by integrins $\alpha 5\beta 1$ or $\alpha V\beta 3$, through either mechanical or topographical regulation: i) stabilization of the matrix by LOXL2 could anchor cells in a stiffer network; ii) remodeling of the fibronectin network with collagen IV self-assembling network could mask cell adhesion sites, as discussed further. This hypothesis is also supported by observation of collagen IV fibrils alignment along cell elongation axis in the drosophila egg chamber, that also correlates with F-actin distribution in epithelial cells (Cerqueira Campos et al., 2020). Of note, similar ECM alignment is observed in tumor-associated stromal collagen, correlating with increased local invasion of tumor cells (Provenzano et al., 2008). In this context, regulation of collagen architecture by LOXL2 rather than molecular content regulates cell responses (Grossman et al., 2016).

Altogether, our data demonstrate that LOXL2 drives spatio-temporal assembly of the basement membrane by promoting association of fibronectin to self-assembled collagen IV. This process could be responsible for regulating architecture and topography of the matrix, making it less prone to cell-mediated remodeling. We thus propose that ECM scaffolding through LOXL2 could mediate cell rearrangements, as supported by the impact of LOXL2 on cortical actin distribution and cell morphology at longer term.

2. Mechanotransduction

The second part of my work aimed to decipher the mechanical response of endothelial cells to the basement membrane they generated. While previous reports had shown the impact of ECM structural/mechanical properties on cell responses, mainly by using micropatterned substrates or ECM geometrical control (Cavalcanti-Adam et al., 2006; Chen et al., 1997), only few studies focused on the role of cell-generated matrix in regulating this process (Cerqueira Campos et al., 2020; Ngandu Mpoyi et al., 2020). Analysis of endothelial mechanotransduction properties demonstrated that LOXL2-mediated basement membrane scaffolding regulates focal adhesions distribution and maturation, and especially distribution of vinculin, pY397-FAK and pY118-paxillin. Interestingly, vinculin and pY397-FAK were detected in large and elongated focal adhesions in LOXL2-depleted cells. Similar alignment of focal adhesions could be triggered by patterning fibronectin in lines (Wang et al., 2018b). Fluorescence levels of pY118-paxillin were very low in these structures, and overall paxillin phosphorylation was decreased upon LOXL2-depletion. Dephosphorylation of paxillin is associated with stabilization of focal adhesions (Zaidel-Bar et al., 2007) and could be responsible for the cytoskeleton reorganization and cell elongation that we have described above. These effects are mediated by defaults in matrix remodeling since paxillin distribution in nascent and focal adhesions was not affected on surface coatings.

In parallel with remodeling of cell-ECM adhesions, LOXL2 depletion also impacted redistribution of vinculin from cell-cell junctions. Vinculin is a well characterized force-sensor at epithelial and endothelial cell junctions, where it functionally regulates stability of cell-cell junctions (le Duc et al., 2010; Huveneers et al., 2012; Thomas et al., 2013). Vinculin was redistributed out of the focal adherens junctions in LOXL2-depleted cells. Recruitment of vinculin to cell-cell junctions is dependent on ECM stiffness (Seddiki et al., 2018). Redistribution of vinculin out of focal adherens junctions could therefore be due to a lower ECM stiffness (Umana-Diaz et al., 2020). pY118-paxillin was also translocated out of cell-cell junctions but did not accumulate in cell-ECM adhesions, as vinculin. Localization of paxillin at cell-cell junctions has been poorly investigated (Birukova et al., 2007; Crawford et al., 2003), even in studies that provided evidence for such distribution (van Geemen et al., 2014). Furthermore, its distribution within adherens junctions was also modified, which could correspond to decreased tension forces at cell-cell junctions. Such translocation out of the cell-cell junctions was indeed accompanied with increased permeability.

3. Angiogenesis

We here show that basement membrane scaffolding by LOXL2 regulates endothelial cell mechanotransduction and we propose that this mechanism could explain the angiogenic response of endothelial cells by regulating mechanics of cell-ECM and cell-cell contacts. Using a 3D *in vitro* capillary formation set-up in which endothelial cells are seeded in collagen I hydrogels, we have recently demonstrated that initial cell spreading in the hydrogel is accompanied by a strong traction of collagen fibers that establish a shell-like organization of material stacked-up at the cell surface (Atlas et al, in preparation, see appendix #). As vascular morphogenesis progresses, collagen IV is deposited in the basement membrane at the interface between fibrillar collagen and cell surface, in parallel with formation of adherens junctions and remodeling of actin cytoskeleton. An interesting hypothesis is that this newly formed basement membrane provides local mechanical anchorage to cells, thus promoting formation and stabilization of cell-cell junctions, at the expense of cell-ECM adhesions. The matrix generated by LOXL2-depleted cells combining lower stiffness (Umana-Diaz et al., 2020) and perturbed topography would thus fail at supporting angiogenesis. We have shown that 3D *in vitro* tube formation was completely abolished within the hydrogel whereas LOXL2-depleted cells could generate capillaries in the vicinity of the stiff culture dish (Bignon et al., 2011). These results strongly suggested that sensed-stiffness of the micro-environment plays an important role in counterbalancing LOXL2-depletion, especially considering that cell contractility in response to stiffness is not altered by LOXL2 depletion. The concept of basement membrane as a mechanical support is illustrated by experiments using *in vitro* capillary models, in which adding soluble RGD peptides is unable to stimulate tube formation, showing that the role of ECM relies on endothelial cell ability to resist mechanical loads more than ability to bind cell receptors (Ingber and Folkman, 1989). LOXL2 stabilizes fibronectin and collagen IV association into basement membrane networks, thus downregulating formation of cell-ECM adhesions and promoting cell-cell adherens junctions. In the absence of LOXL2, prevention of fibronectin remodeling could maintain binding sites for cell receptors such as integrin $\alpha 5\beta 1$, resulting in stress fibers and increased tension exerted by cells. Such mechanoregulation has already been proposed for interactions between fibronectin and collagen I (Kubow et al., 2015). In parallel, decreased translocation of adhesion proteins to cell-cell contacts could prevent junction formation and vascular morphogenesis, as demonstrated for the endothelial knock-out of vinculin (Carvalho et al., 2019). This process would thus prevent generation of capillaries in a 3D environment.

4. Link between interstitial ECM and basement membrane generation

A complementary project developed in the lab aimed to produce collagen I hydrogels with improved angiogenic properties. For that purpose, we used a biomimetic approach consisting in cross-linking collagen I by LOXL2. Indeed, direct cross-linking of collagen I by LOXL2 has been recently demonstrated (Schilter et al., 2019) and such activity has been linked to pathological situations such as cancer or fibrosis (Barry-Hamilton et al., 2010; Cosgrove et al., 2018; Ikenaga et al., 2017; Schilter et al., 2019). Overexpression of LOXL2 is linked to increased collagen cross-links, ECM stiffening, and change in collagen structural properties including alignment and nanoarchitecture of fibers (Jones et al., 2018; Schilter et al., 2019).

We first tuned collagen fibrillogenesis by modulating pH, temperature and collagen concentration of the hydrogels, thus generating a panel of seven gels in a range of bulk stiffness from 50 Pa to 5 kPa, as measured by shear rheology. There was however no direct connection between stiffness or pore size of these hydrogels and capillary formation. We investigated the impact on angiogenesis of LOXL2-mediated modifications of the microenvironment. We focused on two hydrogels with opposed characteristics: a soft gel with low fibrillogenesis that promoted good capillary formation, and a stiffer one with high fibrillogenesis and poor angiogenic properties. LOXL2-mediated cross-linking highly improved mechanical properties of the first hydrogel, without impacting angiogenesis, while it improved capillary formation in the stiffer gel, without noticeable impact on neither structural properties nor bulk stiffness.

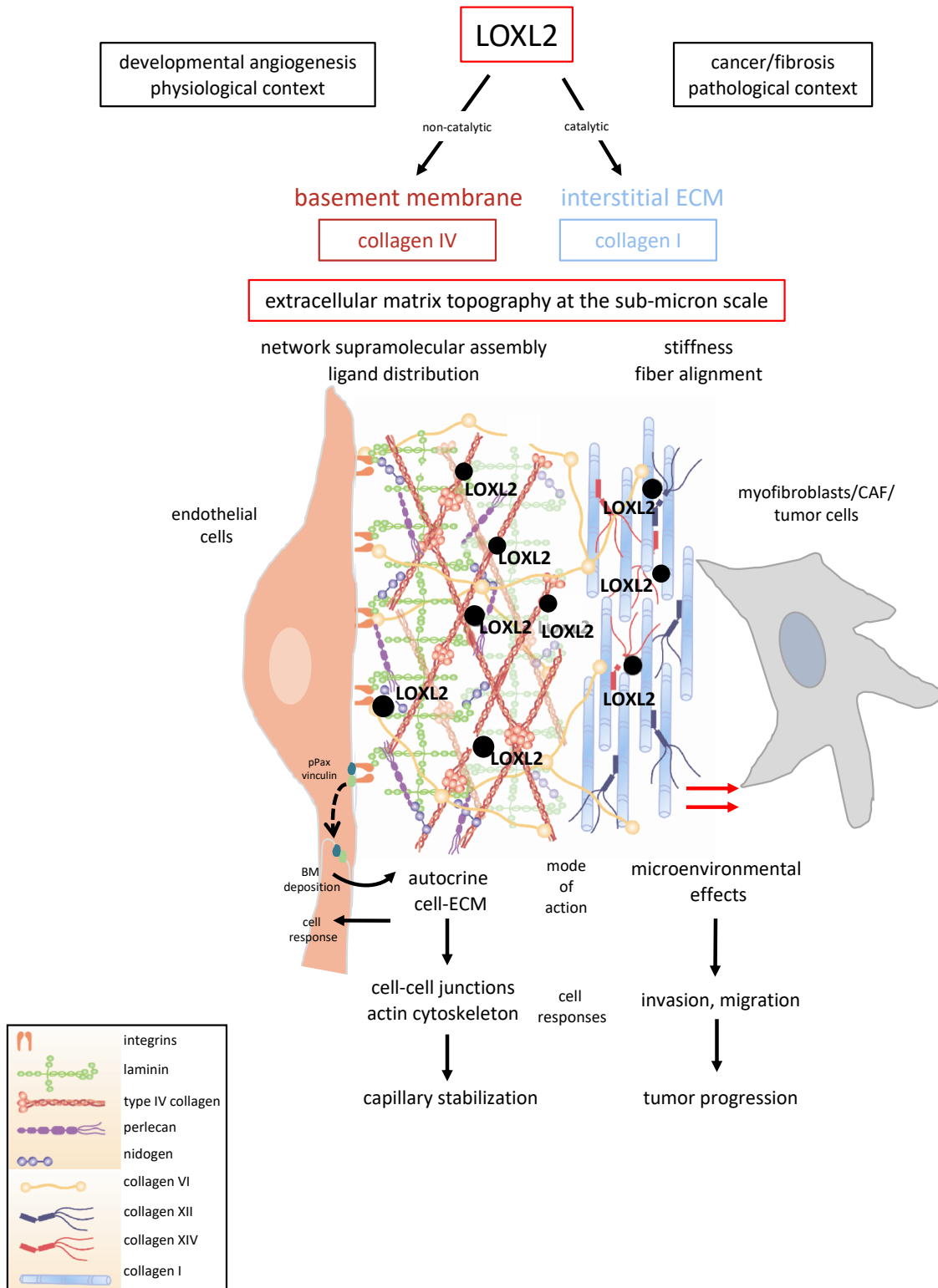
To get better insight into the mechanisms involved in these effects, we turned to high resolution analysis of structural and mechanical properties of the hydrogels. Topographical imaging confirmed the structural analysis performed by second-harmonic generation: LOXL2-mediated cross-linking of the low fibrillogenesis hydrogels increased pore size while it had no impact on the high fibrillogenesis hydrogel. Nanoindentation allowed measurement of the mechanical properties at the fiber level. Such analysis demonstrated that LOXL2 cross-linking had a strong effect on stiffness of bundles of fibers. We thus analyzed collagen remodeling at the initiation of capillary formation, before establishment of the basement membrane. Stacking of collagen at the cell surface was observed in the hydrogel with high fibrillogenesis. However, cross-linking with LOXL2 prevented this process, in agreement with the high elastic properties of collagen in these gels (Sapudom et al., 2019). LOXL2-mediated cross-linking could thus impact endothelial cell behavior at two levels: i) by increasing strain stiffening at the cell scale,

thus promoting cell migration (Doyle et al., 2015; Wang et al., 2019); ii) by preventing excessive collagen packing at cell surface which limits angiogenesis in hydrogels with high fibrillogenesis; similar mechanism has been recently described in breast cancer where collagen shell structure limits endothelial migration (Tien et al., 2020) and also in the context of desmoplasia where inhibition of LOXL2 abolished stromal matrix restraint, unexpectedly resulting in increased tumor progression (Jiang et al., 2020).

5. Conclusion

Although most of the studies I performed aimed to characterize the role of LOXL2 in vascular basement membrane remodeling, my participation to this last project allowed me to enlarge my understanding of LOXL2 function and to propose a general schematic of its impact in ECM remodeling and angiogenesis.

Role of LOXL2 in angiogenesis and microenvironment remodeling



Appendix 1

Marchand et al, Semin. Cell. Dev. Biol. 2019



Contents lists available at ScienceDirect

Seminars in Cell & Developmental Biology

journal homepage: www.elsevier.com/locate/semcdb

Review

Extracellular matrix scaffolding in angiogenesis and capillary homeostasis

Marion Marchand^{a,b}, Catherine Monnot^a, Laurent Muller^a, Stéphane Germain^{a,*}

^a Center for Interdisciplinary Research in Biology (CIRB), Collège de France, CNRS, INSERM, PSL Research University, 11 Place Marcelin Berthelot, 75005, Paris, France
^b Sorbonne Université, Collège Doctoral, F-75005 Paris, France

ARTICLE INFO

Keywords:

Extracellular matrix
 Basement membrane
 Vascular development
 Angiogenesis
 Capillary

ABSTRACT

The extracellular matrix (ECM) of blood vessels, which is composed of both the vascular basement membrane (BM) and the interstitial ECM is identified as a crucial component of the vasculature. We here focus on the unique molecular composition and scaffolding of the capillary ECM, which provides structural support to blood vessels and regulates properties of endothelial cells and pericytes. The major components of the BM are collagen IV, laminins, heparan sulfate proteoglycans and nidogen and also associated proteins such as collagen XVIII and fibronectin. Their organization and scaffolding in the BM is required for proper capillary morphogenesis and maintenance of vascular homeostasis. The BM also regulates vascular mechanosensing. A better understanding of the mechanical and structural properties of the vascular BM and interstitial ECM therefore opens new perspectives to control physiological and pathological angiogenesis and vascular homeostasis. The overall aim of this review is to explain how ECM scaffolding influences angiogenesis and capillary integrity.

1. Introduction

The extracellular matrix (ECM) is a crucial component of the cellular microenvironment and forms a complex three-dimensional network. The vascular ECM is composed of two different compartments: the basement membrane (BM) and the interstitial ECM. Their respective ratio, composition and architecture differ depending on the nature (artery, vein, capillary) and the surrounding environment of the blood vessel. In the wall of large vessels, the interstitial ECM present in the media and embedding vascular smooth muscle cells displays the structural and mechanical properties that are necessary for supporting shear stress and pressure, *i.e.* high stiffness and elasticity. This interstitial ECM is thus mainly composed of elastic fibers and fibrillar collagens, collagen I being by far the most abundant protein in the wall of large vessels. It is crucial for establishing and maintaining the mechanical stability of the vascular system, as demonstrated in mice deficient for the $\alpha 1$ chain of collagen I, which die between E12 and E14 due to rupture of major blood vessels [1]. In capillaries, the vascular wall is limited to the BM. This specialized macromolecular assembly of proteins separates the endothelium from the surrounding stromal tissue [2]. It forms a continuous sheet-like structure of 50 to 150 nm thickness that surrounds the basal surface of the endothelial monolayer and ensheathes perivascular cells, which also participate in, BM synthesis and organization [3,4]. Since capillaries lack smooth muscle cells and the associated interstitial ECM, the BM alone provides the structural and

mechanical features that support the endothelium and vascular integrity, and allows distribution of nutrients and oxygen. BM also plays a major role in pathologies including tumor angiogenesis [5].

We review here the unique molecular properties of the capillary BM, which are crucial to control plasticity of endothelial cells. BM indeed vary in composition in a temporal and tissue-specific manner [6]. BM composition and structure are modified in many ways to generate specialized and context-specific assemblies [7]. Its core components are laminins 411 and 511, collagen IV, perlecan and nidogen 1 and 2. The vascular BM also contains associated proteins including collagen XVIII, VI and VIII and fibronectin. In addition to the properties of each of these components, their scaffolding in the BM is a key process in vascular development and homeostasis. The capillary microenvironment also plays the role of a reservoir for many growth factors and proteins that regulate vascular biology. The complete vascular surroundings therefore orchestrate the capacity of vascular cells to sense and respond to both mechanical and chemical cues from the environment and is thus a key regulator of vascular homeostasis. The aim of the review is to give an overview of the role of BM components and scaffolding in vascular development and homeostasis.

2. Core components of the vascular basement membrane

The two major components of BM are laminins and collagen IV. Both undergo auto-assembly into macromolecular sheets

* Corresponding author.

E-mail address: stephane.germain@college-de-france.fr (S. Germain).<https://doi.org/10.1016/j.semcdb.2018.08.007>Received 3 May 2018; Received in revised form 31 July 2018; Accepted 14 August 2018
1084-9521/© 2018 Elsevier Ltd. All rights reserved.

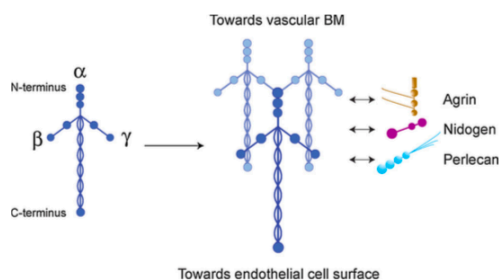


Fig. 1. Organization of laminins in the vascular basement membrane. The laminin network is constituted by the assembly of the α , β and γ chains heterotrimer where the C-terminal long arms are orientated towards the cell surface and the N-terminal short arms towards the collagen IV scaffold. The main interacting ECM components are indicated.

interconnected by nidogen and perlecan. Laminin network is first assembled through interaction with cell surface receptors and then triggers deposition of nidogen and perlecan, which both participate to cross-linking of the collagen IV network in order to generate the core of the BM.

2.1. Laminin

Laminins are a large family of high molecular weight glycoproteins. They consist in heterotrimers composed of disulfide-linked subunits, the α , β and γ chains, and are named according to the composition of the heterotrimer, *i.e.* laminin 411 is composed of $\alpha 4$, $\beta 1$ and $\gamma 1$. Laminins have a cross-shaped structure where the long arm of the cross (80 nm) is an α -helical coiled-coil formed by all three chains, whereas the short arms (35–50 nm) are composed of one chain each [8] (Fig. 1). At the C-terminal extremity of the long arm, the α chains contain five laminin G-like (LG) domains that include the major cell-adhesive sites. The homologous short arms are arranged in a unique globular structure, the laminin N-terminal (LN) domain, connected to tandem repeats of laminin type epidermal growth factor-like (LE) domains. The overall structure is interrupted by two to three internal globular domains [9].

Whereas expression of the β and γ chains is ubiquitous, the α chain is restricted to certain tissues and cell types, thus allowing tissue-specific distribution of laminins. In addition, their expression is also modulated during development and in pathological states [8]. They are found underlying the endothelium and surrounding pericytes in the capillary wall. The most abundant laminins in the vascular BM are composed of the $\alpha 4$ and $\alpha 5$ chains combined with laminin $\beta 1$ and $\gamma 1$ chains to form laminins 411 and 511 [10–13]. Laminin $\alpha 2$ is expressed during development (laminin 211) and also in the mature BM (laminin 221) [14] (Table 1).

Laminin interactions with cellular receptors, such as integrins via the globular domain at the C-terminus of its long arm, support assembly of other protein networks in the BM. Indeed, retention of laminin at the cell surface promotes further polymerization of the network, as demonstrated using *in vitro* planar lipid bilayers containing sulfated glycolipids [15]. The N-terminal short arms of the three chains mediate self-assembly of laminin polymers (Fig. 1). Laminin network undergoes self-assembly at the endothelial cell surface and is considered to initiate BM deposition. The role of laminin scaffolding on vascular development and homeostasis will be further described in chapter 4.1.

2.2. Collagen IV

2.2.1. Synthesis and secretion

Whereas collagen IV is also a heterotrimer, its subunits share quite similar structure with one another. Six distinct collagen IV α chains

Table 1
Laminin isoforms in vascular BM.

Chains	Expression	Heterotrimers	Vascular specificity	Refs.
$\alpha 4$	endothelial and mural cells	411	all blood vessels	[14]
$\beta 1$	ubiquitous			
$\gamma 1$	ubiquitous			
$\alpha 5$	endothelial and mural cells	511	capillaries	[14]
$\beta 1$	ubiquitous			
$\gamma 1$	ubiquitous			
$\alpha 2$	mural cells	211	blood brain barrier vessels	[3,137]
$\beta 1$	ubiquitous			
$\gamma 1$	ubiquitous			
$\alpha 2$	mural cells	221	mature blood vessels	[14,138]
$\beta 2$	widely expressed			
$\gamma 1$	ubiquitous			

Table 2
Collagen IV heterotrimers in BMs.

Heterotrimers	Expression	Vascular orientation	References
$\alpha 1\alpha 1\alpha 2$	all vascular BMs	closely juxtaposed to the endothelium	[16,25]
$\alpha 3\alpha 4\alpha 5$	glomerular, eye, lung, testis BMs	distant from the endothelium	[25]
$\alpha 5\alpha 5\alpha 6$	kidney, skin, smooth muscle BMs	–	[16]

(from $\alpha 1$ to $\alpha 6$ encoded by *COL4A1* to *COL4A6* genes, respectively) are expressed and assemble with a remarkable specificity to form only three distinct heterotrimers ($\alpha 1\alpha 1\alpha 2$, $\alpha 3\alpha 4\alpha 5$ and $\alpha 5\alpha 5\alpha 6$), $\alpha 1\alpha 1\alpha 2$ being the most predominant in all tissues including vascular BM (Table 2). The α chains are approximately 400 nm long and can be separated into three domains: a short N-terminal 75 domain, a long middle triple helical collagenous domain, and a C-terminal globular non-collagenous (NC1) domain (Fig. 2).

The assembly of collagen IV trimers is initiated by interactions between the NC1 globular domains of three α chains that lead to formation of a heterotrimeric protomer. Both the 7S and NC1 domains are then responsible for the assembly of collagen IV networks [16]. Two collagen IV protomers associate via their C-terminal NC1 domains and four protomers are cross-linked at the N-terminal 7S domain. In parallel, lateral associations between these assembled molecules form an elaborate supramolecular scaffold and allow formation of the complex mesh network of collagen IV. Unlike fibrillar collagens, the central collagenous domain of collagen IV is characterized by numerous (21–26 depending on the α chain) interruptions of the Gly-X-Y motifs that confer the structural flexibility responsible for its mesh-like network organization in the BM. In addition, the high level of covalent crosslinks provides stiffness to this structural scaffold.

Collagen IV secretion and supramolecular assembly into the BM require a variety of complex intracellular and extracellular molecular interactions. Among these, interactions with intracellular chaperones such as Hsp47 and the chaperone-binding Tango1 are required for proper collagen IV protomer stability and secretion. Hsp47 does not bind to unfolded or misfolded proteins but preferentially recognizes properly folded triple helices of fibril-forming procollagens and collagen IV protomers in the endoplasmic reticulum (ER). This protein may stabilize collagen IV protomers from the ER to the cis-Golgi [17] and is required for proper BM biosynthesis [18]. Moreover, osteonectin also known as secreted protein acidic and rich in cysteine (SPARC) or

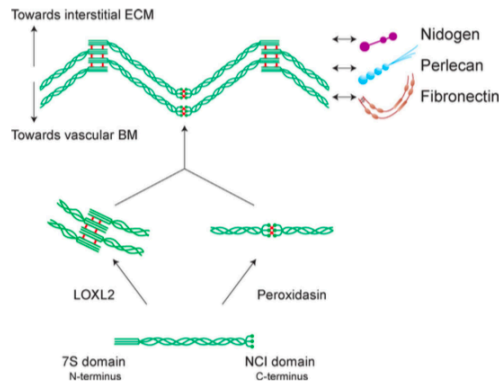


Fig. 2. Organization of collagen IV in the vascular basement membrane. The collagen IV mesh network is constituted by scaffolding of the α chain heterotrimers. The NCI domains cross-linked by the peroxidase enzyme are orientated towards the laminin network. The 7S domains cross-linked after deamination of lysines by LOXL2 are orientated towards the interstitial ECM. 7S and NCI crosslinks are indicated in red. The main interacting ECM components are indicated.

basement-membrane protein 40 (BM-40) has recently been proposed to act as an extracellular chaperone-like protein for collagen IV. It is proposed to ensure the proper deposition and assembly of collagen IV molecules in the BM, and to prevent premature collagen IV organization at sites of production, enabling diffusion and assembly to more distal sites [19].

2.2.2. Assembly in the BM

In all BMs, the collagen IV network is cross-linked to the laminin network through perlecan and nidogen. Synthesis, deposition and scaffolding of collagen IV networks by endothelial cells have been shown to be a central regulator of blood vessel formation and is mandatory for blood vessel survival and maturation *in vivo* ([20] and chapter 4.2 of the present review). Collagen IV networks display a highly oriented macromolecular organization in the BM. For long, the hypothesis has been that collagen IV forms a horizontally organized network through its NCI and 7S domains that serves as the main scaffold for the BM [21]. However, recent studies on $\alpha 3\alpha 4\alpha 5$ heterotrimers in kidney or retina BM have reported a polarized distribution for collagen IV trimers as the N- and C-terminal-domains are localized to opposite sides of the BM [22]. Indeed, the 7S domain is detected at the stromal side whereas the NCI domains is detected as primarily associated to the cell surface. Other recent studies also support this hypothesis [23], suggesting that collagen IV could be organized in such a way that the protein extends throughout the entire width of the vascular BM with the C-terminus pointing out towards the endothelium and the N-terminus towards the interstitial ECM. This highly orientated distribution thus questions not only the horizontal positioning of collagen IV molecules proposed in the current BM model, but also the functional roles of the macromolecular organization of collagen IV. Besides, it has also been demonstrated that distribution of laminin is very similar to NCI collagen IV at the cell-BM interface. These collagen IV and laminin networks are tightly connected by aggregated perlecan [24]. In addition to this specific orientation, the chains composing the collagen IV heterotrimers are also specific depending on their cellular expression. For example, in the kidney glomerular BM, collagen IV $\alpha 1\alpha 1\alpha 2$ protomers produced by the endothelial cells form a network closely juxtaposed to the endothelium, whereas the $\alpha 3\alpha 4\alpha 5$ protomers secreted only by podocytes are tightly attached to the $\alpha 1\alpha 1\alpha 2$ network [25]. These distinct compositions of collagen IV protomers may be

fundamental to establish and maintain the BM architecture therefore suggesting that organization of the BM plays a critical role in its function, and especially in this example, in the filtration capacity of the kidney.

2.2.3. Cross-linking

In addition to disulfide crosslinks, collagen IV network assembly is catalyzed by specific cross-linking enzymes, including peroxidase and lysyl oxidases (LOXs).

Peroxidase has recently been identified as cross-linking collagen IV through formation of sulfilimine bonds between a methionine sulfur and a lysine nitrogen of the NCI domains, thus stabilizing the hexameric structure of collagen IV [26] (Fig. 2). Peroxidase-deficient mice show reduced collagen IV sulfilimine crosslinks and reduced stiffness of the renal tubular BM, thus providing direct evidence for the contribution of collagen IV cross-linking to BM mechanical properties [27]. This however does not result in a vascular phenotype in these mice.

LOXs are secreted copper-containing amine oxidases that catalyze the oxidative deamination of lysines and hydroxylysines in collagens to form semi-aldehydes known as allysines. These highly reactive groups then undergo spontaneous reactions resulting in collagen cross-linking. LOX enzymes thus do not directly cross-link collagens but catalyze the last step required for its cross-linking [28]. They play important roles at different levels of the vascular system. Gene inactivation experiments have demonstrated that whereas LOXL1 only targets elastin [29], LOX cross-links both fibrillar collagen and elastin in the aorta [30,31], and does not affect collagen IV cross-linking or BM assembly [32]. The inactivation of LOX results in defects of aorta development leading to rupture and perinatal birth. Deletion of *Loxl2* gene in mice promotes perinatal lethality with incomplete penetrance associated to congenital heart defects and distension of hepatic blood vessels [33]. We have shown that LOXL2-depletion in endothelial cells results in defects in collagen IV deposition and cross-linking in the ECM [34]. More recently, cross-linking of the 7S N-terminal domain by LOXL2 was demonstrated [35]. Besides, we demonstrated that LOXL2 regulates angiogenesis *in vivo*, as LOXL2 down-regulation inhibits formation of intersomitic vessels in zebrafish embryos, and *in vitro*, using 3D culture models [34].

2.3. Perlecan and nidogen

Perlecan, a secreted heparan sulfate proteoglycan (HSPG), is another major component of the core endothelial BM. Perlecan has a very large multi-domain core protein (approximately 470 kDa), carrying three long N-terminal heparan sulfate (HS) side chains of 65 kDa each. The core protein, composed of five distinct structural domains, is bound to the laminin network, whereas the HS are bound to the collagen IV network [24] most likely at its 7S and NCI domains [8]. Perlecan has the potential to provide a bridge between laminin and the cell surface through its α -DG-binding LG domains [36]. The N-terminal HS side chains also allow perlecan to sequester and present growth factors to their appropriate receptors (see chapter 5). This role is quite important for establishing growth factor gradients required for developmental processes and regulating angiogenesis (reviewed in [37]).

Perlecan can act as a regulator of cell adhesion, proliferation and growth factor signaling [38]. The C-terminal domain, responsible for oligomeric self-assembly and integrin-binding activity, is crucial for developmental and tumor angiogenesis. This domain, named endorepellin, can be processed by various proteases, and displays anti-angiogenic activities [39,40]. In zebrafish embryo, knocking down perlecan expression using morpholinos leads to defects in sprouting of primary intersegmental vessels, showing the importance of perlecan in vascular morphogenesis. The phenotype is partially rescued by micro-injection of human perlecan protein, or endorepellin [41]. Half of the perlecan-deficient mice die early in development, at E10.5, when expression of the Perlecan gene is normally initiated [42]. At E10–11,

many perlecan-deficient embryos show signs of cardiac failure characterized by intrapericardial hemorrhages, weak heartbeats, or even cardiac arrest. Mutants that survive show abnormal BM formation.

Agrin is another secreted HSPG that interacts with core components of the BM. It directly binds the laminin γ 1 chain via its N-terminal domain [8]. The agrin bridge has been shown to strengthen laminin anchorage both *in vitro* and *in vivo* [43,44]. In the BM, agrin was recently shown to have a polarized distribution with the C-terminus pointing to the podocyte or endothelial cell surface, and the N-terminus to the center of the glomerular BM [25]. The functions of agrin are regulated by alternative splicing of its LG3 domain [45]. The non-neuronal splice variant of agrin is responsible for its contribution to BM formation and stability, whereas the neural splice variant plays an important role in the formation of neuromuscular junctions. Agrin might also play a role in the blood-brain-barrier as it accumulates in the BM of cerebral microvessels [46] and contributes to the localization of β -catenin, VE-Cadherin and ZO-1 at the endothelial adherens junctions [47].

Two nidogen proteins, nidogen-1 and -2 (entactin-1 and -2, respectively) are encoded by two different genes but share the same structure. Like perlecan, nidogens act as linkers of the core components of BM. They contain binding sites in the G3 domain for the short arm of the γ 1 laminin subunit and in the G2 domain for collagen IV and perlecan [48–50]. Both isoforms are ubiquitous BM components. However, nidogen-1 is predominant in the vascular BM in adult. Only deletion of both nidogen genes results in perinatal lethality possibly due to cardiovascular and/or respiratory failure, whereas individual knockouts are viable and fertile [51]. Locally restricted bleeding within the heart wall has been reported in mutant embryos. This bleeding seems to be associated to leakage of the microvasculature and absence of capillary BM. Therefore, nidogens do not seem essential for BM formation but may play a role in maintenance of capillary integrity.

3. Extracellular matrix proteins associated to the vascular basement membrane

Besides these core components, many associated proteins also play a role in maintaining the BM functions and in connecting the BM to the interstitial ECM. We will present here collagens associated to the BM and fibronectin, which constitutes a functional bridge between the endothelial cell surface and the surrounding microenvironment.

3.1. Collagens

3.1.1. Collagen XVIII

Collagen XVIII is a ubiquitous BM collagen, reaching high levels in the endothelial BM. It is a high molecular weight protein (approximately 300 kDa) that possesses structural properties of both collagen and proteoglycans, with several glycosaminoglycan chains consisting mainly in HS chains. Collagen XVIII is classified under the group of multiplexins due to the presence of 11 non-collagenous interruptions alternating with 10 collagenous repeats within the central triple helix, conferring high flexibility to the protein. Collagen XV, the other multiplexin collagen specific for BM, is mainly involved in cardiovascular development [52]. Homotrimerization of collagen XVIII is triggered by assembly of the NCI domains. As collagen IV, collagen XVIII displays a very polarized orientation in epidermal and endothelial BMs, the C-terminal domain being orientated towards the cell surface, whereas the N-terminus resides at the BM-interstitial ECM interface [53]. This polarization suggests an anchoring role for collagen XVIII between cells and interstitial ECM. Co-localization of the C-terminal domain of collagen XVIII with perlecan and laminin in the BM is consistent with such polarization [54]. Collagen XVIII binding to the BM could be mediated by HS chains [55]. Collagen XVIII-deficient mice show thickened epidermal BM, suggesting an important structural role for collagen XVIII in maintaining BM physical integrity [56].

Three different tissue-specific isoforms, with core proteins ranging from 135 to 178 kDa, that differ in their N-terminal non-collagenous sequence, have been identified. The shortest variant is found in most vascular BMs. Collagen XVIII became a focus of interest when an 18 kDa C-terminal tryptic peptide, named endostatin, turned out to have anti-angiogenic and tumor-suppressing activities [57]. *In vitro* and *in vivo* anti-angiogenic effects of endostatin have been further confirmed [53]. Several ocular abnormalities including abnormal outgrowth of retinal vessels [58] and reduced susceptibility to high oxygen-induced retinal neovascularization were reported in collagen XVIII-deficient mice [59].

3.1.2. Collagen VIII

Collagen VIII was initially termed endothelial collagen due to its high expression in the endothelial BM [60]. Collagen VIII is a trimeric non-fibrillar short-chain collagen expressed as homotrimers of α 1 or α 2 chains of 74 and 67 kDa, respectively. They are very similar and share an identical domain structure consisting of a short non-collagenous domain 2 (NC2), followed by a collagen triple helix domain and a C-terminal non-collagenous domain 1 (NC1).

While the function of collagen VIII is uncertain, the importance of this collagen in the vasculature has been particularly reported in maintaining the smooth muscle cell phenotype. It may provide a substratum for a variety of cells and facilitate migration of endothelial cells in angiogenesis, smooth muscle cells in intimal invasion and myofibroblasts in fibrotic conditions [61]. Other studies suggest that the close association of collagen VIII to the BM may improve its resistance to compression, and that it would be synthesized during capillary sprouting [62].

3.1.3. Collagen VI

Collagen VI is ubiquitously expressed and has been studied in a wide range of tissues including the vessel wall. Though not considered as a BM associated collagen *per se*, collagen VI is a BM-anchoring protein with specific biosynthetic process and structural organization. Filaments of collagen VI are composed of heterotrimers of α chains ranging from approximately 100 to 350 kDa encoded by six different genes (from *COL6A1* to *COL6A6*). They mostly organize into a heterotrimer composed of α 1 α 2 α 3. The α 4, α 5 and α 6 chains share a structure similar to the α 3 chain and have been proposed to replace the α 3 chain under some pathological conditions [63]. Supra-molecular assembly of collagen VI is driven by a multi-step process and leads to the formation of a characteristic and distinctive network of beaded microfilaments in the ECM. However, in contrast to other types of collagens, collagen VI undergoes an intracellular assembly into large aggregates before being secreted [64]. The three α chains assemble to form a triple-helix monomer that joins into disulfide-bonded anti-parallel dimers, which then align to form large tetramers also stabilized by disulfide bonds. These tetramers are finally secreted in the extracellular space and associate together through non-covalent bonds to form the beaded microfilaments [65]. Collagen VI forms an anchoring meshwork that connects the interstitial matrix to the vascular BM, thus bridging cells to the surrounding environment and organizing the three-dimensional tissue architecture of the vasculature through direct interaction with collagen IV [66]. Interactions with other fibrillar collagens, including collagen I, have also been reported [67]. Collagen VI and fibronectin have been shown to interact together [66,68]. Depletion of collagen VI leads to an increase in both fibronectin expression and extracellular deposition, which is then rearranged into long and parallel fibrils. Exogenous collagen VI restores the basal level of fibronectin deposition, suggesting that collagen VI is a regulator of fibronectin fibrillogenesis [69].

3.2. Fibronectin

3.2.1. Expression and fibrillogenesis

Fibronectin (FN) is a ubiquitously expressed BM-associated protein.

In the vessel wall, it is incorporated between endothelial and perivascular cells. It is a dimeric glycoprotein of high molecular weight, composed of three types of structural repeats (I, II, III). The N-terminal part contains a self-assembly domain that allows for individual fibronectin dimers to assemble in a process termed fibrillogenesis, resulting in a three-dimensional network. Different isoforms of fibronectin are generated by alternative splicing: 1) the soluble form, or plasma form (p-FN) produced by hepatocytes that circulates at high concentration in blood, and 2) the cellular form (c-FN) produced in tissues, that contains additional domains called EDA and EDB, and is incorporated in the ECM [70]. Fibronectin plays a crucial role in cell adhesion, growth, migration, and differentiation. It is essential to wound healing, embryo development and blood vessel morphogenesis. Fibronectin is a unique ECM component because it is detected both close to the cell surface, strongly associated to the endothelial BM but also more distantly, associated to the interstitial ECM. Whereas *in vitro* experiments demonstrate that c-FN is required for autocrine activity on cell-cell and cell-ECM interactions [71] recent *in vivo* loss of function experiments proposed that p-FN could play a critical role during vascular development [72].

3.2.2. Assembly in the extracellular matrix

Fibronectin fibrillogenesis is a non-spontaneous process, mediated by cells *via* integrin binding to the RGD motif. Fibronectin binding to integrins induces their clustering. These integrin clusters locally provide very high concentrations of fibronectin at the cell surface, which may promote fibronectin-fibronectin interactions and fibrillogenesis. Other matrix proteins have been involved in fibronectin fibrillogenesis such as ECM proteoglycans [73]. Transglutaminase-2 (TG2), a calcium-dependent enzyme, stabilizes the ECM through its cross-linking activity. Furthermore, TG2 interacts with $\beta 1$ integrin and fibronectin. This ternary complex promotes fibronectin deposition and pericellular network of fibrils [74].

Direct interaction of fibronectin with type IV collagen has been known for long [75]. A recent study further reported that fibronectin fibrillogenesis is required for type IV collagen deposition [76]. Disruption of fibronectin network affects type IV collagen and laminin deposition in the BM of human trabecular meshwork cells [77]. In a similar manner, interactions between type I collagen and fibronectin suggest that fibronectin acts as a scaffold that may participate to the alignment of collagen fibrils. Fibronectin fibers may thus organize and orient cells so that collagen fibers are aligned and parallel, thus constituting a functional bridge between the endothelial cell surface and the surrounding ECM.

4. Basement membrane scaffolding and function in vascular development and homeostasis

This chapter will focus on the functional role of BM core components in capillary formation and vascular homeostasis described in mouse models and human pathologies.

4.1. Laminins

Among the three main laminin isoforms expressed in vascular BMs, we will here focus on laminins 411 and 511 that are the two major isoforms found in vascular BMs. We will not review laminin $\alpha 2$, present in the mature vessels and vascular smooth muscle BMs [78] but predominantly expressed in striated muscles and peripheral nerves and for which the KO mouse models are reviewed in [79].

4.1.1. Laminin 411

Laminin $\alpha 4$ expression begins at E8.5 and is not restricted to a special type of vessel. The role of laminin $\alpha 4$ has been studied during vascularization of the mouse retina. It regulates tip and stalk cell number and vascular density by regulating the endothelial delta-like 4

(Dll4)/Notch pathways [80]. Laminin $\alpha 4$ is mainly expressed at the growing vascular front in the postnatal retina, and its expression is mostly concentrated at the leading tip cells. It is hypothesized that laminin $\alpha 4$ could induce Dll4 expression specifically in tip cells through a $\beta 1$ integrin-mediated mechanism. The phenotype of the laminin $\alpha 4$ knockout mouse shows a central role for the laminin $\alpha 4$ chain in microvessel growth, resulting in bleeding and hemorrhages of capillaries, leaving large vessels unaffected [81]. The hemorrhages are associated with abnormalities of the BM, *i.e.* reduced deposition of collagen IV, nidogen, and laminin $\alpha 1$ chain. These defects in vascular BM are observed in newborn but not adult null mice [81], suggesting compensation at later stages. Consistent with this observation, laminin $\alpha 4$ knockout mice that survive beyond the perinatal period have a lifespan comparable to the wild-type controls. Mice lacking laminin $\alpha 4$ show excessive filopodia activity and tip cell formation in the retina. This phenotype is close to the phenotype observed when Notch is inhibited *in vivo*, leading to aberrant sprouting angiogenesis and branching [80].

4.1.2. Laminin 511

Laminin $\alpha 5$ is the other major laminin chain strongly expressed in the endothelial BM. Laminin $\alpha 5$ expression begins when the heart starts beating (E10) and blood circulation is initiated, mainly in arteries. It is expressed in the BM of microvessels at much later stages, and may be associated with maturation of the endothelium or its tissue/organ-specific characteristics [82,83]. Laminin $\alpha 5$ is not expressed in fenestrated endothelium of endocrine glands and peritubular capillaries of the kidney [14] suggesting a correlation between absence of laminin $\alpha 5$ and fenestration formation. In postcapillary and larger venules, distribution of laminin $\alpha 5$ is patchy, resulting in BM regions containing only laminin $\alpha 4$ or both laminin $\alpha 4$ and $\alpha 5$ [14]. The exact role of this endothelial laminin in vascular homeostasis has not been fully reported. Deletion of laminin $\alpha 5$ in mouse models results in multiple defects and embryonic lethality at E10-E11 due to placental defects, failure of dorsal aorta closure and structural abnormalities and leakiness of the yolk sac vessels [84]. Kidney defects characterized by abnormal glomerular BM and glomerulogenesis are observed in these Lama5 null embryos [85].

Recent publications indicate that endothelial laminin $\alpha 5$ is essential to the shear stress response [86]. *In vitro* and *in vivo* analyses suggest that laminin $\alpha 5$ binding to $\beta 1$ integrin stabilizes VE-cadherin at adherens junctions, thus increasing the strength of cell-cell adhesion, which is essential to shear stress response and vessel permeability [86]. There is however at this point only little evidence that laminins may be involved in such mechanosensing functions. Other publications support the fact that the RGD-binding integrins, $\alpha 5\beta 1$ or $\alpha v\beta 3$ could play a role in shear-induced intracellular signaling in cultured endothelial cells [87]. Moreover, using a conditional knockout mouse, it was demonstrated that loss of pericyte-produced laminin $\gamma 1$ is involved in the maintenance of the blood brain barrier integrity [88].

4.2. Collagen IV

Double deletion of Col4a1 and Col4a2 results in complete loss of collagen IV in the vascular BM and mouse embryo death at E10.5–11.5 [20]. Embryos display BM structural deficiency associated with dilated, fragile blood vessels and hemorrhages. Brain vascular beds display reduced capillary density and perturbed endothelial protrusions in the neural layers, whereas development of the large vessels is not affected by the deletion [20]. This demonstrates that collagen IV is not critically important for the formation of embryonic BM but is crucial for its structural integrity and function at later stages in development, especially upon mechanical demand after initiation of blood flow. In line with these results, we showed that down-regulating COL4A1 in endothelial cells affects capillary formation in a 3D angiogenesis model in fibrin gels [34].

Mutations in collagen IV are associated with defects in capillary

formation and vessel integrity in human pathologies [89–91]. In the past decade, *COL4A1* and *COL4A2* mutations have been identified as a cause of multi-system disorder for which penetrance and severity of constituent phenotypes can greatly vary. *COL4A1* mutations were found to cause porencephaly. This disease is characterized by cerebral cavities that communicate with the ventricles. Porencephaly is commonly associated with seizures, and mental retardation. It also causes pre- and perinatal hemorrhages, and recurrent intracerebral hemorrhages in young and old patients. The intracerebral hemorrhages can appear spontaneously or can be triggered by specific events. Porencephaly is often associated with systemic small-vessel disease, as mutations in *COL4A1* compromises the BM and weakens the vessels [90,92–94]. More than 100 mutations identified in patients were analyzed, showing that glycine substitutions within the triple helical domain are the most common type of mutations in patients. Glycine is often replaced by a charged amino acid. The position rather than the nature of the mutation is crucial for disease severity [95]. Other mutations responsible for hereditary angiopathy with nephropathy, aneurysms, and muscle cramps (HANAC) syndrome have been identified in the integrin binding region of the collagen domain (G498 V, G519R and G528E). Patients present arteriolar tortuosity in the retina, brain arterial aneurysms and microvessel defects. The vascular BM is interrupted and thinner [91]. Mutations in *COL4A1* and *COL4A2* genes are also associated with systemic small vessel disease and various symptoms especially affecting the eyes, muscles, kidney and brain [96]. The mutations lead to structural instability of all BMs [97]. Perturbations of the matrisome of cerebral blood vessels is a possible proximate cause in familial small vessel disease [98].

A recent study reported the analysis of the BM in human retinal microaneurysms [99]. Interestingly, microaneurysms presented BM thickening associated with increased expression of the core BM proteins (collagen IV, laminin, perlecan and nidogen) along with ECM remodeling enzymes. Indeed, small microaneurysms expressed increased expression of cross-linking enzymes of the LOX family (LOXL2 and LOXL4), whereas large microaneurysms expressed more matrix-metalloproteinase MMP9 and plasminogen activator inhibitor-1. Thickening of the BM by accumulation of collagen IV probably produced by recruited pericytes was thus considered as a compensatory mechanism that would strengthen the vascular wall in the early phase of microaneurysm development [99]. Besides, LOXL2 had already been reported as a susceptibility gene to intracranial aneurysms [100] and further exome sequencing analyses have identified mutations in this gene related to familial intracranial aneurysm [101]. These data confirm the hypothesis of an important role for BM cross-linking by LOXL2 in this pathology.

4.3. Fibronectin

Numerous studies showed that fibronectin and its receptors play a major role in embryogenesis and vascular development [102]. Deletion of the Fibronectin gene in mouse leads to embryo lethality at E8.5, with severe cardiovascular defects including heart malformations and aberrant distribution of blood vessels in the yolk sac [103]. During mouse retina vascularization, endothelial tip cells are guided by pre-existing fibronectin deposited by astrocytes but also synthesize and assemble fibronectin *de novo* [34], a crucial step in the angiogenic process [104]. Accordingly, *in vitro* studies have also demonstrated that growing capillaries deposit their own fibronectin [105] whose assembly regulates and is required for capillary morphogenesis [106].

Whereas many effects of fibronectin are mediated by interaction with its integrin receptors, fibronectin also regulates angiogenesis in an integrin-independent manner, as shown by mutating the heparin-binding domains (HEP-II and HEP-III). Several mutations were identified in patients suffering from glomerulopathy with excessive fibronectin deposition but also in patients with proteinuria, hypertension and massive glomerular deposits of the p-FN, leading to renal failure

[107]. The HEP-II and -III domains play a major role in regulating fibronectin assembly into organized fibrils in the ECM, but also keeps p-FN in a compact soluble form thus preventing its deposition in the ECM. It was suggested that these mutations impair the control of the assembly of fibronectin into fibrils but also the balance between soluble and insoluble FN, leading to abnormal incorporation of the non-fibrillar p-FN. These mutants display lower binding to heparin but also to endothelial cells and podocytes. In endothelial cells, this impairs spreading and cytoskeleton organization [107].

5. The extracellular matrix: a reservoir for growth factors and matricellular proteins

Numerous growth factors, including VEGFs, IGFs, FGFs, TGF- β s, and HGF, have been found to associate with ECM proteins or with HS chains and play a crucial role in vascular development and homeostasis. Some of them are necessary for sprouting angiogenesis, whereas others are tuning this process. We will here review the implication of VEGF and PDGF family of growth factors in vascular homeostasis.

5.1. The VEGF family and its receptors

Vascular endothelial growth factors (VEGFs) are crucial regulators of vasculogenesis and angiogenesis and are essential for vascular homeostasis. The VEGF family comprises several distinct proteins, we here focus on VEGF-A due to its main role in angiogenesis and vascular integrity as well as its predominant association with the vascular BM. Alternative splicing of the VEGF-A pre-mRNA produces several isoforms, each with different affinities for ECM and different biological activity. The predominant form, VEGF₁₆₅, binds to the ECM and to the cell surface by its heparin binding sites. VEGF₁₆₅ binds to the tyrosine kinase receptors VEGFR-1 and VEGFR-2 by diffusion or by presentation through co-receptors such as HSPGs. Binding causes dimerization of receptors, changes in the conformation, and phosphorylation of tyrosine residues that triggers activation of downstream signal transducers and signaling pathways that regulate angiogenesis [108].

ECM-associated HSPGs also bind to VEGF₁₆₅ and potentiate VEGFR-2 signaling [109]. VEGF₁₆₅ signaling in endothelial cells is also fully supported by HS expressed *in trans* by adjacent perivascular smooth muscle cells [110]. Transactivation of VEGFR-2 leads to prolonged and enhanced signal transduction due to HS-dependent trapping of the active VEGFR-2 signaling complex and constitutes a crosstalk mechanism between adjacent cells. Regulation of VEGF₁₆₅ interaction with HSPG by other HSPG-binding proteins can also modulate VEGFR-2 signaling. Indeed, inactivation of Tg2 in mouse resulted in increased vascularization in the retina together as a result of increased phosphorylation of VEGFR-2 at Tyr951 and its downstream targets Src and Akt [105].

Fibronectin also regulates angiogenesis through interactions with growth factors, including TGF- β [111] and VEGF [104]. Indeed, fibronectin binds to VEGF and thus regulates migration and proliferation of endothelial cells. In mouse retina, fibronectin binding to VEGF₁₆₅ secreted by astrocytes promotes the directional migration of tip cells. The role of fibronectin as a “VEGF-A organizer” and as a migration ligand for endothelial cells during sprouting angiogenesis has been well described [104]. Astrocytes are the major source of cellular fibronectin during retinal angiogenesis and its deletion reduced endothelial migration during vascular plexus morphogenesis. This effect could be recapitulated by selectively inhibiting VEGF-A binding to fibronectin *via* injection of blocking peptides. A similar phenotype was reported upon double deletion of fibronectin and HSPGs in the retina, suggesting that both components of the ECM synergize to bind to VEGF-A and support migration and orientation of tip cells. Altogether, these data indicate that fibronectin participates to the vascular branching pattern in the retina *via* binding to VEGF-A.

5.2. The PDGF family and its receptors

Platelet-derived growth factor (PDGF) is a potent mitogen for cells of mesenchymal origin, including fibroblasts, smooth muscle cells and glial cells. It regulates cell growth and division. PDGF plays a significant role in angiogenesis. In both mouse and human, the PDGF signaling network consists of four ligands (PDGF-A, PDGF-B, PDGF-C and PDGF-D) and two tyrosine kinase receptors (PDGFR- α and PDGFR- β). Secreted PDGF acts both in an autocrine and paracrine manner. It regulates angiogenesis through pericyte recruitment and stabilization of neovessels. PDGF-B, released from endothelial tip cells at the migration front, recruits mural cells that express PDGFR- β and especially pericytes [3]. Knockouts of *Pdgfb* and *Pdgfrb* in mouse lead to similar phenotypes of perinatal death due to vascular dysfunction caused by mural cell deficiency [112], leading to vascular leakage and abnormal junctions [113,114]. These defects induced a compensatory mechanism of up-regulation of VEGF-A, which in turn promotes further vascular leakage and hemorrhage [115].

PDGF-B binds to heparin and HSPGs in the ECM via its C-terminal retention motif that limits the range of action of PDGF-B necessary for adhesion of pericytes to the vessel wall. In mice, deletion of this motif perturbs pericyte coverage in microvessels thus showing that PDGF-B-oriented presentation at the endothelial cell surface is crucial for pericyte recruitment [116]. HSPGs actually constitute a PDGF storage compartment at the cell surface and in the ECM, and these interactions regulate spatial distribution and bioavailability of PDGF at sites of pericyte recruitment such as angiogenic sprouts.

5.3. Matricellular proteins

5.3.1. Angiopoietins

Angiopoietins are part of a family of vascular growth factors that play a role in embryonic and postnatal angiogenesis, as well as in stabilization and maturation of blood vessels. Angiopoietins are involved in regulating vascular permeability, vasodilation, and vasoconstriction. Among them, Angiopoietin-1 (Ang-1) interacts with the ECM, whereas Ang-2 is more diffusible [117]. These interactions provide different local concentrations and are thought to account in part for the differences in the biological effect of the angiopoietins. Indeed, matrix-bound Ang-1 induces cell adhesion, motility and Tie2 activation in cell-matrix contacts, eventually translocated to the trailing edge in migrating endothelial cells. In contrast, Ang1-induced Tie2 translocation to cell-cell contacts triggers the formation of homotypic Tie2-Tie2 trans-associated complexes in contacting cells. Distinct signalling proteins are therefore activated by Tie2 in the cell-matrix and cell-cell contacts, where Ang2 inhibits Ang1-induced Tie2 activation [118]. Also, Ang-3 is tethered on

the cell surface via HSPGs [119]. As for angiopoietin like-proteins, angiopoietin like-4 (ANGPTL4), a key regulator of lipoprotein lipase activity thereby impacting processing and distribution of triglycerides and cholesterol, is also secreted by endothelial cells in hypoxia [120] and interacts with HSPGs [121]. It regulates developmental and pathological retinal vascularization by limiting cell adhesion, cell junction organization, pericyte coverage [122]. ANGPTL4 also plays a role in vessel integrity, limiting vascular permeability in ischemic pathologies [122-124].

5.3.2. CCN proteins

Other ECM-associated integrin- and heparin-binding proteins belong to the CCN family and are functionally involved in the development of the vascular system. CCN is an acronym that refers to the initials of the first three family members namely cysteine-rich 61 (CYR61) for CCN1, connective tissue growth factor (CTGF) for CCN2 and nephroblastoma overexpressed (NOV) for CCN3. There are three other members of this family [125]. They all share structural characteristics but are all functionally different. By far, CCN1 and CCN2 display more important roles in vascular development and diseases [126]. They provide the functional bridge between structural macromolecules and growth factors, cytokines, proteases, and other related proteins [127]. Structurally, they are arranged as multimodular molecules composed of four cysteine-rich motifs.

CCN1 and CCN2 are critical regulators of endothelial cell differentiation, mural cell recruitment and BM formation during embryonic vascular development. Once secreted, CCN1 controls adhesion, proliferation and survival through interaction with integrins. CCN1 signaling often requires HSPGs as co-receptors. Mice lacking CCN1 phenocopied $\alpha 4$ and βv integrin-deficiency, leading to similar vascular defects [128]. CCN1 can also bind ECM proteins such as fibronectin or vitronectin and thus potentiates their activation of αv integrins [129]. As for CCN1, the role of CCN2 is context-dependent and is determined by the bioavailability of membrane receptors and/or presence of interacting molecules in the microenvironment. Through direct binding to $\alpha v \beta 3$ integrin, CCN2 promotes endothelial cell adhesion, migration, and tube formation [130,131]. CCN2 also regulates gene expression of growth factors and ECM components [132,133].

6. Concluding remarks

This review describes the specific composition of the vascular BM and highlights the functional roles of this spatially-orientated structure (Fig. 3). In addition to its proteolytic regulation, increasing number of studies demonstrate that regulation of the assembly of the ECM and its components is a decisive process in vascular morphogenesis. Some ECM

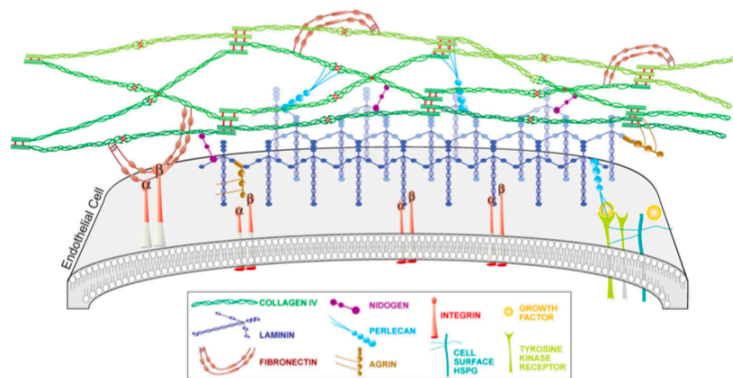


Fig. 3. Polarized basement membrane in capillary wall.

The laminin network interacts with the cell surface directly through the integrins or indirectly through agrin and perlecan. The collagen scaffold interacts with the laminin network through perlecan and nidogen. 7S and N1 crosslinks are indicated in red. Fibronectin is present on the cell surface and interstitial sides of the basement membrane.

remodeling enzymes play a key role, by allowing scaffolding and organization of protein components.

The ECM is a reservoir for growth factors that influence angiogenesis by controlling specific signaling pathways. Regulation of their bioavailability directly impacts on vascular morphogenesis and homeostasis. These combined processes are key events of the dynamic regulation that leads to a specifically and functionally orientated structure, as discussed earlier for the collagen IV and XVIII polarization in the vascular BM.

The ECM is a crucial regulator of the cell microenvironment and tissue organization. Cells assemble soluble proteins into insoluble fibrils embedded in a hydrophilic polysaccharide-based ECM with unique mechanical properties and chemical composition thus generating the cues that will regulate cell-cell interactions and morphogenesis. Cellular traction forces are indeed considered as effectors activated by mechanosensing in order to regulate matrix remodeling [134]. Cells thus both sense and influence ECM mechanics to maintain tissue homeostasis. Works developed over the last 15 years have demonstrated the crucial role of ECM-mediated mechanotransduction as a major regulator of morphogenetic processes including angiogenesis. Fluid shear stress has been considered as the main source of mechanical signals regulating vascular function for long and is still under deep investigation [135,136]. It is now also established that substrate mechanical properties can also influence sprouting and vascular network formation. Endothelial cells establish perfused vessels in any tissue but cartilage, thus encountering a huge diversity of microenvironments. Such context pushes forward the role of the vascular BM as the stable structural feature that will allow vascular interactions with- and functions in- any tissue. The mechanisms that stand behind these relationships however still require deep investigation. Overall, a better understanding of the mechanical and structural properties of the vascular BM and interstitial ECM undoubtedly opens new perspectives to control physiological and pathological angiogenesis and vascular homeostasis.

Fundings

This work was partially supported by Fondation pour la Recherche Médicale and INSERM.

Conflict of interests

The authors declare no competing financial interest.

Acknowledgement

The authors wish to thank France Maloumian for designing the figures.

References

- [1] J. Lohler, R. Timpl, R. Jaenisch, Embryonic lethal mutation in mouse collagen I gene causes rupture of blood vessels and is associated with erythropoietic and mesenchymal cell death, *Cell* 38 (1984) 597–607.
- [2] G.E. Davis, D.R. Senger, Endothelial extracellular matrix: biosynthesis, remodeling, and functions during vascular morphogenesis and neovessel stabilization, *Circ. Res.* 97 (2005) 1093–1107.
- [3] A. Armulik, G. Genove, C. Beisholtz, Pericytes: developmental, physiological, and pathological perspectives, problems, and promises, *Dev. Cell* 21 (2011) 193–215.
- [4] A.N. Stratman, G.E. Davis, Endothelial cell-pericyte interactions stimulate basement membrane matrix assembly: influence on vascular tube remodeling, maturation, and stabilization, *Microsc. Microanal.* 18 (2012) 68–80.
- [5] R. Kalluri, Basement membranes: structure, assembly and role in tumour angiogenesis, *Nat. Rev. Cancer* 3 (2003) 422–433.
- [6] R.O. Hynes, A. Naba, Overview of the matrisome—an inventory of extracellular matrix constituents and functions, *Cold Spring Harb. Perspect. Biol.* 4 (2012) a004903.
- [7] G. Uechi, Z. Sun, E.M. Schreiber, W. Halfter, M. Balasubramani, Proteomic view of basement membranes from human retinal blood vessels, inner limiting membranes, and lens capsules, *J. Proteome Res.* (2014).
- [8] E. Hohenester, P.D. Yurchenco, Laminins in basement membrane assembly, *Cell Adh. Migr.* 7 (2013) 56–63.
- [9] P.D. Yurchenco, Integrating activities of Laminins that drive basement membrane assembly and function, *Curr. Top. Membr.* 76 (2015) 1–30.
- [10] M. Frieser, H. Nockel, F. Pausch, C. Roder, A. Hahn, R. Deutzmann, et al., Cloning of the mouse laminin alpha 4 cDNA. Expression in a subset of endothelium, *Eur. J. Biochem.* 246 (1997) 727–735.
- [11] A. Iivanainen, K. Sainio, H. Sariola, K. Tryggvason, Primary structure and expression of a novel human laminin alpha 4 chain, *FEBS Lett.* 365 (1995) 183–188.
- [12] L. Sorokin, W. Girg, T. Gopfert, R. Hallmann, R. Deutzmann, Expression of novel 400-kDa laminin chains by mouse and bovine endothelial cells, *Eur. J. Biochem.* 223 (1994) 603–610.
- [13] L.M. Sorokin, F. Pausch, M. Frieser, S. Kroger, E. Ohage, R. Deutzmann, Developmental regulation of the laminin alpha5 chain suggests a role in epithelial and endothelial cell maturation, *Dev. Biol. (Basel)* 189 (1997) 285–300.
- [14] L.F. Youssif, J. Di Russo, L. Sorokin, Laminin isoforms in endothelial and perivascular basement membranes, *Cell Adh. Migr.* 7 (2013) 101–110.
- [15] E. Kalb, J. Engel, Binding and calcium-induced aggregation of laminin onto lipid bilayers, *J. Biol. Chem.* 266 (1991) 19047–19052.
- [16] J. Khoshnoodi, V. Pedchenko, B.G. Hudson, Mammalian collagen IV, *Microsc. Res. Tech.* 71 (2008) 357–370.
- [17] T. Kolde, Y. Takahara, S. Asada, K. Nagata, Xaa-Arg-Gly triplets in the collagen triple helix are dominant binding sites for the molecular chaperone HSP47, *J. Biol. Chem.* 277 (2002) 6178–6182.
- [18] N. Nagai, M. Hosokawa, S. Itohara, E. Adachi, T. Matsushita, N. Hosokawa, et al., Embryonic lethality of molecular chaperone hsp47 knockout mice is associated with defects in collagen biosynthesis, *J. Cell Biol.* 150 (2000) 1499–1506.
- [19] A. Chioran, S. Duncan, A. Catalano, T.J. Brown, M.J. Ringuette, Collagen IV trafficking: the inside-out and beyond story, *Dev. Biol. (Basel)* 431 (2017) 124–133.
- [20] E. Poschi, U. Schlötzer-Schrehardt, B. Brachvogel, K. Saito, Y. Ninomiya, U. Mayer, Collagen IV is essential for basement membrane stability but dispensable for initiation of its assembly during early development, *Development* 131 (2004) 1619–1628.
- [21] R. Timpl, H. Wiedemann, V. van Delden, H. Furthmayr, K. Kuhn, A network model for the organization of type IV collagen molecules in basement membranes, *Eur. J. Biochem.* 120 (1981) 203–211.
- [22] W. Halfter, C. Monnier, D. Muller, P. Oertle, G. Uechi, M. Balasubramani, et al., The bi-functional organization of human basement membranes, *PLoS ONE* 8 (2013) e67660.
- [23] R. Jayadev, D.R. Sherwood, Basement membranes, *Curr. Biol.* 27 (2017) R207–R211.
- [24] D.T. Behrens, D. Villone, M. Koch, G. Brunner, L. Sorokin, H. Robenek, et al., The epidermal basement membrane is a composite of separate laminin- or collagen IV-containing networks connected by aggregated perlecan, but not by nidogens, *J. Biol. Chem.* 287 (2012) 18700–18709.
- [25] H. Suleiman, L. Zhang, R. Roth, J.E. Heuser, J.H. Miner, A.S. Shaw, et al., Nanoscale protein architecture of the kidney glomerular basement membrane, *Elife* 2 (2013) e01149.
- [26] G. Bhavé, C.F. Cummings, R.M. Vanacore, C. Kumagai-Cresse, I.A. Ero-Tolliver, M. Rafi, et al., Peroxidase forms sulfilimine chemical bonds using hypohalous acids in tissue genesis, *Nat. Chem. Biol.* 8 (2012) 784–790.
- [27] G. Bhavé, S. Colon, N. Ferrell, The sulfilimine cross-link of collagen IV contributes to kidney tubular basement membrane stiffness, *Am. J. Physiol. Renal Physiol.* 313 (2017) F596–F602.
- [28] P.C. Trackman, Enzymatic and non-enzymatic functions of the lysyl oxidase family in bone, *Matrix Biol.* 52–54 (2016) 7–18.
- [29] X. Liu, Y. Zhao, J. Gao, B. Pawlyk, B. Starcher, J.A. Spencer, et al., Elastic fiber homeostasis requires lysyl oxidase-like 1 protein, *Nat. Genet.* 36 (2004) 178–182.
- [30] I.K. Hornstra, S. Birge, B. Starcher, A.J. Bailey, R.P. Mecham, S.D. Shapiro, Lysyl oxidase is required for vascular and diaphragmatic development in mice, *J. Biol. Chem.* 278 (2003) 14387–14393.
- [31] J.M. Maki, J. Rasanen, H. Tikkanen, R. Sormunen, K. Makikallio, K.I. Kivirikko, et al., Inactivation of the lysyl oxidase gene *Lox* leads to aortic aneurysms, cardiovascular dysfunction, and perinatal death in mice, *Circulation* 106 (2002) 2503–2509.
- [32] J.M. Maki, R. Sormunen, S. Lippo, R. Kaarteenaho-Wiik, R. Soininen, J. Myllyharju, Lysyl oxidase is essential for normal development and function of the respiratory system and for the integrity of elastic and collagen fibers in various tissues, *Am. J. Pathol.* 167 (2005) 927–936.
- [33] A. Martin, F. Salvador, G. Moreno-Bueno, A. Floristan, C. Ruiz-Herguido, E.P. Cuevas, et al., Lysyl oxidase-like 2 represses Notch1 expression in the skin to promote squamous cell carcinoma progression, *EMBO J.* 34 (2015) 1090–1109.
- [34] M. Bignon, C. Pichol-Thievent, J. Hardouin, M. Malbouyres, N. Brechot, L. Nasciutti, et al., Lysyl oxidase-like protein-2 regulates sprouting angiogenesis and type IV collagen assembly in the endothelial basement membrane, *Blood* 118 (2011) 3979–3989.
- [35] C. Anazzo, A.J. Lopez-Jimenez, M. Rafi, L. Vega-Montoto, M.Z. Zhang, B.G. Hudson, et al., Lysyl Oxidase-like-2 cross-links collagen IV of glomerular basement membrane, *J. Biol. Chem.* 291 (2016) 25999–26012.
- [36] E. Hohenester, D. Tisi, J.F. Tals, R. Timpl, The crystal structure of a laminin G-like module reveals the molecular basis of alpha-dystroglycan binding to laminins, perlecan, and agrin, *Mol. Cell* 4 (1999) 783–792.
- [37] M.A. Gubbiotti, T. Neill, R.V. Iozzo, A current view of perlecan in physiology and pathology: a mosaic of functions, *Matrix Biol.* 57–58 (2017) 285–298.
- [38] M.S. Lord, C.Y. Chuang, J. Melrose, M.J. Davies, R.V. Iozzo, J.M. Whitelock, The role of vascular-derived perlecan in modulating cell adhesion, proliferation and

- growth factor signaling, *Matrix Biol.* 35 (2014) 112–122.
- [39] S. Douglass, A. Goyal, R.V. Iozzo, The role of perlecan and endorepellin in the control of tumor angiogenesis and endothelial cell autophagy, *Connect. Tissue Res.* 56 (2015) 381–391.
- [40] C. Poluzzi, R.V. Iozzo, L. Schaefer, Endostatin and endorepellin: a common route of action for similar angiostatic cancer avengers, *Adv. Drug Deliv. Rev.* 97 (2016) 156–173.
- [41] J.J. Zoeller, A. McQuillan, J. Whitelock, S.Y. Ho, R.V. Iozzo, A central function for perlecan in skeletal muscle and cardiovascular development, *J. Cell Biol.* 181 (2008) 381–394.
- [42] M. Costell, E. Gustafsson, A. Aszodi, M. Morgelin, W. Bloch, E. Hunziker, et al., Perlecan maintains the integrity of cartilage and some basement membranes, *J. Cell Biol.* 147 (1999) 1109–1122.
- [43] K.K. McKee, S. Capizzi, P.D. Yurchenco, Scaffold-forming and adhesive contributions of synthetic laminin-binding proteins to basement membrane assembly, *J. Biol. Chem.* 284 (2009) 8984–8994.
- [44] J. Moll, P. Barzaghi, S. Lin, G. Bezakova, H. Lochmuller, E. Engvall, et al., An agrin minigene rescues dystrophic symptoms in a mouse model for congenital muscular dystrophy, *Nature* 413 (2001) 302–307.
- [45] G. Bezakova, M.A. Ruegg, New insights into the roles of agrin, *Nat. Rev. Mol. Cell Biol.* 4 (2003) 295–308.
- [46] A.J. Barber, E. Lieth, Agrin accumulates in the brain microvascular basal lamina during development of the blood-brain barrier, *Dev. Dyn.* 208 (1997) 62–74.
- [47] E. Steiner, G.U. Enzmann, R. Lyck, S. Lin, M.A. Ruegg, S. Kroger, et al., The heparan sulfate proteoglycan agrin contributes to barrier properties of mouse brain endothelial cells by stabilizing adherens junctions, *Cell Tissue Res.* 358 (2014) 465–479.
- [48] J.W. Fox, U. Mayer, R. Nischt, M. Aumailley, D. Reinhardt, H. Wiedemann, et al., Recombinant nidogen consists of three globular domains and mediates binding of laminin to collagen type IV, *EMBO J.* 10 (1991) 3137–3146.
- [49] M. Hopf, W. Gohring, A. Ries, R. Timpl, E. Hohenester, Crystal structure and mutational analysis of a perlecan-binding fragment of nidogen-1, *Nat. Struct. Biol.* 8 (2001) 634–640.
- [50] U. Mayer, R. Nischt, E. Poschl, K. Mann, K. Fukuda, M. Gerl, et al., A single EGF-like motif of laminin is responsible for high affinity nidogen binding, *EMBO J.* 12 (1993) 1879–1885.
- [51] B.L. Bader, N. Smyth, S. Nedbal, N. Miosge, A. Baranowsky, S. Mokkaipati, et al., Compound genetic ablation of nidogen 1 and 2 causes basement membrane defects and perinatal lethality in mice, *Mol. Cell Biol.* 25 (2005) 6846–6856.
- [52] K. Rasi, J. Pihola, M. Czabanka, R. Sormunen, M. Ilves, H. Leskinen, et al., Collagen XV is necessary for modeling of the extracellular matrix and its deficiency predisposes to cardiomyopathy, *Circ. Res.* 107 (2010) 1241–1252.
- [53] L. Seppinen, T. Pihlajaniemi, The multiple functions of collagen XVIII in development and disease, *Matrix Biol.* 30 (2011) 83–92.
- [54] K. Javaherian, S.Y. Park, W.F. Pickl, K.R. LaMontagne, R.T. Sjin, S. Gillies, et al., Laminin modulates morphogenic properties of the collagen XVIII endostatin domain, *J. Biol. Chem.* 277 (2002) 45211–45218.
- [55] S. Dong, G.J. Cole, W. Hallfrer, Expression of collagen XVIII and localization of its glycosaminoglycan attachment sites, *J. Biol. Chem.* 278 (2003) 1700–1707.
- [56] A. Utraiainen, R. Sormunen, M. Kettunen, L.S. Carvalhaes, E. Sajanti, L. Eklund, et al., Structurally altered basement membranes and hydrocephalus in a type XVIII collagen deficient mouse line, *Hum. Mol. Genet.* 13 (2004) 2089–2099.
- [57] M.S. O'Reilly, T. Boehm, Y. Shing, N. Fukui, G. Vasios, W.S. Lane, et al., Endostatin: an endogenous inhibitor of angiogenesis and tumor growth, *Cell* 88 (1997) 277–285.
- [58] A.G. Mameros, D.R. Keene, U. Hansen, N. Fukai, K. Moulton, P.L. Goletz, et al., Collagen XVIII/endostatin is essential for vision and retinal pigment epithelial function, *EMBO J.* 23 (2004) 89–99.
- [59] M. Hurskainen, L. Eklund, P.O. Hagg, M. Fruttiger, R. Sormunen, M. Ilves, et al., Abnormal maturation of the retinal vasculature in type XVIII collagen/endostatin deficient mice and changes in retinal glial cells due to lack of collagen types XV and XVIII, *FASEB J.* 19 (2005) 1564–1566.
- [60] H. Sage, B. Trueb, P. Bornstein, Biosynthetic and structural properties of endothelial cell type VIII collagen, *J. Biol. Chem.* 258 (1983) 13391–13401.
- [61] G. Hou, D. Mulholland, M.A. Gronski, M.P. Bendeck, Type VIII collagen stimulates smooth muscle cell migration and matrix metalloproteinase synthesis after arterial injury, *Am. J. Pathol.* 156 (2000) 467–476.
- [62] H. Sage, M.L. Iruela-Arispe, Type VIII collagen in murine development. Association with capillary formation in vitro, *Ann. N. Y. Acad. Sci.* 580 (1990) 17–31.
- [63] S.K. Gara, P. Grumati, A. Urciuolo, P. Bonaldo, B. Kobbe, M. Koch, et al., Three novel collagen VI chains with high homology to the alpha3 chain, *J. Biol. Chem.* 283 (2008) 10658–10670.
- [64] A. Colombatti, M.T. Mucignat, P. Bonaldo, Secretion and matrix assembly of recombinant type VI collagen, *J. Biol. Chem.* 270 (1995) 13105–13111.
- [65] C. Baldock, M.J. Sherratt, C.A. Shuttleworth, C.M. Kielty, The supramolecular organization of collagen VI microfibrils, *J. Mol. Biol.* 330 (2003) 297–307.
- [66] H.J. Kuo, C.L. Maslen, D.R. Keene, R.W. Glanville, Type VI collagen anchors endothelial basement membranes by interacting with type IV collagen, *J. Biol. Chem.* 272 (1997) 26522–26529.
- [67] P. Bonaldo, V. Russo, F. Buccicotti, R. Doliana, A. Colombatti, Structural and functional features of the alpha 3 chain indicate a bridging role for chicken collagen VI in connective tissues, *Biochemistry* 29 (1990) 1245–1254.
- [68] E. Tillet, H. Wiedemann, R. Golbik, T.C. Pan, R.Z. Zhang, K. Mann, et al., Recombinant expression and structural and binding properties of alpha 1(VI) and alpha 2(VI) chains of human collagen type VI, *Eur. J. Biochem.* 221 (1994) 177–185.
- [69] J.F. Groulx, D. Gagne, Y.D. Benoit, D. Martel, N. Basora, J.F. Beaulieu, Collagen VI is a basement membrane component that regulates epithelial cell-fibronectin interactions, *Matrix Biol.* 30 (2011) 195–206.
- [70] S. Astrof, R.O. Hynes, Fibronectins in vascular morphogenesis, *Angiogenesis* 12 (2009) 165–175.
- [71] B. Cseh, S. Fernandez-Sauze, D. Grall, S. Schaub, E. Doma, E. Van Obberghen-Schilling, Autocrine fibronectin directs matrix assembly and crosstalk between cell-matrix and cell-cell adhesion in vascular endothelial cells, *J. Cell. Sci.* 123 (2010) 3989–3999.
- [72] H. Kumra, L. Sabatier, A. Hassan, T. Sakai, D.F. Mosher, J. Brinckmann, et al., Roles of fibronectin isoforms in neonatal vascular development and matrix integrity, *PLoS Biol.* 16 (2018) e2004812.
- [73] C.Y. Chung, H.P. Erickson, Glycosaminoglycans modulate fibronectin matrix assembly and are essential for matrix incorporation of tenascin-C, *J. Cell. Sci.* 110 (Pt 12) (1997) 1413–1419.
- [74] S.S. Akimov, A.M. Belkin, Cell-surface transglutaminase promotes fibronectin assembly via interaction with the gelatin-binding domain of fibronectin: a role in TGFbeta-dependent matrix deposition, *J. Cell. Sci.* 114 (2001) 2989–3000.
- [75] M. Aumailley, R. Timpl, Attachment of cells to basement membrane collagen type IV, *J. Cell Biol.* 103 (1986) 1569–1575.
- [76] C.G. Miller, A. Pozzi, R. Zent, J.E. Schwarzbauer, Effects of high glucose on integrin activity and fibronectin matrix assembly by mesangial cells, *Mol. Biol. Cell* 25 (2014) 2342–2350.
- [77] M.S. Filla, K.D. Dimeo, T. Tong, D.M. Peters, Disruption of fibronectin matrix affects type IV collagen, fibrillin and laminin deposition into extracellular matrix of human trabecular meshwork (HTM) cells, *Exp. Eye Res.* 165 (2017) 7–19.
- [78] U. Rauch, A. Saxena, S. Lorkowski, J. Rauterberg, H. Bjorkbacka, M. Durbeek, et al., Laminin isoforms in atherosclerotic arteries from mice and man, *Histol. Histopathol.* 26 (2011) 711–724.
- [79] Y. Yao, Laminin: loss-of-function studies, *Cell. Mol. Life Sci.* 74 (2017) 1095–1115.
- [80] D. Stenzel, C.A. Franco, S. Estrach, A. Mettouchi, D. Sauvaget, I. Rosewell, et al., Endothelial basement membrane limits tip cell formation by inducing Dll4/Notch signalling in vivo, *EMBO Rep.* 12 (2011) 1135–1143.
- [81] J. Thyboll, J. Kortessmaa, R. Cao, R. Soininen, L. Wang, A. Iivanainen, et al., Deletion of the laminin alpha4 chain leads to impaired microvessel maturation, *Mol. Cell Biol.* 22 (2002) 1194–1202.
- [82] R. Hallmann, N. Horn, M. Selg, O. Wendler, F. Pausch, L.M. Sorokin, Expression and function of laminins in the embryonic and mature vasculature, *Physiol. Rev.* 85 (2005) 979–1000.
- [83] L.M. Sorokin, F. Pausch, M. Durbeek, P. Ekblom, Differential expression of five laminin alpha (1–5) chains in developing and adult mouse kidney, *Dev. Dyn.* 210 (1997) 446–462.
- [84] E.G. Coles, L.S. Gammill, J.H. Miner, M. Bronner-Fraser, Abnormalities in neural crest cell migration in laminin alpha5 mutant mice, *Dev. Biol. (Basel)* 289 (2006) 218–228.
- [85] J.H. Miner, C. Li, Defective glomerulogenesis in the absence of laminin alpha5 demonstrates a developmental role for the kidney glomerular basement membrane, *Dev. Biol. (Basel)* 217 (2000) 278–289.
- [86] J. Di Russo, A.L. Luik, L. Yousif, S. Budny, H. Oberleithner, V. Hofschroer, et al., Endothelial basement membrane laminin 511 is essential for shear stress response, *EMBO J.* 36 (2017) 183–201.
- [87] E. Tzima, M.A. del Pozo, S.J. Shattil, S. Chien, M.A. Schwartz, Activation of integrins in endothelial cells by fluid shear stress mediates Rho-dependent cytoskeletal alignment, *EMBO J.* 20 (2001) 4639–4647.
- [88] J. Gautam, X. Zhang, Y. Yao, The role of pericytic laminin in blood brain barrier integrity maintenance, *Sci. Rep.* 6 (2016) 36450.
- [89] D.B. Gould, F.C. Phalan, G.J. Breedveld, S.E. van Mil, R.S. Smith, J.C. Schimenti, et al., Mutations in Col4a1 cause perinatal cerebral hemorrhage and porencephaly, *Science* 308 (2005) 1167–1171.
- [90] D.B. Gould, F.C. Phalan, S.E. van Mil, J.P. Sundberg, K. Vahedi, P. Massin, et al., Role of COL4A1 in small-vessel disease and hemorrhagic stroke, *N. Engl. J. Med.* 354 (2006) 1489–1496.
- [91] E. Plaisier, O. Gribouval, S. Alamowitch, B. Mougnot, C. Prost, M.C. Verpont, et al., COL4A1 mutations and hereditary angiopathy, nephropathy, aneurysms, and muscle cramps, *N. Engl. J. Med.* 357 (2007) 2687–2695.
- [92] A. Federico, I. Di Donato, S. Bianchi, C. Di Palma, I. Taglia, M.T. Dotti, Hereditary cerebral small vessel diseases: a review, *J. Neurol. Sci.* 322 (2012) 25–30.
- [93] D.S. Kuo, C. Labelle-Dumais, D.B. Gould, COL4A1 and COL4A2 mutations and disease: insights into pathogenic mechanisms and potential therapeutic targets, *Hum. Mol. Genet.* 21 (2012) R97–110.
- [94] K. Vahedi, S. Alamowitch, Clinical spectrum of type IV collagen (COL4A1) mutations: a novel genetic multisystem disease, *Curr. Opin. Neurol.* 24 (2011) 63–68.
- [95] M. Jeanne, D.B. Gould, Genotype-phenotype correlations in pathology caused by collagen type IV alpha 1 and 2 mutations, *Matrix Biol.* 57–58 (2017) 29–44.
- [96] J. Favor, C.J. Gloeckner, D. Janik, M. Klempt, A. Neuhauser-Klaus, W. Pletsch, et al., Type IV procollagen missense mutations associated with defects of the eye, vascular stability, the brain, kidney function and embryonic or postnatal viability in the mouse, *Mus musculus*: an extension of the Col4a1 allelic series and the identification of the first two Col4a2 mutant alleles, *Genetics* 175 (2007) 725–736.
- [97] T. Van Agtmael, U. Schlötzer-Schrehardt, L. McKie, D.G. Brownstein, A.W. Lee, S.H. Cross, et al., Dominant mutations of Col4a1 result in basement membrane defects which lead to anterior segment dysgenesis and glomerulopathy, *Hum. Mol. Genet.* 14 (2005) 3161–3168.
- [98] A. Joutel, I. Haddad, J. Ratelade, M.T. Nelson, Perturbations of the cerebrovascular matrisome: A convergent mechanism in small vessel disease of the

- brain? *J. Cereb. Blood Flow Metab.* 36 (2016) 143–157.
- [99] M. Lopez-Luppo, V. Nacher, D. Ramos, J. Catita, M. Navarro, A. Carretero, et al., Blood vessel basement membrane alterations in human retinal microaneurysms during aging, *Invest. Ophthalmol. Vis. Sci.* 58 (2017) 1116–1131.
- [100] H. Akagawa, A. Narita, H. Yamada, A. Tajima, B. Krschek, H. Kasuya, et al., Systematic screening of lysyl oxidase-like (LOXL) family genes demonstrates that LOXL2 is a susceptibility gene to intracranial aneurysms, *Hum. Genet.* 121 (2007) 377–387.
- [101] Y. Wu, Z. Li, Y. Shi, L. Chen, H. Tan, Z. Wang, et al., Exome sequencing identifies LOXL2 mutation as a cause of familial intracranial aneurysm, *World Neurosurg.* 109 (2018) e812–e818.
- [102] E. Van Obberghen-Schilling, R.P. Tucker, F. Saupe, I. Gasser, B. Cseh, G. Orend, Fibronectin and tenascin-C: accomplices in vascular morphogenesis during development and tumor growth, *Int. J. Dev. Biol.* 55 (2011) 511–525.
- [103] E.L. George, E.N. Georges-Labouesse, R.S. Patel-King, H. Rayburn, R.O. Hynes, Defects in mesoderm, neural tube and vascular development in mouse embryos lacking fibronectin, *Development* 119 (1993) 1079–1091.
- [104] D. Stenzel, A. Lundkvist, D. Sauvaget, M. Busse, M. Graupera, A. van der Flier, et al., Integrin-dependent and -independent functions of astrocytic fibronectin in retinal angiogenesis, *Development* 138 (2011) 4451–4463.
- [105] N. Beckouche, M. Bignon, V. Lelarge, T. Mathivet, C. Pichol-Thievend, S. Berndt, et al., The interaction of heparan sulfate proteoglycans with endothelial transglutaminase-2 limits VEGF165-induced angiogenesis, *Sci. Signal.* 8 (2015) ra70.
- [106] X. Zhou, R.G. Rowe, N. Hiraoka, J.P. George, D. Wirtz, D.F. Mosher, et al., Fibronectin fibrillogenesis regulates three-dimensional neovessel formation, *Genes Dev.* 22 (2008) 1231–1243.
- [107] F. Castelletti, R. Donadelli, F. Banterla, F. Hildebrandt, P.F. Zipfel, E. Bresin, et al., Mutations in FN1 cause glomerulopathy with fibronectin deposits, *Proc. Natl. Acad. Sci. U. S. A.* 105 (2008) 2538–2543.
- [108] S. Karaman, V.M. Leppanen, K. Alitalo, Vascular endothelial growth factor signaling in development and disease, *Development* 145 (2018).
- [109] F. Cecchi, D. Pajalunga, C.A. Fowler, A. Uren, D.C. Rabe, B. Peruzzi, et al., Targeted disruption of heparan sulfate interaction with hepatocyte and vascular endothelial growth factors blocks normal and oncogenic signaling, *Cancer Cell* 22 (2012) 250–262.
- [110] L. Jakobsson, J. Kreuger, K. Holmbom, L. Lundin, I. Eriksson, L. Kjellen, et al., Heparan sulfate in trans potentiates VEGFR-mediated angiogenesis, *Dev. Cell* 10 (2006) 625–634.
- [111] L. Fontana, Y. Chen, P. Prijatelj, T. Sakai, R. Fassler, L.Y. Sakai, et al., Fibronectin is required for integrin α 5 β 1-mediated activation of latent TGF- β complexes containing LTBP-1, *FASEB J.* 19 (2005) 1798–1808.
- [112] P. Lindahl, B.R. Johansson, P. Leveen, C. Betsholtz, Pericyte loss and microaneurysm formation in PDGF-B-deficient mice, *Science* 277 (1997) 242–245.
- [113] P. Leveen, M. Pekny, S. Gebre-Medhin, B. Swolin, E. Larsson, C. Betsholtz, Mice deficient for PDGF B show renal, cardiovascular, and hematological abnormalities, *Genes Dev.* 8 (1994) 1875–1887.
- [114] P. Soriano, Abnormal kidney development and hematological disorders in PDGF beta-receptor mutant mice, *Genes Dev.* 8 (1994) 1888–1896.
- [115] M. Hellstrom, H. Gerhardt, M. Kalen, X. Li, U. Eriksson, H. Wolburg, et al., Lack of pericytes leads to endothelial hyperplasia and abnormal vascular morphogenesis, *J. Cell Biol.* 153 (2001) 543–553.
- [116] P. Lindblom, H. Gerhardt, S. Liebner, A. Abramsson, M. Enge, M. Hellstrom, et al., Endothelial PDGF-B retention is required for proper investment of pericytes in the microvessel wall, *Genes Dev.* 17 (2003) 1835–1840.
- [117] Y. Xu, Q. Yu, Angiotensin-1, unlike angiotensin-2, is incorporated into the extracellular matrix via its linker peptide region, *J. Biol. Chem.* 276 (2001) 34990–34998.
- [118] P. Saharinen, L. Eklund, J. Miettinen, R. Wirkkala, A. Anisimov, M. Winderlich, et al., Angiotensins assemble distinct Tie2 signalling complexes in endothelial cell-cell and cell-matrix contacts, *Nat. Cell Biol.* 10 (2008) 527–537.
- [119] Y. Xu, Y.J. Liu, Q. Yu, Angiotensin-3 is tethered on the cell surface via heparan sulfate proteoglycans, *J. Biol. Chem.* 279 (2004) 41179–41188.
- [120] S. Le Jan, C. Amy, A. Cazes, C. Monnot, N. Lamané, J. Favier, et al., Angiotensin-like 4 is a proangiogenic factor produced during ischemia and in conventional renal cell carcinoma, *Am. J. Pathol.* 162 (2003) 1521–1528.
- [121] C. Chomel, A. Cazes, C. Faye, M. Bignon, E. Gomez, C. Ardidié-Robouant, et al., Interaction of the coiled-coil domain with glycosaminoglycans protects angiotensin-like 4 from proteolysis and regulates its antiangiogenic activity, *FASEB J.* 23 (2009) 940–949.
- [122] E.G. Perdiguerro, A. Galatup, M. Durand, J. Teillon, J. Philippe, D.M. Valenzuela, et al., Alteration of developmental and pathological retinal angiogenesis in *angptl4*-deficient mice, *J. Biol. Chem.* 286 (2011) 36841–36851.
- [123] A. Galaup, E. Gomez, R. Soultani, M. Durand, A. Cazes, C. Monnot, et al., Protection against myocardial infarction and no-reflow through preservation of vascular integrity by angiotensin-like 4, *Circulation* 125 (2012) 140–149.
- [124] E. Gomez Perdiguerro, A. Liabotis-Fontugne, M. Durand, C. Faye, S. Ricard-Blum, M. Simonutti, et al., ANGPTL4- α 5 β 3 interaction counteracts hypoxia-induced vascular permeability by modulating Src signalling downstream of vascular endothelial growth factor receptor 2, *J. Pathol.* 240 (2016) 461–471.
- [125] D.R. Brigstock, R. Goldschmeding, K.I. Katsube, S.C. Lam, L.F. Lau, K. Lyons, et al., Proposal for a unified CCN nomenclature, *Mol. Pathol.* 56 (2003) 127–128.
- [126] A. Leask, D.J. Abraham, All in the CCN family: essential matricellular signaling modulators emerge from the bunker, *J. Cell. Sci.* 119 (2006) 4803–4810.
- [127] B. Chaqour, Molecular control of vascular development by the matricellular proteins CCN1 (Cyr61) and CCN2 (CTGF), *Trends Dev. Biol.* 7 (2013) 59–72.
- [128] B.L. Bader, H. Rayburn, D. Crowley, R.O. Hynes, Extensive vasculogenesis, angiogenesis, and organogenesis precede lethality in mice lacking all α v integrins, *Cell* 95 (1998) 507–519.
- [129] S.J. Jim Leu, J.S. Sung, M.L. Huang, M.Y. Chen, T.W. Tsai, A novel anti-CCN1 monoclonal antibody suppresses Rac-dependent cytoskeletal reorganization and migratory activities in breast cancer cells, *Biochem. Biophys. Res. Commun.* 434 (2013) 885–891.
- [130] R.A. Dean, G.S. Butler, Y. Hamma-Kourbali, J. Delbe, D.R. Brigstock, J. Courty, et al., Identification of candidate angiogenic inhibitors processed by matrix metalloproteinase 2 (MMP-2) in cell-based proteomic screens: disruption of vascular endothelial growth factor (VEGF)/heparin affinity regulatory peptide (pleiotrophin) and VEGF/Connective tissue growth factor angiogenic inhibitory complexes by MMP-2 proteolysis, *Mol. Cell. Biol.* 27 (2007) 8454–8465.
- [131] J.M. Schober, N. Chen, T.M. Grzeskiewicz, I. Jovanovic, E.E. Emeson, T.P. Ugarova, et al., Identification of integrin α 5 β 1 as an adhesion receptor on peripheral blood monocytes for Cyr61 (CCN1) and connective tissue growth factor (CCN2): immediate-early gene products expressed in atherosclerotic lesions, *Blood* 99 (2002) 4457–4465.
- [132] L.R. James, C. Le, H. Doherty, H.S. Kim, N. Maeda, Connective tissue growth factor (CTGF) expression modulates response to high glucose, *PLoS ONE* 8 (2013) e70441.
- [133] T. Tsoutsman, X. Wang, K. Garchow, B. Riser, S. Twigg, C. Semsarian, CCN2 plays a key role in extracellular matrix gene expression in severe hypertrophic cardiomyopathy and heart failure, *J. Mol. Cell. Cardiol.* 62 (2013) 164–178.
- [134] L. Boldock, C. Wittkowske, C.M. Perrault, Microfluidic traction force microscopy to study mechanotransduction in angiogenesis, *Microcirculation* 24 (2017).
- [135] V. Gebala, R. Collins, I. Geudens, L.K. Phng, H. Gerhardt, Blood flow drives lumen formation by inverse membrane blebbing during angiogenesis in vivo, *Nat. Cell Biol.* 18 (2016) 443–450.
- [136] H. Nakajima, K. Yamamoto, S. Agarwala, K. Terai, H. Fukui, S. Fukuhara, et al., Flow-dependent endothelial YAP regulation contributes to vessel maintenance, *Dev. Cell* 40 (2017) 523–536 e6.
- [137] M.J. Menezes, F.K. McClenahan, C.V. Leiton, A. Aranmolate, X. Shan, H. Colognato, The extracellular matrix protein laminin α 2 regulates the maturation and function of the blood-brain barrier, *J. Neurosci.* 34 (2014) 15260–15280.
- [138] M. Glukhova, V. Kotliansky, C. Fondacci, F. Marotte, L. Rappaport, Laminin variants and integrin laminin receptors in developing and adult human smooth muscle, *Dev. Biol. (Basel)* 157 (1993) 437–447.

Appendix 2

Atlas*, Bidault* et al, in prep

Biomimetic cross-linking of collagen hydrogels by LOXL2 improves pre-vascularization of tissue constructs

Yoann Atlas^{1,2,x}, Laurent Bidault^{1,x}, Marion F Marchand^{1,2}, Christophe Helary⁴, Romain Salza⁵, Tristan Piolot¹, Philippe Mailly¹, Alain Barret¹, Catherine Monnot¹, Sylvie Ricard-Blum⁵, Jurgen Brinckman⁶, Thibaud Coradin³, Stéphane Germain^{1,+}, Laurent Muller^{1,+,*}

¹: CIRB, CNRS UMR7241, INSERM U1050, Collège de France, PSL University, Paris, France

²: Sorbonne Université, Collège doctoral, Paris, France

³: LCMCP, UPMC, Paris, France

⁵: IGFL, CNRS UMR5242, ENS Lyon, France

⁶: Institute of virology and cell biology, University of Lübeck, Lübeck, Germany

^{x,+} : contributed equally to this work

^{*} : corresponding author

SHORT TITLE

Cross-linking collagen for prevascularization

ABSTRACT

Vascularization of tissue constructs is a hindrance to success of regenerative medicine approaches based on tissue engineering. One option considered for improving blood perfusion consists in *in vitro* pre-vascularization, which requires characterization of hydrogels supporting formation of microvascular networks and stiff enough for manipulation. Angiogenesis is associated with complex matrix remodeling targeting both fibrillar collagen I of the biomaterial and network-forming collagen IV of the basement membrane generated by endothelial cells. We here investigated the impact of collagen I organization on *in vitro* pre-vascularization of constructs. Enhancing fibrillogenesis increased stiffness but decreased capillary formation. In order to further modulate the mechanical and structural properties of hydrogels, we used a biomimetic strategy taking advantage of lysyl oxidase-like 2 cross-linking activity. Hydrogels crosslinked under weak fibrillogenesis conditions displayed higher stiffness and preserved angiogenic properties. Cross-linking stiffer hydrogels with low angiogenic properties improved capillary formation with limited macroscopic impact on stiffness. Measuring the local properties of collagen by atomic force microscopy however demonstrated the strong impact of LOXL2 cross-linking on fibers at the cell-scale. Altogether, LOXL2-mediated cross-linking of collagen hydrogels allowed the production of stiffer gels with increased angiogenic properties, thus constituting a promising option for pre-vascularization of tissue constructs.

197 words

KEYWORDS :

Pre-vascularization, collagen, crosslink, lysyl oxidase

INTRODUCTION

Tissue engineering is now considered to be the most promising approach for promoting regeneration of failing organs. This strategy consists in combining the therapeutic potential of regenerating stem cells with the mechanical support of biomaterials. Its success is however directly subject to blood perfusion of the grafted tissue-engineered construct for cell survival and differentiation (Novosel, Kleinhans, and Kluger 2011; Auger, Gibot, and Lacroix 2013). Promoting angiogenesis *in situ* after implantation of the tissue construct is often considered as inefficient, particularly in the context of hard or thick tissues (Grosso et al. 2017). *In vitro* prevascularization is a more promising approach consisting in generating a microvascular network *in vitro* and relying on inosculation with the host circulation for perfusion. Using dental pulp stem cells co-seeded with endothelial cells in a scaffold, we have recently demonstrated that such prevascularized construct result in high perfusion and protection from apoptosis (Atlas, Gorin et al. submitted). *In vitro* microvascularization of that construct occurred as a response to the angiogenic factors released by stem cells conditioned with FGF-2 (Gorin et al. 2016).

A huge amount of studies has been focusing on secreted factors or cell-cell interactions involving stem cells included in tissue constructs (Kerschnitzki et al. 2013; Rademakers et al. 2019). Much less attention has been given to the nature of scaffolds that would provide the best environment to endothelial cells for *in vitro* capillary morphogenesis. This is however getting even more important in the context of tissue construct pre-vascularization using techniques such as biofabrication or 3D printing (Novosel, Kleinhans, and Kluger 2011; Kolesky et al. 2016; H.-H. Greco Song et al. 2018). Indeed, stiffness and composition of matrix plays a major role in controlling cell proliferation, migration, and even differentiation (Engler et al. 2006; Ulrich, Pardo, and Kumar 2009). Many studies have indeed proven the high impact of mechanical constraints on endothelial cell behavior (Sieminski, Hebbel, and Gooch 2004; Mammoto et al. 2009; Raghavan et al. 2010; Lesman et al. 2016).

Whereas macroporous scaffolds and cell-derived microenvironments like cell-sheets could provide interesting tools for *in vivo* angiogenesis, they might not be able to provide the immediate support required for rapid *in vitro* formation of capillaries (X. Li et al. 2017; Gibot et al. 2016). Hydrogels of natural polymers thus appear as more adapted biomaterials, and collagen has indeed been extensively used in this context, including for the development of angiogenesis models over the last 20 years (Montesano et al. 1996). One of the major defaults of such hydrogels as biomaterials dedicated to implantation is however their softness which makes them difficult to handle, even more in the context for manipulation of fragile microvascular networks.

Collagen is a very versatile material that can be used in many different ways, and improving the physical properties of collagen gels has been achieved using several approaches (Soroushanova et al. 2019). The requirements for a material dedicated to capillary morphogenesis include stiffness and pore size for promotion of cell migration and matrix remodeling for allowing vascular morphogenesis. Indeed, migration requirement varies with cell types, but nucleus plasticity has recently been identified as the major limiting factor (Wolf et al. 2013; Thiam et al. 2016), with cells encountering nuclear envelop deformation and rupture as they migrate in pores under 2 μm (Raab et al. 2016). Furthermore, in parallel with migration, endothelial cells need to organize into tubular structures with a diameter of 10 to 20 μm whose establishment requires matrix remodeling for generating space and for synthesizing their own vascular microenvironment. We here used collagen hydrogels generated under conditions that support fibrillogenesis by self-assembly. We first investigated the remodeling of such collagen hydrogels during the process of capillary formation. We then modulated collagen fibrillogenesis in order to obtain a wide panel of hydrogels with distinct physical characteristics. Among the different factors that control collagen fibrillogenesis, we chose to modulate temperature and pH as their impact has already been extensively documented (Y. Li et al. 2009; Harris, Soliakov, and Lewis 2013; Ramírez-Rodríguez et al. 2014; Xie et al. 2017). Even though ionic composition also controls fibrillogenesis, this condition was imposed by the culture medium required for capillary formation (Carey et al. 2012; Harris and Reiber 2007).

In order to further extend the range of physical properties of the hydrogels, we also used a biomimetic approach based on the cross-linking activity of lysyl-oxidase like 2 (LOXL2). Enzymes of the LOX family are indeed responsible for the covalent cross-linking of collagens by catalyzing the

deamination of lysines and hydroxylysines both in physiological and pathological contexts (H.-J. Moon et al. 2014). They share a conserved catalytic domain that contains a copper-binding site and a lysyl tyrosylquinone cofactor (Fig. S6). LOXL2 also contains 4 repeats of SRCR domains that extend as a string of pearls without interaction with the catalytic domain (Schmelzer et al. 2019). Oxidation of collagens and tropoelastin by LOXL2 has been known for long, but it is only recently that the resulting cross-linking of these proteins has been demonstrated (Anazco et al. 2016; Schilter et al. 2019; Schmelzer et al. 2019). This enzyme has indeed been associated with pathological contexts involving matrix stiffening, i.e. fibrosis and tumor growth (Barry-Hamilton et al. 2010; Yang et al. 2016; Y. Wei et al. 2017), and also with the regulation of angiogenesis during development (Bignon et al. 2011). We here took advantage of the specificity of LOXL2 for a limited spectrum of sites in collagen in order to promote cross-linking of hydrogels that would increase their mechanical properties without blocking cell progression and vascular morphogenesis as a result of excessive cross-linking.

Our aim was thus to determine optimal conditions for producing collagen hydrogels that were stiff enough for handling and supportive of *in vitro* pre-vascularization of tissue constructs. Analysis of matrix stiffness and pore size both at a bulk scale and at the cell-scale allowed characterization of the conditions required for capillary formation and of a candidate approach for generating such conditions in cross-linked collagen gels.

RESULTS

- **Capillary formation is associated with remodeling of the fibrillar microenvironment and generation of basement membrane**

When spheroids of endothelial cells are seeded in collagen hydrogels and cultivated in complete endothelial growth medium supplemented with 5 ng/ml VEGF, individual cells invade the hydrogel without maintaining cell-cell junctions, in a mesenchymal manner (Fig. S1A; movie 1). When cultivated in conditioned medium from dermal fibroblasts containing 5 ng/ml VEGF, these cells invade the hydrogel as organized angiogenic sprouts consisting in tip and stalk cells to generate capillaries (Fig. S1B; movie 2), as previously described in fibrin hydrogels (Nakatsu et al. 2003; Bignon et al. 2011). We here analyzed the matrix remodeling associated with such capillary formation. Twenty hours after seeding cells in collagen, they elongated and polarized as they explored the environment with long protrusions bearing filopodia (Fig. 1A.i). They established large areas of cell-cell contacts mediated by CD31 and VE-Cadherin (Fig. 1A.iii-iv) with no lumen formation (Fig. 1Aii). Both proteins display a patchy distribution typical of junction-associated intermittent lamellipodia (JAIL) (Cao et al. 2017) (Fig. 1A.iii-iv). Intracellular aggregates of co-localized VE-cadherin and CD31 were also detected at the tip of the protrusions (Fig. 1A.i). After 3 days in culture, cells have organized into lumenized and branched capillaries (Fig. 1B.i-ii). VE-Cadherin was localized to mature adherens junctions (Fig. 1B.iv). During the process of capillary formation cytoskeleton underwent remodeling as actin was redistributed from a cortical network at 20 hours (Fig. 1A.i) to stress fibers and cell junctions (Fig. 1B.v). Endothelial cells indeed organized in angiogenic sprouts and acquired typical specification into tip and stalk cells, as demonstrated by VE-cadherin and β -catenin co-localization either as aggregates in protrusions of tip cells, or at cell adherens junctions in stalk cells (Fig. 1C).

Capillary morphogenesis was also associated with major matrix remodeling. Twenty hours after seeding, fibrillar collagen was strikingly stacked up at the cell surface, as detected using second harmonic generation in 2P-microscopy (Fig. 2A.i). In addition, bundles of radial collagen fibers were detected at the cell vicinity, demonstrating transmission of cell contraction to the microenvironment. Deposition of collagen IV at the cell surface was limited at this early time point, compared to intracellular immuno-staining (Fig. 2A.ii). After 72 hours, packed collagen was still detected in some areas at the cell surface (Fig. 2D.i), but radial bundles of collagen fibers were no more present along capillaries (Fig. 2B.i and S1A). Collagen IV was deposited in the basement membrane at the interface between fibrillar collagen and cell surface (Fig. 2C.iv and D.iv). We investigated collagen I degradation using Marimastat, a matrix metalloproteinase inhibitor. Marimastat treatment inhibited capillary formation in a dose-dependent manner (Fig. 3A-B). Lumen formation was also abolished and cell surface bore numerous filopodia (Fig. 3C). Collagen I remained stacked up at the surface of endothelial cells after 3 days in culture (Fig. 3D.i) with similar levels to those observed after 20 hours under control conditions (Fig. 2B.i and S1A.i), supporting inhibition of its remodeling. Only limited amount and shorter radial bundles of fibers were detected, indicating inhibition of cell contraction or of its transmission to the matrix. Using an antibody specific for cleaved collagen I (anti-Col1-3/4C), we verified that Marimastat did inhibit collagen degradation (Fig. S2). Cleaved collagen I was only detected after 96 hours incubation, and co-localized with the SHG signal stacked up along basement membrane of the capillaries (Fig. S2A and B). Treatment with Marimastat strongly decreased the signal detected with anti-Col1-3/4C (Fig. S2C and D). The strongest staining actually appeared to be intracellular (Fig. S2D), suggesting processing by cysteine or serine lysosomal proteases. The amount of collagen IV deposition was not affected by Marimastat (Fig. 3D.ii), but its distribution however overlapped with packed collagen I instead of generating an interface between fibrillar collagen and cell surface (Fig. 3D). In addition, Marimastat neither inhibited formation of capillary network nor did it alter lumen formation in fibrin hydrogel (Fig. S3), demonstrating that it is the remodeling of collagen I from the scaffold that is affected by MMP inhibition rather than cell-generated material. These observations also suggested that remodeling of collagen at the cell surface consisted in a fine tuning between stacking up and breaking down fibrillar collagen for providing support to cell mechanotransduction, rather than coarse degradation generating channels for cell progression. They also raised questions as to whether and to which extent collagen I fibrillogenesis could modulate capillary formation.

- **Capillary formation is regulated by collagen fibrillogenesis**

Collagen fibrillogenesis was thus tuned in order to characterize the optimal microenvironment supporting capillary formation. Fibrillogenesis of collagen I at 2 or 4.5 mg/ml was triggered at pH 6.5, 7 or 8.5 and at either 20 or 37°C. These conditions provided hydrogels with elastic properties in a stiffness range from 50 to 5000 Pa (Fig. 4A-C). Increasing concentration of collagen or pH, and lowering temperature enhanced collagen storage modulus, as previously described in several studies (X. Li et al. 2017; Holder et al. 2018). The structural properties of the hydrogels were analyzed using SHG (Fig. 4D). Collagen fibers were thinner and shorter and reached higher densities at 4.5 mg/ml than at 2 mg/ml. At both concentrations, length and diameter of the fibers increased together with stiffness at higher pH. Pore size was assessed over 100 μm stacks. Collagen concentration was the factor affecting the more distribution of pore size (Fig. 4E and F). In gels containing 4.5 mg/ml collagen, 50% of the total pore area was achieved by pores smaller than 1.5 μm , and the largest pores reached 3.4 μm in diameter. Low concentration (2 mg/ml) gels contained a wider range of pore size, with 12 to 28% of the total pore size made up by pores above 4 μm , and the largest pores reaching 9 μm . There was no overall direct correlation between stiffness and distribution of pore size under the fibrillogenesis conditions that we investigated.

Angiogenesis was then assessed by embedding endothelial cells in hydrogels right after neutralization, as fibrillogenesis was initiated. We thus verified that cell encapsulation did not alter fibrillogenesis (Fig S3). Capillary formation was inversely correlated with stiffness of the hydrogels (Fig. 4G). The higher amounts of endothelial cells engaged in capillaries was measured in the softer gels, independently of the concentration of collagen and size of the pores. Pore size was not limiting capillary formation, except for the stiffer (5 kPa) gel generated at higher concentration and lower pH. Surprisingly, among the 2 mg/ml gels, increasing pore size and stiffness by generating the gel at higher pH (20°C and pH 8.5) limited capillary formation. This result was quite unexpected considering the positive impact of both increased stiffness and enlarged pores on cell migration described in the literature (Wolf et al. 2013).

- **LOXL2-mediated increased mechanical and structural properties impact vascularization of collagen hydrogels**

In order to improve collagen as a biomaterial for generating pre-vascularized tissue constructs, we used a biomimetic cross-linking approach. We recently described the purification of active recombinant human LOXL2 (Schmelzer et al. 2019). LOXL2 was added upon neutralization of collagen, when fibrillogenesis was initiated. We first verified that LOXL2 treatment resulted in collagen cross-linking by measuring the total amount of hydroxylysinoxidation (HLNL) cross-links after acidic lysis of the gels (Fig. 5A). We then analyzed the consequence of LOXL2 treatment on the mechanical and structural properties of the collagen hydrogels. Gel points were assessed as the time where the storage modulus G' becomes larger than the loss modulus G'' , thus shifting from a viscoelastic substance to a viscoelastic solid. Gel point was modulated by collagen concentration and temperature but not by pH (Fig. S4). It was actually not possible to measure the gel point of hydrogels prepared at 37°C (Fig. S4A and B) because gelation was too fast (Holder et al. 2018), even though fibrillogenesis was limited at this temperature (Fig. 4D). We thus only treated with LOXL2 the gels prepared at 20°C. LOXL2 differently affected physical properties of the hydrogels depending on their initial fibrillogenesis level in the absence of enzyme, resulting in bulk aspect of collagen organization by SHG imaging quite similar compared to what was observed in the absence of LOXL2 (Fig. 5C). Stiffness, pore size and fiber length were all increased by LOXL2 in the three gels produced at either pH 6.5 or 7 and at both concentrations of collagen (Fig. 5B-E). Whereas the increase resulted in a limited availability of large pores above 4 μm (less than 10%) in the 4.5 mg/ml gels (Fig. 5E), the 2 mg/ml gels reached values of 20 and 28% of the total pore area corresponding to pores larger than 4 μm (Fig. 5D). No significant change was detected for stiffness measured by shear rheology and for the distribution of pore size in the gels produced at pH 8.5. In order to demonstrate the involvement of the lysyl oxidase activity, LOXL2 was pre-incubated with 500 μM β -APN for 30 minutes prior to addition to neutralized collagen. β -APN treatment inhibited LOXL2-mediated increase in stiffness and pore size, but did not affect the fiber length. These data suggested that LOXL2 could cross-link collagen I through both catalytic-dependent and -independent

mechanisms. LOXL2 also increased the gel point of all gels, but this effect was not reversed by β -APN either (Fig. S4), further suggesting that some non-catalytic interactions with collagen I could modulate collagen organization. We thus investigated direct interactions between LOXL2 and collagen I using surface plasmon resonance (SPR). In addition to full-length LOXL2, we purified a truncated form consisting in the 2 N-terminal SRCR domains alone (termed SRCR12) (Umana-Diaz et al. in revision) (Fig. S5), which corresponds to a naturally occurring form in many cell types (López-Jiménez, Basak, and Vanacore 2017; Okada et al. 2018; Schmelzer et al. 2019). Interactions with collagen I were measured using immobilized collagen I with analytes being either full-length LOXL2 or the SRCR12 truncated form. We determined two dissociation constants for LOXL2 (681 and 5.7 nM) and one for SRCR12 (20.4 nM) (table 1), indicating that the two N-terminal domains of LOXL2 could bind collagen I with a similar affinity whereas they were in the full-length protein or after their proteolytic removal. This hypothesis was further supported by our recent structural data showing the string of pearl organization of LOXL2 with no interactions between the N-terminal SRCR domains and the C-terminal domain of LOXL2 (Schmelzer et al. 2019). These data supported the non-enzymatic cross-linking of collagen I through interactions with the SRCR and the catalytic domain of LOXL2, resulting in increased fiber length with no impact on hydrogel stiffness nor on pore size.

We then assessed capillary formation in the collagen gels cross-linked by LOXL2 (Fig. 6). LOXL2 had no impact in the less reticulated hydrogel prepared with 2mg/ml collagen I at pH6.5, even though mechanical properties of this hydrogel displayed the largest increase. LOXL2 did not improve capillary formation in the stiffer high-density gel either. In the three other gels, LOXL2 improved capillary formation with no correlation with the increase of mechanical and structural properties. We thus pushed further the characterization of the 2 mg/ml collagen gels generated either at pH 6.5, which have highest changes in mechanical properties with no impact on capillary formation, or at pH 8.5, which have no modification of pore size and smallest effect on stiffness, but yet highest impact on angiogenesis.

We used atomic force microscopy (AFM) to collect force-distance curves by probing the surface of thick collagen hydrogels. Topographical analysis confirmed the SHG data demonstrating low pore size increased by LOXL2 in gels generated at pH 6.5, and large pores with no impact of LOXL2 at pH 8.5 (Fig. 7A and B). Elastic modulus (E) was then calculated in hydrogels generated at pH 6.5 using colloidal probes of 6 μ m diameter. These analyses confirmed the increase in gel stiffness measured by shear rheology (Fig. 7C). It was however not possible to fit the force-distance curves with the Hertz model when we probed the hydrogels generated at pH 8.5, due to the large size of the pores compared to the size of the probe, and to the lower density of longer fibers (fig. 7B). Considering the topography of these hydrogels, we thus turned to a more specific approach to measure stiffness of bundles of collagen fibers using AFM Quantitative Imaging (QI) mode used conical shape probes, which allows to record complete force-distance curves at each pixel and extraction of elasticity. We found that LOXL2 increased the stiffness of collagen fibers in hydrogels generated at pH 8.5 (Fig.7 D-E and G). We measured a very heterogeneous distribution of the stiffness, with some bundles reaching values of above one kPa, almost 10-fold higher than in the control gels. Treatment with β -APN abolished this effect (Fig. 7F and G). Such a strong local stiffening of collagen at the cell-scale could be responsible for the important improvement of capillary formation mediated by LOXL2 treatment. Indeed, endothelial cells could not stack up the collagen fibers cross-linked by LOXL2 at their surface 24 hours after seeding as they do in control gels (Fig. 7H). This was not due to their confinement as cells spread in 3D to a similar extent (movie 3).

DISCUSSION

In this study, we used a biomimetic approach based on the physiological cross-linking of collagen by the lysyl-oxidase LOXL2 to produce hydrogels with improved characteristics for generation of micro-vascularized tissue constructs. Whereas many studies have focused on the impact of modulation of the 3D microenvironment, they are often limited to the investigation of cell spreading and migration. Our work further assessed vascular morphogenesis, which includes deeper matrix remodeling and generation of vascular basement membrane. Whereas the current paradigm consists in associating increased stiffness with migration and vascularization, there is an overall contradiction between studies that show either the positive impact of mechanical constraints (Raghavan et al. 2010; van der Meer et al. 2013), or inhibition by increasing stiffness (Crosby et al. 2019; Stevenson et al. 2013; Francis-Sedlak et al. 2010).

Capillary formation in collagen gels is associated with major remodeling of the ECM consisting in reorganization and degradation of the fibrillar collagen, and *de novo* generation of vascular basement membrane. Whereas the first processes are common with most cell types, including mesenchymal or tumor cells, the latter is specific to epithelial and endothelial cells and participates to micro-vascular morphogenesis (Pöschl et al. 2004; Bignon et al. 2011; X. Zhou et al. 2008). We observed strong fibrillar collagen stacking at the cell surface and radial bundles of fibers extending in the hydrogel. At the same time point, cells displayed protrusions in the gel, associated with strong cortical actin staining, suggesting that cell-matrix interactions were responsible for such collagen organization. Similar collagen reorganization had already been described in endothelial cells (P.-F. Lee, Yeh, and Bayless 2009; McLeod et al. 2013) as well as in fibroblasts (Pena et al. 2010). Cells could nevertheless exert traction forces beyond this collagen shell-like organization, as indicated by the radial bundles of collagen fibers, and as measured by 3D traction force microscopy (Jorge-Peñas et al. 2017). Such bundles of collagen were actually used by endothelial cells for migration and establishment of cell-cell interactions required for capillary morphogenesis (McLeod et al. 2013). Forty-eight hours later, endothelial cells had established cell-cell junctions and organized in lumenized capillaries. Most of the fibrillar collagen packed at the cell surface was simultaneously lost, except at the level of branching points (P.-F. Lee, Yeh, and Bayless 2009). Loss of this collagen I shell corresponded to the proteolytic activity of matrix metalloproteases (van Hinsbergh and Koolwijk 2008), as demonstrated by inhibition with an MMP inhibitor and by co-localization with cleaved collagen I. Similar observations were done by Lee and collaborators, who also showed that delaying addition of MMP inhibitor resulted in inhibition of the expansion of lumen diameter (P.-F. Lee, Yeh, and Bayless 2009). Quite remarkably, detection of cleaved collagen did not extend further from the cell surface, suggesting a major role for MT1-MMP rather than soluble MMP2 or MMP9 (van Hinsbergh and Koolwijk 2008). In parallel with lumen formation, we observed -1) cortical actin redistribution to cell-cell junctions and stress fibers, -2) loss of the radial bundles of collagen fibers and -3) deposition of collagen IV at the interface between cell surface and fibrillar collagen. These observations indicated a clear shift of endothelial cell interactions with the ECM, and thus a major role for basement membrane generation, as already demonstrated (X. Zhou et al. 2008; Bignon et al. 2011). The inhibition of ECM degradation was very instructive as it revealed that neither collagen I stacking nor basement membrane deposition were altered, but that there was disorganization of the ECM at the cell surface, with co-localization of packed fibrillar collagen and collagen IV. Altogether, these experiments allowed deciphering the steps of ECM remodeling during capillary formation in collagen hydrogels. They suggested a central role for stacking of collagen I at the cell surface in the early steps of capillary formation, for allowing both cell migration and organization of the basement membrane-Interstitial ECM interface. These data also suggested the possibility to modulate capillary formation through the tuning of collagen fibrillogenesis.

Capillary formation is regulated by mechanical cues at several levels, starting with regulation of endothelial gene expression by stiffness (Mammoto et al. 2009; Santos et al. 2015), but modulation of 3D environments in order to analyze single factors like porosity or stiffness is difficult to set up. Indeed, increasing stiffness does not always improve capillary morphogenesis, and translating conclusions from one material to another is complex. In this regard, fibrin has also been used for modulation of angiogenesis, but its fibrillar component is too different from collagen's to compare these studies

(Lesman et al. 2016). Using hydrogels made by combinations of synthetic peptides, inversely proportional extent of microvascularization and stiffness was demonstrated (Stevenson et al. 2013). Contradictory results have also been generated using similar approaches to increase physical properties of collagen (Francis-Sedlak et al. 2009; 2010; Mason et al. 2013). These studies all dealt with relatively soft hydrogels under 500 Pa. Our three softer gel formulations ranging from 56 to 221 Pa showed no impact on vascularization. It is only once 500 Pa is reached that 10% inhibition is detected, and stiffer gels induced more inhibition of micro-vascularization. Soft hydrogels under 500 Pa are however not appropriate for manipulation of micro-vascularized tissue constructs which requires at least 1 kPa bulk stiffness to prevent collapsing upon handling. Whereas this can be achieved by increasing concentration, the matrix density results in cell confinement too high to allow cell spreading and migration (Stevenson et al. 2013; McLeod et al. 2013; Crosby et al. 2019). We also observed cell rounding and inhibition of morphogenesis in our hydrogels at 4.5 mg/mL and high pH.

Cross-linking collagen hydrogels is not always an appropriate solution to reach high enough stiffness, as described above using glucose (Francis-Sedlak et al. 2009; 2010; Mason et al. 2013). Stronger cross-linking agents like genipin are potent factors in cardiovascular engineering for controlling release of molecules (Del Gaudio et al. 2013) or evolution of vascular grafts (Madhavan et al. 2010). Genipin is also used for preventing cell infiltration as a way to control degradation and matrix replacement *in vivo* (Liang et al. 2004). Such approaches are however not adapted to rapid *in vitro* vascularization. Common chemical cross-linkers are also impossible to use with cells, unless they target specific modifications of the polymers used to generate the hydrogels, which is not the case using native collagen. We thus turned to a biomimetic approach for cross-linking, using LOXL2, a physiologically relevant collagen cross-linking enzyme. Whereas the lack of availability of purified LOX has hindered its use in biomaterial science, LOXL2 turns out to be more readily available and we have already demonstrated that cross-linking tropoelastin with recombinant human LOXL2 resulted in the generation of a material with similar elastic properties as elastin (Schmelzer et al. 2019). One recent study has also demonstrated the improvement of tensile properties of collagen after addition of exogenous LOXL2, resulting in two-fold increase in cartilage generated *in vitro*, and further three-fold increase after implantation (Makris et al. 2014). In the present work, LOXL2 increased hydroxylysinoxidation (HLNL) within 24 hours and strongly impacted collagen hydrogels, but to different extents depending on the fibrillogenesis conditions. In gels with limited fibrillogenesis, LOXL2 increased both gel structure and stiffness. In gels with higher fibrillogenesis, LOXL2 had limited impact on gel structure and bulk stiffness. In a similar manner, LOXL2 had no impact on the compressive moduli of engineered bone constructs, while increasing pyridinoline (PYR) cross-links (Mitra et al. 2019).

In terms of functional impact, we observed the largest increase in capillary formation upon LOXL2-mediated cross-linking of the hydrogel that was the less modified in terms of pore size and stiffness. We thus investigated collagen mechanical properties at the cell-scale using AFM. Whereas the topographical observations confirmed the SHG results, measuring elastic moduli of bundles of fibers revealed a very high and heterogeneous increase, as some of the bundles reached values 10 times higher than the average measurement performed in the control gels not treated with LOXL2. Quite remarkably, these modifications of mechanical properties translated into inhibition of the compaction of collagen at the cell surface 24 hours after cell embedding. These observations corresponded to the higher elasticity of bundles of fibers that we measured resulting in higher strain stiffening at the cell scale. Modulation of matrix properties at the local cell-scale has been highlighted recently (Doyle et al. 2015; Sapudom et al. 2019; W. Y. Wang et al. 2019). These studies pointed to the role of fiber elasticity in promotion of cell migration. In a similar manner, LOXL2-mediated cross-linking of collagen under conditions of high fibrillogenesis improved transmission of cell forces as a result of storage of elastic energy (W. Y. Wang et al. 2019). Furthermore, such collagen fiber elasticity could also participate in increased efficiency of lumen formation by limiting collagen stacking at the cell surface during the first hours of cell spreading in the 3D microenvironment.

Altogether, our data demonstrate that microvascularization in collagen hydrogels is associated to complex matrix remodeling consisting in stacking of fibrillar collagen followed by its degradation at the cell-surface in order to allow for generation of basement membrane. Furthermore, we showed that,

rather than bulk physical properties of matrices, it is the microarchitecture of collagen gels that limits micro-vascularization. Whether cell confinement plays an important role, elasticity of bundles of fibers at the cell-scale trumps the bulk stiffness by regulating both cell migration and microarchitecture remodeling for lumen formation. The LOXL2-based biomimetic cross-linking that we described here might thus provide a powerful tool for production of micro-vascularized collagen hydrogels that better support both remodeling by endothelial cells and handling for transplantation.

MATERIALS AND METHODS

- **Cell culture**

Normal human dermal fibroblasts were purchased from Promocell (Heidelberg, Germany) and cultured in the dedicated medium (FGM-2). Conditioned media were prepared using complete endothelial cells medium (ECGM-2, Promocell). Human umbilical vein endothelial cells (HUVEC) were isolated and cultured as previously described (Chomel et al. 2009). Experiments were performed up to passage 5.

- **Collagen hydrogels**

Collagen was acid-extracted from rat tails and stored at 4°C in 500 mM acetic acid for long term storage. Batches were dialysed with Spectra-Por with 20 mM acetic acid. Hydrogels were prepared by diluting collagen to 2 or 4.5 mg/ml in 20mM acetic acid. Concentrated (10X) M199 culture medium (Thermo Fisher Scientific, MA, USA) was added and pH was raised to the indicated values by addition of NaHCO₃ on ice. Gelation was performed at 20 or 37°C during 60 min. In some experiments, LOXL2 (325 U/ml) was added to the collagen solution right after neutralization of the pH at the initiation of gelation at 20°C. LOXL2 inhibition was performed by pre-incubation of LOXL2 with 500 µM β-APN (SIGMA-Aldrich) for 30 minutes at room temperature before addition to the neutralized collagen solution.

- **Capillary formation assay**

Capillary formation was performed by encapsulating 1 to 1.5 10⁶ HUVEC/ml in collagen right after pH neutralization at the initiation of fibrillogenesis. After 60 min of polymerization at the indicated temperature, fibroblast-conditioned medium containing 5 ng/ml VEGF (R&D Systems, Minneapolis, MN, USA) was added and the hydrogels were further incubated at 37°C in 5% CO₂. Culture medium was changed every 24h for up to 5 days. Marimastat was also replaced every day, together with the conditioned medium. Each hydrogel formulation was analyzed in triplicate wells in at least two independent experiments (n≥6).

- **Immunofluorescence, microscopy and image analysis**

For immunofluorescence experiments, hydrogels were fixed with 4% paraformaldehyde for 30 min. They were then washed 3 times with PBS and permeabilised for 30 min in PBS containing 1% triton-X-100 (Thermo Fisher Scientific). Immunostaining and fluorescent labeling of cytoskeleton and nuclei were performed in PBS-Triton-X-100 0.2%. β-catenin was detected with antibody #4627 coupled to AlexaFluor 647 from Cell Signalling Technologies (Danvers, MA, USA); VE-cadherin with antibody #53-1449 coupled to AlexaFluor 488 from Affymetrix (Santa Clara, CA, USA); CD31 with antibody #MO823 from Agilent Technologies (Santa Clara, CA, USA); collagen IV with antibody #MAB1910 from Thermo Fisher Scientific; cleaved collagen I with antibody #0217-050 from Immunoglobe (Himmelstadt, Germany). Secondary antibodies coupled to AlexaFluor dyes were purchased from Thermo Fisher Scientific.

For imaging of endothelial cell organization and collagen remodeling, images were acquired with a Leica SP5-MP confocal microscope equipped with a Leica HCX PL APO X25 objective lens, (water immersion, 0.95 NA) (Leica, Wetzlar, Germany). Multiphoton excitation was performed using a Maitai SP laser (Newport Corporation, Irvine, CA, USA). Second harmonic generation (SHG) signal was collected by external non-descanned detector at 440 nm, using laser excitation at 880 nm.

For analysis of pore size, z-stacks were acquired 100 µm beyond the surface of the hydrogels and over 100 µm depth with a 4 µm step. Three independently cast hydrogels were analyzed. Three fields of view were acquired per sample. Pore size was quantified using a macro developed in ImageJ function 'Local Thickness (Hildebrand and Rüeggsegger, 1997) and Matlab (Mathworks, Natick, MA, USA). Average of 25 planes per sample was calculated, and the cumulative pore area per field was plotted.

For quantification of capillary formation, hydrogels were stained with DAPI and phalloidin coupled to either AlexaFluor 488 or AlexaFluor 555 (Thermo Fisher Scientific). For the Marimastat experiments, images were acquired with a Zeiss Observer equipped with Apotome 2 (Zeiss, Heidelberg, Germany).

Capillary network were segmented with Imaris 8.2 (Bitplane, Belfast, UK) and quantified with a software developed in-house using Matlab as previously described (Atlas, Gorin et al. submitted) and based open-source plugging (Arganda-Carreras et al. 2010; Kerschnitzki et al. 2013).

For analysis of the impact of fibrillogenesis on capillary formation, images were acquired with a confocal spinning-disk microscope equipped with a 10X objective lens (0.3 NA) (Roper Technologies, Lakewood Ranch, FL, USA and Nikon Instruments, Amsterdam, Netherlands). Z-stacks were acquired 100 μm beyond the surface of the hydrogel over a depth of 300 μm using a step size of 5 μm . Four independent fields per well were imaged. Quantification of capillary formation was performed with Fiji using macros designed in our group. Briefly, 3D coordinates of nuclei centroids were extracted from DAPI staining and assigned in 3D masks of capillaries that were generated from the phalloidin staining. Number of nuclei per capillary was then calculated, considering structures containing 6 or more nuclei as capillaries, based on observation of lumenized structures.

- **Shear rheology**

Rheological experiments were performed on MCR302 with Rheocompass V1.12 (Anton Paar, Graz, Austria). Temperature was controlled with a peltier system equipped with an insert for disposable cups and deformation was applied with a cone of $\Theta = 2^\circ\text{C}$ with a diameter of 25mm. Collagen hydrogels were prepared as described above and cast on the rheometer. Polymerization was followed for 60 min with a deformation $\gamma = 0.1\%$ applied at a 1 Hz frequency at the indicated temperature. Each experimental condition was performed independently at least three times.

- **LOXL2 purification and activity measurement**

Recombinant human LOXL2 was purified from the secretion medium of CHO cells and activity was assessed as previously described using cadaverin (Sigma-Aldrich, Saint Louis, MO, USA) as a substrate (Palamakumbura et al, 2002; Schmelzer et al, 2019). The capacity of LOXL2 to oxidize lysines after fibrillogenesis was also measured. Gels were cast in 96 well plates. After 60 minutes of polymerization, gels were washed with 50 mM borate buffer pH 8 before addition of 325 U/ml LOXL2 and 2.75 $\mu\text{g}/\text{ml}$ Amplex UltraRed and 1 U/ml horse radish peroxidase (Thermo Fisher Scientific). Reactions were followed with a spectrometer ENVISION (Perkin Elmer, Waltham, MA, USA) during 60min at 37°C using $\lambda_{\text{ex}} = 535\text{nm}$ and $\lambda_{\text{em}} = 610\text{nm}$. The amount of H_2O_2 produced by LOXL2 activity was determined with a standard of peroxide (100 to 4000 mM) generated in the same conditions without LOXL2.

- **SPR binding assays**

SPR binding assays were carried out in a Biacore T100 system (GE Healthcare, Protein Science Facility, UMS 3444, Lyon, France) using human placenta collagen IV and human plasma fibronectin (C7521 and F2006, Sigma). They were covalently immobilized on a dextran-covered CM5 sensor chip using the amine coupling kit (GE Healthcare) according to the manufacturer's instructions at a flow rate of 5 $\mu\text{L}/\text{min}$ with 10 mM HEPES, 150 mM NaCl, P20 0.05% pH 7.4 as running buffer. The carboxyl groups of CM5 sensor chips were activated by injecting N-hydroxysuccinimide/1-ethyl-3-(3-dimethylaminopropyl)carbodiimide for 420 s. Collagen I was injected for 420 s at 100 $\mu\text{g}/\text{mL}$ over the activated sensor chip. The residual activated groups were blocked by injecting 1M ethanolamine pH 8.5 for 420 s. Two injections of running buffer of 60 s each were then performed.

Several concentrations of full-length LOXL2 (8, 16, 32, 64 and 128 nM) and SRCR12 domains (62.5, 125, 250, 500 nM and 1 μM) were injected at 30 $\mu\text{l}/\text{min}$ for 180s over immobilized collagen I and over a control flow cell submitted to the coupling steps without ligand to evaluate non-specific binding, which was subtracted from raw data. The association (k_a) and dissociation rate (k_d) constants and the equilibrium dissociation constant (KD) were calculated using the Biaevaluation software (version 2.0.3).

- **Quantification of cross-links**

Hydrogels were hydrolyzed in 6 N HCl at 110 °C for 24 h. Purification and enrichment of the cross-links were performed by solid-phase extraction, then measured by HPLC.

- **AFM nanoindentation experiments**

Global elastic modulus (E) of collagen hydrogels was determined by colloidal probe force spectroscopy using a scanning force microscope (NanoWizard 4, JPK Instruments, Berlin, Germany) mounted on an AxioObserver microscope (Zeiss) placed on a vibration isolation table. Briefly, a gold coated cantilever (0.01 N/m) with a 6.44 μm bead probe (NanoAndMore, Paris, France) was used. Exact spring constant was determined upon calibration in PBS by the thermal noise method (Hutter and Bechhoefer 1993) prior to each experiment. Each AFM measurement consists in the acquisition of 255 force-distance curves extracted as 16 x 16 matrices with indentation points spaced 6 μm apart. Measurements were conducted at 3 different positions in 2 independent gel preparations. Approach and retraction speeds were kept constant at 5 $\mu\text{m}/\text{s}$, ramping the cantilever by 7 μm with a 1.2 nN threshold in a closed z loop that keeps the maximal force applied to the hydrogel constant.

As colloidal probe indentation did not produce valid force-distance curves for stiffer collagen hydrogels generated at pH 8.5 (data not shown), we performed an analysis of fiber stiffness using a conical shape probe with typical tip radius of curvature < 30nm mounted on a gold coated cantilever (0.03-0.09 N/m). Quantitative imaging (QI) (JPK, Berlin, Germany) was conducted to acquire a complete force-distance curve at each pixel. Scanning speed was kept constant to 200 $\mu\text{m}/\text{s}$, ramping the cantilever by 10 μm with a 1 nN threshold, to prevent damage to the samples. At least 3 different fields of 30 x 4 μm (while collecting 100 x 27 pixels) were imaged on each hydrogel, in 2 independent gel preparations.

For AFM imaging experiments, collagen hydrogels were fixed with 2% PFA 2,5% glutaraldehyde in PBS and subsequently washed and conserved in PBS-azide at 4°C. AFM topography images were recorded using a NanoWizard 4, JPK under the same conditions as for fiber stiffness measurement. Typically, an AFM image of 20 x 10 μm corresponding to 200 x 100 pixels was acquired at an appropriate scan rate between 200 and 300 kHz and the setpoint was kept as low as possible to prevent damage to the sample. AFM image processing and analysis were performed using JPK and ImageJ. Second order flattening is applied to AFM topography images to remove tilt and bow. Median filter and Gaussian convolution were also applied.

- **Automated fitting of force-indentation curves and data processing**

As a measure of matrix elasticity, we used the Young's modulus of the 3D collagen matrices. AFM force-distance curves were both transformed to force-indentation curves and fitted using the JPK data processing software. Curves were fitted from the end downward using the contact-point independent linear Hertz-Sneddon model (Carl and Schillers 2008) depending on the indenter geometry, i.e. for bead-shaped measurements, we extracted E from [1]:

$$F^{2/3} = \frac{4}{3} \frac{E}{1-\nu^2} \sqrt{R} \delta \quad [1]$$

where F is the force, R is the bead radius, E is the Young's modulus, δ is the indentation depth, ν is the Poisson ratio, which was set to 0.5. The Hertz model assumes infinite sample thickness, which was approximated by using small indentation (typical indentation depth 1-4 μm) on at least 1 mm thick hydrogels, assuming that the underlying plastic dish did not interfere with the measurements. We also passed over the fact that the Poisson ratio (reflecting the behavior of the material under compression) was set to 0.5 (for soft incompressible biological samples) and may be asymmetric and nonlinear for collagen (Steinwachs et al. 2016). Automated curve fitting was applied using fitting range of 100% of curve for a batch of force-distance curves for each condition.

- **Fiber stiffness measurements**

We used automated curve fitting on QI images to generate height maps as well as stiffness maps. We collected individual regions of interest on height maps corresponding to collagen fibers and selected the corresponding ROI on the stiffness map. We then extracted the mean stiffness of fibers *a posteriori*. We quantified individual stiffness of about 6 groups of fibers in at least 3 different fields in 2 independent experiments. Exemplary force-distance curve and corresponding fits of the Hertz model are shown figure S2.

TABLE 1: Interactions of LOXL2 with collagen I:

ligand	analyte	K_{D1} (nM)	K_{D2} (nM)	Chi ²
Collagen I	LOXL2	681 ± 7.8	5.7 ± 5.8	< 2.09
Collagen I	SRCR12		20.5 ± 0.9	<9.81

BIBLIOGRAPHY

- Anazco, Carolina, Alberto J. Lopez-Jimenez, Mohamed Rafi, Lorenzo Vega-Montoto, Ming-Zhi Zhang, Billy G. Hudson, and Roberto M. Vanacore. 2016. "Lysyl Oxidase Like-2 Crosslinks Collagen IV of Glomerular Basement Membrane." *Journal of Biological Chemistry*, October, jbc.M116.738856. <https://doi.org/10.1074/jbc.M116.738856>.
- Arganda-Carreras, Ignacio, Rodrigo Fernández-González, Arrate Muñoz-Barrutia, and Carlos Ortiz-De-Solorzano. 2010. "3D Reconstruction of Histological Sections: Application to Mammary Gland Tissue." *Microscopy Research and Technique* 73 (11): 1019–29. <https://doi.org/10.1002/jemt.20829>.
- Auger, François A., Laure Gibot, and Dan Lacroix. 2013. "The Pivotal Role of Vascularization in Tissue Engineering." *Annual Review of Biomedical Engineering* 15 (1): 177–200. <https://doi.org/10.1146/annurev-bioeng-071812-152428>.
- Barry-Hamilton, Vivian, Rhyannon Spangler, Derek Marshall, Scott McCauley, Hector M Rodriguez, Miho Oyasu, Amanda Mikels, et al. 2010. "Allosteric Inhibition of Lysyl Oxidase-like-2 Impedes the Development of a Pathologic Microenvironment." *Nature Medicine* 16 (9): 1009–17. <https://doi.org/10.1038/nm.2208>.
- Bignon, M., C. Pichol-Thievend, J. Hardouin, M. Malbouyres, N. Brechot, L. Nasciutti, A. Barret, et al. 2011. "Lysyl Oxidase-like Protein-2 Regulates Sprouting Angiogenesis and Type IV Collagen Assembly in the Endothelial Basement Membrane." *Blood* 118 (14): 3979–89. <https://doi.org/10.1182/blood-2010-313296>.
- Cao, Jiahui, Manuel Ehling, Sigrid März, Jochen Seebach, Katsiaryna Tarbashevich, Tomas Sixta, Mara E. Pitulescu, et al. 2017. "Polarized Actin and VE-Cadherin Dynamics Regulate Junctional Remodelling and Cell Migration during Sprouting Angiogenesis." *Nature Communications* 8 (1). <https://doi.org/10.1038/s41467-017-02373-8>.
- Carey, Shawn P., Casey M. Kraning-Rush, Rebecca M. Williams, and Cynthia A. Reinhart-King. 2012. "Biophysical Control of Invasive Tumor Cell Behavior by Extracellular Matrix Microarchitecture." *Biomaterials* 33 (16): 4157–65. <https://doi.org/10.1016/j.biomaterials.2012.02.029>.
- Carl, Philippe, and Hermann Schillers. 2008. "Elasticity Measurement of Living Cells with an Atomic Force Microscope: Data Acquisition and Processing." *Pflügers Archiv - European Journal of Physiology* 457 (2): 551–59. <https://doi.org/10.1007/s00424-008-0524-3>.
- Chomel, Clémence, Aurélie Cazes, Clément Faye, Marine Bignon, Elisa Gomez, Corinne Ardidie-Robouant, Alain Barret, et al. 2009. "Interaction of the Coiled-Coil Domain with Glycosaminoglycans Protects Angiopoietin-like 4 from Proteolysis and Regulates Its Antiangiogenic Activity." *The FASEB Journal* 23 (3): 940–49. <https://doi.org/10.1096/fj.08-115170>.
- Crosby, Cody O., Deepti Valliappan, David Shu, Sachin Kumar, Chengyi Tu, Wei Deng, Sapun H. Parekh, and Janet Zoldan. 2019. "Quantifying the Vasculogenic Potential of Induced Pluripotent Stem Cell-Derived Endothelial Progenitors in Collagen Hydrogels." *Tissue Engineering Part A* 25 (9–10): 746–58. <https://doi.org/10.1089/ten.tea.2018.0274>.
- Del Gaudio, Costantino, Silvia Baiguera, Margherita Boieri, Benedetta Mazzanti, Domenico Ribatti, Alessandra Bianco, and Paolo Macchiarini. 2013. "Induction of Angiogenesis Using VEGF Releasing Genipin-Crosslinked Electrospun Gelatin Mats." *Biomaterials* 34 (31): 7754–65. <https://doi.org/10.1016/j.biomaterials.2013.06.040>.
- Doyle, Andrew D., Nicole Carvajal, Albert Jin, Kazue Matsumoto, and Kenneth M. Yamada. 2015. "Local 3D Matrix Microenvironment Regulates Cell Migration through Spatiotemporal Dynamics of Contractility-Dependent Adhesions." *Nature Communications* 6 (1). <https://doi.org/10.1038/ncomms9720>.
- Engler, Adam J., Shamik Sen, H. Lee Sweeney, and Dennis E. Discher. 2006. "Matrix Elasticity Directs Stem Cell Lineage Specification." *Cell* 126 (4): 677–89. <https://doi.org/10.1016/j.cell.2006.06.044>.
- Francis-Sedlak, Megan E., Monica L. Moya, Jung-Ju Huang, Stephanie A. Lucas, Nivedita Chandrasekharan, Jeffery C. Larson, Ming-Huei Cheng, and Eric M. Brey. 2010. "Collagen Glycation Alters Neovascularization in Vitro and in Vivo." *Microvascular Research* 80 (1): 3–9. <https://doi.org/10.1016/j.mvr.2009.12.005>.
- Francis-Sedlak, Megan E., Shiri Uriel, Jeffery C. Larson, Howard P. Greisler, David C. Venerus, and Eric M. Brey. 2009. "Characterization of Type I Collagen Gels Modified by Glycation." *Biomaterials* 30 (9): 1851–56. <https://doi.org/10.1016/j.biomaterials.2008.12.014>.
- Gibot, Laure, Todd Galbraith, Bryan Kloos, Suvendu Das, Dan A. Lacroix, François A. Auger, and Mihaela Skobe. 2016. "Cell-Based Approach for 3D Reconstruction of Lymphatic Capillaries in Vitro Reveals Distinct Functions of HGF and VEGF-C in Lymphangiogenesis." *Biomaterials* 78 (February): 129–39. <https://doi.org/10.1016/j.biomaterials.2015.11.027>.
- Gorin, Caroline, Gael Y. Rochefort, Rumezha Bascetin, Hanru Ying, Julie Lesieur, Jérémy Sadoine, Nathan Beckouche, et al. 2016. "Priming Dental Pulp Stem Cells With Fibroblast Growth Factor-2 Increases Angiogenesis of Implanted Tissue-Engineered Constructs Through Hepatocyte Growth Factor and Vascular Endothelial Growth Factor Secretion: FGF-2 Priming Enhances Angiogenesis by DPSCs." *STEM CELLS Translational Medicine* 5 (3): 392–404. <https://doi.org/10.5966/sctm.2015-0166>.
- Grosso, Andrea, Maximilian G. Burger, Alexander Lunger, Dirk J. Schaefer, Andrea Banfi, and Nunzia Di Maggio. 2017. "It Takes Two to Tango: Coupling of Angiogenesis and Osteogenesis for Bone Regeneration." *Frontiers in Bioengineering and Biotechnology* 5. <https://doi.org/10.3389/fbioe.2017.00068>.
- Harris, J. Robin, and Andreas Reiber. 2007. "Influence of Saline and PH on Collagen Type I Fibrillogenesis in Vitro: Fibril Polymorphism and Colloidal Gold Labelling." *Micron* 38 (5): 513–21. <https://doi.org/10.1016/j.micron.2006.07.026>.
- Harris, J. Robin, Andrei Soliakov, and Richard J. Lewis. 2013. "In Vitro Fibrillogenesis of Collagen Type I in Varying Ionic and PH Conditions." *Micron* 49 (June): 60–68. <https://doi.org/10.1016/j.micron.2013.03.004>.
- Hinsbergh, Victor W. M. van, and Pieter Koolwijk. 2008. "Endothelial Sprouting and Angiogenesis: Matrix Metalloproteinases in the Lead." *Cardiovascular Research* 78 (2): 203–12. <https://doi.org/10.1093/cvr/cvm102>.
- Holder, A. J., N. Badiie, K. Hawkins, C. Wright, P. R. Williams, and D. J. Curtis. 2018. "Control of Collagen Gel Mechanical Properties through Manipulation of Gelation Conditions near the Sol-Gel Transition." *Soft Matter* 14 (4): 574–80. <https://doi.org/10.1039/C7SM01933E>.
- Hutter, Jeffrey L., and John Bechhoefer. 1993. "Calibration of Atomic-force Microscope Tips." *Review of Scientific Instruments* 64 (7): 1868–73. <https://doi.org/10.1063/1.1143970>.
- Jorge-Peñas, Alvaro, Hannelore Bové, Kathleen Sanen, Marie-Mo Vaeyens, Christian Steuwe, Maarten Roeffaers, Marcel Ameloot, and Hans Van Oosterwyck. 2017. "3D Full-Field Quantification of Cell-Induced Large Deformations in Fibrillar Biomaterials by Combining Non-Rigid Image Registration with Label-Free Second Harmonic Generation." *Biomaterials* 136 (August): 86–97. <https://doi.org/10.1016/j.biomaterials.2017.05.015>.
- Kerschnitzki, Michael, Philip Kollmannsberger, Manfred Burghammer, Georg N. Duda, Richard Weinkamer, Wolfgang Wagermaier, and Peter Fratzl. 2013. "Architecture of the Osteocyte Network Correlates with Bone Material Quality." *Journal of Bone and Mineral Research* 28 (8): 1837–45. <https://doi.org/10.1002/jbmr.1927>.

- Kolesky, David B., Kimberly A. Homan, Mark A. Skylar-Scott, and Jennifer A. Lewis. 2016. "Three-Dimensional Bioprinting of Thick Vascularized Tissues." *Proceedings of the National Academy of Sciences* 113 (12): 3179–84. <https://doi.org/10.1073/pnas.1521342113>.
- Lee, Po-Feng, Alvin T. Yeh, and Kayla J. Bayless. 2009. "Nonlinear Optical Microscopy Reveals Invading Endothelial Cells Anisotropically Alter Three-Dimensional Collagen Matrices." *Experimental Cell Research* 315 (3): 396–410. <https://doi.org/10.1016/j.yexcr.2008.10.040>.
- Lesman, Ayelet, Dekel Rosenfeld, Shira Landau, and Shulamit Levenberg. 2016. "Mechanical Regulation of Vascular Network Formation in Engineered Matrices." *Advanced Drug Delivery Reviews* 96 (January): 176–82. <https://doi.org/10.1016/j.addr.2015.07.005>.
- Li, Xuguang, Yuankun Dai, Tao Shen, and Changyou Gao. 2017. "Induced Migration of Endothelial Cells into 3D Scaffolds by Chemoattractants Secreted by Pro-Inflammatory Macrophages in Situ." *Regenerative Biomaterials* 4 (3): 139–48. <https://doi.org/10.1093/rb/rbx005>.
- Li, Yuping, Amran Asadi, Margo R. Monroe, and Elliot P. Douglas. 2009. "PH Effects on Collagen Fibrillogenesis in Vitro: Electrostatic Interactions and Phosphate Binding." *Materials Science and Engineering: C* 29 (5): 1643–49. <https://doi.org/10.1016/j.msec.2009.01.001>.
- Liang, Huang-Chien, Wen-Hisung Chang, Hsiang-Fa Liang, Meng-Horng Lee, and Hsing-Wen Sung. 2004. "Crosslinking Structures of Gelatin Hydrogels Crosslinked with Genipin or a Water-Soluble Carbodiimide." *Journal of Applied Polymer Science* 91 (6): 4017–26. <https://doi.org/10.1002/app.13563>.
- López-Jiménez, Alberto J., Trayambak Basak, and Roberto M. Vanacore. 2017. "Proteolytic Processing of Lysyl Oxidase-like-2 in the Extracellular Matrix Is Required for Crosslinking of Basement Membrane Collagen IV." *Journal of Biological Chemistry* 292 (41): 16970–82. <https://doi.org/10.1074/jbc.M117.798603>.
- Madhavan, Krishna, Dmitry Belchenko, Antonella Motta, and Wei Tan. 2010. "Evaluation of Composition and Crosslinking Effects on Collagen-Based Composite Constructs." *Acta Biomaterialia* 6 (4): 1413–22. <https://doi.org/10.1016/j.actbio.2009.09.028>.
- Makris, Eleftherios A., Donald J. Responde, Nikolaos K. Paschos, Jerry C. Hu, and Kyriacos A. Athanasiou. 2014. "Developing Functional Musculoskeletal Tissues through Hypoxia and Lysyl Oxidase-Induced Collagen Cross-Linking." *Proceedings of the National Academy of Sciences* 111 (45): E4832–41. <https://doi.org/10.1073/pnas.1414271111>.
- Mammoto, Akiko, Kip M. Connor, Tadanori Mammoto, Chong Wing Yung, Dongeun Huh, Christopher M. Aderman, Gustavo Mostoslavsky, Lois E. H. Smith, and Donald E. Ingber. 2009. "A Mechanosensitive Transcriptional Mechanism That Controls Angiogenesis." *Nature* 457 (7233): 1103–8. <https://doi.org/10.1038/nature07765>.
- Mason, Brooke N., Alina Starchenko, Rebecca M. Williams, Lawrence J. Bonassar, and Cynthia A. Reinhart-King. 2013. "Tuning Three-Dimensional Collagen Matrix Stiffness Independently of Collagen Concentration Modulates Endothelial Cell Behavior." *Acta Biomaterialia* 9 (1): 4635–44. <https://doi.org/10.1016/j.actbio.2012.08.007>.
- McLeod, Claire, John Higgins, Yekaterina Miroshnikova, Rachel Liu, Alisha Garrett, and Alisha L. Sarang-Sieminski. 2013. "Microscopic Matrix Remodeling Precedes Endothelial Morphological Changes During Capillary Morphogenesis." *Journal of Biomechanical Engineering* 135 (7). <https://doi.org/10.1115/1.4023984>.
- Meer, Andries D. van der, Valeria V. Orlova, Peter ten Dijke, Albert van den Berg, and Christine L. Mummery. 2013. "Three-Dimensional Co-Cultures of Human Endothelial Cells and Embryonic Stem Cell-Derived Pericytes inside a Microfluidic Device." *Lab on a Chip* 13 (18): 3562. <https://doi.org/10.1039/c3lc50435b>.
- Mitra, Debika, Osamu W. Yasui, Jenna N. Harvestine, Jarrett M. Link, Jerry C. Hu, Kyriacos A. Athanasiou, and J. Kent Leach. 2019. "Exogenous Lysyl Oxidase-Like 2 and Perfusion Culture Induce Collagen Crosslink Formation in Osteogenic Grafts." *Biotechnology Journal* 14 (3): 1700763. <https://doi.org/10.1002/biot.201700763>.
- Montesano, R., S. Kumar, L. Orci, and M. S. Pepper. 1996. "Synergistic Effect of Hyaluronan Oligosaccharides and Vascular Endothelial Growth Factor on Angiogenesis in Vitro." *Laboratory Investigation; a Journal of Technical Methods and Pathology* 75 (2): 249–62.
- Moon, Hee-Jung, Joel Finney, Trey Ronnebaum, and Minae Mure. 2014. "Human Lysyl Oxidase-like 2." *Bioorganic Chemistry* 57 (December): 231–41. <https://doi.org/10.1016/j.bioorg.2014.07.003>.
- Nakatsu, Martin N., Richard C. A. Sainson, Jason N. Aoto, Kevin L. Taylor, Mark Aitkenhead, Sofia Pérez-del-Pulgar, Philip M. Carpenter, and Christopher C. W. Hughes. 2003. "Angiogenic Sprouting and Capillary Lumen Formation Modeled by Human Umbilical Vein Endothelial Cells (HUVEC) in Fibrin Gels: The Role of Fibroblasts and Angiopoietin-1." *Microvascular Research* 66 (2): 102–12. [https://doi.org/10.1016/S0026-2862\(03\)00045-1](https://doi.org/10.1016/S0026-2862(03)00045-1).
- Novosel, Esther C., Claudia Kleinhans, and Petra J. Kluger. 2011. "Vascularization Is the Key Challenge in Tissue Engineering." *Advanced Drug Delivery Reviews* 63 (4–5): 300–311. <https://doi.org/10.1016/j.addr.2011.03.004>.
- Okada, Kazushi, Hee-Jung Moon, Joel Finney, Alex Meier, and Minae Mure. 2018. "Extracellular Processing of Lysyl Oxidase-like 2 and Its Effect on Amine Oxidase Activity." *Biochemistry* 57 (51): 6973–83. <https://doi.org/10.1021/acs.biochem.8b01008>.
- Pena, Ana-Maria, Dominique Fagot, Christian Olive, Jean-François Michelet, Jean-Baptiste Galey, Frederic Leroy, Emmanuel Beaupaire, Jean-Louis Martin, Anne Colonna, and Marie-Claire Schanne-Klein. 2010. "Multiphoton Microscopy of Engineered Dermal Substitutes: Assessment of 3-D Collagen Matrix Remodeling Induced by Fibroblast Contraction." *Journal of Biomedical Optics* 15 (February): 056018. <https://doi.org/10.1117/1.3503411>.
- Pöschl, Ernst, Ursula Schlötzer-Schrehardt, Bent Brachvogel, Kenji Saito, Yoshifumi Ninomiya, and Ulrike Mayer. 2004. "Collagen IV Is Essential for Basement Membrane Stability but Dispensable for Initiation of Its Assembly during Early Development." *Development* 131 (7): 1619–28. <https://doi.org/10.1242/dev.01037>.
- Raab, Matthew, Matteo Gentili, Henry de Belly, Hawa-Racine Thiam, Pablo Vargas, Ana Joaquina Jimenez, Franziska Lautenschlaeger, et al. 2016. "ESCR1 III Repairs Nuclear Envelope Ruptures during Cell Migration to Limit DNA Damage and Cell Death." *Science* 352 (6283): 359–62. <https://doi.org/10.1126/science.1247611>.
- Rademakers, Timo, Judith Horvath, Clemens Blitterswijk, and Vanessa LaPointe. 2019. "Oxygen and Nutrient Delivery in Tissue Engineering: Approaches to Graft Vascularization." *Journal of Tissue Engineering and Regenerative Medicine* 13 (July). <https://doi.org/10.1002/term.2932>.
- Raghavan, Srivatsan, Celeste M. Nelson, Jan D. Baranski, Emerson Lim, and Christopher S. Chen. 2010. "Geometrically Controlled Endothelial Tubulogenesis in Micropatterned Gels." *Tissue Engineering Part A* 16 (7): 2255–63. <https://doi.org/10.1089/ten.tea.2009.0584>.
- Ramírez-Rodríguez, Gloria Belén, Michele Iafisco, Anna Tampieri, Jaime Gómez-Morales, and José Manuel Delgado-López. 2014. "PH-Responsive Collagen Fibrillogenesis in Confined Droplets Induced by Vapour Diffusion." *Journal of Materials Science: Materials in Medicine* 25 (10): 2305–12. <https://doi.org/10.1007/s10856-014-5189-1>.
- Santos, Livia, Gregor Fuhrmann, Maya Juenet, Nadav Amdursky, Christine-Maria Horejs, Paola Campagnolo, and Molly M. Stevens. 2015. "Extracellular Stiffness Modulates the Expression of Functional Proteins and Growth Factors in Endothelial Cells." *Advanced Healthcare Materials* 4 (14): 2056–63. <https://doi.org/10.1002/adhm.201500338>.
- Sapudom, Jiranuwat, Liv Kalbitzer, Xiancheng Wu, Steve Martin, Klaus Kroy, and Tilo Pompe. 2019. "Fibril Bending Stiffness of 3D Collagen Matrices Instructs Spreading and Clustering of Invasive and Non-Invasive Breast Cancer Cells." *Biomaterials* 193 (February): 47–57.

- <https://doi.org/10.1016/j.biomaterials.2018.12.010>.
- Schilter, Heidi, Alison D. Findlay, Lara Perryman, Tin T. Yow, Joshua Moses, Amna Zahoor, Craig I. Turner, et al. 2019. "The Lysyl Oxidase like 2/3 Enzymatic Inhibitor, PXS-5153A, Reduces Crosslinks and Ameliorates Fibrosis." *Journal of Cellular and Molecular Medicine* 23 (3): 1759–70. <https://doi.org/10.1111/jcmm.14074>.
- Schmelzer, Christian E. H., Andrea Heinz, Helen Troilo, Michael P. Lockhart-Cairns, Thomas A. Jowitt, Marion F. Marchand, Laurent Bidault, et al. 2019. "Lysyl Oxidase-like 2 (LOXL2)-Mediated Cross-Linking of Tropoelastin." *The FASEB Journal* 33 (4): 5468–81. <https://doi.org/10.1096/fj.201801860RR>.
- Sieminski, A. L. R. P. Hebbel, and K. J. Gooch. 2004. "The Relative Magnitudes of Endothelial Force Generation and Matrix Stiffness Modulate Capillary Morphogenesis in Vitro." *Experimental Cell Research* 297 (2): 574–84. <https://doi.org/10.1016/j.yexcr.2004.03.035>.
- Song, H.-H. Greco, Rowza T. Rumma, C. Keith Ozaki, Elazer R. Edelman, and Christopher S. Chen. 2018. "Vascular Tissue Engineering: Progress, Challenges, and Clinical Promise." *Cell Stem Cell* 22 (3): 340–54. <https://doi.org/10.1016/j.stem.2018.02.009>.
- Sorushanova, Anna, Luis M. Delgado, Zhuning Wu, Naledi Shologu, Aniket Kshirsagar, Rufus Raghunath, Anne M. Mullen, et al. 2019. "The Collagen Suprafamily: From Biosynthesis to Advanced Biomaterial Development." *Advanced Materials* 31 (1): 1801651. <https://doi.org/10.1002/adma.201801651>.
- Steinwachs, Julian, Claus Metzner, Kai Skodzek, Nadine Lang, Ingo Thievensen, Christoph Mark, Stefan Münster, Katerina E Aifantis, and Ben Fabry. 2016. "Three-Dimensional Force Microscopy of Cells in Biopolymer Networks." *Nature Methods* 13 (2): 171–76. <https://doi.org/10.1038/nmeth.3685>.
- Stevenson, M.D., H. Pirstine, N.J. Hogrebe, T.M. Nocera, M.W. Boehm, R.K. Reen, K.W. Koelling, G. Agarwal, A.L. Sarang-Sieminski, and K.J. Gooch. 2013. "A Self-Assembling Peptide Matrix Used to Control Stiffness and Binding Site Density Supports the Formation of Microvascular Networks in Three Dimensions." *Acta Biomaterialia* 9 (8): 7651–61. <https://doi.org/10.1016/j.actbio.2013.04.002>.
- Thiam, Hawa-Racine, Pablo Vargas, Nicolas Carpi, Carolina Lage Crespo, Matthew Raab, Emmanuel Terriac, Megan C. King, et al. 2016. "Perinuclear Arp2/3-Driven Actin Polymerization Enables Nuclear Deformation to Facilitate Cell Migration through Complex Environments." *Nature Communications* 7 (1): 1–14. <https://doi.org/10.1038/ncomms10997>.
- Ulrich, Theresa A., Elena M. de Juan Pardo, and Sanjay Kumar. 2009. "The Mechanical Rigidity of the Extracellular Matrix Regulates the Structure, Motility, and Proliferation of Glioma Cells." *Cancer Research* 69 (10): 4167–74. <https://doi.org/10.1158/0008-5472.CAN-08-4859>.
- Umana-Diaz, Claudia, Cathy Pichol-Thievend, Marion Marchand, Yoann Atlas, Romain Salza, Marilyne Malbouyres, Jérémie Teillon, et al. in revision. "Scavenger Receptor Cysteine-Rich Domains of Lysyl Oxidase-Like2 Regulate Endothelial ECM and Angiogenesis through Non-Catalytic Scaffolding Mechanisms."
- Wang, William Y., Christopher D. Davidson, Daphne Lin, and Brendon M. Baker. 2019. "Actomyosin Contractility-Dependent Matrix Stretch and Recoil Induces Rapid Cell Migration." *Nature Communications* 10 (1). <https://doi.org/10.1038/s41467-019-09121-0>.
- Wei, Ying, Thomas J. Kim, David H. Peng, Dana Duan, Don L. Gibbons, Mitsuo Yamauchi, Julia R. Jackson, et al. 2017. "Fibroblast-Specific Inhibition of TGF- β 1 Signaling Attenuates Lung and Tumor Fibrosis." *The Journal of Clinical Investigation* 127 (10): 3675–88. <https://doi.org/10.1172/JCI94624>.
- Wolf, Katarina, Mariska te Lindert, Marina Krause, Stephanie Alexander, Joost te Riet, Amanda L. Willis, Robert M. Hoffman, Carl G. Figdor, Stephen J. Weiss, and Peter Friedl. 2013. "Physical Limits of Cell Migration: Control by ECM Space and Nuclear Deformation and Tuning by Proteolysis and Traction Force." *The Journal of Cell Biology* 201 (7): 1069–84. <https://doi.org/10.1083/jcb.201210152>.
- Xie, Jing, Min Bao, Stéphanie M. C. Bruekers, and Wilhelm T. S. Huck. 2017. "Collagen Gels with Different Fibrillar Microarchitectures Elicit Different Cellular Responses." *ACS Applied Materials & Interfaces* 9 (23): 19630–37. <https://doi.org/10.1021/acsami.7b03883>.
- Yang, Jin, Konstantinos Savvatis, Jong Seok Kang, Peidong Fan, Hongyan Zhong, Karen Schwartz, Vivian Barry, et al. 2016. "Targeting LOXL2 for Cardiac Interstitial Fibrosis and Heart Failure Treatment." *Nature Communications* 7 (1). <https://doi.org/10.1038/ncomms13710>.
- Zhou, Xiaoming, R. Grant Rowe, Nobuaki Hiraoka, Jerry P. George, Denis Wirtz, Deane F. Mosher, Ismo Virtanen, Michael A. Chernousov, and Stephen J. Weiss. 2008. "Fibronectin Fibrillogenesis Regulates Three-Dimensional Neovessel Formation." *Genes & Development* 22 (9): 1231–43. <https://doi.org/10.1101/gad.1643308>.

FIGURE 1

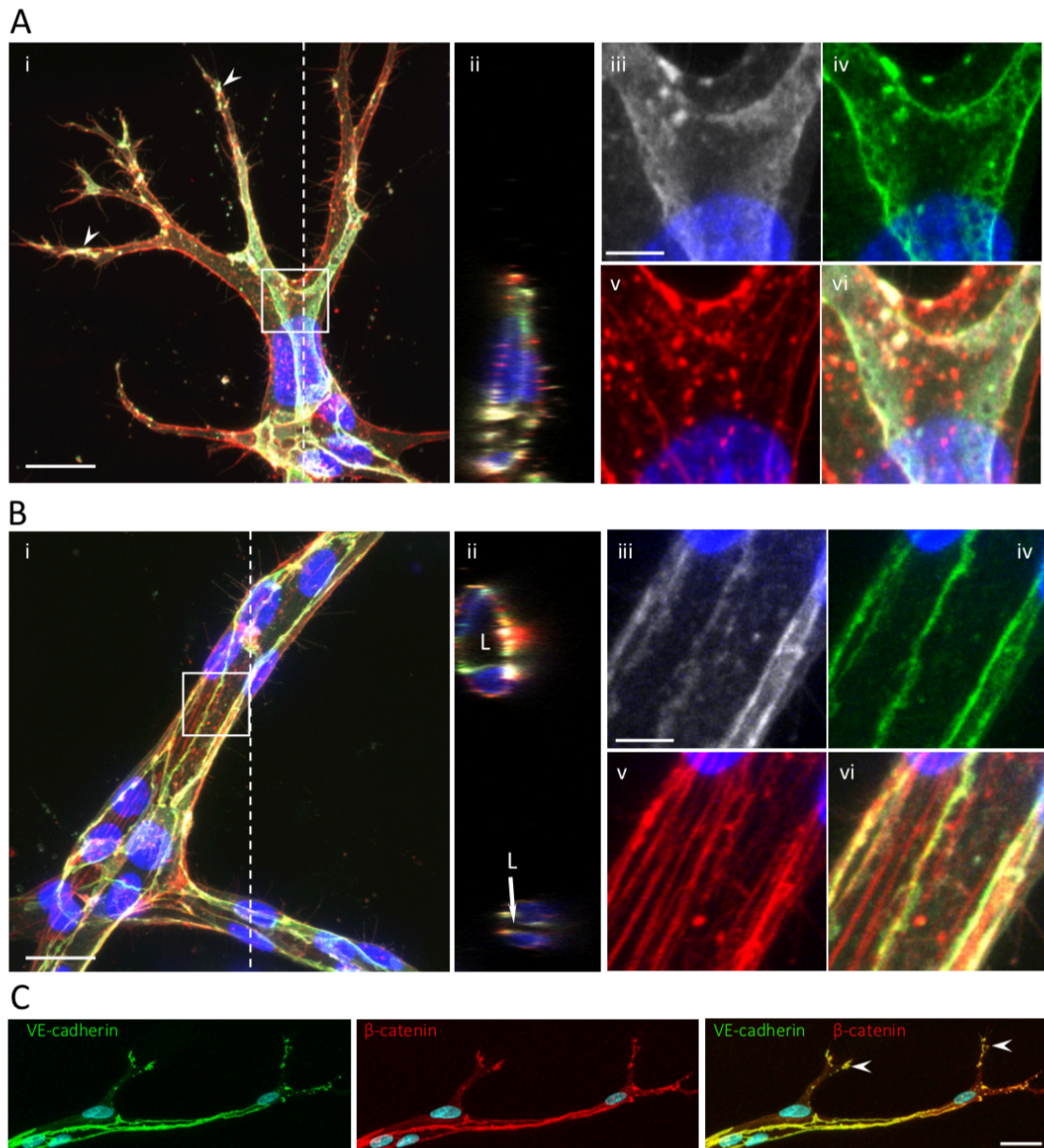


Figure 1: Capillary formation in collagen hydrogels. Endothelial cells seeded in collagen hydrogel were cultured for 24 (**A**) or 72 (**B** and **C**) hours before fixation. **A** and **B**: Gels were immuno-stained for CD31 (white) and VE-Cadherin (green). F-actin was labeled with phalloidin (red) and nuclei with DAPI (blue). Channels were merged (i, ii vi) or overlaid with DAPI staining (iii-v). Z-stacks of images were projected (i) and orthogonally sectioned (ii) along the white dotted line. White boxed area corresponds to the zoomed images (iii to vi). L and arrows indicate lumen. Scale bars: 20 (i-ii) and 5 (iii-vi) μm . **C**: Gels were immuno-stained for VE-cadherin (green) and β -catenin (red). Nuclei were stained with DAPI. Scale bars: 30 μm . Arrowheads indicate aggregates of VE-Cadherin in tip cell protrusions.

FIGURE 2

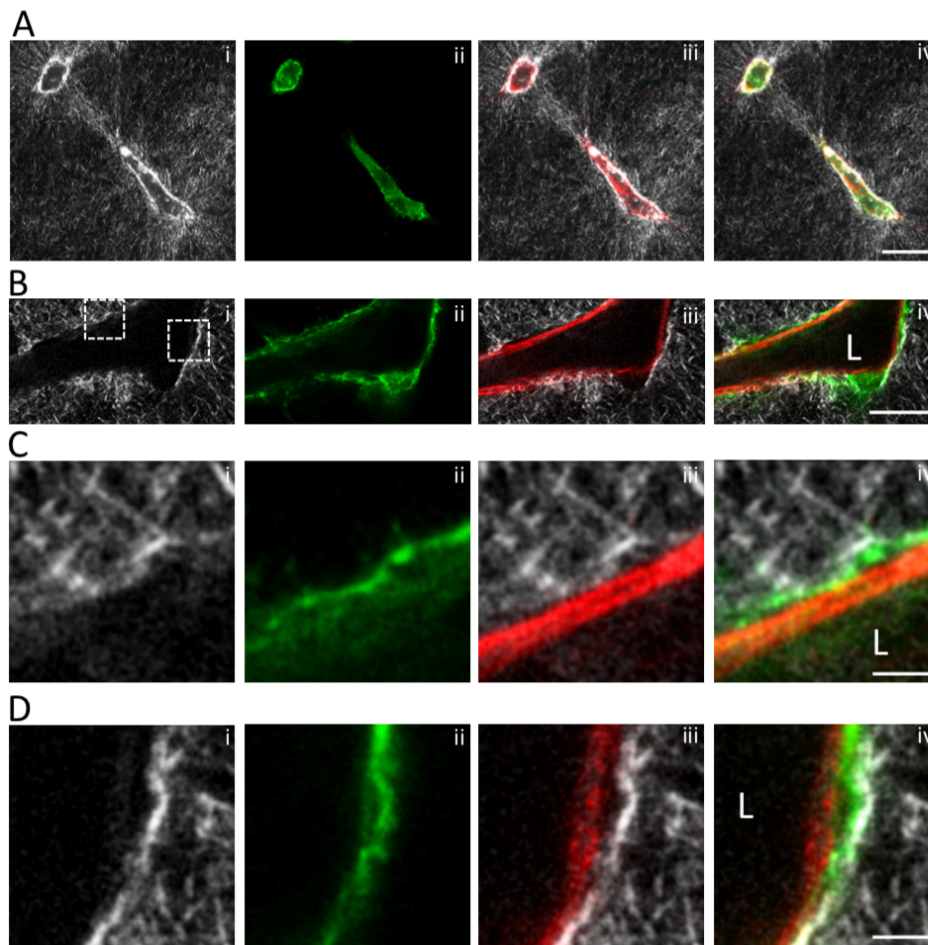


Figure 2: Matrix remodeling associated to capillary formation. Endothelial cells seeded in collagen hydrogel were cultured for 24 (**A**) or 72 (**B-D**) hours before fixation. Gels were immuno-stained for collagen IV (green) for basement membrane detection (**ii**). F-actin was labeled with phalloidin (red). Second harmonic generation in 2P-microscopy was detected (white) (**i**) and merged with phalloidin (**iii**) or phalloidin and collagen IV (**iv**). White boxes indicate the zoomed areas presented in **C** and **D**. L indicates lumen. A single confocal plane is shown. Scale bars: 25 (**A** and **B**) and 5 (**C** and **D**) μm .

FIGURE 3

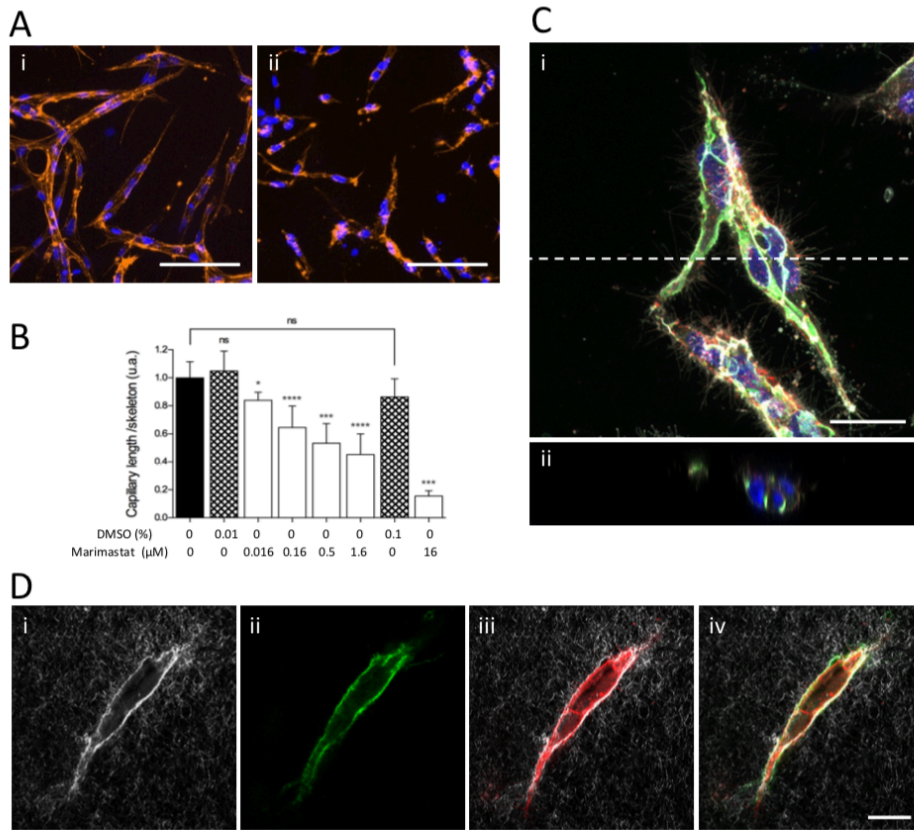


Figure 3: MMP inhibition prevents matrix remodeling and capillary formation. Endothelial cells seeded in collagen hydrogel were cultured for 96 hours under control conditions (**Ai**) or in the presence of 1.6 μ M Marimastat (**Aii**, **C** and **D**). **A-B:** Gels were fixed and F-actin was labeled with phalloidin (orange) for quantification of capillary formation. **C:** CD31 (white) and VE-cadherin (green) were immuno-stained. F-actin was labeled with phalloidin (red) and nuclei were stained with DAPI (blue). Channels were all merged. Z-stacks of images were projected (**i**) and orthogonally sectioned (**ii**) along the white dotted line. **D:** Collagen IV (green) was immunostained for basement membrane detection (**ii**). F-actin was labeled with phalloidin (red). Second harmonic generation in 2P-microscopy was detected (white) (**i**) and merged with phalloidin (**iii**) or phalloidin and collagen IV (**iv**). Scale bar: 100 (**A**) and 20 (**C** and **D**) μ m.

FIGURE 4

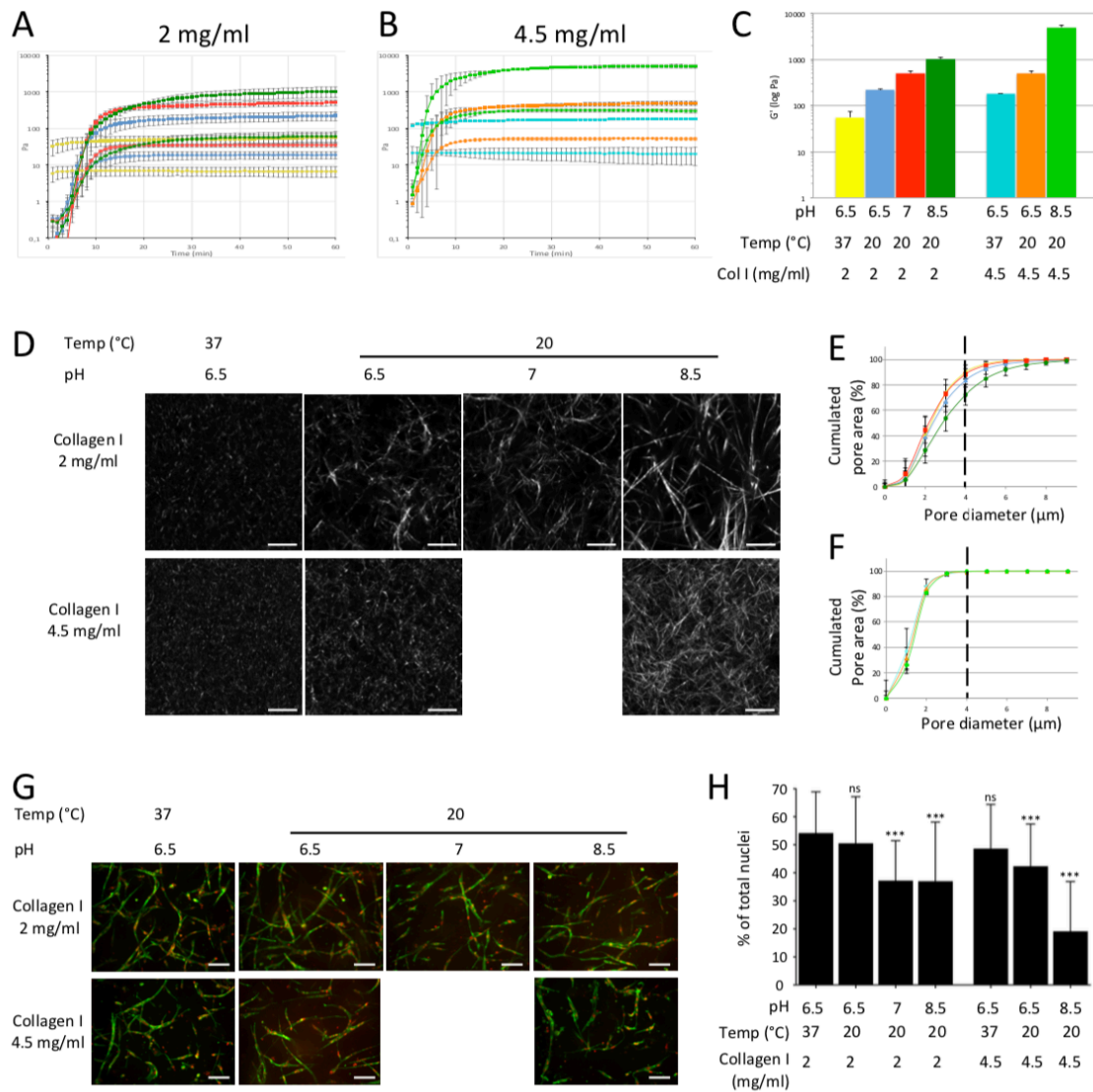


Figure 4: Tuning collagen fibrillogenesis impacts capillary formation. **A-C:** Mechanical properties of collagen hydrogels were measured using shear rheology. Gels were prepared at the indicated pH, temperature and concentration (**C**) and color-coded for plotting (**A** and **B**). Storage G' (square) and loss G'' (diamond) moduli were measured at 2 (**A**) and 4.5 (**B**) mg/ml of collagen I over the first hour of polymerization. G' values at equilibrium were plotted (**C**). **D-F:** Structural properties of hydrogels were assessed using SHG in 2P-microscopy. Gels were prepared under the same conditions as above and incubated at the indicated temperature for 60 minutes before overnight incubation at 37° C in ECBM2. And assessment of fibrillogenesis (**D**). Scale bar: 10 μ m. Pore size was measured and cumulative area of the pores at 2 (**E**) and 4.5 (**F**) mg/ml is represented. **G** and **H:** Capillary formation was measured as described in the methods section. Endothelial cells seeded in collagen gels were cultured for 96 hours. F-actin was stained with phalloidin (green) and nuclei with DAPI (red). Scale bar: 200 μ m.

FIGURE 5

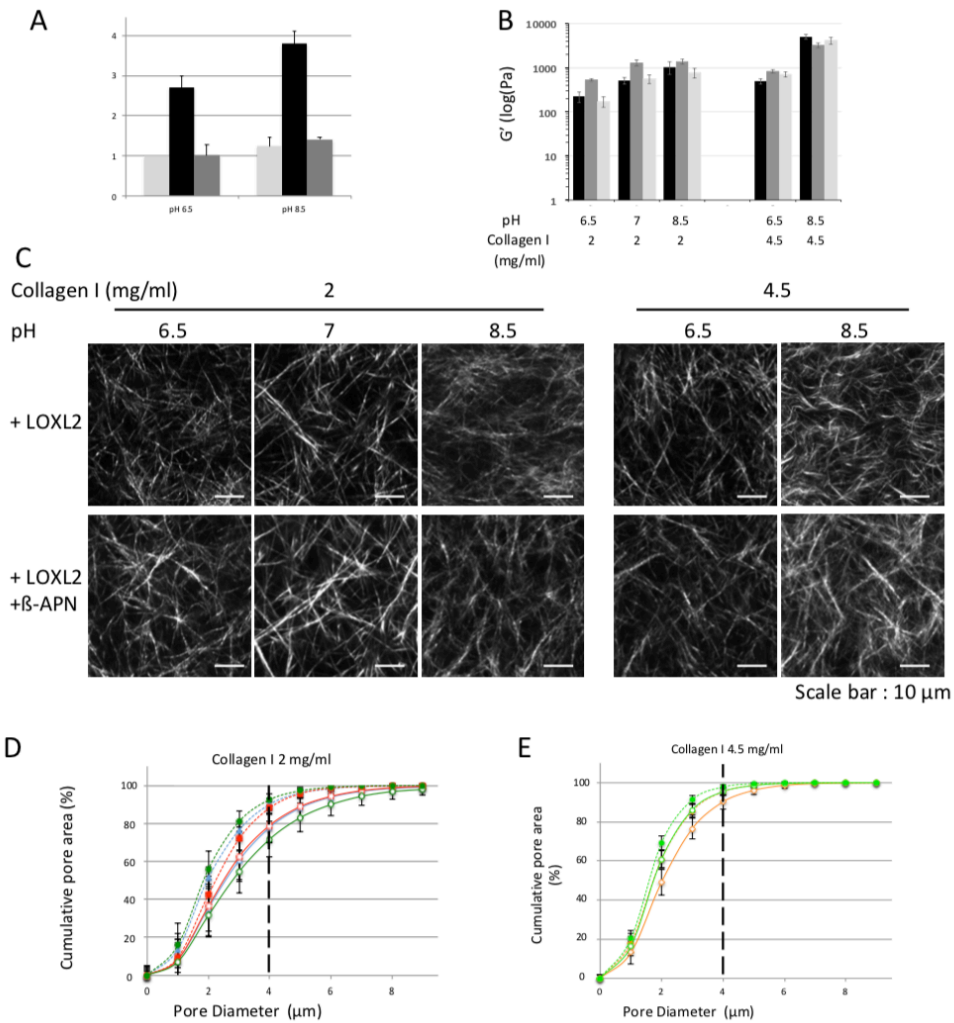


Figure 5: Collagen hydrogels were prepared at the indicated pH, temperature and concentration either in control conditions or in the presence of LOXL2 or of LOXL2 pre-treated with 500 μ M β -APN. **A:** Collagen hydrogels prepared at pH 6.5 and 8.5 were hydrolyzed in 6 N HCl at 110 $^{\circ}$ C for 24 h. Amount of HLNL cross-links were identified by HPLC. **B:** Mechanical properties were measured using shear rheology. Storage G' and loss G'' moduli were measured at 2 and 4.5 mg/ml of collagen I over the first hour of polymerization. G' at equilibrium were plotted. **C-E:** Structural properties of hydrogels were assessed using SHG in 2P-microscopy. Gels were prepared under the same conditions as above for 60 minutes and incubated at 37 $^{\circ}$ C in ECM2 for 16-20 hours before analysis of fibrillogenesis (**C**). Scale bar: 10 μ m. Pore size was assessed and cumulative area of the pores at 2 (**D**) and 4.5 (**E**) mg/ml is represented.

FIGURE 6

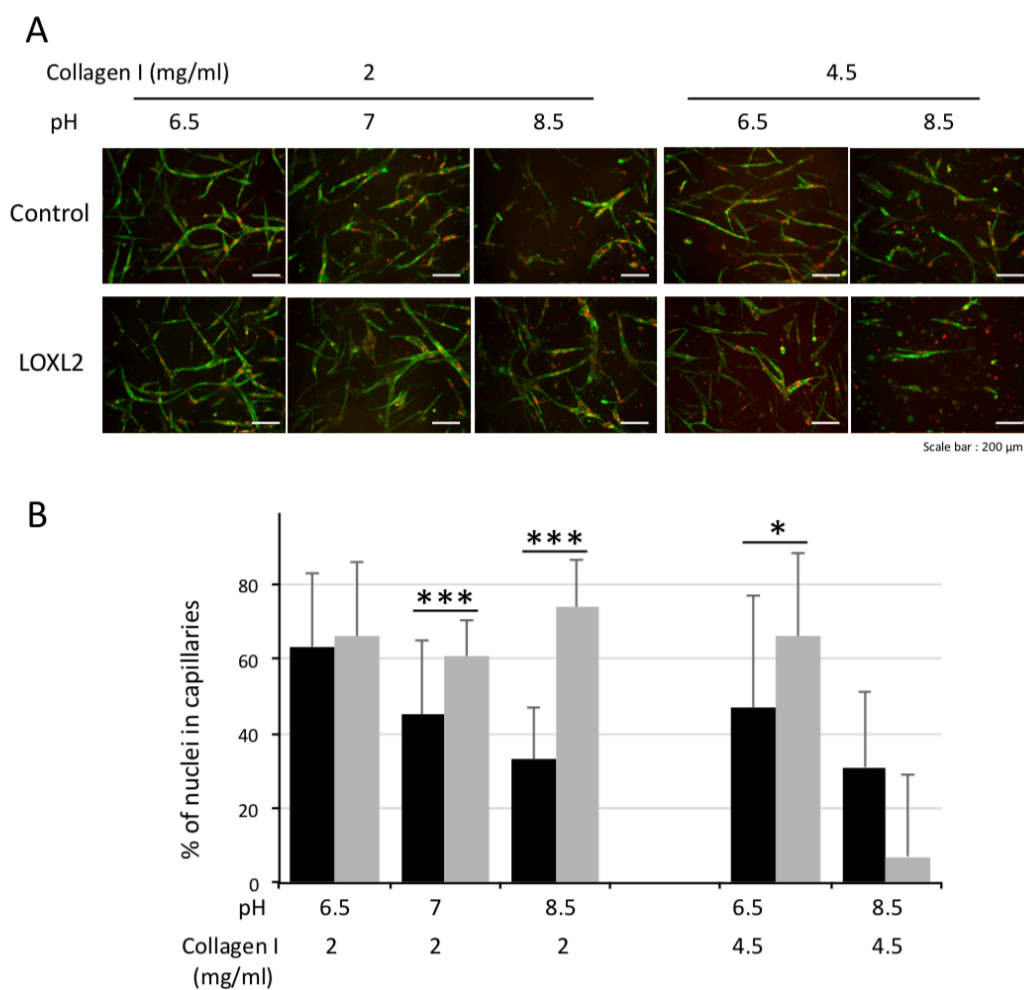


Figure 6: A and B: Endothelial cells were seeded in collagen prepared at 20 ° C and at the indicated collagen I concentration and pH, in the presence or absence of LOXL2. They were then cultured for 96 hours. F-actin was stained with phalloidin (green and nuclei with DAPI (red). Capillary formation was assessed as described in the methods sections. Scale bar: 200 μ m.

FIGURE 7

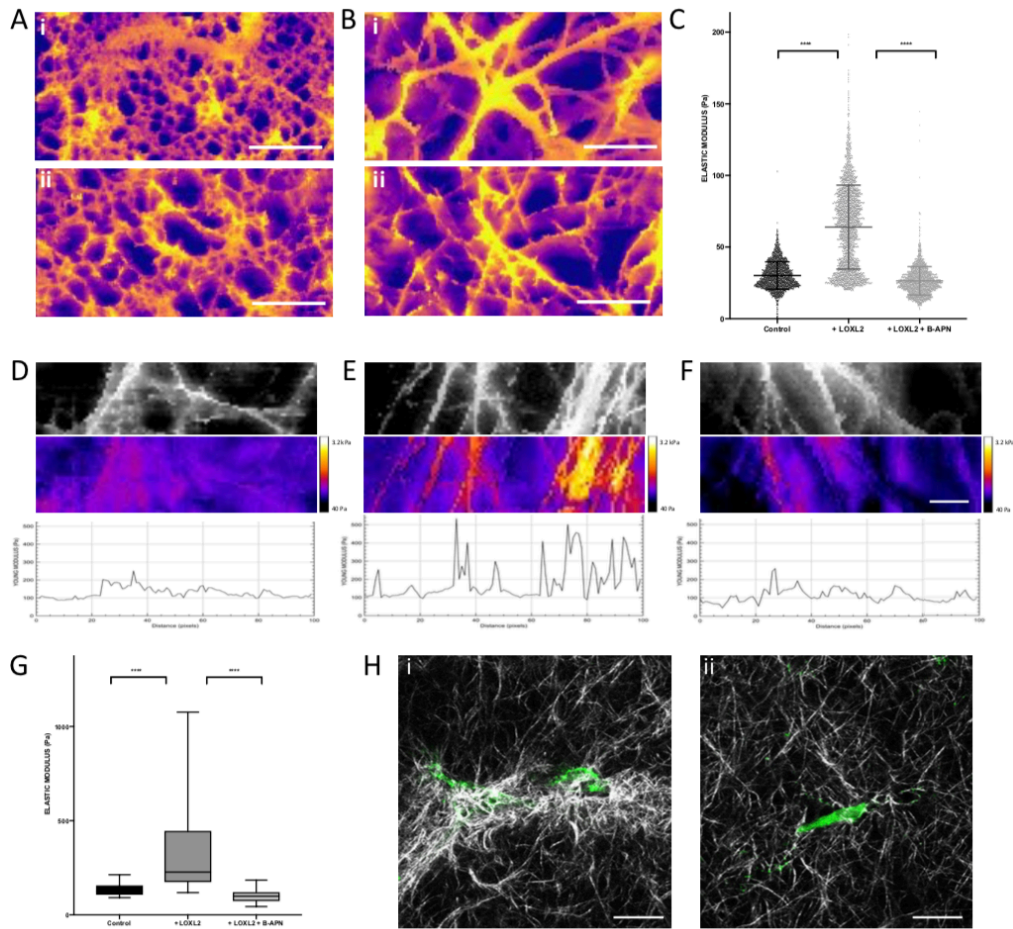


Figure 7: **A** and **B:** AFM topographical analysis of 2 mg/mL collagen hydrogels generated at pH 6.5 (**A**) or 8.5 (**B**) in control conditions (**i**) or in the presence of LOXL2 (**ii**). Representative QI AFM images of 20 x 10 μm (pixel size 100 nm in **A** and 133 nm in **B**). Scale bar: 5 μm . **C:** Elastic modulus of 2 mg/mL collagen hydrogels generated at pH 6.5 was determined by colloidal probe force spectroscopy. Sets of measurement of at least 255 force-distance curves were conducted at 3 different positions of collagen hydrogels from 2 independent experiments. Data are represented as individual values. Line is at mean \pm SD. **D-F:** Analysis of fiber stiffness was determined by using a pyramidal probe on 2 mg/mL collagen hydrogels generated at pH 8.5 in control conditions (**D**), or crosslinked with LOXL2 (**E**) or with LOXL2 treated with β -APN (**F**). QI imaging was performed at each pixel. At least 3 different fields of 30x4 μm were analyzed on each hydrogel from 2 independent experiments. Top row represents height measurements and middle row represents corresponding stiffness maps (logarithmic scale). Bottom row represents stiffness along a line scan (non logarithmic scale). Scale bar: 4 μm . **G:** Individual fiber stiffness quantification was performed by collecting regions of interest corresponding to fibers on height maps and mean stiffness was extracted. Data represent the means and min to max (whiskers) values. Kruskal-Wallis test: **** P<0.0001. **H:** Hydrogels prepared at pH 8.5 and seeded with endothelial cells were fixed at 24 hours. F-actin was stained with phalloidin (green). Second harmonic generation was acquired. One single confocal plane of the z-stack (movie 3) is represented. Scale bar: 25 μm

SUPPLEMENTARY FIGURE 1

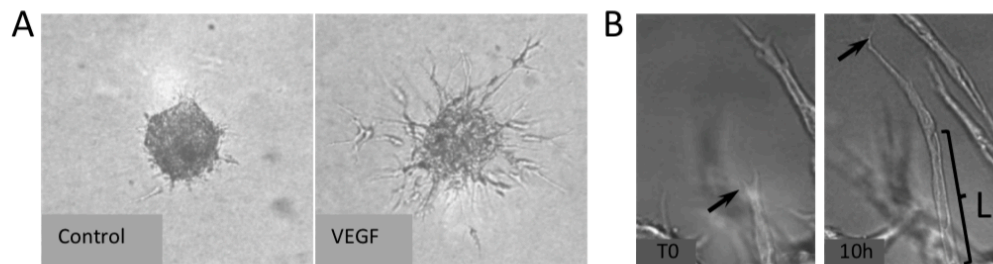


Figure S1: HUVEC spheroids were embedded in collagen hydrogels and cultured either in ECGM2 alone or in the presence of VEGF (**A**), or in fibroblast-conditioned medium containing VEGF (**B**). Time-lapse acquisitions were performed within the first 24 hours in culture (**A** and associated movie 1) or after 3 days of culture and for 10 hours (**B** and associated movie 2).

SUPPLEMENTARY FIGURE 2

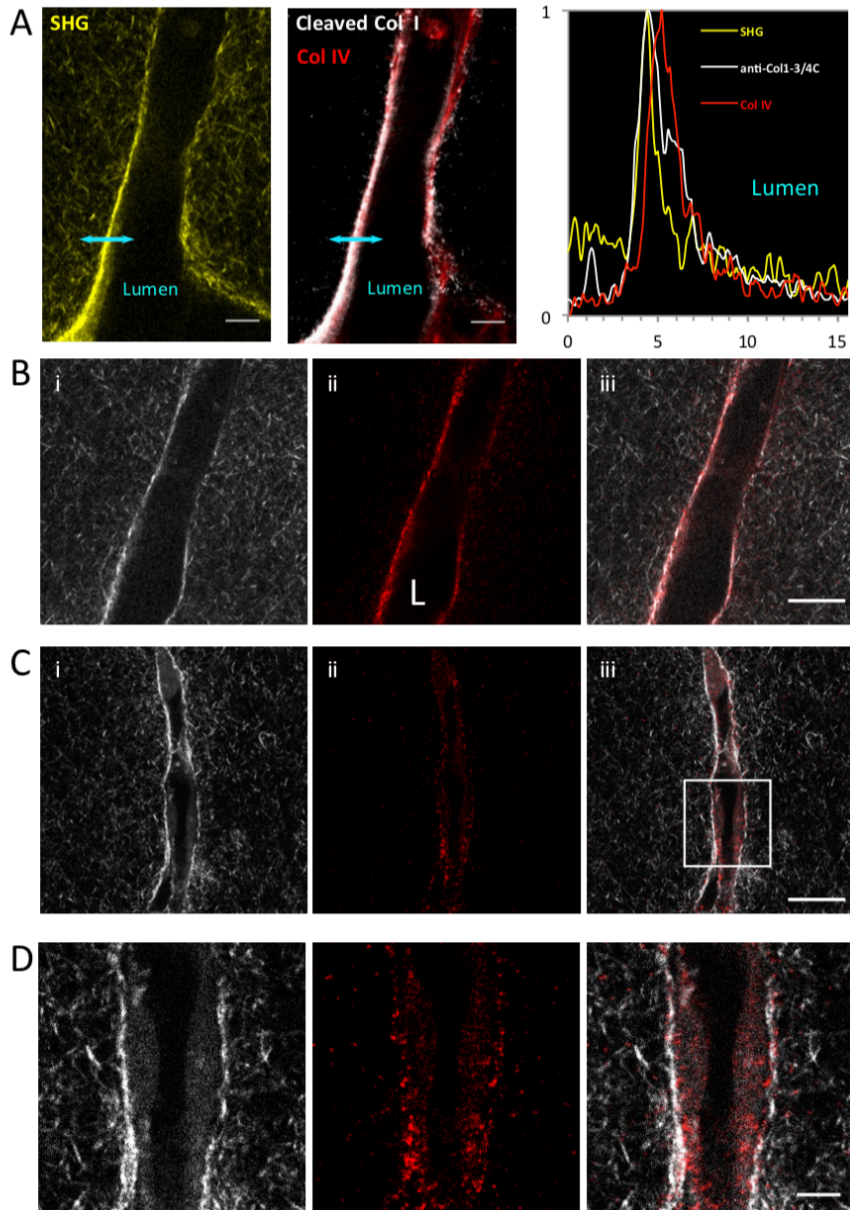


Figure S2: Matrix remodeling associated to capillary formation was assessed for collagen I cleavage. Endothelial cells seeded in collagen hydrogel were cultured for 72 hours in control conditions (A and B) or in the presence of 1.6 μ M Marimastat (C-D) before fixation. Gels were immuno-stained for processed collagen I (white in A and red in ii). Second harmonic generation in 2P-microscopy was detected (yellow in A and white in i) and merged (iii). White box indicate the zoomed area presented in C. A single confocal plane is shown. Scale bars: XXXXXXXX (A), 20 (B and C) and 5 (D) μ m.

SUPPLEMENTARY FIGURE 3

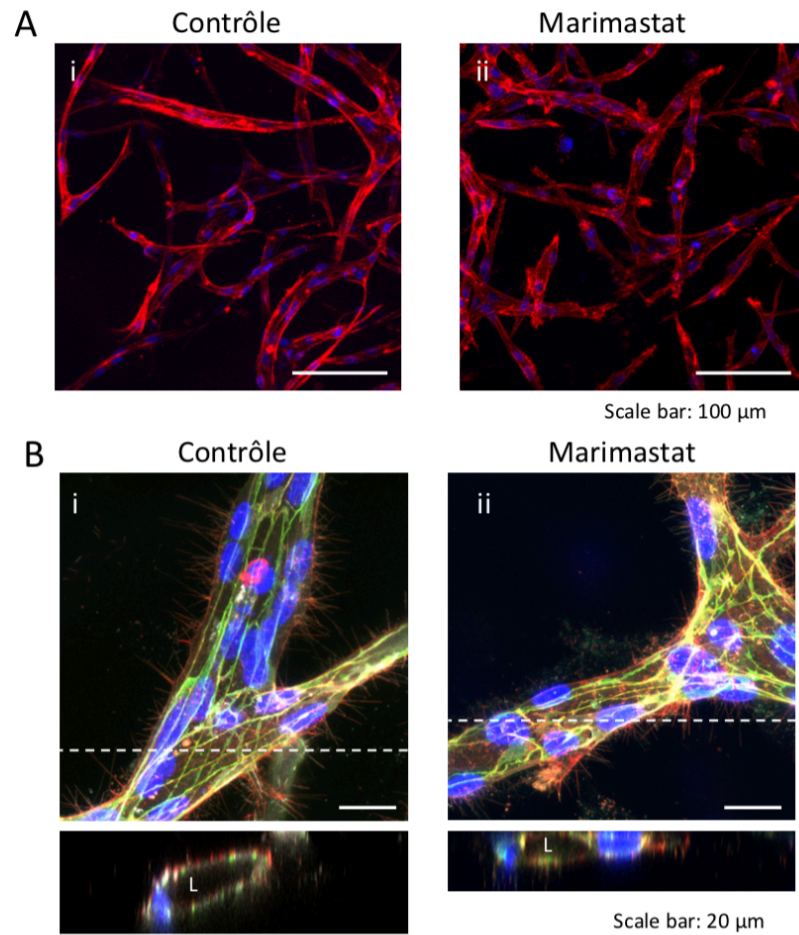


Figure S3: MMP inhibition does not affect capillary formation in fibrin hydrogels. Endothelial cells seeded in fibrin hydrogel were cultured for 96 hours under control conditions (**Ai** and **Bi**) or in the presence of 1.6 μM Marimastat (**Aii** and **Bii**). Gels were fixed and F-actin was labeled with phalloidin (red) (**A**) and immunostained for VE-cadherin (green) (**B**). Nuclei were stained with DAPI (blue). Channels were all merged. Z-stacks of images were projected (**top**) and orthogonally sectioned (**bottom**) along the white dotted line. Scale bar: 100 (**A**) and 20 (**B**) μm .

SUPPLEMENTARY FIGURE 4

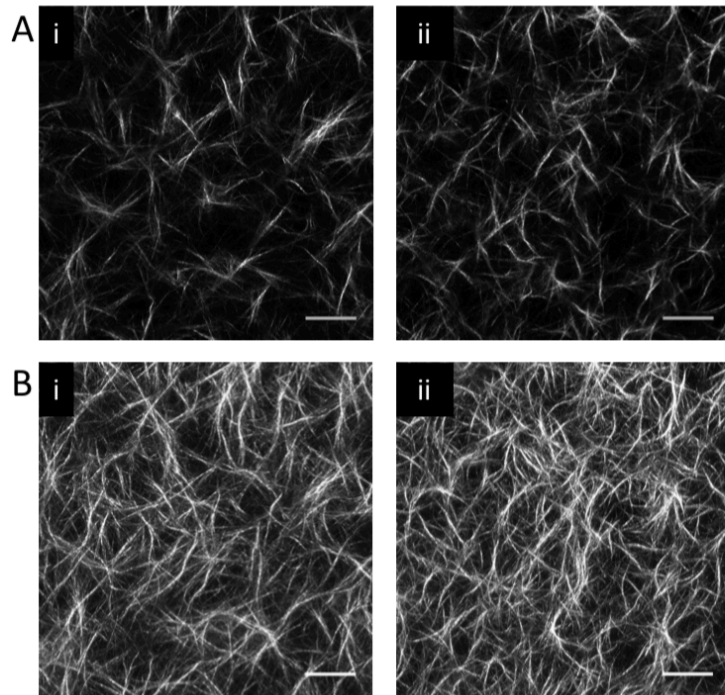


Figure S4: Collagen I hydrogels were generated in the absence (i) or presence of 1.0×10^6 cells/mL (ii). Second harmonic generation was detected (white). Single focal plane (A) or projection of 20 planes (step: $1 \mu\text{m}$) (B) are illustrated. Scale bar: $30 \mu\text{m}$.

SUPPLEMENTARY FIGURE 5

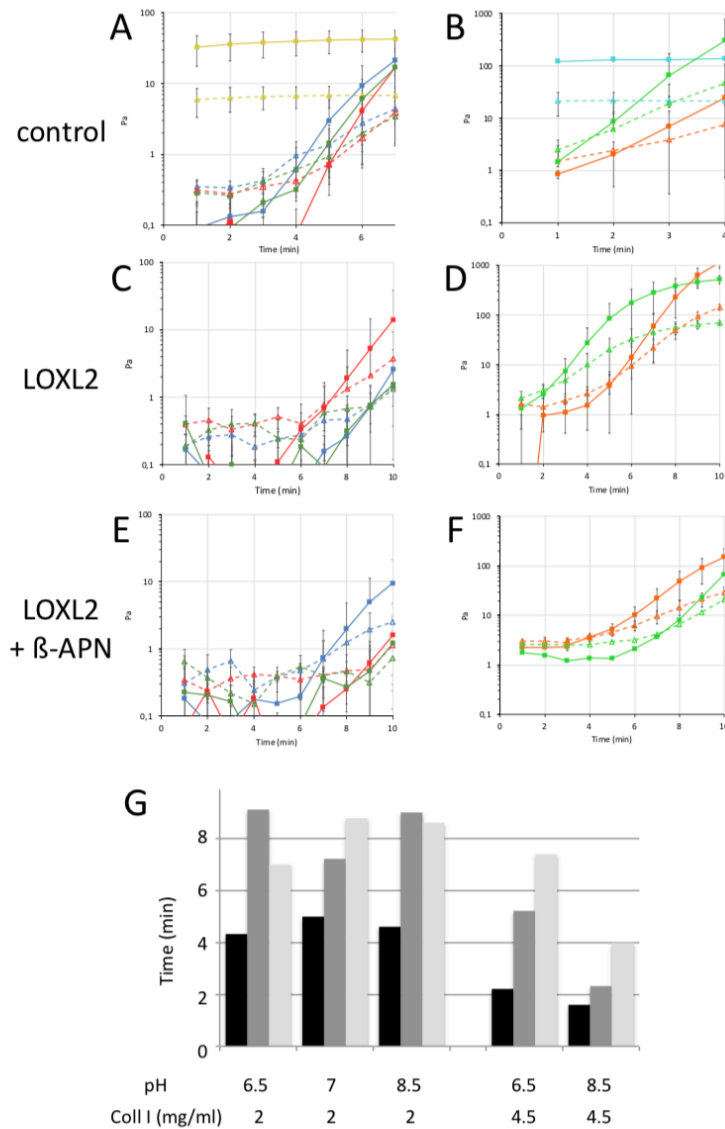


Figure S5: Gel points were extracted from the shear rheology data. **A-F:** Enlargement of the rheology curves corresponding to the first 4 to 10 minutes of the measurements done to generate figures 4C and 5B. Gel point values were assessed from each curves and plotted (**G**).

SUPPLEMENTARY FIGURE 6

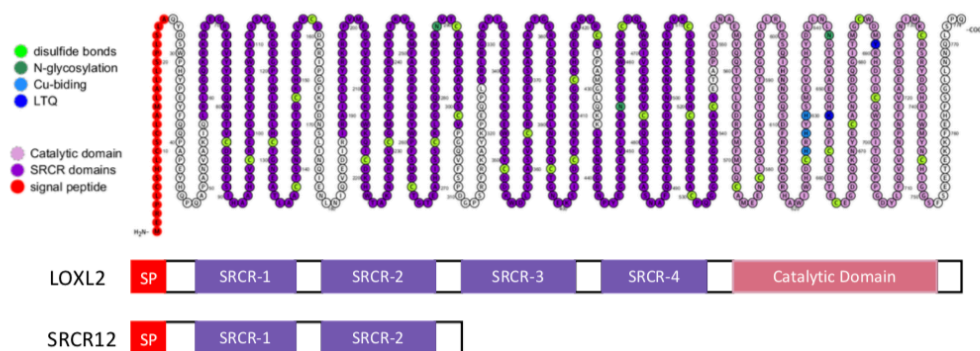


Figure S6: Schematic representation of the structure of LOXL2 and of the SRCR12 construct. SP is for signal peptide and SRCR for the scavenger receptor cysteine rich domain.

SUPPLEMENTARY FIGURE 7

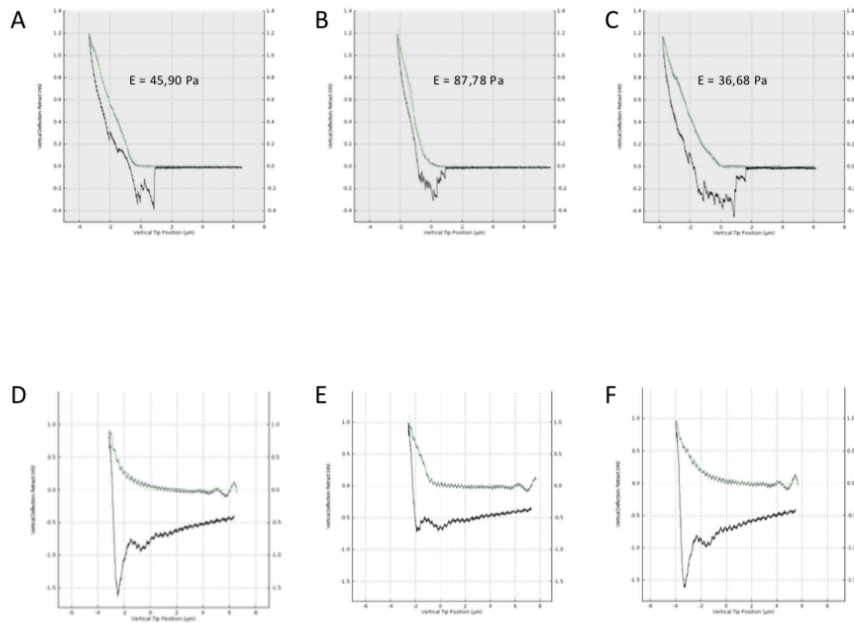


Figure S7. Determination of Young's moduli by fitting force indentation curves according to the linear Hertz model. **A to C:** Representative plots of force-distance curves for the mechanical characterization of collagen I hydrogels by colloidal probe force spectroscopy are shown for hydrogels generated at pH 6.5 (**A**), with LOXL2 (**B**) or LOXL2 + β -APN (**C**). Linear fitting of approach curves is shown (green line) and corresponding elastic moduli. **D to F:** Representative plots of force-distance curves for the mechanical characterization of collagen I hydrogels generated at pH 8.5 (**A**) with LOXL2 (**B**) or LOXL2 + β -APN (**C**). Linear fitting of approach curves is shown (green line).

Online movies:

Movie 1 : spherode sans co-culture = migration individuelle ([Spher -NHDF VEGF.AVI](#))

Movie 2 : spherode avec co-culture pour formation de capillaires ([Spher1 1z zoom.AVI](#)).

Movie 3 : z-stack of 3D cell spreading in control or LOXL2-treated collagen gel produced at pH 8.5

References

- Abedi, H., and Zachary, I. (1997). Vascular endothelial growth factor stimulates tyrosine phosphorylation and recruitment to new focal adhesions of focal adhesion kinase and paxillin in endothelial cells. *J. Biol. Chem.* *272*, 15442–15451.
- Abu Taha, A., and Schnittler, H.-J. (2014). Dynamics between actin and the VE-cadherin/catenin complex: novel aspects of the ARP2/3 complex in regulation of endothelial junctions. *Cell Adhes. Migr.* *8*, 125–135.
- Adams, R.H., and Eichmann, A. (2010). Axon Guidance Molecules in Vascular Patterning. *Cold Spring Harb. Perspect. Biol.* *2*, a001875.
- Akagawa, H., Narita, A., Yamada, H., Tajima, A., Krischek, B., Kasuya, H., Hori, T., Kubota, M., Saeki, N., Hata, A., et al. (2007). Systematic screening of lysyl oxidase-like (LOXL) family genes demonstrates that LOXL2 is a susceptibility gene to intracranial aneurysms. *Hum. Genet.* *121*, 377–387.
- Akimov, S.S., and Belkin, A.M. (2001). Cell-surface transglutaminase promotes fibronectin assembly via interaction with the gelatin-binding domain of fibronectin: a role in TGFbeta-dependent matrix deposition. *J. Cell Sci.* *114*, 2989–3000.
- Albiges-Rizo, C., Destaing, O., Fourcade, B., Planus, E., and Block, M.R. (2009). Actin machinery and mechanosensitivity in invadopodia, podosomes and focal adhesions. *J. Cell Sci.* *122*, 3037–3049.
- Añazco, C., López-Jiménez, A.J., Rafi, M., Vega-Montoto, L., Zhang, M.-Z., Hudson, B.G., and Vanacore, R.M. (2016). Lysyl Oxidase-like-2 Cross-links Collagen IV of Glomerular Basement Membrane. *J. Biol. Chem.* *291*, 25999–26012.
- Armulik, A., Genové, G., and Betsholtz, C. (2011). Pericytes: Developmental, Physiological, and Pathological Perspectives, Problems, and Promises. *Dev. Cell* *21*, 193–215.
- Astrof, S., Crowley, D., and Hynes, R.O. (2007). Multiple cardiovascular defects caused by the absence of alternatively spliced segments of fibronectin. *Dev. Biol.* *311*, 11–24.
- Aumailley, M., and Timpl, R. (1986). Attachment of cells to basement membrane collagen type IV. *J. Cell Biol.* *103*, 1569–1575.
- Aumiller, V., Strobel, B., Romeike, M., Schuler, M., Stierstorfer, B.E., and Kreuz, S. (2017). Comparative analysis of lysyl oxidase (like) family members in pulmonary fibrosis. *Sci. Rep.* *7*, 149.
- Bachir, A.I., Zareno, J., Moissoglu, K., Plow, E.F., Gratton, E., and Horwitz, A.R. (2014). Integrin-associated complexes form hierarchically with variable stoichiometry in nascent adhesions. *Curr. Biol. CB* *24*, 1845–1853.
- Bailey, A.J., Sims, T.J., and Light, N. (1984). Cross-linking in type IV collagen. *Biochem. J.* *218*, 713–723.
- Balaban, N.Q., Schwarz, U.S., Rivelino, D., Goichberg, P., Tzur, G., Sabanay, I., Mahalu, D., Safran, S., Bershadsky, A., Addadi, L., et al. (2001). Force and focal adhesion assembly: a close relationship studied using elastic micropatterned substrates. *Nat. Cell Biol.* *3*, 466–472.
- Barber-Pérez, N., Georgiadou, M., Guzmán, C., Isomursu, A., Hamidi, H., and Ivaska, J. (2020). Mechano-responsiveness of fibrillar adhesions on stiffness-gradient gels. *J. Cell Sci.*
- Barker, H.E., Chang, J., Cox, T.R., Lang, G., Bird, D., Nicolau, M., Evans, H.R., Gartland, A., and Erler, J.T. (2011). LOXL2-mediated matrix remodeling in metastasis and mammary gland involution. *Cancer Res.* *71*, 1561–1572.
- Barker, H.E., Bird, D., Lang, G., and Erler, J.T. (2013). Tumor-Secreted LOXL2 Activates Fibroblasts through FAK Signaling. *Mol. Cancer Res.* *11*, 1425–1436.

- Barry-Hamilton, V., Spangler, R., Marshall, D., McCauley, S., Rodriguez, H.M., Oyasu, M., Mikels, A., Vaysberg, M., Ghermazien, H., Wai, C., et al. (2010). Allosteric inhibition of lysyl oxidase-like-2 impedes the development of a pathologic microenvironment. *Nat. Med.* *16*, 1009–1017.
- Bastounis, E.E., Yeh, Y.-T., and Theriot, J.A. (2019). Subendothelial stiffness alters endothelial cell traction force generation while exerting a minimal effect on the transcriptome. *Sci. Rep.* *9*, 18209.
- Bays, J.L., and DeMali, K.A. (2017). Vinculin in cell–cell and cell–matrix adhesions. *Cell. Mol. Life Sci.* *74*, 2999–3009.
- Bays, J.L., Peng, X., Tolbert, C.E., Guilluy, C., Angell, A.E., Pan, Y., Superfine, R., Burrige, K., and DeMali, K.A. (2014). Vinculin phosphorylation differentially regulates mechanotransduction at cell–cell and cell–matrix adhesions. *J. Cell Biol.* *205*, 251–263.
- Bécam, I.E., Tanentzapf, G., Lepesant, J.-A., Brown, N.H., and Huynh, J.-R. (2005). Integrin-independent repression of cadherin transcription by talin during axis formation in *Drosophila*. *Nat. Cell Biol.* *7*, 510–516.
- Beckouche, N., Bignon, M., Lelarge, V., Mathivet, T., Pichol-Thievend, C., Berndt, S., Hardouin, J., Garand, M., Ardidie-Robouant, C., Barret, A., et al. (2015). The interaction of heparan sulfate proteoglycans with endothelial transglutaminase-2 limits VEGF165-induced angiogenesis. *Sci. Signal.* *8*, ra70.
- Bhave, G., Cummings, C.F., Vanacore, R.M., Kumagai-Cresse, C., Ero-Tolliver, I.A., Rafi, M., Kang, J.-S., Pedchenko, V., Fessler, L.I., Fessler, J.H., et al. (2012). Peroxidase forms sulfilimine chemical bonds using hypohalous acids in tissue genesis. *Nat. Chem. Biol.* *8*, 784–790.
- Bhave, G., Colon, S., and Ferrell, N. (2017). The Sulfilimine Cross-Link of Collagen IV Contributes to Kidney Tubular Basement Membrane Stiffness. *Am. J. Physiol. Renal Physiol.* *ajprenal.00096.2017*.
- Bignon, M., Pichol-Thievend, C., Hardouin, J., Malbouyres, M., Brechot, N., Nasciutti, L., Barret, A., Teillon, J., Guillon, E., Etienne, E., et al. (2011). Lysyl oxidase-like protein-2 regulates sprouting angiogenesis and type IV collagen assembly in the endothelial basement membrane. *Blood* *118*, 3979–3989.
- Birukova, A.A., Malyukova, I., Poroyko, V., and Birukov, K.G. (2007). Paxillin-beta-catenin interactions are involved in Rac/Cdc42-mediated endothelial barrier-protective response to oxidized phospholipids. *Am. J. Physiol. Lung Cell. Mol. Physiol.* *293*, L199–211.
- Blum, Y., Belting, H.-G., Ellertsdottir, E., Herwig, L., Lüders, F., and Affolter, M. (2008). Complex cell rearrangements during intersegmental vessel sprouting and vessel fusion in the zebrafish embryo. *Dev. Biol.* *316*, 312–322.
- Borghi, N., Sorokina, M., Shcherbakova, O.G., Weis, W.I., Pruitt, B.L., Nelson, W.J., and Dunn, A.R. (2012). E-cadherin is under constitutive actomyosin-generated tension that is increased at cell-cell contacts upon externally applied stretch. *Proc. Natl. Acad. Sci.* *109*, 12568–12573.
- Boscher, C., Gaonac'h-Lovejoy, V., Delisle, C., and Gratton, J.-P. (2019). Polarization and sprouting of endothelial cells by angiopoietin-1 require PAK2 and paxillin-dependent Cdc42 activation. *Mol. Biol. Cell* *30*, 2227–2239.
- Bouchet, B.P., Gough, R.E., Ammon, Y.-C., van de Willige, D., Post, H., Jacquemet, G., Altelaar, A.M., Heck, A.J., Goult, B.T., and Akhmanova, A. (2016). Talin-KANK1 interaction controls the recruitment of cortical microtubule stabilizing complexes to focal adhesions. *ELife* *5*.
- Bouleti, C., Mathivet, T., Coqueran, B., Serfaty, J.-M., Lesage, M., Berland, E., Ardidie-Robouant, C., Kauffenstein, G., Henrion, D., Lapergue, B., et al. (2013). Protective effects of angiopoietin-like 4 on cerebrovascular and functional damages in ischaemic stroke. *Eur. Heart J.* *34*, 3657–3668.

- Bouvard, C., Segaula, Z., De Arcangelis, A., Galy-Fauroux, I., Mauge, L., Fischer, A.-M., Georges-Labouesse, E., and Helley, D. (2014). Tie2-dependent deletion of $\alpha 6$ integrin subunit in mice reduces tumor growth and angiogenesis. *Int. J. Oncol.* *45*, 2058–2064.
- Braren, R., Hu, H., Kim, Y.H., Beggs, H.E., Reichardt, L.F., and Wang, R. (2006). Endothelial FAK is essential for vascular network stability, cell survival, and lamellipodial formation. *J. Cell Biol.* *172*, 151–162.
- Brown, K.L., Cummings, C.F., Vanacore, R.M., and Hudson, B.G. (2017). Building collagen IV smart scaffolds on the outside of cells. *Protein Sci. Publ. Protein Soc.* *26*, 2151–2161.
- Brugnera, E., Haney, L., Grimsley, C., Lu, M., Walk, S.F., Tosello-Tramont, A.-C., Macara, I.G., Madhani, H., Fink, G.R., and Ravichandran, K.S. (2002). Unconventional Rac-GEF activity is mediated through the Dock180-ELMO complex. *Nat. Cell Biol.* *4*, 574–582.
- Burrige, K., and Wennerberg, K. (2004). Rho and Rac take center stage. *Cell* *116*, 167–179.
- Cao, J., and Schnittler, H. (2019). Putting VE-cadherin into JAIL for junction remodeling. *J. Cell Sci.* *132*.
- Cao, J., Ehling, M., März, S., Seebach, J., Tarbashevich, K., Sixta, T., Pitulescu, M.E., Werner, A.-C., Flach, B., Montanez, E., et al. (2017). Polarized actin and VE-cadherin dynamics regulate junctional remodelling and cell migration during sprouting angiogenesis. *Nat. Commun.* *8*, 2210.
- Carmeliet, P., Lampugnani, M.G., Moons, L., Breviario, F., Compernelle, V., Bono, F., Balconi, G., Spagnuolo, R., Oosthuysen, B., Dewerchin, M., et al. (1999). Targeted deficiency or cytosolic truncation of the VE-cadherin gene in mice impairs VEGF-mediated endothelial survival and angiogenesis. *Cell* *98*, 147–157.
- Carvalho, J.R., Fortunato, I.C., Fonseca, C.G., Pezzarossa, A., Barbacena, P., Dominguez-Cejudo, M.A., Vasconcelos, F.F., Santos, N.C., Carvalho, F.A., and Franco, C.A. (2019). Non-canonical Wnt signaling regulates junctional mechanocoupling during angiogenic collective cell migration. *ELife* *8*.
- Cavalcanti-Adam, E.A., Micoulet, A., Blümmel, J., Auernheimer, J., Kessler, H., and Spatz, J.P. (2006). Lateral spacing of integrin ligands influences cell spreading and focal adhesion assembly. *Eur. J. Cell Biol.* *85*, 219–224.
- Cavalcanti-Adam, E.A., Volberg, T., Micoulet, A., Kessler, H., Geiger, B., and Spatz, J.P. (2007). Cell spreading and focal adhesion dynamics are regulated by spacing of integrin ligands. *Biophys. J.* *92*, 2964–2974.
- Cazaux, S., Sadoun, A., Biarnes-Pelicot, M., Martinez, M., Obeid, S., Bongrand, P., Limozin, L., and Puech, P.-H. (2016). Synchronizing atomic force microscopy force mode and fluorescence microscopy in real time for immune cell stimulation and activation studies. *Ultramicroscopy* *160*, 168–181.
- Cebrià-Costa, J.P., Pascual-Reguant, L., Gonzalez-Perez, A., Serra-Bardenys, G., Querol, J., Cosín, M., Verde, G., Cigliano, R.A., Sanseverino, W., Segura-Bayona, S., et al. (2020). LOXL2-mediated H3K4 oxidation reduces chromatin accessibility in triple-negative breast cancer cells. *Oncogene* *39*, 79–121.
- Cerqueira Campos, F., Dennis, C., Alégot, H., Fritsch, C., Isabella, A., Pouchin, P., Bardot, O., Horne-Badovinac, S., and Mirouse, V. (2020). Oriented basement membrane fibrils provide a memory for F-actin planar polarization via the Dystrophin-Dystroglycan complex during tissue elongation. *Dev.* *147*.
- Chang, J., Nicolau, M.M., Cox, T.R., Wetterskog, D., Martens, J.W.M., Barker, H.E., and Erler, J.T. (2013). LOXL2 induces aberrant acinar morphogenesis via ErbB2 signaling. *Breast Cancer Res. BCR* *15*, R67.
- Chaturvedi, R.R., Stevens, K.R., Solorzano, R.D., Schwartz, R.E., Eyckmans, J., Baranski, J.D., Stapleton, S.C., Bhatia, S.N., and Chen, C.S. (2015). Patterning vascular networks in vivo for tissue engineering applications. *Tissue Eng. Part C Methods* *21*, 509–517.

- Chen, C.S., Mrksich, M., Huang, S., Whitesides, G.M., and Ingber, D.E. (1997). Geometric control of cell life and death. *Science* 276, 1425–1428.
- Chen, X.L., Nam, J.-O., Jean, C., Lawson, C., Walsh, C.T., Goka, E., Lim, S.-T., Tomar, A., Tancioni, I., Uryu, S., et al. (2012). VEGF-induced vascular permeability is mediated by FAK. *Dev. Cell* 22, 146–157.
- Chen, Y., Ju, L., Rushdi, M., Ge, C., and Zhu, C. (2017a). Receptor-mediated cell mechanosensing. *Mol. Biol. Cell* 28, 3134–3155.
- Chen, Y., Lee, H., Tong, H., Schwartz, M., and Zhu, C. (2017b). Force regulated conformational change of integrin $\alpha\text{V}\beta 3$. *Matrix Biol.* 60–61, 70–85.
- Cheng, F., Miao, L., Wu, Q., Gong, X., Xiong, J., and Zhang, J. (2016). Vinculin b deficiency causes epicardial hyperplasia and coronary vessel disorganization in zebrafish. *Dev.* 143, 3522–3531.
- Chioran, A., Duncan, S., Catalano, A., Brown, T.J., and Ringuette, M.J. (2017). Collagen IV trafficking: The inside-out and beyond story. *Dev. Biol.* 431, 124–133.
- Chlasta, J., Milani, P., Runel, G., Duteyrat, J.-L., Arias, L., Lamiré, L.-A., Boudaoud, A., and Grammont, M. (2017). Variations in basement membrane mechanics are linked to epithelial morphogenesis. *Dev.* 144, 4350–4362.
- Choi, C.K., Vicente-Manzanares, M., Zareno, J., Whitmore, L.A., Mogilner, A., and Horwitz, A.R. (2008). Actin and α -actinin orchestrate the assembly and maturation of nascent adhesions in a myosin II motor-independent manner. *Nat. Cell Biol.* 10, 1039–1050.
- Chung, C.Y., and Erickson, H.P. (1997). Glycosaminoglycans modulate fibronectin matrix assembly and are essential for matrix incorporation of tenascin-C. *J. Cell Sci.* 110 (Pt 12), 1413–1419.
- Conway, D.E., Breckenridge, M.T., Hinde, E., Gratton, E., Chen, C.S., and Schwartz, M.A. (2013). Fluid shear stress on endothelial cells modulates mechanical tension across VE-cadherin and PECAM-1. *Curr. Biol. CB* 23, 1024–1030.
- Cosgrove, D., Dufek, B., Meehan, D.T., Delimont, D., Hartnett, M., Samuelson, G., Gratton, M.A., Phillips, G., MacKenna, D.A., and Bain, G. (2018). Lysyl oxidase like-2 contributes to renal fibrosis in Col4a3/Alport mice. *Kidney Int.* 94, 303–314.
- Crawford, B.D., Henry, C.A., Clason, T.A., Becker, A.L., and Hille, M.B. (2003). Activity and distribution of paxillin, focal adhesion kinase, and cadherin indicate cooperative roles during zebrafish morphogenesis. *Mol. Biol. Cell* 14, 3065–3081.
- Crest, J., Diz-Muñoz, A., Chen, D.-Y., Fletcher, D.A., and Bilder, D. (2017). Organ sculpting by patterned extracellular matrix stiffness. *ELife* 6.
- Cseh, B., Fernandez-Sauze, S., Grall, D., Schaub, S., Doma, E., and Van Obberghen-Schilling, E. (2010). Autocrine fibronectin directs matrix assembly and crosstalk between cell-matrix and cell-cell adhesion in vascular endothelial cells. *J. Cell Sci.* 123, 3989–3999.
- Csiszar, K. (2001). Lysyl oxidases: A novel multifunctional amine oxidase family. B.-P. in N.A.R. and M. Biology, ed. (Academic Press), pp. 1–32.
- Cuevas, E.P., Moreno-Bueno, G., Canesin, G., Santos, V., Portillo, F., and Cano, A. (2014). LOXL2 catalytically inactive mutants mediate epithelial-to-mesenchymal transition. *Biol. Open* 3, 129–137.
- Cuevas, E.P., Eraso, P., Mazón, M.J., Santos, V., Moreno-Bueno, G., Cano, A., and Portillo, F. (2017). LOXL2 drives epithelial-mesenchymal transition via activation of IRE1-XBP1 signalling pathway. *Sci. Rep.* 7, 44988.

- De Franceschi, N., Hamidi, H., Alanko, J., Sahgal, P., and Ivaska, J. (2015). Integrin traffic - the update. *J. Cell Sci.* *128*, 839–852.
- Dejana, E., and Orsenigo, F. (2013). Endothelial adherens junctions at a glance. *J. Cell Sci.* *126*, 2545–2549.
- DeMali, K.A., Wennerberg, K., and Burridge, K. (2003). Integrin signaling to the actin cytoskeleton. *Curr. Opin. Cell Biol.* *15*, 572–582.
- Di Russo, J., Luik, A., Yousif, L., Budny, S., Oberleithner, H., Hofschroer, V., Klingauf, J., van Bavel, E., Bakker, E.N., Hellstrand, P., et al. (2017). Endothelial basement membrane laminin 511 is essential for shear stress response. *EMBO J.* *36*, 183–201.
- Discher, D.E. (2005). Tissue Cells Feel and Respond to the Stiffness of Their Substrate. *Science* *310*, 1139–1143.
- Domigan, C.K., Warren, C.M., Antanesian, V., Happel, K., Ziyad, S., Lee, S., Krall, A., Duan, L., Torres-Collado, A.X., Castellani, L.W., et al. (2015). Autocrine VEGF maintains endothelial survival through regulation of metabolism and autophagy. *J. Cell Sci.* *128*, 2236–2248.
- Doss, B.L., Pan, M., Gupta, M., Greci, G., Mège, R.-M., Lim, C.T., Sheetz, M.P., Voituriez, R., and Ladoux, B. (2020). Cell response to substrate rigidity is regulated by active and passive cytoskeletal stress. *Proc. Natl. Acad. Sci. U. S. A.* *117*, 12817–12825.
- Doyle, A.D., Carvajal, N., Jin, A., Matsumoto, K., and Yamada, K.M. (2015). Local 3D matrix microenvironment regulates cell migration through spatiotemporal dynamics of contractility-dependent adhesions. *Nat. Commun.* *6*, 8720.
- van den Dries, K., Linder, S., Maridonneau-Parini, I., and Poincloux, R. (2019). Probing the mechanical landscape - new insights into podosome architecture and mechanics. *J. Cell Sci.* *132*.
- le Duc, Q., Shi, Q., Blonk, I., Sonnenberg, A., Wang, N., Leckband, D., and de Rooij, J. (2010). Vinculin potentiates E-cadherin mechanosensing and is recruited to actin-anchored sites within adherens junctions in a myosin II-dependent manner. *J. Cell Biol.* *189*, 1107–1115.
- Dufour, S., Mège, R.-M., and Thiery, J.P. (2013). α -catenin, vinculin, and F-actin in strengthening E-cadherin cell-cell adhesions and mechanosensing. *Cell Adhes. Migr.* *7*, 345–350.
- Duncan, S., Delage, S., Chioran, A., Sirbu, O., Brown, T.J., and Ringuette, M.J. (2020). The predicted collagen-binding domains of Drosophila SPARC are essential for survival and for collagen IV distribution and assembly into basement membranes. *Dev. Biol.* *461*, 197–209.
- Ebrahim, Q., Chaurasia, S.S., Vasanji, A., Qi, J.H., Klenotic, P.A., Cutler, A., Asosingh, K., Erzurum, S., and Anand-Apte, B. (2010). Cross-Talk between Vascular Endothelial Growth Factor and Matrix Metalloproteinases in the Induction of Neovascularization in Vivo. *Am. J. Pathol.* *176*, 496–503.
- Efimova, N., and Svitkina, T.M. (2018). Branched actin networks push against each other at adherens junctions to maintain cell-cell adhesion. *J. Cell Biol.* *217*, 1827–1845.
- Eftymiou, G., Saint, A., Ruff, M., Rekad, Z., Ciais, D., and Obberghen-Schilling, E. (2020). Shaping Up the Tumor Microenvironment With Cellular Fibronectin. *Front. Oncol.* *10*, 641.
- Eichmann, A., Yuan, L., Moyon, D., Lenoble, F., Pardanaud, L., and Breant, C. (2005). Vascular development: from precursor cells to branched arterial and venous networks. *Int. J. Dev. Biol.* *49*, 259–267.
- Eliceiri, B.P., and Cheresh, D.A. (1998). The role of α v integrins during angiogenesis. *Mol. Med. Camb. Mass* *4*, 741–750.
- Eliceiri, B.P., and Cheresh, D.A. (1999). The role of α v integrins during angiogenesis: insights into

- potential mechanisms of action and clinical development. *J. Clin. Invest.* *103*, 1227–1230.
- Eliceiri, B.P., Puente, X.S., Hood, J.D., Stupack, D.G., Schlaepfer, D.D., Huang, X.Z., Sheppard, D., and Cheresh, D.A. (2002). Src-mediated coupling of focal adhesion kinase to integrin $\alpha(v)\beta5$ in vascular endothelial growth factor signaling. *J. Cell Biol.* *157*, 149–160.
- El-Kirat-Chatel, S., and Beaussart, A. (2018). Probing Bacterial Adhesion at the Single-Molecule and Single-Cell Levels by AFM-Based Force Spectroscopy. *Methods Mol. Biol. Clifton NJ* *1814*, 403–414.
- Ellertsdóttir, E., Lenard, A., Blum, Y., Krudewig, A., Herwig, L., Affolter, M., and Belting, H.-G. (2010). Vascular morphogenesis in the zebrafish embryo. *Dev. Biol.* *341*, 56–65.
- Elosegui-Artola, A., Oria, R., Chen, Y., Kosmalska, A., Pérez-González, C., Castro, N., Zhu, C., Trepats, X., and Roca-Cusachs, P. (2016). Mechanical regulation of a molecular clutch defines force transmission and transduction in response to matrix rigidity. *Nat. Cell Biol.* *18*, 540–548.
- Erler, J.T., and Giaccia, A.J. (2006). Lysyl Oxidase Mediates Hypoxic Control of Metastasis. *Cancer Res.* *66*, 10238–10241.
- Etienne-Manneville, S., and Hall, A. (2003). Cell polarity: Par6, aPKC and cytoskeletal crosstalk. *Curr. Opin. Cell Biol.* *15*, 67–72.
- Farge, E. (2011). Mechanotransduction in Development. In *Current Topics in Developmental Biology*, (Elsevier), pp. 243–265.
- Fässler, R., and Meyer, M. (1995). Consequences of lack of beta 1 integrin gene expression in mice. *Genes Dev.* *9*, 1896–1908.
- Faurobert, E., Rome, C., Lisowska, J., Manet-Dupé, S., Boulday, G., Malbouyres, M., Balland, M., Bouin, A.-P., Kéramidas, M., Bouvard, D., et al. (2013). CCM1–ICAP-1 complex controls $\beta1$ integrin-dependent endothelial contractility and fibronectin remodeling. *J. Cell Biol.* *202*, 545–561.
- Filla, M.S., Dimeo, K.D., Tong, T., and Peters, D.M. (2017). Disruption of fibronectin matrix affects type IV collagen, fibrillin and laminin deposition into extracellular matrix of human trabecular meshwork (HTM) cells. *Exp. Eye Res.* *165*, 7–19.
- Fogelgren, B., Polgár, N., Szauter, K.M., Ujfaludi, Z., Laczkó, R., Fong, K.S.K., and Csiszar, K. (2005). Cellular fibronectin binds to lysyl oxidase with high affinity and is critical for its proteolytic activation. *J. Biol. Chem.* *280*, 24690–24697.
- Friedlander, M., Theesfeld, C.L., Sugita, M., Fruttiger, M., Thomas, M.A., Chang, S., and Cheresh, D.A. (1996). Involvement of integrins $\alpha v \beta 3$ and $\alpha v \beta 5$ in ocular neovascular diseases. *Proc. Natl. Acad. Sci. U. S. A.* *93*, 9764–9769.
- Fujimoto, E., and Tajima, S. (2009). Reciprocal regulation of LOX and LOXL2 expression during cell adhesion and terminal differentiation in epidermal keratinocytes. *J. Dermatol. Sci.* *55*, 91–98.
- Galaup, A., Gomez, E., Souktani, R., Durand, M., Cazes, A., Monnot, C., Teillon, J., Le Jan, S., Bouleti, C., Briois, G., et al. (2012). Protection Against Myocardial Infarction and No-Reflow Through Preservation of Vascular Integrity by Angiopoietin-Like 4. *Circulation* *125*, 140–149.
- Galbraith, C.G., Yamada, K.M., and Sheetz, M.P. (2002). The relationship between force and focal complex development. *J. Cell Biol.* *159*, 695–705.
- Gasiorowski, J.Z., Murphy, C.J., and Nealey, P.F. (2013). Biophysical cues and cell behavior: the big impact of little things. *Annu. Rev. Biomed. Eng.* *15*, 155–176.
- Gebala, V., Collins, R., Geudens, I., Phng, L.-K., and Gerhardt, H. (2016). Blood flow drives lumen formation by inverse membrane blebbing during angiogenesis in vivo. *Nat. Cell Biol.* *18*, 443–450.

- van Geemen, D., Smeets, M.W.J., van Stalborch, A.-M.D., Woerdeman, L.A.E., Daemen, M.J.A.P., Hordijk, P.L., and Huvencers, S. (2014). F-actin-anchored focal adhesions distinguish endothelial phenotypes of human arteries and veins. *Arterioscler. Thromb. Vasc. Biol.* *34*, 2059–2067.
- Geiger, B., Tokuyasu, K.T., Dutton, A.H., and Singer, S.J. (1980). Vinculin, an intracellular protein localized at specialized sites where microfilament bundles terminate at cell membranes. *Proc. Natl. Acad. Sci. U. S. A.* *77*, 4127–4131.
- George, E.L., Georges-Labouesse, E.N., Patel-King, R.S., Rayburn, H., and Hynes, R.O. (1993). Defects in mesoderm, neural tube and vascular development in mouse embryos lacking fibronectin. *Dev.* *119*, 1079–1091.
- Georgiadou, M., and Ivaska, J. (2017). Tensins: Bridging AMP-Activated Protein Kinase with Integrin Activation. *Trends Cell Biol.* *27*, 703–711.
- Georgiadou, M., Lilja, J., Jacquemet, G., Guzmán, C., Rafeeva, M., Alibert, C., Yan, Y., Sahgal, P., Lerche, M., Manneville, J.-B., et al. (2017). AMPK negatively regulates tensin-dependent integrin activity. *J. Cell Biol.* *216*, 1107–1121.
- Gerhardt, H. (2003). VEGF guides angiogenic sprouting utilizing endothelial tip cell filopodia. *J. Cell Biol.* *161*, 1163–1177.
- Gerhardt, H., and Betsholtz, C. (2003). Endothelial-pericyte interactions in angiogenesis. *Cell Tissue Res.* *314*, 15–23.
- Germain, S., Monnot, C., Muller, L., and Eichmann, A. (2010). Hypoxia-driven angiogenesis: role of tip cells and extracellular matrix scaffolding. *Curr. Opin. Hematol.* *17*, 245–251.
- German, A.E., Mammoto, T., Jiang, E., Ingber, D.E., and Mammoto, A. (2014). Paxillin controls endothelial cell migration and tumor angiogenesis by altering neuropilin 2 expression. *J. Cell Sci.* *127*, 1672–1683.
- Geudens, I., and Gerhardt, H. (2011). Coordinating cell behaviour during blood vessel formation. *Dev.* *138*, 4569–4583.
- Gomez Perdiguero, E., Liabotis-Fontugne, A., Durand, M., Faye, C., Ricard-Blum, S., Simonutti, M., Augustin, S., Robb, B.M., Paques, M., Valenzuela, D.M., et al. (2016). ANGPTL4- $\alpha\text{v}\beta\text{3}$ interaction counteracts hypoxia-induced vascular permeability by modulating Src signalling downstream of vascular endothelial growth factor receptor 2. *J. Pathol.* *240*, 461–471.
- Gorin, C., Rochefort, G.Y., Bascetin, R., Ying, H., Lesieur, J., Sadoine, J., Beckouche, N., Berndt, S., Novais, A., Lesage, M., et al. (2016). Priming Dental Pulp Stem Cells With Fibroblast Growth Factor-2 Increases Angiogenesis of Implanted Tissue-Engineered Constructs Through Hepatocyte Growth Factor and Vascular Endothelial Growth Factor Secretion. *Stem Cells Transl. Med.* *5*, 392–404.
- Gould, D.B. (2005). Mutations in Col4a1 Cause Perinatal Cerebral Hemorrhage and Porencephaly. *Science* *308*, 1167–1171.
- Gould, D.B., Phalan, F.C., van Mil, S.E., Sundberg, J.P., Vahedi, K., Massin, P., Bousser, M.G., Heutink, P., Miner, J.H., Tournier-Lasserre, E., et al. (2006). Role of COL4A1 in Small-Vessel Disease and Hemorrhagic Stroke. *N. Engl. J. Med.* *354*, 1489–1496.
- Grashoff, C., Hoffman, B.D., Brenner, M.D., Zhou, R., Parsons, M., Yang, M.T., McLean, M.A., Sligar, S.G., Chen, C.S., Ha, T., et al. (2010). Measuring mechanical tension across vinculin reveals regulation of focal adhesion dynamics. *Nature* *466*, 263–266.
- Grossman, M., Ben-Chetrit, N., Zhuravlev, A., Afik, R., Bassat, E., Solomonov, I., Yarden, Y., and Sagi, I. (2016). Tumor Cell Invasion Can Be Blocked by Modulators of Collagen Fibril Alignment That Control Assembly of the Extracellular Matrix. *Cancer Res.* *76*, 4249–4258.
- Gupta, M., Sarangi, B.R., Deschamps, J., Nematbakhsh, Y., Callan-Jones, A., Margadant, F., Mège,

- R.-M., Lim, C.T., Voituriez, R., and Ladoux, B. (2015). Adaptive rheology and ordering of cell cytoskeleton govern matrix rigidity sensing. *Nat. Commun.* 6, 7525.
- Gupta, M., Doss, B., Lim, C.T., Voituriez, R., and Ladoux, B. (2016). Single cell rigidity sensing: A complex relationship between focal adhesion dynamics and large-scale actin cytoskeleton remodeling. *Cell Adhes. Migr.* 10, 554–567.
- Hagel, M., George, E.L., Kim, A., Tamimi, R., Opitz, S.L., Turner, C.E., Imamoto, A., and Thomas, S.M. (2002). The adaptor protein paxillin is essential for normal development in the mouse and is a critical transducer of fibronectin signaling. *Mol. Cell. Biol.* 22, 901–915.
- Halfter, W., Monnier, C., Müller, D., Oertle, P., Uechi, G., Balasubramani, M., Safi, F., Lim, R., Loparic, M., and Henrich, P.B. (2013). The Bi-Functional Organization of Human Basement Membranes. *PLoS ONE* 8, e67660.
- Han, M.K.L., and de Rooij, J. (2016). Converging and Unique Mechanisms of Mechanotransduction at Adhesion Sites. *Trends Cell Biol.* 26, 612–623.
- Han, X., Li, P., Yang, Z., Huang, X., Wei, G., Sun, Y., Kang, X., Hu, X., Deng, Q., Chen, L., et al. (2017). Zyxin regulates endothelial von Willebrand factor secretion by reorganizing actin filaments around exocytic granules. *Nat. Commun.* 8, 14639.
- Hellström, M., Phng, L.-K., Hofmann, J.J., Wallgard, E., Coultas, L., Lindblom, P., Alva, J., Nilsson, A.-K., Karlsson, L., Gaiano, N., et al. (2007). Dll4 signalling through Notch1 regulates formation of tip cells during angiogenesis. *Nature* 445, 776–780.
- van Helvert, S., and Friedl, P. (2016). Strain Stiffening of Fibrillar Collagen during Individual and Collective Cell Migration Identified by AFM Nanoindentation. *ACS Appl. Mater. Interfaces* 8, 21946–21955.
- Herranz, N., Dave, N., Millanes-Romero, A., Pascual-Reguant, L., Morey, L., Díaz, V.M., Lórenz-Fonfría, V., Gutierrez-Gallego, R., Jerónimo, C., Iturbide, A., et al. (2016). Lysyl oxidase-like 2 (LOXL2) oxidizes trimethylated lysine 4 in histone H3. *FEBS J.* 283, 4263–4273.
- Hirata, H., Tatsumi, H., and Sokabe, M. (2008). Mechanical forces facilitate actin polymerization at focal adhesions in a zyxin-dependent manner. *J. Cell Sci.* 121, 2795–2804.
- Hodivala-Dilke, K. (2008). α v β 3 integrin and angiogenesis: a moody integrin in a changing environment. *Curr. Opin. Cell Biol.* 20, 514–519.
- Hoffman, L.M., Jensen, C.C., Kloeker, S., Wang, C.-L.A., Yoshigi, M., and Beckerle, M.C. (2006). Genetic ablation of zyxin causes Mena/VASP mislocalization, increased motility, and deficits in actin remodeling. *J. Cell Biol.* 172, 771–782.
- Hohenester, E., and Yurchenco, P.D. (2013). Laminins in basement membrane assembly. *Cell Adhes. Migr.* 7, 56–63.
- Hong, X., and Yu, J.-J. (2019). Silencing of lysyl oxidase-like 2 inhibits the migration, invasion and epithelial-to-mesenchymal transition of renal cell carcinoma cells through the Src/FAK signaling pathway. *Int. J. Oncol.* 54, 1676–1690.
- Hornstra, I.K., Birge, S., Starcher, B., Bailey, A.J., Mecham, R.P., and Shapiro, S.D. (2003). Lysyl Oxidase Is Required for Vascular and Diaphragmatic Development in Mice. *J. Biol. Chem.* 278, 14387–14393.
- Horton, E.R., Byron, A., Askari, J.A., Ng, D.H.J., Millon-Frémillon, A., Robertson, J., Koper, E.J., Paul, N.R., Warwood, S., Knight, D., et al. (2015). Definition of a consensus integrin adhesome and its dynamics during adhesion complex assembly and disassembly. *Nat. Cell Biol.* 17, 1577–1587.
- Hu, X., Jing, C., Xu, X., Nakazawa, N., Cornish, V.W., Margadant, F.M., and Sheetz, M.P. (2016).

Cooperative Vinculin Binding to Talin Mapped by Time-Resolved Super Resolution Microscopy. *Nano Lett.* 16, 4062–4068.

Humphries, J.D. (2006). Integrin ligands at a glance. *J. Cell Sci.* 119, 3901–3903.

Humphries, J.D., Wang, P., Streuli, C., Geiger, B., Humphries, M.J., and Ballestrem, C. (2007). Vinculin controls focal adhesion formation by direct interactions with talin and actin. *J. Cell Biol.* 179, 1043–1057.

Humphries, J.D., Chastney, M.R., Askari, J.A., and Humphries, M.J. (2019). Signal transduction via integrin adhesion complexes. *Curr. Opin. Cell Biol.* 56, 14–21.

Huveneers, S., Oldenburg, J., Spanjaard, E., van der Krogt, G., Grigoriev, I., Akhmanova, A., Rehmann, H., and de Rooij, J. (2012). Vinculin associates with endothelial VE-cadherin junctions to control force-dependent remodeling. *J. Cell Biol.* 196, 641–652.

Hynes, R.O. (2007). Cell-matrix adhesion in vascular development: Cell-matrix adhesion in vascular development. *J. Thromb. Haemost.* 5, 32–40.

Hytönen, V.P., and Vogel, V. (2008). How force might activate talin's vinculin binding sites: SMD reveals a structural mechanism. *PLoS Comput. Biol.* 4, e24.

Ichihara-Tanaka, K., Maeda, T., Titani, K., and Sekiguchi, K. (1992). Matrix assembly of recombinant fibronectin polypeptide consisting of amino-terminal 70 kDa and carboxyl-terminal 37 kDa regions. *FEBS Lett.* 299, 155–158.

Ikenaga, N., Peng, Z.-W., Vaid, K.A., Liu, S.B., Yoshida, S., Sverdlov, D.Y., Mikels-Vigdal, A., Smith, V., Schuppan, D., and Popov, Y.V. (2017). Selective targeting of lysyl oxidase-like 2 (LOXL2) suppresses hepatic fibrosis progression and accelerates its reversal. *Gut* 66, 1697–1708.

Ingber, D.E., and Folkman, J. (1989). Mechanochemical switching between growth and differentiation during fibroblast growth factor-stimulated angiogenesis in vitro: role of extracellular matrix. *J. Cell Biol.* 109, 317–330.

Iruela-Arispe, M.L., and Davis, G.E. (2009). Cellular and Molecular Mechanisms of Vascular Lumen Formation. *Dev. Cell* 16, 222–231.

Isabella, A.J., and Horne-Badovinac, S. (2015). Dynamic regulation of basement membrane protein levels promotes egg chamber elongation in *Drosophila*. *Dev. Biol.* 406, 212–221.

Jain, R.K. (2003). Molecular regulation of vessel maturation. *Nat. Med.* 9, 685–693.

Jansen, K.A., Atherton, P., and Ballestrem, C. (2017). Mechanotransduction at the cell-matrix interface. *Semin. Cell Dev. Biol.* 71, 75–83.

Jean, C., Chen, X.L., Nam, J.-O., Tancioni, I., Uryu, S., Lawson, C., Ward, K.K., Walsh, C.T., Miller, N.L.G., Ghassemian, M., et al. (2014). Inhibition of endothelial FAK activity prevents tumor metastasis by enhancing barrier function. *J. Cell Biol.* 204, 247–263.

Jiang, H., Torphy, R.J., Steiger, K., Hongo, H., Ritchie, A.J., Kriegsmann, M., Horst, D., Umetsu, S.E., Joseph, N.M., McGregor, K., et al. (2020). Pancreatic ductal adenocarcinoma progression is restrained by stromal matrix. *J. Clin. Invest.* 130, 4704–4709.

Jin, S.-W., Beis, D., Mitchell, T., Chen, J.-N., and Stainier, D.Y.R. (2005). Cellular and molecular analyses of vascular tube and lumen formation in zebrafish. *Dev.* 132, 5199–5209.

Jin, Y., Liu, Y., Lin, Q., Li, J., Druso, J.E., Antonyak, M.A., Meininger, C.J., Zhang, S.L., Dostal, D.E., Guan, J.-L., et al. (2013). Deletion of Cdc42 enhances ADAM17-mediated vascular endothelial growth factor receptor 2 shedding and impairs vascular endothelial cell survival and vasculogenesis. *Mol. Cell Biol.* 33, 4181–4197.

- Jones, M.G., Andriotis, O.G., Roberts, J.J., Lunn, K., Tear, V.J., Cao, L., Ask, K., Smart, D.E., Bonfanti, A., Johnson, P., et al. (2018). Nanoscale dysregulation of collagen structure-function disrupts mechano-homeostasis and mediates pulmonary fibrosis. *ELife* 7.
- de Jong, O.G., van der Waals, L.M., Kools, F.R.W., Verhaar, M.C., and van Balkom, B.W.M. (2019). Lysyl oxidase-like 2 is a regulator of angiogenesis through modulation of endothelial-to-mesenchymal transition. *J. Cell. Physiol.* 234, 10260–10269.
- Jorge-Peñas, A., Bové, H., Sanen, K., Vaeyens, M.-M., Steuwe, C., Roeffaers, M., Ameloot, M., and Van Oosterwyck, H. (2017). 3D full-field quantification of cell-induced large deformations in fibrillar biomaterials by combining non-rigid image registration with label-free second harmonic generation. *Biomaterials* 136, 86–97.
- Joutel, A., Haddad, I., Ratelade, J., and Nelson, M.T. (2016). Perturbations of the cerebrovascular matrisome: A convergent mechanism in small vessel disease of the brain? *J. Cereb. Blood Flow Metab. Off. J. Int. Soc. Cereb. Blood Flow Metab.* 36, 143–157.
- Ke, H., Feng, Z., Liu, M., Sun, T., Dai, J., Ma, M., Liu, L.-P., Ni, J.-Q., and Pastor-Pareja, J.C. (2018). Collagen secretion screening in *Drosophila* supports a common secretory machinery and multiple Rab requirements. *J. Genet. Genomics* 45, 299–313.
- Kechagia, J.Z., Ivaska, J., and Roca-Cusachs, P. (2019). Integrins as biomechanical sensors of the microenvironment. *Nat. Rev. Mol. Cell Biol.* 20, 457–473.
- Kim, D.-H., and Wirtz, D. (2013). Focal adhesion size uniquely predicts cell migration. *FASEB J. Off. Publ. Fed. Am. Soc. Exp. Biol.* 27, 1351–1361.
- Kim, B.-R., Dong, S.M., Seo, S.H., Lee, J.-H., Lee, J.M., Lee, S.-H., and Rho, S.B. (2014). Lysyl oxidase-like 2 (LOXL2) controls tumor-associated cell proliferation through the interaction with MARCKSL1. *Cell. Signal.* 26, 1765–1773.
- Kim, S., Harris, M., and Varner, J.A. (2000). Regulation of integrin alpha vbeta 3-mediated endothelial cell migration and angiogenesis by integrin alpha5beta1 and protein kinase A. *J. Biol. Chem.* 275, 33920–33928.
- Klepfish, M., Gross, T., Vugman, M., Afratis, N.A., Havusha-Laufer, S., Brazowski, E., Solomonov, I., Varol, C., and Sagi, I. (2020). LOXL2 Inhibition Paves the Way for Macrophage-Mediated Collagen Degradation in Liver Fibrosis. *Front. Immunol.* 11, 480.
- Koenderink, G.H., and Paluch, E.K. (2018). Architecture shapes contractility in actomyosin networks. *Curr. Opin. Cell Biol.* 50, 79–85.
- Kong, F., García, A.J., Mould, A.P., Humphries, M.J., and Zhu, C. (2009). Demonstration of catch bonds between an integrin and its ligand. *J. Cell Biol.* 185, 1275–1284.
- Kragl, M., Schubert, R., Karsjens, H., Otter, S., Bartosinska, B., Jeruschke, K., Weiss, J., Chen, C., Alsteens, D., Kuss, O., et al. (2016). The biomechanical properties of an epithelial tissue determine the location of its vasculature. *Nat. Commun.* 7, 13560.
- Krieg, M., Arboleda-Estudillo, Y., Puech, P.-H., Käfer, J., Graner, F., Müller, D.J., and Heisenberg, C.-P. (2008). Tensile forces govern germ-layer organization in zebrafish. *Nat. Cell Biol.* 10, 429–436.
- Kubow, K.E., Vukmirovic, R., Zhe, L., Klotzsch, E., Smith, M.L., Gourdon, D., Luna, S., and Vogel, V. (2015). Mechanical forces regulate the interactions of fibronectin and collagen I in extracellular matrix. *Nat. Commun.* 6, 8026.
- Kukkurainen, S., Määttä, J.A., Saeger, J., Valjakka, J., Vogel, V., and Hytönen, V.P. (2014). The talin-integrin interface under mechanical stress. *Mol. Biosyst.* 10, 3217–3228.
- Ladoux, B., Nelson, W.J., Yan, J., and Mège, R.M. (2015). The mechanotransduction machinery at work

at adherens junctions. *Integr. Biol. Quant. Biosci. Nano Macro* 7, 1109–1119.

Lampugnani, M.G., Resnati, M., Dejana, E., and Marchisio, P.C. (1991). The role of integrins in the maintenance of endothelial monolayer integrity. *J. Cell Biol.* 112, 479–490.

LeBleu, V.S., MacDonald, B., and Kalluri, R. (2007). Structure and Function of Basement Membranes. *Exp. Biol. Med.* 232, 1121–1129.

Lecuit, T., Lenne, P.-F., and Munro, E. (2011). Force Generation, Transmission, and Integration during Cell and Tissue Morphogenesis. *Annu. Rev. Cell Dev. Biol.* 27, 157–184.

Lee, C.Y., and Bautch, V.L. (2011). Ups and downs of guided vessel sprouting: the role of polarity. *Physiol. Bethesda Md* 26, 326–333.

Lee, S.-W., Kim, H.-K., Naidansuren, P., Ham, K.A., Choi, H.S., Ahn, H.-Y., Kim, M., Kang, D.H., Kang, S.W., and Joe, Y.A. (2020). Peroxidase is essential for endothelial cell survival and growth signaling by sulfhydryl crosslink-dependent matrix assembly. *FASEB J.*

Lehnert, D., Wehrle-Haller, B., David, C., Weiland, U., Ballestrem, C., Imhof, B.A., and Bastmeyer, M. (2004). Cell behaviour on micropatterned substrata: limits of extracellular matrix geometry for spreading and adhesion. *J. Cell Sci.* 117, 41–52.

Li, Q., Zhang, Y., Pluchon, P., Robens, J., Herr, K., Mercade, M., Thiery, J.-P., Yu, H., and Viasnoff, V. (2016). Extracellular matrix scaffolding guides lumen elongation by inducing anisotropic intercellular mechanical tension. *Nat. Cell Biol.* 18, 311–318.

Liliensiek, S.J., Nealey, P., and Murphy, C.J. (2009). Characterization of Endothelial Basement Membrane Nanotopography in Rhesus Macaque as a Guide for Vessel Tissue Engineering. *Tissue Eng. Part A* 15, 2643–2651.

Lindahl, P., Johansson, B.R., Levéen, P., and Betsholtz, C. (1997). Pericyte loss and microaneurysm formation in PDGF-B-deficient mice. *Science* 277, 242–245.

Lo, C.-M., Wang, H.-B., Dembo, M., and Wang, Y. (2000). Cell Movement Is Guided by the Rigidity of the Substrate. *Biophys. J.* 79, 144–152.

Löhler, J., Timpl, R., and Jaenisch, R. (1984). Embryonic lethal mutation in mouse collagen I gene causes rupture of blood vessels and is associated with erythropoietic and mesenchymal cell death. *Cell* 38, 597–607.

Loirand, G., and Pacaud, P. (2014). Involvement of Rho GTPases and their regulators in the pathogenesis of hypertension. *Small GTPases* 5.

López-Colomé, A.M., Lee-Rivera, I., Benavides-Hidalgo, R., and López, E. (2017). Paxillin: a crossroad in pathological cell migration. *J. Hematol. Oncol. J Hematol Oncol* 10, 50.

López-Jiménez, A.J., Basak, T., and Vanacore, R.M. (2017). Proteolytic processing of lysyl oxidase-like-2 in the extracellular matrix is required for crosslinking of basement membrane collagen IV. *J. Biol. Chem.* 292, 16970–16982.

López-Luppo, M., Nacher, V., Ramos, D., Catita, J., Navarro, M., Carretero, A., Rodriguez-Baeza, A., Mendes-Jorge, L., and Ruberte, J. (2017). Blood Vessel Basement Membrane Alterations in Human Retinal Microaneurysms During Aging. *Invest. Ophthalmol. Vis. Sci.* 58, 1116–1131.

Lu, J., Doyle, A.D., Shinsato, Y., Wang, S., Bodendorfer, M.A., Zheng, M., and Yamada, K.M. (2020). Basement Membrane Regulates Fibronectin Organization Using Sliding Focal Adhesions Driven by a Contractile Winch. *Dev. Cell* 52, 631–646.e4.

Mahjour, F., Dambal, V., Shrestha, N., Singh, V., Noonan, V., Kantarci, A., and Trackman, P.C. (2019). Mechanism for oral tumor cell lysyl oxidase like-2 in cancer development: synergy with PDGF-AB.

Oncogenesis 8, 34.

Maki, J.M. (2002). Inactivation of the Lysyl Oxidase Gene *Lox* Leads to Aortic Aneurysms, Cardiovascular Dysfunction, and Perinatal Death in Mice. *Circulation* 106, 2503–2509.

Mäki, J.M., Sormunen, R., Lippo, S., Kaarteenaho-Wiik, R., Soininen, R., and Myllyharju, J. (2005). Lysyl oxidase is essential for normal development and function of the respiratory system and for the integrity of elastic and collagen fibers in various tissues. *Am. J. Pathol.* 167, 927–936.

Mammoto, T., and Ingber, D.E. (2010). Mechanical control of tissue and organ development. *Development* 137, 1407–1420.

Marchand, M., Monnot, C., Muller, L., and Germain, S. (2019). Extracellular matrix scaffolding in angiogenesis and capillary homeostasis. *Semin. Cell Dev. Biol.* 89, 147–156.

Margadant, F., Chew, L.L., Hu, X., Yu, H., Bate, N., Zhang, X., and Sheetz, M. (2011). Mechanotransduction in vivo by repeated talin stretch-relaxation events depends upon vinculin. *PLoS Biol.* 9, e1001223.

Martin, A., Salvador, F., Moreno-Bueno, G., Floristán, A., Ruiz-Herguido, C., Cuevas, E.P., Morales, S., Santos, V., Csiszar, K., Dubus, P., et al. (2015). Lysyl oxidase-like 2 represses Notch1 expression in the skin to promote squamous cell carcinoma progression. *EMBO J.* 34, 1090–1109.

Marutani, T., Yamamoto, A., Nagai, N., Kubota, H., and Nagata, K. (2004). Accumulation of type IV collagen in dilated ER leads to apoptosis in Hsp47-knockout mouse embryos via induction of CHOP. *J. Cell Sci.* 117, 5913–5922.

Maruthamuthu, V., Sabass, B., Schwarz, U.S., and Gardel, M.L. (2011). Cell-ECM traction force modulates endogenous tension at cell-cell contacts. *Proc. Natl. Acad. Sci.* 108, 4708–4713.

McCleverty, C.J., Lin, D.C., and Liddington, R.C. (2007). Structure of the PTB domain of tensin1 and a model for its recruitment to fibrillar adhesions. *Protein Sci. Publ. Protein Soc.* 16, 1223–1229.

Mierke, C.T., Kollmannsberger, P., Zitterbart, D.P., Smith, J., Fabry, B., and Goldmann, W.H. (2008). Mechano-coupling and regulation of contractility by the vinculin tail domain. *Biophys. J.* 94, 661–670.

Millanes-Romero, A., Herranz, N., Perrera, V., Iturbide, A., Loubat-Casanovas, J., Gil, J., Jenuwein, T., García de Herreros, A., and Peiró, S. (2013). Regulation of heterochromatin transcription by Snail1/LOXL2 during epithelial-to-mesenchymal transition. *Mol. Cell* 52, 746–757.

Miller, C.G., Pozzi, A., Zent, R., and Schwarzbauer, J.E. (2014). Effects of high glucose on integrin activity and fibronectin matrix assembly by mesangial cells. *Mol. Biol. Cell* 25, 2342–2350.

Mitra, S.K., and Schlaepfer, D.D. (2006). Integrin-regulated FAK-Src signaling in normal and cancer cells. *Curr. Opin. Cell Biol.* 18, 516–523.

Mitrossilis, D., Fouchard, J., Guiroy, A., Desprat, N., Rodriguez, N., Fabry, B., and Asnacios, A. (2009). Single-cell response to stiffness exhibits muscle-like behavior. *Proc. Natl. Acad. Sci. U. S. A.* 106, 18243–18248.

Monkley, S.J., Kostourou, V., Spence, L., Petrich, B., Coleman, S., Ginsberg, M.H., Pritchard, C.A., and Critchley, D.R. (2011). Endothelial cell talin1 is essential for embryonic angiogenesis. *Dev. Biol.* 349, 494–502.

Monteiro, P., Rossé, C., Castro-Castro, A., Irondelle, M., Lagoutte, E., Paul-Gilloteaux, P., Desnos, C., Formstecher, E., Darchen, F., Perrais, D., et al. (2013). Endosomal WASH and exocyst complexes control exocytosis of MT1-MMP at invadopodia. *J. Cell Biol.* 203, 1063–1079.

Moon, H.-J., Finney, J., Xu, L., Moore, D., Welch, D.R., and Mure, M. (2013). MCF-7 cells expressing nuclear associated lysyl oxidase-like 2 (LOXL2) exhibit an epithelial-to-mesenchymal transition (EMT)

phenotype and are highly invasive in vitro. *J. Biol. Chem.* 288, 30000–30008.

Moon, H.-J., Finney, J., Ronnebaum, T., and Mure, M. (2014). Human lysyl oxidase-like 2. *Bioorganic Chem.* 57, 231–241.

Moreno, V., Gonzalo, P., Gómez-Escudero, J., Pollán, Á., Acín-Pérez, R., Breckenridge, M., Yáñez-Mó, M., Barreiro, O., Orsenigo, F., Kadomatsu, K., et al. (2014). An EMMPRIN- γ -catenin-Nm23 complex drives ATP production and actomyosin contractility at endothelial junctions. *J. Cell Sci.* 127, 3768–3781.

Moreno-Bueno, G., Salvador, F., Martín, A., Floristán, A., Cuevas, E.P., Santos, V., Montes, A., Morales, S., Castilla, M.A., Rojo-Sebastián, A., et al. (2011). Lysyl oxidase-like 2 (LOXL2), a new regulator of cell polarity required for metastatic dissemination of basal-like breast carcinomas. *EMBO Mol. Med.* 3, 528–544.

Naba, A., Clauser, K.R., Hoersch, S., Liu, H., Carr, S.A., and Hynes, R.O. (2012). The Matrisome: In Silico Definition and In Vivo Characterization by Proteomics of Normal and Tumor Extracellular Matrices. *Mol. Cell. Proteomics MCP* 11.

Nakatsu, M.N., Davis, J., and Hughes, C.C.W. (2007). Optimized Fibrin Gel Bead Assay for the Study of Angiogenesis. *J. Vis. Exp.* 186.

Neumann, P., Jaé, N., Knau, A., Glaser, S.F., Fouani, Y., Rossbach, O., Krüger, M., John, D., Bindereif, A., Grote, P., et al. (2018). The lncRNA GATA6-AS epigenetically regulates endothelial gene expression via interaction with LOXL2. *Nat. Commun.* 9, 237.

Ngandu Mpoyi, E., Cantini, M., Sin, Y.Y., Fleming, L., Zhou, D.W., Costell, M., Lu, Y., Kadler, K., García, A.J., Van Agtmael, T., et al. (2020). Material-driven fibronectin assembly rescues matrix defects due to mutations in collagen IV in fibroblasts. *Biomaterials* 252, 120090.

Nguyen, D.-H.T., Gao, L., Wong, A., and Chen, C.S. (2017). Cdc42 regulates branching in angiogenic sprouting in vitro. *Microcirc. N. Y. N* 1994 24.

Nguyen, E.V., Pereira, B.A., Lawrence, M.G., Ma, X., Rebello, R.J., Chan, H., Niranjana, B., Wu, Y., Ellem, S., Guan, X., et al. (2019). Proteomic Profiling of Human Prostate Cancer-associated Fibroblasts (CAF) Reveals LOXL2-dependent Regulation of the Tumor Microenvironment. *Mol. Cell. Proteomics MCP* 18, 1410–1427.

Okada, K., Moon, H.-J., Finney, J., Meier, A., and Mure, M. (2018). Extracellular Processing of Lysyl Oxidase-like 2 and Its Effect on Amine Oxidase Activity. *Biochemistry* 57, 6973–6983.

Oldenburg, J., and de Rooij, J. (2014). Mechanical control of the endothelial barrier. *Cell Tissue Res.* 355, 545–555.

Olsson, A.-K., Dimberg, A., Kreuger, J., and Claesson-Welsh, L. (2006). VEGF receptor signalling - in control of vascular function. *Nat. Rev. Mol. Cell Biol.* 7, 359–371.

Oria, R., Wiegand, T., Escribano, J., Elosegui-Artola, A., Uriarte, J.J., Moreno-Pulido, C., Platzman, I., Delcanale, P., Albertazzi, L., Navajas, D., et al. (2017). Force loading explains spatial sensing of ligands by cells. *Nature* 552, 219–224.

Pankov, R., Cukierman, E., Katz, B.Z., Matsumoto, K., Lin, D.C., Lin, S., Hahn, C., and Yamada, K.M. (2000). Integrin dynamics and matrix assembly: tensin-dependent translocation of $\alpha(5)\beta(1)$ integrins promotes early fibronectin fibrillogenesis. *J. Cell Biol.* 148, 1075–1090.

Park, J.E., Keller, G.A., and Ferrara, N. (1993). The vascular endothelial growth factor (VEGF) isoforms: differential deposition into the subepithelial extracellular matrix and bioactivity of extracellular matrix-bound VEGF. *Mol. Biol. Cell* 4, 1317–1326.

Parsons, J.T., Horwitz, A.R., and Schwartz, M.A. (2010). Cell adhesion: integrating cytoskeletal dynamics and cellular tension. *Nat. Rev. Mol. Cell Biol.* 11, 633–643.

- Peinado, H., Del Carmen Iglesias-de la Cruz, M., Olmeda, D., Csiszar, K., Fong, K.S.K., Vega, S., Nieto, M.A., Cano, A., and Portillo, F. (2005). A molecular role for lysyl oxidase-like 2 enzyme in snail regulation and tumor progression. *EMBO J.* 24, 3446–3458.
- Peng, D.H., Ungewiss, C., Tong, P., Byers, L.A., Wang, J., Canales, J.R., Villalobos, P.A., Uraoka, N., Mino, B., Behrens, C., et al. (2017). ZEB1 induces LOXL2-mediated collagen stabilization and deposition in the extracellular matrix to drive lung cancer invasion and metastasis. *Oncogene* 36, 1925–1938.
- Peng, L., Ran, Y.-L., Hu, H., Yu, L., Liu, Q., Zhou, Z., Sun, Y.-M., Sun, L.-C., Pan, J., Sun, L.-X., et al. (2009). Secreted LOXL2 is a novel therapeutic target that promotes gastric cancer metastasis via the Src/FAK pathway. *Carcinogenesis* 30, 1660–1669.
- Peng, T., Deng, X., Tian, F., Li, Z., Jiang, P., Zhao, X., Chen, G., Chen, Y., Zheng, P., Li, D., et al. (2019). The interaction of LOXL2 with GATA6 induces VEGFA expression and angiogenesis in cholangiocarcinoma. *Int. J. Oncol.*
- Petropoulos, C., Oddou, C., Emadali, A., Hiriart-Bryant, E., Boyault, C., Faurobert, E., Vande Pol, S., Kim-Kaneyama, J.-R., Kraut, A., Coute, Y., et al. (2016). Roles of paxillin family members in adhesion and ECM degradation coupling at invadosomes. *J. Cell Biol.* 213, 585–599.
- Phng, L.-K., and Gerhardt, H. (2009). Angiogenesis: A Team Effort Coordinated by Notch. *Dev. Cell* 16, 196–208.
- Phng, L.-K., Gebala, V., Bentley, K., Philippides, A., Wacker, A., Mathivet, T., Sauter, L., Stanchi, F., Belting, H.-G., Affolter, M., et al. (2015). Formin-mediated actin polymerization at endothelial junctions is required for vessel lumen formation and stabilization. *Dev. Cell* 32, 123–132.
- Plaisier, E., Gribouval, O., Alamowitch, S., Mougnot, B., Prost, C., Verpont, M.C., Marro, B., Desmettre, T., Cohen, S.Y., Roulet, E., et al. (2007). COL4A1 mutations and hereditary angiopathy, nephropathy, aneurysms, and muscle cramps. *N. Engl. J. Med.* 357, 2687–2695.
- Polacheck, W.J., and Chen, C.S. (2016). Measuring cell-generated forces: a guide to the available tools. *Nat. Methods* 13, 415–423.
- Pöschl, E., Schlötzer-Schrehardt, U., Brachvogel, B., Saito, K., Ninomiya, Y., and Mayer, U. (2004). Collagen IV is essential for basement membrane stability but dispensable for initiation of its assembly during early development. *Dev.* 131, 1619–1628.
- Potente, M., Gerhardt, H., and Carmeliet, P. (2011). Basic and therapeutic aspects of angiogenesis. *Cell* 146, 873–887.
- Prager-Khoutorsky, M., Lichtenstein, A., Krishnan, R., Rajendran, K., Mayo, A., Kam, Z., Geiger, B., and Bershadsky, A.D. (2011). Fibroblast polarization is a matrix-rigidity-dependent process controlled by focal adhesion mechanosensing. *Nat. Cell Biol.* 13, 1457–1465.
- Provenzano, P.P., Inman, D.R., Eliceiri, K.W., Trier, S.M., and Keely, P.J. (2008). Contact guidance mediated three-dimensional cell migration is regulated by Rho/ROCK-dependent matrix reorganization. *Biophys. J.* 95, 5374–5384.
- Puech, P.-H., Poole, K., Knebel, D., and Muller, D.J. (2006). A new technical approach to quantify cell-cell adhesion forces by AFM. *Ultramicroscopy* 106, 637–644.
- Pulous, F.E., and Petrich, B.G. (2019). Integrin-dependent regulation of the endothelial barrier. *Tissue Barriers* 7.
- Pulous, F.E., Grimsley-Myers, C.M., Kansal, S., Kowalczyk, A.P., and Petrich, B.G. (2019). Talin-Dependent Integrin Activation Regulates VE-Cadherin Localization and Endothelial Cell Barrier Function. *Circ. Res.* 124, 891–903.

- Radwanska, A., Grall, D., Schaub, S., Divonne, S.B. la F., Ciais, D., Rekima, S., Rupp, T., Sudaka, A., Orend, G., and Van Obberghen-Schilling, E. (2017). Counterbalancing anti-adhesive effects of Tenascin-C through fibronectin expression in endothelial cells. *Sci. Rep.* 7, 12762.
- Raghavan, S., Nelson, C.M., Baranski, J.D., Lim, E., and Chen, C.S. (2010). Geometrically controlled endothelial tubulogenesis in micropatterned gels. *Tissue Eng. Part A* 16, 2255–2263.
- Rahimi, N. (2012). The Ubiquitin-Proteasome System Meets Angiogenesis. *Mol. Cancer Ther.* 11, 538–548.
- Reynolds, L.E., Wyder, L., Lively, J.C., Taverna, D., Robinson, S.D., Huang, X., Sheppard, D., Hynes, R.O., and Hodivala-Dilke, K.M. (2002). Enhanced pathological angiogenesis in mice lacking beta3 integrin or beta3 and beta5 integrins. *Nat. Med.* 8, 27–34.
- del Rio, A., Perez-Jimenez, R., Liu, R., Roca-Cusachs, P., Fernandez, J.M., and Sheetz, M.P. (2009). Stretching single talin rod molecules activates vinculin binding. *Science* 323, 638–641.
- Risau, W., and Lemmon, V. (1988). Changes in the vascular extracellular matrix during embryonic vasculogenesis and angiogenesis. *Dev. Biol.* 125, 441–450.
- Rodríguez Fernández, J.L., Geiger, B., Salomon, D., and Ben-Ze'ev, A. (1993). Suppression of vinculin expression by antisense transfection confers changes in cell morphology, motility, and anchorage-dependent growth of 3T3 cells. *J. Cell Biol.* 122, 1285–1294.
- Saito, T., Uzawa, K., Terajima, M., Shiiba, M., Amelio, A.L., Tanzawa, H., and Yamauchi, M. (2019). Aberrant Collagen Cross-linking in Human Oral Squamous Cell Carcinoma. *J. Dent. Res.* 98, 517–525.
- San Antonio, J.D., Zoeller, J.J., Habursky, K., Turner, K., Pimtong, W., Burrows, M., Choi, S., Basra, S., Bennett, J.S., DeGrado, W.F., et al. (2009). A Key Role for the Integrin $\alpha 2\beta 1$ in Experimental and Developmental Angiogenesis. *Am. J. Pathol.* 175, 1338–1347.
- Sapudom, J., Kalbitzer, L., Wu, X., Martin, S., Kroy, K., and Pompe, T. (2019). Fibril bending stiffness of 3D collagen matrices instructs spreading and clustering of invasive and non-invasive breast cancer cells. *Biomaterials* 193, 47–57.
- Sauteur, L., Krudewig, A., Herwig, L., Ehrenfeuchter, N., Lenard, A., Affolter, M., and Belting, H.-G. (2014). Cdh5/VE-cadherin promotes endothelial cell interface elongation via cortical actin polymerization during angiogenic sprouting. *Cell Rep.* 9, 504–513.
- Schilter, H., Findlay, A.D., Perryman, L., Yow, T.T., Moses, J., Zahoor, A., Turner, C.I., Deodhar, M., Foot, J.S., Zhou, W., et al. (2019). The lysyl oxidase like 2/3 enzymatic inhibitor, PXS-5153A, reduces crosslinks and ameliorates fibrosis. *J. Cell. Mol. Med.* 23, 1759–1770.
- Schmelzer, C.E.H., Heinz, A., Troilo, H., Lockhart-Cairns, M.P., Jowitt, T.A., Marchand, M.F., Bidault, L., Bignon, M., Hedtke, T., Barret, A., et al. (2019). Lysyl oxidase-like 2 (LOXL2)-mediated cross-linking of tropoelastin. *FASEB J. Off. Publ. Fed. Am. Soc. Exp. Biol.* 33, 5468–5481.
- Seano, G., Chiaverina, G., Gagliardi, P.A., di Blasio, L., Puliafito, A., Bouvard, C., Sessa, R., Tarone, G., Sorokin, L., Helley, D., et al. (2014). Endothelial podosome rosettes regulate vascular branching in tumour angiogenesis. *Nat. Cell Biol.* 16, 931–941, 1–8.
- Sechler, J.L., Takada, Y., and Schwarzbauer, J.E. (1996). Altered rate of fibronectin matrix assembly by deletion of the first type III repeats. *J. Cell Biol.* 134, 573–583.
- Seddiki, R., Narayana, G.H.N.S., Strale, P.-O., Balcioglu, H.E., Peyret, G., Yao, M., Le, A.P., Teck Lim, C., Yan, J., Ladoux, B., et al. (2018). Force-dependent binding of vinculin to α -catenin regulates cell–cell contact stability and collective cell behavior. *Mol. Biol. Cell* 29, 380–388.
- Selhuber-Unkel, C., López-García, M., Kessler, H., and Spatz, J.P. (2008). Cooperativity in Adhesion

Cluster Formation during Initial Cell Adhesion. *Biophys. J.* 95, 5424–5431.

Senger, D.R., Claffey, K.P., Benes, J.E., Perruzzi, C.A., Sergiou, A.P., and Detmar, M. (1997). Angiogenesis promoted by vascular endothelial growth factor: Regulation through $\alpha 1$ and $\beta 1$ integrins. *Proc. Natl. Acad. Sci.* 94, 13612–13617.

Silva, R., D'Amico, G., Hovalva-Dilke, K.M., and Reynolds, L.E. (2008). Integrins: The Keys to Unlocking Angiogenesis. *Arterioscler. Thromb. Vasc. Biol.* 28, 1703–1713.

Sims, D.E. (1986). The pericyte—a review. *Tissue Cell* 18, 153–174.

Smith, M.L., Gourdon, D., Little, W.C., Kubow, K.E., Eguiluz, R.A., Luna-Morris, S., and Vogel, V. (2007). Force-induced unfolding of fibronectin in the extracellular matrix of living cells. *PLoS Biol.* 5, e268.

Song, J., Zhang, X., Buscher, K., Wang, Y., Wang, H., Di Russo, J., Li, L., Lütke-Enking, S., Zarbock, A., Stadtmann, A., et al. (2017). Endothelial Basement Membrane Laminin 511 Contributes to Endothelial Junctional Tightness and Thereby Inhibits Leukocyte Transmigration. *Cell Rep.* 18, 1256–1269.

Sorokin, L.M., Pausch, F., Frieser, M., Kröger, S., Ohage, E., and Deutzmann, R. (1997). Developmental Regulation of the Laminin $\alpha 5$ Chain Suggests a Role in Epithelial and Endothelial Cell Maturation. *Dev. Biol.* 189, 285–300.

Stenzel, D., Franco, C.A., Estrach, S., Mettouchi, A., Sauvaget, D., Rosewell, I., Schertel, A., Armer, H., Domogatskaya, A., Rodin, S., et al. (2011a). Endothelial basement membrane limits tip cell formation by inducing Dll4/Notch signalling in vivo. *EMBO Rep.* 12, 1135–1143.

Stenzel, D., Lundkvist, A., Sauvaget, D., Busse, M., Graupera, M., van der Flier, A., Wijelath, E.S., Murray, J., Sobel, M., Costell, M., et al. (2011b). Integrin-dependent and -independent functions of astrocytic fibronectin in retinal angiogenesis. *Development* 138, 4451–4463.

Steppan, J., Wang, H., Bergman, Y., Rauer, M.J., Tan, S., Jandu, S., Nandakumar, K., Barreto-Ortiz, S., Cole, R.N., Boronina, T.N., et al. (2019). Lysyl oxidase-like 2 depletion is protective in age-associated vascular stiffening. *Am. J. Physiol. Heart Circ. Physiol.* 317, H49–H59.

Steuwe, C., Vaeyens, M.-M., Jorge-Peñas, A., Cokelaere, C., Hofkens, J., Roeffaers, M.B.J., and Van Oosterwyck, H. (2020). Fast quantitative time lapse displacement imaging of endothelial cell invasion. *PloS One* 15, e0227286.

Stockton, R.A., Shenkar, R., Awad, I.A., and Ginsberg, M.H. (2010). Cerebral cavernous malformations proteins inhibit Rho kinase to stabilize vascular integrity. *J. Exp. Med.* 207, 881–896.

Stratman, A.N., and Davis, G.E. (2012). Endothelial cell-pericyte interactions stimulate basement membrane matrix assembly: influence on vascular tube remodeling, maturation, and stabilization. *Microsc. Microanal. Off. J. Microsc. Soc. Am. Microbeam Anal. Soc. Microsc. Soc. Can.* 18, 68–80.

Stratman, A.N., Schwindt, A.E., Malotte, K.M., and Davis, G.E. (2010). Endothelial-derived PDGF-BB and HB-EGF coordinately regulate pericyte recruitment during vasculogenic tube assembly and stabilization. *Blood* 116, 4720–4730.

Strilić, B., Kucera, T., Eglinger, J., Hughes, M.R., McNagny, K.M., Tsukita, S., Dejana, E., Ferrara, N., and Lammert, E. (2009). The molecular basis of vascular lumen formation in the developing mouse aorta. *Dev. Cell* 17, 505–515.

Stutchbury, B., Atherton, P., Tsang, R., Wang, D.-Y., and Ballestrem, C. (2017). Distinct focal adhesion protein modules control different aspects of mechanotransduction. *J. Cell Sci.* 130, 1612–1624.

Suchting, S., Freitas, C., Noble, F. le, Benedito, R., Bréant, C., Duarte, A., and Eichmann, A. (2007). The Notch ligand Delta-like 4 negatively regulates endothelial tip cell formation and vessel branching. *Proc. Natl. Acad. Sci.* 104, 3225–3230.

- Suleiman, H., Zhang, L., Roth, R., Heuser, J.E., Miner, J.H., Shaw, A.S., and Dani, A. (2013). Nanoscale protein architecture of the kidney glomerular basement membrane. *ELife* 2, e01149.
- Sumida, G.M., Tomita, T.M., Shih, W., and Yamada, S. (2011). Myosin II activity dependent and independent vinculin recruitment to the sites of E-cadherin-mediated cell-cell adhesion. *BMC Cell Biol.* 12, 48.
- Sun, Z., Guo, S.S., and Fässler, R. (2016a). Integrin-mediated mechanotransduction. *J. Cell Biol.* 215, 445–456.
- Sun, Z., Tseng, H.-Y., Tan, S., Senger, F., Kurzawa, L., Dedden, D., Mizuno, N., Wasik, A.A., They, M., Dunn, A.R., et al. (2016b). Kank2 activates talin, reduces force transduction across integrins and induces central adhesion formation. *Nat. Cell Biol.* 18, 941–953.
- Szymborska, A., and Gerhardt, H. (2018). Hold Me, but Not Too Tight-Endothelial Cell-Cell Junctions in Angiogenesis. *Cold Spring Harb. Perspect. Biol.* 10.
- Takagi, J., Petre, B.M., Walz, T., and Springer, T.A. (2002). Global Conformational Rearrangements in Integrin Extracellular Domains in Outside-In and Inside-Out Signaling. *Cell* 110, 599–611.
- Tanjore, H., Zeisberg, E.M., Gerami-Naini, B., and Kalluri, R. (2008). β 1 integrin expression on endothelial cells is required for angiogenesis but not for vasculogenesis. *Dev. Dyn.* 237, 75–82.
- Tavora, B., Batista, S., Reynolds, L.E., Jadeja, S., Robinson, S., Kostourou, V., Hart, I., Fruttiger, M., Parsons, M., and Hodivala-Dilke, K.M. (2010). Endothelial FAK is required for tumour angiogenesis. *EMBO Mol. Med.* 2, 516–528.
- Tello, M., Spenlé, C., Hemmerlé, J., Mercier, L., Fabre, R., Allio, G., Simon-Assmann, P., and Goetz, J.G. (2016). Generating and characterizing the mechanical properties of cell-derived matrices using atomic force microscopy. *Methods San Diego Calif* 94, 85–100.
- They, M., Racine, V., Piel, M., Pepin, A., Dimitrov, A., Chen, Y., Sibarita, J.-B., and Bornens, M. (2006). Anisotropy of cell adhesive microenvironment governs cell internal organization and orientation of polarity. *Proc. Natl. Acad. Sci.* 103, 19771–19776.
- Théry, M., Pépin, A., Dressaire, E., Chen, Y., and Bornens, M. (2006). Cell distribution of stress fibres in response to the geometry of the adhesive environment. *Cell Motil. Cytoskeleton* 63, 341–355.
- Thomas, W.A., Boscher, C., Chu, Y.-S., Cuvelier, D., Martinez-Rico, C., Seddiki, R., Heysch, J., Ladoux, B., Thiery, J.P., Mege, R.-M., et al. (2013). α -Catenin and vinculin cooperate to promote high E-cadherin-based adhesion strength. *J. Biol. Chem.* 288, 4957–4969.
- Thyboll, J., Kortessmaa, J., Cao, R., Soininen, R., Wang, L., Iivanainen, A., Sorokin, L., Risling, M., Cao, Y., and Tryggvason, K. (2002). Deletion of the laminin alpha4 chain leads to impaired microvessel maturation. *Mol. Cell. Biol.* 22, 1194–1202.
- Tien, J., Ghani, U., Dance, Y.W., Seibel, A.J., Karakan, M.C., Ekinici, K.L., and Nelson, C.M. (2020). Matrix pore size governs escape of human breast cancer cells from a microtumor to an empty cavity. *iScience* 23, 101673.
- Tiwari, S., Askari, J.A., Humphries, M.J., and Balleid, N.J. (2011). Divalent cations regulate the folding and activation status of integrins during their intracellular trafficking. *J. Cell Sci.* 124, 1672–1680.
- del Toro, R., Prahst, C., Mathivet, T., Siegfried, G., Kaminker, J.S., Larrivee, B., Breant, C., Duarte, A., Takakura, N., Fukamizu, A., et al. (2010). Identification and functional analysis of endothelial tip cell-enriched genes. *Blood* 116, 4025–4033.
- Trichet, L., Le Digabel, J., Hawkins, R.J., Vedula, S.R.K., Gupta, M., Ribault, C., Hersen, P., Voituriez, R., and Ladoux, B. (2012). Evidence of a large-scale mechanosensing mechanism for cellular adaptation to substrate stiffness. *Proc. Natl. Acad. Sci. U. S. A.* 109, 6933–6938.

- Tseng, Q., Duchemin-Pelletier, E., Deshiere, A., Balland, M., Guillou, H., Filhol, O., and Thery, M. (2012). Spatial organization of the extracellular matrix regulates cell-cell junction positioning. *Proc. Natl. Acad. Sci.* *109*, 1506–1511.
- Turner, C.J., Badu-Nkansah, K., and Hynes, R.O. (2017). Endothelium-derived fibronectin regulates neonatal vascular morphogenesis in an autocrine fashion. *Angiogenesis* *20*, 519–531.
- Uechi, G., Sun, Z., Schreiber, E.M., Halfter, W., and Balasubramani, M. (2014). Proteomic View of Basement Membranes from Human Retinal Blood Vessels, Inner Limiting Membranes, and Lens Capsules. *J Proteome Res.*
- Umana-Diaz, C., Pichol-Thievend, C., Marchand, M.F., Atlas, Y., Salza, R., Malbouyres, M., Barret, A., Teillon, J., Ardidie-Robouant, C., Ruggiero, F., et al. (2020). Scavenger Receptor Cysteine-Rich domains of Lysyl Oxidase-Like2 regulate endothelial ECM and angiogenesis through non-catalytic scaffolding mechanisms. *Matrix Biol.* *88*, 23-52.
- Uroz, M., Garcia-Puig, A., Tekeli, I., Elosegui-Artola, A., Abenza, J.F., Marín-Llauradó, A., Pujals, S., Conte, V., Albertazzi, L., Roca-Cusachs, P., et al. (2019). Traction forces at the cytokinetic ring regulate cell division and polyploidy in the migrating zebrafish epicardium. *Nat. Mater.* *18*, 1015–1023.
- Vadasz, Z., Kessler, O., Akiri, G., Gengrinovitch, S., Kagan, H.M., Baruch, Y., Izhak, O.B., and Neufeld, G. (2005). Abnormal deposition of collagen around hepatocytes in Wilson's disease is associated with hepatocyte specific expression of lysyl oxidase and lysyl oxidase like protein-2. *J. Hepatol.* *43*, 499–507.
- Wang, W.Y., Pearson, A.T., Kutys, M.L., Choi, C.K., Wozniak, M.A., Baker, B.M., and Chen, C.S. (2018a). Extracellular matrix alignment dictates the organization of focal adhesions and directs uniaxial cell migration. *APL Bioeng.* *2*, 046107.
- Wang, W.Y., Pearson, A.T., Kutys, M.L., Choi, C.K., Wozniak, M.A., Baker, B.M., and Chen, C.S. (2018b). Extracellular matrix alignment dictates the organization of focal adhesions and directs uniaxial cell migration. *APL Bioeng.* *2*, 046107.
- Wang, W.Y., Davidson, C.D., Lin, D., and Baker, B.M. (2019). Actomyosin contractility-dependent matrix stretch and recoil induces rapid cell migration. *Nat. Commun.* *10*, 1186.
- Warren, C.M., and Iruela-Arispe, M.L. (2014). Podosome rosettes precede vascular sprouts in tumour angiogenesis. *Nat. Cell Biol.* *16*, 928–930.
- Webster, K.D., Crow, A., and Fletcher, D.A. (2011). An AFM-based stiffness clamp for dynamic control of rigidity. *PloS One* *6*, e17807.
- Wijelath, E.S., Rahman, S., Namekata, M., Murray, J., Nishimura, T., Mostafavi-Pour, Z., Patel, Y., Suda, Y., Humphries, M.J., and Sobel, M. (2006). Heparin-II domain of fibronectin is a vascular endothelial growth factor-binding domain: enhancement of VEGF biological activity by a singular growth factor/matrix protein synergism. *Circ. Res.* *99*, 853–860.
- Wilson, D.G., Phamluong, K., Li, L., Sun, M., Cao, T.C., Liu, P.S., Modrusan, Z., Sandoval, W.N., Rangell, L., Carano, R.A.D., et al. (2011). Global defects in collagen secretion in a Mia3/TANGO1 knockout mouse. *J. Cell Biol.* *193*, 935–951.
- Winograd-Katz, S.E., Fässler, R., Geiger, B., and Legate, K.R. (2014). The integrin adhesome: from genes and proteins to human disease. *Nat. Rev. Mol. Cell Biol.* *15*, 273–288.
- Wong, C.C.-L., Tse, A.P.-W., Huang, Y.-P., Zhu, Y.-T., Chiu, D.K.-C., Lai, R.K.-H., Au, S.L.-K., Kai, A.K.-L., Lee, J.M.-F., Wei, L.L., et al. (2014). Lysyl oxidase-like 2 is critical to tumor microenvironment and metastatic niche formation in hepatocellular carcinoma. *Hepatol. Baltim. Md* *60*, 1645–1658.
- Wozniak, M.A., and Chen, C.S. (2009). Mechanotransduction in development: a growing role for contractility. *Nat. Rev. Mol. Cell Biol.* *10*, 34–43.

- Wu, S., Zheng, Q., Xing, X., Dong, Y., Wang, Y., You, Y., Chen, R., Hu, C., Chen, J., Gao, D., et al. (2018a). Matrix stiffness-upregulated LOXL2 promotes fibronectin production, MMP9 and CXCL12 expression and BMDCs recruitment to assist pre-metastatic niche formation. *J. Exp. Clin. Cancer Res. CR* 37, 99.
- Wu, Y., Li, Z., Shi, Y., Chen, L., Tan, H., Wang, Z., Yin, C., Liu, L., and Hu, J. (2018b). Exome Sequencing Identifies LOXL2 Mutation as a Cause of Familial Intracranial Aneurysm. *World Neurosurg.* 109, e812–e818.
- Xu, H., Pumiglia, K., and LaFlamme, S.E. (2020). Laminin-511 and $\alpha 6$ integrins regulate the expression of CXCR4 to promote endothelial morphogenesis. *J. Cell Sci.* 133.
- Yamamoto, H., Ehling, M., Kato, K., Kanai, K., van Lessen, M., Frye, M., Zeuschner, D., Nakayama, M., Vestweber, D., and Adams, R.H. (2015). Integrin $\beta 1$ controls VE-cadherin localization and blood vessel stability. *Nat. Commun.* 6, 6429.
- Yang, J., Savvatis, K., Kang, J.S., Fan, P., Zhong, H., Schwartz, K., Barry, V., Mikels-Vigdal, A., Karpinski, S., Kornyejev, D., et al. (2016). Targeting LOXL2 for cardiac interstitial fibrosis and heart failure treatment. *Nat. Commun.* 7, 13710.
- Yang, J.T., Rayburn, H., and Hynes, R.O. (1993). Embryonic mesodermal defects in alpha 5 integrin-deficient mice. *Dev.* 119, 1093–1105.
- Ye, M., Song, Y., Pan, S., Chu, M., Wang, Z.-W., and Zhu, X. (2020). Evolving roles of lysyl oxidase family in tumorigenesis and cancer therapy. *Pharmacol. Ther.* 215, 107633.
- Yurchenco, P.D. (2011). Basement membranes: cell scaffoldings and signaling platforms. *Cold Spring Harb. Perspect. Biol.* 3.
- Zaffryar-Eilot, S., Marshall, D., Voloshin, T., Bar-Zion, A., Spangler, R., Kessler, O., Ghermazien, H., Brekhan, V., Suss-Toby, E., Adam, D., et al. (2013). Lysyl oxidase-like-2 promotes tumour angiogenesis and is a potential therapeutic target in angiogenic tumours. *Carcinogenesis* 34, 2370–2379.
- Zaidel-Bar, R., Ballestrem, C., Kam, Z., and Geiger, B. (2003). Early molecular events in the assembly of matrix adhesions at the leading edge of migrating cells. *J. Cell Sci.* 116, 4605–4613.
- Zaidel-Bar, R., Milo, R., Kam, Z., and Geiger, B. (2007). A paxillin tyrosine phosphorylation switch regulates the assembly and form of cell-matrix adhesions. *J. Cell Sci.* 120, 137–148.
- Zamir, E., Katz, M., Posen, Y., Erez, N., Yamada, K.M., Katz, B.Z., Lin, S., Lin, D.C., Bershadsky, A., Kam, Z., et al. (2000). Dynamics and segregation of cell-matrix adhesions in cultured fibroblasts. *Nat. Cell Biol.* 2, 191–196.
- Zeeb, M., Strilic, B., and Lammert, E. (2010). Resolving cell-cell junctions: lumen formation in blood vessels. *Curr. Opin. Cell Biol.* 22, 626–632.
- Zhan, X.-H., Jiao, J.-W., Zhang, H.-F., Xu, X.-E., He, J.-Z., Li, R.-L., Zou, H.-Y., Wu, Z.-Y., Wang, S.-H., Wu, J.-Y., et al. (2019). LOXL2 Upregulates Phosphorylation of Ezrin to Promote Cytoskeletal Reorganization and Tumor Cell Invasion. *Cancer Res.* 79, 4951–4964.
- Zhang, X., Jiang, G., Cai, Y., Monkley, S.J., Critchley, D.R., and Sheetz, M.P. (2008). Talin depletion reveals independence of initial cell spreading from integrin activation and traction. *Nat. Cell Biol.* 10, 1062–1068.
- Zhang, X., Wang, Q., Wu, J., Wang, J., Shi, Y., and Liu, M. (2018). Crystal structure of human lysyl oxidase-like 2 (hLOXL2) in a precursor state. *Proc. Natl. Acad. Sci. U. S. A.* 115, 3828–3833.
- Zhou, X., Rowe, R.G., Hiraoka, N., George, J.P., Wirtz, D., Mosher, D.F., Virtanen, I., Chernousov, M.A.,

and Weiss, S.J. (2008). Fibronectin fibrillogenesis regulates three-dimensional neovessel formation. *Genes Dev.* 22, 1231–1243.

Zhou, Z.-H., Ji, C.-D., Xiao, H.-L., Zhao, H.-B., Cui, Y.-H., and Bian, X.-W. (2017). Reorganized Collagen in the Tumor Microenvironment of Gastric Cancer and Its Association with Prognosis. *J. Cancer* 8, 1466–1476.

Zovein, A.C., Luque, A., Turlo, K.A., Hofmann, J.J., Yee, K.M., Becker, M.S., Fassler, R., Mellman, I., Lane, T.F., and Iruela-Arispe, M.L. (2010). Beta1 integrin establishes endothelial cell polarity and arteriolar lumen formation via a Par3-dependent mechanism. *Dev. Cell* 18, 39–51.